



NEW STRATEGIES FOR C(SP³)-H FUNCTIONALIZATION

Daniel Bafaluy Español

ADVERTIMENT. L'accés als continguts d'aquesta tesi doctoral i la seva utilització ha de respectar els drets de la persona autora. Pot ser utilitzada per a consulta o estudi personal, així com en activitats o materials d'investigació i docència en els termes establerts a l'art. 32 del Text Refós de la Llei de Propietat Intel·lectual (RDL 1/1996). Per altres utilitzacions es requereix l'autorització prèvia i expressa de la persona autora. En qualsevol cas, en la utilització dels seus continguts caldrà indicar de forma clara el nom i cognoms de la persona autora i el títol de la tesi doctoral. No s'autoritza la seva reproducció o altres formes d'explotació efectuades amb finalitats de lucre ni la seva comunicació pública des d'un lloc aliè al servei TDX. Tampoc s'autoritza la presentació del seu contingut en una finestra o marc aliè a TDX (framing). Aquesta reserva de drets afecta tant als continguts de la tesi com als seus resums i índexs.

ADVERTENCIA. El acceso a los contenidos de esta tesis doctoral y su utilización debe respetar los derechos de la persona autora. Puede ser utilizada para consulta o estudio personal, así como en actividades o materiales de investigación y docencia en los términos establecidos en el art. 32 del Texto Refundido de la Ley de Propiedad Intelectual (RDL 1/1996). Para otros usos se requiere la autorización previa y expresa de la persona autora. En cualquier caso, en la utilización de sus contenidos se deberá indicar de forma clara el nombre y apellidos de la persona autora y el título de la tesis doctoral. No se autoriza su reproducción u otras formas de explotación efectuadas con fines lucrativos ni su comunicación pública desde un sitio ajeno al servicio TDR. Tampoco se autoriza la presentación de su contenido en una ventana o marco ajeno a TDR (framing). Esta reserva de derechos afecta tanto al contenido de la tesis como a sus resúmenes e índices.

WARNING. Access to the contents of this doctoral thesis and its use must respect the rights of the author. It can be used for reference or private study, as well as research and learning activities or materials in the terms established by the 32nd article of the Spanish Consolidated Copyright Act (RDL 1/1996). Express and previous authorization of the author is required for any other uses. In any case, when using its content, full name of the author and title of the thesis must be clearly indicated. Reproduction or other forms of for profit use or public communication from outside TDX service is not allowed. Presentation of its content in a window or frame external to TDX (framing) is not authorized either. These rights affect both the content of the thesis and its abstracts and indexes.



UNIVERSITAT
ROVIRA I VIRGILI

DOCTORAL THESIS

NEW STRATEGIES FOR C(sp³)-H FUNCTIONALIZATION

DANIEL BAFALUY ESPAÑOL

DOCTORAL THESIS
2020

UNIVERSITAT ROVIRA I VIRGLI
NEW STRATEGIES FOR C(SP³)-H FUNCTIONALIZATION
Daniel Bafaluy Español

UNIVERSITAT ROVIRA I VIRGLI
NEW STRATEGIES FOR C(SP³)-H FUNCTIONALIZATION
Daniel Bafaluy Español

New Strategies for C(sp³)-H Functionalization

Daniel Bafaluy Español

Doctoral Thesis

Supervised by Prof. Dr. Kilian Muñiz Klein and Prof. Dr. Rubén Martín Romo

Institute of Chemical Research of Catalonia (ICIQ)



Tarragona
2020

UNIVERSITAT ROVIRA I VIRGLI
NEW STRATEGIES FOR C(SP³)-H FUNCTIONALIZATION
Daniel Bafaluy Español



Prof. Dr. Rubén Martín Romo, Group Leader at the Institute of Chemical Research of Catalonia (ICIQ) and Research Professor at the Catalan Institution of Research and Advanced Studies (ICREA):

I confirm that the present thesis manuscript, entitled “New Strategies for C(sp³)-H Functionalization”, presented by Daniel Bafaluy Español to receive the degree of Doctor, has been carried out under the supervision of Prof. Dr. Kilian Muñoz Klein at the Institute of Chemical Research of Catalonia (ICIQ) and that I have cosupervised this Thesis after the sudden loss of Prof. Muñoz.

Tarragona, June 30th, 2020

Doctoral Thesis Supervisors

Prof. Dr. Kilian Muñoz Klein

Prof. Dr. Rubén Martín Romo

In memoriam

UNIVERSITAT ROVIRA I VIRGLI
NEW STRATEGIES FOR C(SP³)-H FUNCTIONALIZATION
Daniel Bafaluy Español

“Yo soy un hombre, y lo soy precisamente porque me equivoco. Nadie llega a una verdad sin haberse equivocado catorce veces, o ciento catorce, y esto es, acaso, un honor para el género humano. Pero no sabemos ser originales ni siquiera para equivocarnos. Un error original acaso valga más que una verdad insignificante.”

Crimen y Castigo, Fiódor Dostoyevski

UNIVERSITAT ROVIRA I VIRGLI
NEW STRATEGIES FOR C(SP³)-H FUNCTIONALIZATION
Daniel Bafaluy Español

Acknowledgements

All the work summarized at the present Thesis is the result of a long journey that started 4 years ago. During these years, I was not alone, and now it is time to say thanks to those that enormously contributed in many different ways.

Obviously, the first person to which I am immensely grateful is my PhD supervisor Prof. Kilian Muñiz. His unexpected and dramatic loss irrupted at our lives in a terrible manner. Almost at the end of my PhD studies, I never thought that I would have to write these lines with this bitter-sweet feeling. Kilian was one of the smartest persons that I ever met. His knowledge and passion for chemistry was a model that he always tried to transmit to the members of his group. He was the source of all what I learned, and I feel lucky that I had been able to absorb a tiny part of his knowledge these last 5 years, when I first joined the group as a master student. I will miss those Monday morning seminars where he asked about which famous professor (quite often of German nationality) developed a certain reaction, or who was the PhD advisor of some of the big scientific names we were talking about. Apart of the scientific aspect, he was always in close contact with all the members or the group, including myself. Quite often he entered the lab just to talk about whatever (including chemistry) with us. In general, he was a person of strong opinions which was never afraid to openly express what he thought. I cannot help but draw a melancholic smile while writing these words when I remember those afternoons when Kilian walked into the lab just to chat about how terrible the political situation is. Or about how Cristiano Ronaldo is way better than Messi. Or how Lufthansa is the best airline to use. Or many other topics that he loved like Asturias, Japan, literature or art.

From a personal perspective, I always felt very supported and valued by Kilian as his student. Some of the best experiences that I had during these years, like the congress in Japan and many other congresses and symposiums outside and inside Spain that I assisted were thanks to him. I am particularly grateful to the first congress that I assisted, the biennial meeting of organic chemistry in Punta Umbría, when I was only a young and inexperienced master student. Obviously, Kilian also played a crucial role in the development and accomplishment of the results discussed in this Thesis. He taught me how to be honest and critical, even with my own work, and how to be an effective and independent researcher. I am sure that he would have been proud of all the accomplished work.

Subsequently, after Kilian's loss, there were some people who did their best in order to help the group and myself during those terrible days. First I am grateful to Prof. Miquel Pericàs and Dr. Lluís Solà, who took care of all the group and respected our requests. In the same manner, I am extremely grateful to Prof. Rubén Martín, who kindly accepted the responsibility of taking care of my thesis these last months. I am thankful to Rubén for the help and guidance through the publishing process of the last project and for the supervision and correction of the thesis. It was really a lot of work that you accepted selflessly Rubén, thanks for all.

Regarding my labmates, who highly contributed to this Thesis, I should start in chronological order. First, I am obliged to say thanks to those that helped me at my first times in the group. I particularly refer to Dr. Claudio Martínez, Laura Fra and Martín Romero. In this sense, Claudio had to suffer an abusive number of questions (most of them quite silly) from my side. In his role of Group Coordinator, he was the security net for the younger researches. The same applies to Laura and Martín, who also suffered my constant requests, but taught me how to effectively work in a lab. Particularly, I had the chance to work side-by-side with Laura, from who I learned a lot. In addition, we usually shared our daily-basis adventures.

Also during my first year I had the opportunity to work with many other amazing people such as Calvin, my Irish friend. I had the opportunity to learn some nice Chinese expressions thanks to Dr. Hongwei Zhang (*aka* Johnny or Chino loco), with who I worked in close contact for a time. Additional labmates with which I initially worked on my first year were Dr. Matilde Aguilar, Belén, Ricardo, Laura Barreiro, Nicola, Anda, Dr. Terry Tomakinian and Dr. Peter Becker. In particular, I had the chance to share with Anda an amazing travel to Japan. I will also miss (maybe only sometimes) her intense talkative character. At some point I moved to laboratory 2.4, to share my current desk with Laura Barreiro. There were really tough times which we shared. At some point more people joined the group, like Estefi, Thomas, Francesca or Anastasia, shaping it to the friendly and dynamic place that it is now. Thanks to Estefi, who definitely contributed to my nice experience in the group with her nice character and conversation (sometimes maybe too focused on calories-counting). Thomas was an amazing labmate, with who I enjoyed not only the casual chatting but also the scientific discussions. He contributed to my work as a source of good ideas and solutions. I also shared my time with some awesome catalan labmates, Andrea and Èric. With Èric, I shared his marvelous music taste and the amazing experience of attending some crazy metal music festivals. I hope that next summer we can repeat the experience.

I also had the opportunity to share time inside and outside the lab with some exemplary postdocs of the group. I am talking about Dr. Mario Martínez, Dr. Julien Bergès and Dr. Sebastian Herold. From Mario I will miss those funny moments at the lab and his

amazing cooking skills. By far the best beach-cooker that I met. Concerning Julien, I truly enjoyed spend time with him, his endless energy was really contagious. Furthermore, those discussions about the *Spanish cuisine* (which, of course, is not even comparable with the French 'gourmet' gastronomy) were a constant source of fun. Finally, Sebastian (*aka* Dr. Herold) demonstrated to be an awesome coworker. I had the opportunity to work in close contact with him, sharing the research projects discussed in Chapters II and III, as well as other (unsuccessful) scientific challenges. In this sense, he was really the electrochemical expert, and tough me all the possibilities that this field can offer to a pure synthetic chemist. Apart of the scientific expertise, he really instructed me on how to take the things 'tranquilito', because constant rushing is not good sometimes. I will miss those moments when someone randomly told me: "Bafa, Dr. Herold wants to meet you at his office." I truly enjoyed these discussions on how, as chemist, we are not only scientist but artist as well. Eventually, new people joined the group configuring it in its actual shape. Eleni, Dr. Kang Chen, Aliénor, Jiayu and Jixiang. With Eleni and Ali I had the chance to share the lab 2.4 and to enjoy some nice after-work moments. The happiness of Ali is truly contagious, and it was really funny to annoy Eleni early in the mornings. Finally, I want to acknowledge all the people that temporarily joined the group such as Eric, Jorge, Cristian, Matthew or Zoritsa.

I have the honor consider as friends to most of the aforementioned colleges with which I shared unforgettable experiences.

Last, but not least, I feel very grateful for the received administrative support from Noemi Panadès at the beginning and from Sorania Jiménez through last years. Special thanks to Sorania, which took care of all of us, including myself, these last terrible months. I feel very grateful to the external colleagues that worked with me in the project described in Chapter III. Many thanks to Prof. Feliu Maseras and Prof. Pedro Pérez, as well as to their group members Adiran and Funes (ICIQ), and Dr. José María Muñoz-Molina and Prof. Tomás Balderrain (UHU). Additional special thanks to Estefi, Sebastian and Mario for the corrections on the Thesis manuscript. Special thanks also to the ICIQ facilities such as NMR, X-ray, HTE, ChromTAE, Material Characterization, MS and many others like Glass blowing, Mechanical workshop or IT. Additional special thanks also for the logistic guys!

However, the interactions within ICIQ people did not stop here. I am grateful to the awesome community. In particular, I want to thank Marcos, Joan, Ana and Èric, for this amazing musical project that we started some months ago. It is a pity that COVID ruined our opportunity to debut as a group. However, I truly enjoyed playing with all of them and to recall the forgotten drummer that is inside me. I will really miss the practice sessions.

Ahora toca hacer un cambio de registro para agradecer a aquellos que, estando fuera del ambiente profesional, han contribuido enormemente a lo que soy a día de hoy. En primer lugar, tengo que agradecer a mi núcleo familiar más cercano. A mi madre Reyes, mi padre José Luis y mi hermano Álvaro. No sabría por dónde empezar a agradecer a mis padres, ya que son quienes me lo han dado todo. Ellos me han enseñado a ser una persona responsable, tolerante y trabajadora. Que, si algo te gusta, tienes que esforzarte, y al final siempre acabas por conseguirlo. Su incondicional apoyo y cariño han hecho de mí la persona que soy hoy. Espero que estén tan orgullosos de mí como yo lo estoy de ellos. Tengo que extender todo este agradecimiento al apoyo incondicional que también he recibido por parte del resto de mi familia, en especial a mis tíos y mis primos. Es un privilegio pertenecer a una familia tan unida como es el clan Español, especialmente apuntalado sobre mi madre y mis tías. En el momento de nostalgia y emotividad desenfundado que supone para mí escribir estas líneas no puedo menos que acordarme de mis abuelos Luis y Felisa, que desafortunadamente no pueden estar aquí para ver en lo que me he convertido. También debo agradecer a quienes prácticamente considero como mi familia, aún sin serlo. Hablo de Andrés, Alvarito, Miguel, Sancho y Rivera, en gran medida gracias a los cuales me siento tan unido a Monzón. Me han acompañado desde que tengo recuerdo y espero que lo sigan haciendo. También agradezco a mis amigos de Zaragoza César, Campillo, Dani, Víctor, Cristina, Raquel, Miriam y Laura, cuyas recurrentes visitas a Tarragona en el puente de diciembre, en las que mi piso se convertía en una comuna hippie, han hecho que cada año espere dichas fechas con especial ilusión.

Por último, he reservado para el final el agradecimiento a una de las personas más importantes en mi vida. Judith, los años que he compartido a tu lado han sido maravillosos, como espero que lo sean los que están por venir. Por tu cariño, comprensión y apoyo continuo te estoy eternamente agradecido. Sé que he contado contigo en todas las decisiones que he tomado y en las que tomaré en el futuro. Has contribuido a hacerme enormemente feliz durante este tiempo, y espero poder devolvarte aunque sólo sea una pequeña parte de todo lo que me has dado. Lo que en esta Tesis se incluye también te pertenece. Muchas gracias.

List of publications resulting from this Thesis

Anodic benzylic C(sp³)-H amination: unified access to pyrrolidines and piperidines. S. Herold, D. Bafaluy, K. Muñiz, *Green Chem.* **2018**, *20*, 3191-3196.

Copper-Catalyzed N-F Bond Activation for Uniform Intramolecular C-H Amination Yielding Pyrrolidines and Piperidines. D. Bafaluy, J. M. Muñoz-Molina, I. Funes-Ardoiz, S. Herold, A. J. de Aguirre, H. Zhang, F. Maseras, T. R. Belderrain, P. J. Pérez, K. Muñiz, *Angew. Chem. Int. Ed.* **2019**, *58*, 8912-8916.

Iodine Catalysis for C(sp³)-H Fluorination with a Nucleophilic Fluorine Source.* D. Bafaluy, Z. Georgieva, K. Muñiz, *Angew. Chem. Int. Ed.* **2020**, *59*, 14241-14245.

* Highlighted at the front cover of *Angewandte Chemie International Edition*. Highlighted as 'hot paper'.

UNIVERSITAT ROVIRA I VIRGLI
NEW STRATEGIES FOR C(SP³)-H FUNCTIONALIZATION
Daniel Bafaluy Español

Abbreviation list

Ac	Acetyl
Ar	Aryl
bc.....	Bathocuproine
BDE	Bond Dissociation Energy
BHT	2,6-Di- <i>tert</i> -butyl-4-methylphenol
Bn	Benzyl
Boc.....	Tert-butyloxy carbonyl
bpy	2,2'-Bipyridine
Bz.....	Benzoyl
Cbz.....	Benzyloxycarbonyl
CFL.....	Compact Fluorescent Lamp
DBDMH.....	1,3-dibromo-5,5-dimethylhydantoin
DCDMH.....	1,3-dichloro-5,5-dimethylhydantoin
DCE	1,2-Dichloroethanol
DFT	Density Functional Theory
DIDMH.....	1,3-diiodo-5,5-dimethylhydantoin
DMAc.....	N,N-Dimethylacetamide
DMF.....	N,N-Dimethylformamide
DMSO	Dimethylsulfoxide
DNA	Deoxyribonucleic acid
dr	Diastereomeric ratio
dtbbpy	4,4'-Bis- <i>tert</i> -butyl-2,2'-bipyridine
ee	Enantiomeric excess
EPR	Electron Paramagnetic Resonance
esp.....	$\alpha,\alpha,\alpha',\alpha'$ -tetramethyl-1,3-benzenedipropionic acid
HAA	Hydrogen Atom Abstraction
HAT.....	Hydrogen Atom Transfer
HFIP	1,1,1,3,3,3-Hexafluoroisopropanol
HPLC	High Performance Liquid Chromatography
HRMS.....	High Resolution Mass Spectrometry
IPr	1,3-Bis(2,6-diisopropylphenyl)-1,3-dihydro-2H-imidazol-2-ylidene
IR	Infrared
LED	Light-Emitting Diode
<i>m</i> CBA.....	<i>m</i> -Chlorobenzoic acid
<i>m</i> CPBA.....	<i>m</i> -Chloroperbenzoic acid
MECP.....	Minimum Energy Crossing Points
Mes.....	2,4,6-Trimethylbenzyl / Mesytl
<i>m,m</i> OMeBA.....	<i>m,m</i> -Bismethoxybenzoic acid
MOM.....	Methoxymethyl

mOMeBA.....	<i>m</i> -Methoxybenzoic acid
mp	Melting point
Ms	Methanesulfonyl
MS	Molecular Sieves
NBS.....	N-Bromosuccinimide
NCS.....	N-Chlorosuccinimide
NDHPI.....	N,N-dihydroxypyromellitimide
NFPY.....	N-Fluoropyridinium tetrafluoroborate
NFSI	N-Fluorobenzenesulfonimide
NHPI	N-Hydroxyphthalimide
NIS	N-Iodosuccinimide
NMR	Nuclear Magnetic Resonance
Ns	4-Nitrobenzenesulfonyl
oFBA	<i>o</i> -Fluorobenzoic acid
pBBA.....	<i>p</i> -Bromobenzoic acid
PET.....	Positron Emission Tomography
phen	1,10-Phenanthroline
Phth.....	Phthalimide
Phs.....	Phenylsulfonyl
PMB.....	<i>p</i> -Methoxybenzene
pMeBA.....	<i>p</i> -Methylbenzoic acid
pOMeBA.....	<i>p</i> -Methoxybenzoic acid
ppy	Pyridinylphenyl
RVC.....	Reticulated Vitreous Carbon
SES.....	2-(Trimethylsilyl)ethanesulfonyl
TBS.....	Tert-butyldimethylsilyl
Tces	2,2,2-Trichloroethoxy-1-sulfonyl
TDG.....	Transient Directing Group
TEMPO	2,2,6,6-Tetramethyl-1-piperidinyloxy
Tf	Trifluoromethanesulfonyl
TFA	Trifluoroacetic acid
Tol	Toluene
Tp	Hydrotrispyrazolylborate
TPMA.....	Tris(2-pyridylmethyl)amine
TPT.....	Triphenylpyrylium tetrafluoroborate
Troc	2,2,2-Trichloroethoxycarbonyl
Ts.....	4-Methylbenzenesulfonyl
TS.....	Transition State
UV.....	Ultraviolet

Table of Contents

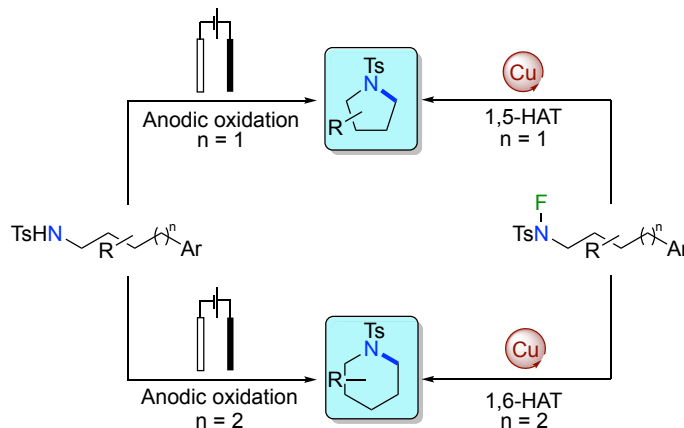
Summary of the Thesis	1
Chapter I. Introduction on C(sp³)-H Functionalization	3
1.1. C(sp ³)-H functionalization	5
1.2. Importance of C(sp ³)-N bonds in bioactive molecules	6
1.3. C(sp ³)-H amination	7
1.3.1. Transition metal-promoted C(sp ³)-H amination	7
1.3.1.1. Amination via C(sp ³)-H metallation	7
1.3.1.2. Nitrene insertion	10
1.3.1.3. Radical-mediated C(sp ³)-H amination	16
1.3.2. Metal free C(sp ³)-H amination	18
1.4. Importance of C(sp ³)-F bonds in bioactive molecules	28
1.5. C(sp ³)-H fluorination	29
1.5.1. Transition metal-mediated C(sp ³)-H fluorination	29
1.5.1.1. Fluorination via C(sp ³)-H metallation	29
1.5.1.2. Radical-mediated C(sp ³)-H fluorination	31
1.5.2. Metal free C(sp ³)-H fluorination	36
1.6. Global objectives	40
Chapter II. Anodic Benzylic C(sp³)-H Amination: A Unified Access to Pyrrolidines and Piperidines	41
2.1. Introduction: Electrochemical amination	43
2.2. Results and discussion	49
2.3. Conclusions	62
2.4. Experimental section	62
Chapter III. Copper-Catalyzed N-F Bond Activation for Uniform Intramolecular C-H Amination Yielding Pyrrolidines and Piperidines	91
3.1. Introduction: N-fluorosulfonamide activation	93
3.2. Results and discussion	100
3.3. Conclusions	114
3.4. Experimental section	115
Chapter IV. Iodine Catalysis for C(sp³)-H Fluorination with a Nucleophilic Fluorine Source	147
4.1. Introduction: Interrupted Hofmann-Löffler reaction	149
4.2. Results and discussion	154
4.3. Conclusions	164
4.4. Experimental section	164
Overall conclusions	185

UNIVERSITAT ROVIRA I VIRGLI
NEW STRATEGIES FOR C(SP³)-H FUNCTIONALIZATION
Daniel Bafaluy Español

Summary of the Thesis

Aliphatic C-H functionalization has been established as an alternative new method to build up sp^3 hybridized carbons. Particularly, C(sp^3)-H methods for formation of carbon-heteroatom bonds are in high demand since such approach allows for direct preparation of complex molecules bearing interesting functionalities from rather simple starting materials. The general aim of this doctoral thesis involves the development of novel directed sp^3 C-H functionalization techniques for C-N and C-F bond formation based on the Hofmann-Löffler reaction scaffold.

In this PhD thesis, we have designed a new electrochemical pyrrolidine formation protocol involving aliphatic sp^3 C-H functionalization. This approach is particularly attractive if one takes into consideration that electrochemical amination techniques predominantly rely on the functionalization of sp^2 and sp C-H bonds. Our technology represents an environmentally benign method for enabling an anodic sp^3 C-H oxidation en route to pyrrolidines, piperidines and oxygen-containing heterocycles (Scheme I, left).

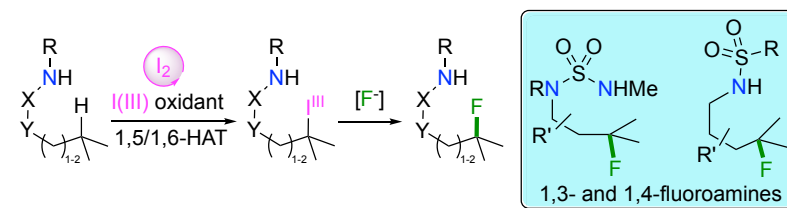


Scheme I: Uniform access to pyrrolidine and piperidine formation via anodic oxidation (left) or copper-catalyzed N-F bond activation (right).

Aiming at extending the range of protocols for preparing saturated nitrogen-containing heterocycles, we have developed a Cu-catalyzed technique that makes use of N-F bonds as vehicles for enabling intramolecular sp^3 C-H amination (Scheme I, right). Interestingly, this protocol overrides the inherent proclivity for 1,5-HAT processes, allowing to access piperidine scaffolds via 1,6-HAT instead. Kinetic experiments, isotope effects, EPR studies, control experiments with stoichiometric complexes, mass spectrometric measurements and DFT calculations were performed to unravel the mechanistic intricacies of this reaction.

Summary of the Thesis

Finally, we developed a novel approach for directed sp^3 C-H fluorination employing nucleophilic fluoride as fluorine source. Even though various methods for aliphatic C-H fluorination are known, most of them rely on the generation of electron-rich carbon-centered radicals that require the employment of electrophilic NFSI or Selectfluor to form the targeted sp^3 C-F bond. To overcome this limitation, we designed an iodine catalyzed method that enables a Hofmann-Löffler-type reaction via the intermediacy of hypervalent alkyl-iodine(III) species that can be intercepted with nucleophilic fluoride, thus holding promise for the implementation of PET-imaging techniques with ^{18}F sources (Scheme II). In addition, we identified two nitrogen-containing directing groups that could efficiently promote the fluorination reaction in a site-selective manner, either triggering a 1.5- or 1,6-HAT for the preparation of densely functionalized pyrrolidine or piperidine scaffolds.



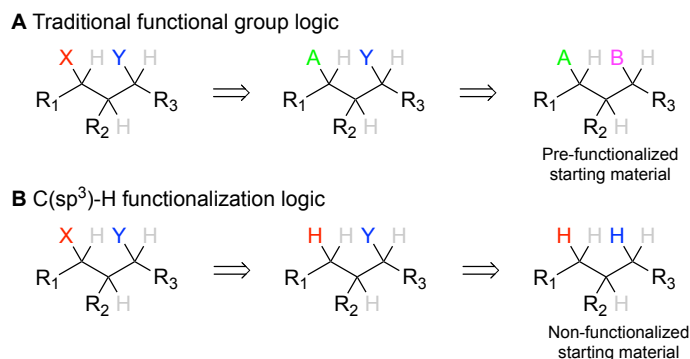
Scheme II: Iodine-catalyzed directed C-H fluorination.

Chapter I. Introduction on C(sp³)-H Functionalization

Chapter I. Introduction on C(sp³)-H Functionalization

1.1. C(sp³)-H functionalization

Through last decades, C(sp³)-H functionalization has emerged as an entire field in synthetic organic chemistry. The conceptually new approach underlying the development of this field implies that synthetic chemist can now access new disconnections that no longer rely on pre-installed functional group interconversions (Scheme 1.1).¹ In this manner, C-H bonds can now be identified as synthons for C-heteroatom and C-C bond formation.



Scheme 1.1: Functional group interconversion logic vs. C(sp³)-H functionalization logic.

A particularly attractive endeavor in C(sp³)-H activation is the ability to convert petrochemical commodity feedstocks such as alkanes into added-value compounds.² However, site-selectivity issues might come into play as saturated hydrocarbons possess multiple number of similarly reactive C-H linkages.³ A close look into the literature, however, reveals that new technologies have been implemented to forge C-C, C-O, C-N, C-S or C-halogen bond formation via C-H functionalization. These transformations can be achieved by means of transition-metal catalysis⁴ (C(sp³)-H metalation and carbene/nitrene insertions), radical processes⁵ (mainly via Hydrogen Atom Transfer) or enzymatic functionalization.⁶ The prospective potential of these methods have been tested in a broad spectrum of total synthesis of natural products, such as Aspidophytine, Rhazinicine or N-methylwelwitindolinone C isothiocyanate,

¹ a) H. M. L. Davies, J. Du Bois, J.-Q. Yu, *Chem. Soc. Rev.* **2011**, *40*, 1855-1856. b) J. F. Hartwig, M. A. Larsen, *ACS Cent. Sci.* **2016**, *2*, 281-292.

² R. G. Bergman, *Science* **2007**, *446*, 391-393.

³ R. Giri, B.-F. Shi, K. M. Engle, N. Maugel, J.-Q. Yu, *Chem. Soc. Rev.* **2009**, *38*, 3242-3272.

⁴ P. Gandeepan, T. Müller, D. Zell, G. Cera, S. Warratz, L. Ackermann, *Chem. Rev.* **2019**, *119*, 2192-2452.

⁵ J. C. K. Chu, T. Rovis, *Angew. Chem. Int. Ed.* **2018**, *57*, 62-101.

⁶ J. C. Lewis, P. S. Coelho, F. H. Arnold, *Chem. Soc. Rev.* **2011**, *40*, 2003-2021.

Chapter I. Introduction on C(sp³)-H Functionalization

where sp³ C-H functionalization was the critical step on the sequence.⁷ Not surprisingly, C-H functionalization has been rapidly embraced by medicinal chemists in late-stage functionalization approaches for the discovery of target leads in drug discovery.⁸

1.2. Importance of C(sp³)-N bonds in bioactive molecules

Nitrogen-containing molecules are ubiquitous compounds of mayor importance for living organisms.⁹ The basicity of the nitrogen lone pair and the ability to enable hydrogen bonding (both as donor and acceptor) are particularly important. For example, selective recognition through hydrogen bonding allows the formation and replication of DNA's double helix, and are responsible for macromolecular folding of proteins and peptides. Therefore, it comes as no surprise that nitrogen-containing molecules rank amongst the most prevalent motifs in marketed drugs for pharmaceutical applications. Indeed, approximately 84% of commercial drugs contain at least one nitrogen atom, with an average ratio of nitrogen atoms per drug of 2.3.¹⁰

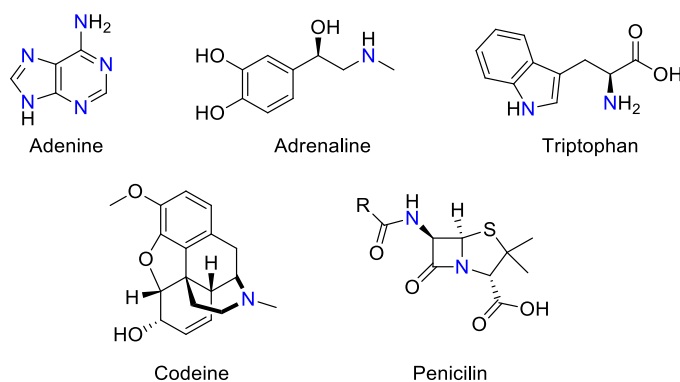


Figure 1.1: Selected nitrogen-containing bioactive molecules.

Given that the C-H oxidation machinery of living organisms is limited to the formation of C-O bonds, the formation of nitrogen-containing molecules in nature is typically obtained via cascade reactions or reductive amination techniques by promoting a condensation reactions of pre-existing carbonyl compounds with amines in the presence of a suitable reductant. Prompted by the inherent limitation of nature to

⁷ a) W. R. Gutekunst, P. S. Baran, *Chem. Soc. Rev.* **2011**, *40*, 1976-1991. b) Y. Qiu, S. Gao, *Nat. Prod. Rep.* **2016**, *33*, 562-581. c) R. R. Karimov, J. F. Hartwig, *Angew. Chem. Int. Ed.* **2018**, *57*, 4234-4241.

⁸ T. Cernak, K. D. Dykstra, S. Tyagarajan, P. Vachal, S. W. Krska, *Chem. Soc. Rev.* **2016**, *45*, 546-576.

⁹ A. Ricci (Ed.), *Amino Group Chemistry: From Synthesis to the Life Sciences*; Wiley-VCH, Weinheim, Germany, **2007**.

¹⁰ E. Vitaku, D. T. Smith, J. T. Mjardarson, *J. Med. Chem.* **2014**, *57*, 10257-10274.

introduce nitrogen linkages, chemists have recently developed artificial amination technologies that allow to promote the targeted C-N bond-formation via direct C-H functionalization.¹¹

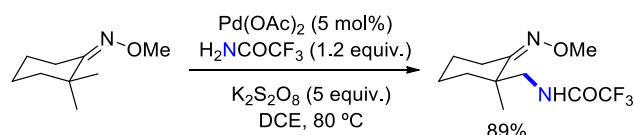
1.3. C(sp³)-H amination

1.3.1. Transition metal-promoted C(sp³)-H amination

From a synthetic point of view, the current available methodologies for sp³ C-H amination can be divided into three different categories: (1) Amination via C(sp³)-H metallation, (2) nitrene insertion and (3) radical-based amination.

1.3.1.1. Amination via C(sp³)-H metallation

In this strategy, a transition metal inserts into a C-H bond by forming a discrete organometallic intermediate prior to reaction with an appropriate nitrogen source, thus setting the basis for a reductive elimination of nucleophilic insertion event. Due to the inherent low reactivity of C(sp³)-H bonds compared with its C(sp²)-H counterparts (higher bond-dissociation energy and lack of empty low-energy orbitals for interaction with the transition metal), a chelating directing group is often employed in these reactions. In 2006, the pioneering work of Che demonstrated the ability of palladium complexes to enable an intermolecular C(sp³)-H amination.¹² The reaction employed O-methyloximes as directing groups and it was postulated to work through the formation of a high oxidation state Pd^{IV} metallacycle intermediates (Scheme 1.2).



Scheme 1.2: Palladium catalyzed aliphatic amination of oximes.

Prompted by these precedents, chemists discovered new pathways for triggering sp³ C-H amination based on metals other than palladium, culminating in a series of procedures catalyzed by Rh, Ir or Co, among others.¹³ For instance, You reported a rhodium catalyzed procedure which employs pyridine as directing group,¹⁴ thus allowing to trigger an amination event at homobenzylic positions with an exquisite control of the site-selectivity profile (Scheme 1.3).

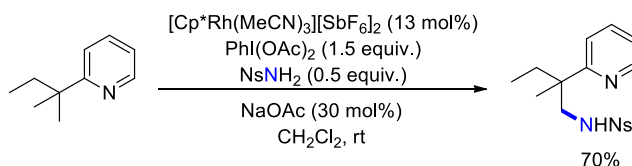
¹¹ R. Hili, A. K. Yudin, *Nature Chem. Biol.* **2006**, *2*, 283.

¹² H.-Y. Thu, W.-Y. Yu, C.-M. Che, *J. Am. Chem. Soc.* **2006**, *128*, 9048-9049.

¹³ Y. Park, Y. Kim, S. Chang, *Chem. Rev.* **2017**, *117*, 9247-9301.

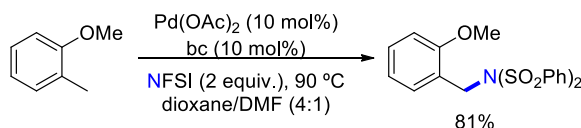
¹⁴ X. Huang, Y. Wang, J. Lan, J. You, *Angew. Chem. Int. Ed.* **2015**, *54*, 9404-9408.

Chapter I. Introduction on C(sp³)-H Functionalization



Scheme 1.3: Pyridine-directed C-H amination

As judged by the wealth of literature data, a wide range of nitrogen sources can be introduced in C-H amination protocols, including the utilization of organic azides,¹⁵ dioxazolones,¹⁶ anthranils¹⁷, N-acyloxyamides¹⁸ or even fluorosulphonamides.¹⁹ The latter case is particularly relevant, as Pd catalysts have shown the ability to promote C-H amination technologies by using N-fluorobenzenesulfonimide (NFSI) as both nitrogen source and oxidant (Scheme 1.4).



Scheme 1.4: Palladium-catalyzed amination employing NFSI as nitrogen source.

In 2009, Glorius reported a Pd-catalyzed indoline synthesis from 2-alkylphenylacetamides.²⁰ The authors discussed two potential pathways by which this reaction might operate. While the first one involves direct reductive elimination from a metallated Pd^{II} intermediate, an alternative pathway consisting of the intermediacy of Pd^{IV} intermediates could also be considered in the presence of strongly oxidizing conditions.

¹⁵ a) T. Kang, Y. Kim, D. Lee, Z. Wang, S. Chang, *J. Am. Chem. Soc.* **2014**, *136*, 4141-4144. b) N. Wang, R. Li, L. Li, S. Xu, H. Song, B. Wang, *J. Org. Chem.* **2014**, *79*, 5379-5385. c) B. Liu, B. Li, B. Wang, *Chem. Commun.* **2015**, *51*, 16334-16337. d) T. Kang, H. Kim, J. G. Kim, S. Chang, *Chem. Commun.* **2014**, *50*, 12073-12075

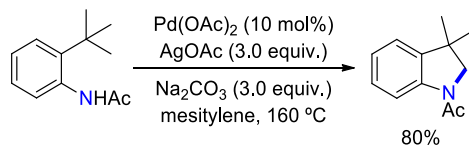
¹⁶ a) H. Wang, G. Tang, X. Li, *Angew. Chem. Int. Ed.* **2015**, *54*, 13049-13052. b) N. Barsu, M. A. Rahman, M. Sen, B. Sundararaju, *Chem. Eur. J.* **2016**, *22*, 9135-9138.

¹⁷ a) S. Yu, G. Tang, Y. Li, X. Zhou, Y. Lan, X. Li, *Angew. Chem. Int. Ed.* **2016**, *55*, 8696-8700. b) C. Tang, M. Zou, J. Liu, X. Wen, X. Sun, Y. Zhang, N. Jiao, *Chem. Eur. J.* **2016**, *22*, 11165-11169.

¹⁸ J. He, T. Shigenari, J.-Q. Yu, *Angew. Chem. Int. Ed.* **2015**, *54*, 6545-6549.

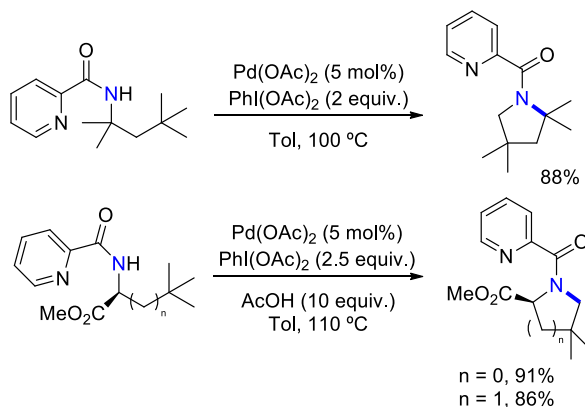
¹⁹ A. Iglesias, R. Alvarez, A. R. de Lera, K. Muñiz, K. *Angew. Chem. Int. Ed.* **2012**, *51*, 2225-2228.

²⁰ J. J. Neumann, S. Rakshit, T. Dröge, F. Glorius, *Angew. Chem. Int. Ed.* **2009**, *48*, 6892-6895.



Scheme 1.5: Glorius' indoline synthesis through intramolecular amination.

Different pyridine-based chelating groups such as picolinamide or 2-(Pyridin-2-yl)isopropyl amine²¹ were explored in the context of Pd-catalyzed C-H amination. Daugulis²² and Chen²³ independently developed similar picolinamide-directed palladium catalyzed procedures for accessing pyrrolidine backbones (Scheme 1.6). Furthermore, Chen's procedure was extended to the synthesis of four-membered ring azetidines (Scheme 1.6, bottom). Both authors proposed the formation of a high oxidation state Pd^{IV} intermediates via oxidation of Pd^{II} cyclometallated intermediate by reaction with an appropriate hypervalent iodine(III) reagent.



Scheme 1.6: Top: Daugulis' picolinamide-directed pyrrolidine synthesis. Bottom: Chen's picolinamide-directed pyrrolidine and azetidine synthesis.

Despite the popularity of palladium-based C-H amination protocols, various first-row transition metals such as Cu,²⁴ Ni²⁵ or Co²⁶ were also successfully applied to intramolecular C(sp³)-H amination technologies by utilizing quinoline-base directing group.

²¹ Q. Zhang, K. Chen, W. Rao, Y. Zhang, F. J. Chen, B.-F. Shi, *Angew. Chem. Int. Ed.* **2013**, *52*, 13588-13592.

²² E. T. Nades, O. Daugulis, *J. Am. Chem. Soc.* **2012**, *134*, 7-10.

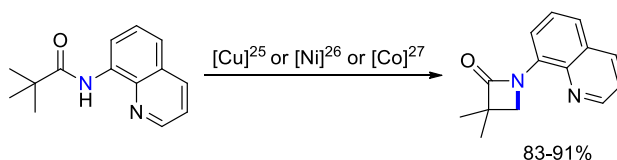
²³ G. He, Y. Zhao, S. Zhang, C. Lu, G. Chen, *J. Am. Chem. Soc.* **2012**, *134*, 3-6.

²⁴ a) Z. Wang, J. Ni, Y. Kuninobu, M. Kanai, *Angew. Chem. Int. Ed.* **2014**, *53*, 3496-3499. b) X. Wu, Y. Zhao, G. Zhang, H. Ge, *Angew. Chem. Int. Ed.* **2014**, *53*, 3706-3710.

²⁵ X. Wu, Y. Zhao, H. Ge, *Chem. Eur. J.* **2014**, *20*, 9530-9533.

²⁶ X. Wu, K. Yang, Y. Zhao, H. Sun, G. Li, H. Ge, *Nat. Commun.* **2015**, *6*, 6462.

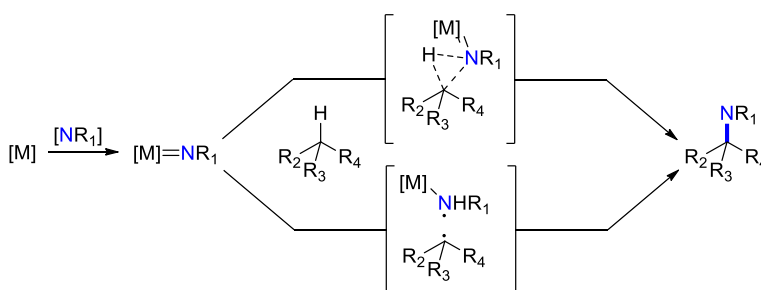
Chapter I. Introduction on C(sp³)-H Functionalization



Scheme 1.7: Copper, nickel and cobalt catalyzed β -lactam synthesis.

1.3.1.2. Nitrene insertion

Catalytic nitrene insertion was first studied by Breslow for the amination of cyclohexane in an attempt to mimic cytochrome P-450 system.²⁷ By identifying iminoiodanes as suitable nitrene precursors, Mansui studied the preparation of aziridines starting from the corresponding alkenes through nitrene insertion.²⁸ This strategy still represents an important approach for the preparation of aziridines.²⁹ The mechanism for C(sp³)-H nitrene insertion has been widely discussed through last decades. The reaction starts with the formation of a metallated nitrenoid (also called nitrene complex) from the reaction of the metal catalyst and a suitable nitrene precursor such as an organic azide or an iminoiodane. In the most widely accepted mechanism, a concerted direct insertion of the metallated nitrene species into the C-H bond takes place (Scheme 1.8, top). However, an alternative mechanism has been postulated in which the nitrene complex reacts in a stepwise hydrogen atom abstraction (HAA) reaction, after which radical recombination affords the final aminated product (Scheme 1.8, bottom). The later scenario has been supported by extensive mechanistic investigations and computational studies for some systems.³⁰



²⁷ R. Breslow, S. H. Gellman, *J. Chem. Soc., Chem. Commun.* **1982**, 1400.

²⁸ D. Mansui, J.-P. Mahy, A. Dureault, G. Bedi, P. Battioni, *J. Chem. Soc., Chem. Commun.* **1984**, 1161.

²⁹ P. Müller, C. Fruit, *Chem. Rev.* **2003**, *103*, 2905-2919.

³⁰ a) M. J. B. Aguila, Y. M. Badiei, T. H. Warren, *J. Am. Chem. Soc.* **2013**, *135*, 9399-9406. b) H. Xu, X. Zhang, Z. Ke, C. Zhao, *RSC Adv.* **2016**, *6*, 29045-29053.

Scheme 1.8: Mechanistic pathways in nitrene insertions. Concerted pathway (top) and stepwise HAA pathway (bottom).

Recently, notorious advances has been achieved by employing porphyrin-based complexes. Particularly, Che, White and Zhang have explored the use of these complexes with abundant first-row transition metals like manganese,³¹ iron³² or cobalt³³ in catalytic intra- and intermolecular amination reactions (Figure 1.2). Additionally, it is possible to directly employ preactivated nitrene precursors such as sulphonyl azides and iminoiodanes as nitrogen sources, or to form them in situ by oxidation of amides or sulphonamides with hypervalent iodine (III) reagents. In addition to first row transition metals, Ruthenium-based porphyrins have also been successfully employed as catalysts in nitrene insertion reactions.³⁴

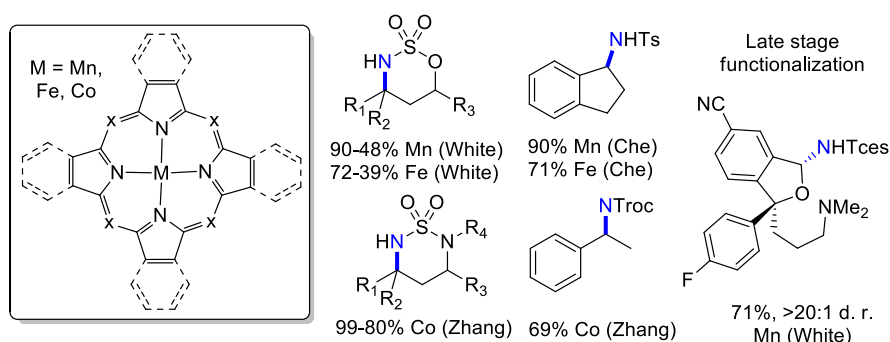


Figure 1.2: Recent advances on first row transition metal porphyrin-based catalytic systems for aliphatic C-H nitrene insertions.

Moving away from heme's inspired porphyrin ligands, different ligand scaffolds were explored for the development of related catalytic scenarios. Indeed, less sophisticated ligand scaffolds have shown to promote equally well nitrene insertions, thus improving the synthetic applicability of these processes in the context of first-row transition metal

³¹ a) X.-Q. Yu, J.-S. Huang, X.-G. Zhou, C.-M. Che, *Org. Lett.* **2000**, *2*, 2233-2236. b) S. M. Paradine, J. R. Griffin, J. Zhao, A. L. Petronico, S. M. Miller, M. C. White, *Nat. Chem.* **2015**, *7*, 987-994. c) J. R. Clark, K. Feng, A. Sookezian, M. C. White, *Nat. Chem.* **2018**, *10*, 583-591.

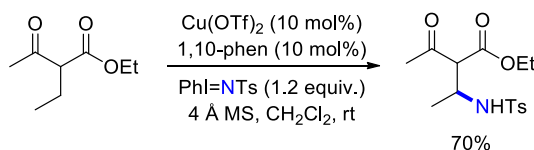
³² a) Y. Liu, C.-M. Che, *Chem. Eur. J.* **2010**, *16*, 10494-10501. b) S. M. Paradine, M. C. White, *J. Am. Chem. Soc.* **2012**, *134*, 2036-2039.

³³ a) H. Lu, H. Jiang, L. Wojtas, X. P. Zhang, *Angew. Chem. Int. Ed.* **2010**, *49*, 10192-10196. b) H. Lu, V. Subbarayan, J. Tao, X. P. Zhang, *Organometallics* **2010**, *29*, 389-393. c) V. Lyaskovskyy, A. I. O. Suarez, H. Lu, H. Jiang, X. P. Zhang, B. de Bruin, *J. Am. Chem. Soc.* **2011**, *133*, 12264-12273. d) H. Lu, C. Li, H. Jiang, C. L. Lizardi, X. P. Zhang, *Angew. Chem. Int. Ed.* **2014**, *53*, 7028-7032.

³⁴ a) S. Fantauzzi, E. Gallo, A. Caselli, F. Ragaini, N. Casati, P. Macchi, S. Cenini, *Chem. Commun.* **2009**, 3952-3954. b) D. Intriери, A. Caselli, F. Ragaini, P. Macchi, N. Casati, E. Gallo, *Eur. J. Inorg. Chem.* **2012**, *2012*, 569-580.

Chapter I. Introduction on C(sp³)-H Functionalization

catalysis.³⁵ For example, Driver reported an indole synthesis via a nitrene insertion-aromatization tandem processes using simple FeBr₂ as active catalyst.³⁶ Additionally, the use of Salen ligands allowed the development of enantioselective variants for manganese catalyzed nitrene insertions.³⁷ Copper was also shown to be a suitable metal for intermolecular nitrene insertions, as demonstrated by the pioneering work of Pérez that employed trispyrazolylborates (Tp) as ligands.³⁸ Some years later, Chan described a copper-catalyzed amination of 2-alkyl substituted β-ketoesters with simple 1,10-phenanthroline as ligand (Scheme 1.9).³⁹ Du Bois reported a system based on a dinuclear ruthenium catalyst which is able to access high levels of regioselectivity for substrates bearing competing positions such as allylic systems.⁴⁰ Furthermore, Blakey and Katsuki reported ruthenium-based catalytic procedures based on the use of Pybox and Salem ligands for intramolecular and intermolecular aminations, respectively.⁴¹



Scheme 1.9: Copper catalyzed nitrene insertion.

Despite the recent popularity of 3d and 4d transition metals in C-H nitrene insertions, this field has largely been dominated by the use of noble rhodium catalysts. The key independent finding from the group of Che and Du Bois enabled the in situ oxidation of amides and related surrogates with commercially available PhI(OAc)₂ and dramatically improved the amide scope as suitable nitrene precursors.^{32a,42} Indeed, dirhodium catalysts bearing two dicarboxylate ligands led to the implementation of highly robust catalytic systems, which do not suffer for oxidative degradation. Bis{rhodium(α,α,α',α'-tetramethyl-1,3-benzenedipropionate)} – known as Rh₂(esp)₂ – was extensively used as

³⁵ a) E. R. King, E. T. Hennessy, T. A. Betley, *J. Am. Chem. Soc.* **2011**, *133*, 4917-4923. b) Y. Liu, X. Guan, E. L.-M. Wong, P. Liu, J.-S. Huang, C.-M. Che, *J. Am. Chem. Soc.* **2013**, *135*, 7194-7204. c) O. Villanueva, N. M. Weldy, S. B. Blakey, C. E. MacBeth, *Chem. Sci.* **2015**, *6*, 6672-6675.

³⁶ Q. Nguyen, T. Nguyen, T. G. Driver, *J. Am. Chem. Soc.* **2013**, *135*, 620-623.

³⁷ a) Y. Kohmura, T. Katsuki, *Tetrahedron Lett.* **2001**, *42*, 3339-3342. b) J. Zhang, P. W. H. Chan, C.-M. Che, *Tetrahedron Lett.* **2005**, *46*, 5403-5408.

³⁸ a) A. Caballero, M. M. Díaz-Requejo, T. R. Belderráin, M. C. Nicasio, S. Trofimenko, P. J. Pérez, *J. Am. Chem. Soc.* **2003**, *125*, 1446-1447. b) M. R. Fructos, S. Trofimenko, M. M. Diaz-Requejo, P. J. Perez, *J. Am. Chem. Soc.* **2006**, *128*, 11784-11791.

³⁹ T. M. U. Ton, C. Tejo, D. L. Y. Tiong, P. W. H. Chan, *J. Am. Chem. Soc.* **2012**, *134*, 7344-7350.

⁴⁰ M. E. Harvey, D. G. Musaev, J. Du Bois, *J. Am. Chem. Soc.* **2011**, *133*, 17207-17216.

⁴¹ a) E. Milczek, N. Boudet, S. Blakey, *Angew. Chem. Int. Ed.* **2008**, *47*, 6825-6828. b) Y. Nishioka, T. Uchida, T. Katsuki, *Angew. Chem. Int. Ed.* **2013**, *52*, 1739-1742.

⁴² C. G. Espino, J. Du Bois, *Angew. Chem. Int. Ed.* **2001**, *40*, 598-600.

catalyst for intramolecular nitrene insertion reactions. This methodology allowed the access to a wide variety of heterocycles with high ring-size selectivity depending on the tether group chosen (Figure 1.3). It was observed that the use of sulphonamides and phosphoramides led to the formation of six membered rings whereas the use of amides led to the corresponding five-membered ring cyclization. In addition, the reaction showed a general selectivity trend, with tertiary alkyl sites being considerable more reactive than the corresponding secondary or primary sites.⁴³

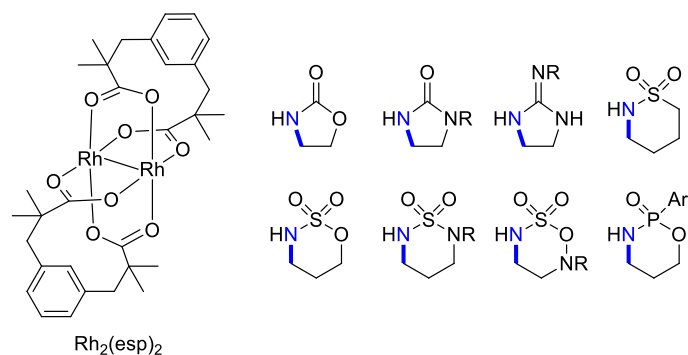


Figure 1.3: $\text{Rh}_2(\text{esp})_2$ and its accessible heterocyclic motifs through intramolecular nitrene insertions.

For instance, Du Bois, Schomaker and Driver employed $\text{Rh}_2(\text{esp})_2$ for diastereoselective intramolecular cyclization of sulfamides, azides and carbamates at either benzylic, homobenzylic or propargylic positions.^{44,45,46}

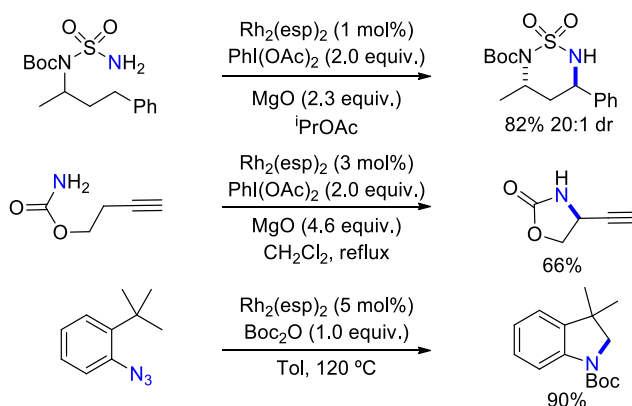
⁴³ a) J. L. Roizen, M. E. Harvey, J. Du Bois, *Acc. Chem. Res.* **2012**, *45*, 911-922. b) J. Du Bois, *Org. Process Res. Dev.* **2011**, *15*, 758-762. c) F. Collet, C. Lescot, C. Liang, P. Dauban, *Dalton Trans.* **2010**, *39*, 10401-10413. d) D. N. Zalatan, J. Du Bois, *Top. Curr. Chem.* **2009**, *292*, 347-378.

⁴⁴ T. Kurokawa, M. Kim, J. Du Bois, *Angew. Chem. Int. Ed.* **2009**, *48*, 2777-2779.

⁴⁵ R. D. Grigg, J. W. Rigoli, S. D. Pearce, J. M. Schomaker, *Org. Lett.* **2012**, *14*, 280-283.

⁴⁶ N. Quyen, K. Sun, T. G. Driver, *J. Am. Chem. Soc.* **2012**, *134*, 7262-7265.

Chapter I. Introduction on C(sp³)-H Functionalization



Scheme 1.10: Selected applications of Rh₂(esp)₂ in C-H amination. Top: diastereoselective synthesis of 1,3-diamines. Center: nitrene insertion at propargylic position. Bottom: indoline synthesis from benzyl-azides.

While the vast majority of C-H nitrene insertions rely on intramolecular approaches, Du Bois and Bach utilized Rh₂(esp)₂ as catalyst for intermolecular settings employing engineered amine sources which enabled orthogonal controlled selectivities.⁴⁷ Furthermore, fine-tuning of the reaction conditions allowed for the smooth amination of rather complex molecules such as natural products and pharmaceuticals.⁴⁸

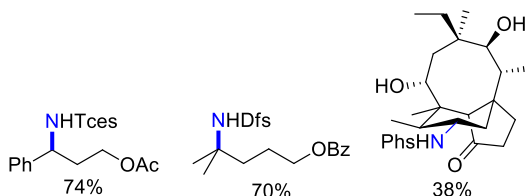


Figure 1.4: Selected examples accessed by rhodium-catalyzed intermolecular nitrene insertion.

More importantly, introduction of chiral ligands in dirhodium catalytic system allowed Davies,⁴⁹ Du Bois⁵⁰ and Bach⁵¹ to access enantioselective procedures for the intramolecular cyclization of carbonates and sulfamates at activated benzylic and allylic

⁴⁷ a) J. L. Roizen, D. N. Zalatan, J. Du Bois, *Angew. Chem. Int. Ed.* **2013**, *52*, 11343-11346. b) A. Nörder, P. Herrmann, E. Herdtweck, T. Bach, *Org. Lett.* **2010**, *12*, 3690-3692. c) K. W. Fiori, J. Du Bois, *J. Am. Chem. Soc.* **2007**, *129*, 562-568. d) E. N. Bess, R. J. DeLuca, D. J. Tindall, M. S. Oderinde, J. L. Roizen, J. Du Bois, M. Sigman, *J. Am. Chem. Soc.* **2014**, *136*, 5783-5789.

⁴⁸ N. D. Chiappini, J. B. C. Mack, J. Du Bois, *Angew. Chem. Int. Ed.* **2018**, *57*, 495-4959.

⁴⁹ R. P. Reddy, H. M. L. Davies, *Org. Lett.* **2006**, *8*, 5013-5016.

⁵⁰ D. N. Zalatan, J. Du Bois, *J. Am. Chem. Soc.* **2008**, *130*, 9220-9221.

⁵¹ T. Hoke, E. Herdtweck, T. Bach, *Chem. Commun.* **2013**, *49*, 8009-8011.

positions respectively. Subsequently, Dauban⁵² and Lebel⁵³ developed diastereoselective amination conditions employing enantiopure chiral sulfonimidamides and carbamates as nitrene precursors to access the corresponding diastereomerically pure products.

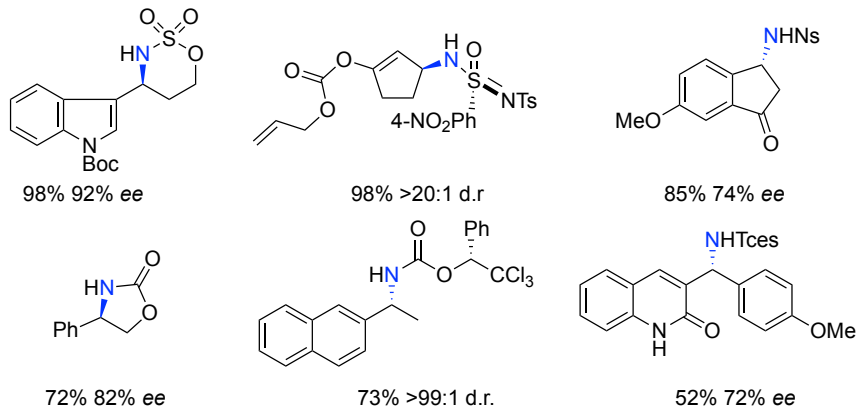


Figure 1.5: Selected examples of non-racemic aminated products accessed through rhodium catalyzed enantioselective and diastereoselective nitrene insertion.

Recently, Schomaker reported an interesting Ag-catalyzed system in which the selectivity for intramolecular aziridination or nitrene insertion of carbamates over allylic systems can be perfectly regulated by the ratio between AgOTf catalyst and 1,10-phenanthroline ligand.⁵⁴ Finally, third row transition metals have been barely used in such reactions, with few exceptions on iridium and gold catalysis. Driver reported an activation of organic azides for intramolecular amination⁵⁵ whereas Katsuki disclosed an enantioselective version of such protocol by means of salem-iridium complexes.⁵⁶

⁵² a) C. Liang, F. Robert-Peillard, C. Fruit, P. Müller, R. H. Dodd, P. Dauban, *Angew. Chem. Int. Ed.* **2006**, *45*, 4641-4644. b) C. Liang, F. Collet, F. Robert-Peillard, P. Müller, R. H. Dodd, P. Dauban, *J. Am. Chem. Soc.* **2008**, *130*, 343-350. c) C. Lescot, B. Darses, F. Collet, P. Retailleau, P. Dauban, *J. Org. Chem.* **2012**, *77*, 7232-7240. d) J. Buendia, B. Darses, P. Dauban, *Angew. Chem. Int. Ed.* **2015**, *54*, 5697-5701.

⁵³ a) H. Lebel, C. Spitz, O. Leogane, C. Trudel, M. Parmentier, *Org. Lett.* **2011**, *13*, 5460-5463. b) H. Lebel, C. Trudel, C. Spitz, *Chem. Commun.* **2012**, *48*, 7799-7801.

⁵⁴ a) J. W. Rigoli, C. D. Weatherly, J. M. Alderson, B. T. Vo, J. M. Schomaker, *J. Am. Chem. Soc.* **2013**, *135*, 17238-17241. b) J. M. Alderson, A. M. Phelps, R. J. Scamp, N. S. Dolan, J. M. Schomaker, *J. Am. Chem. Soc.* **2014**, *136*, 16720-16723

⁵⁵ K. Sun, R. Sachwani, K. J. Richert, T. G. Driver, *Org. Lett.* **2009**, *11*, 3598-3601.

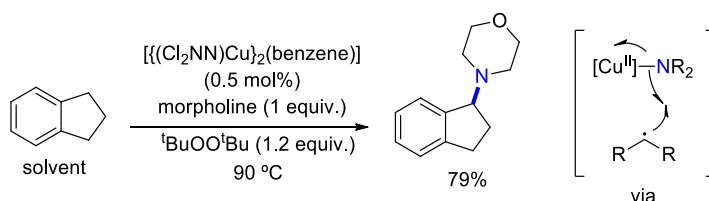
⁵⁶ M. Ichinose, H. Suematsu, Y. Yasutomi, Y. Nishioka, T. Uchida, T. Katsuki, *Angew. Chem. Int. Ed.* **2011**, *50*, 9884-9887.

Chapter I. Introduction on C(sp³)-H Functionalization

The single example in gold catalysis was reported by Feng for the intermolecular amination at benzylic positions employing tosylamide as nitrogen source.⁵⁷

1.3.1.3. Radical-mediated C(sp³)-H amination

Few examples of radical-based mechanisms have been disclosed within the general area of *sp*³ C-H amination. These strategies use photoredox or transition metal catalysts for the generation of radical species (such as nitrogen-centered or carbon-centered radicals) that trigger the targeted amination event via intramolecular or intermolecular hydrogen abstraction pathways. Pioneering work by Warren demonstrated that copper catalysis could be applied for intermolecular aliphatic C-H amination using *di-tert*-butyl peroxide as radical initiator (Scheme 1.11).⁵⁸ The authors discussed a dinuclear-Cu^I/Cu^{II} catalytic system in which hydrogen abstraction of the substrate generates a carbon-centered radical intermediate that reacts with a Cu^{II} intermediate bearing a nitrogen group.



Scheme 1.11: Copper catalyzed benzylic C-H amination.

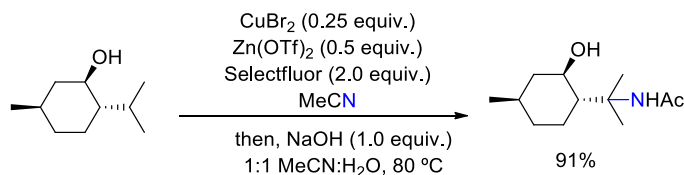
Hartwig reported a similar system for the efficient intermolecular amidation of non-activated alkanes.⁵⁹ The authors proposed a Cu^{III}/Cu^I catalytic system in which the activation of the nitrogen source proceeds in a similar pathway from what already discussed by Warren. Interestingly, this methodology showed an amination selectivity for secondary and primary positions over tertiary ones. The group of Baran developed a directed Ritter-type amination of aliphatic sites catalyzed by copper with Selectfluor as oxidant (Scheme 1.12).⁶⁰ The authors postulated a mechanism in which the carbon centered radical is oxidized by the copper catalyst to a carbocation which gets trapped by acetonitrile.

⁵⁷ Y. Zhang, B. Feng, C. Zhu, *Org. Biomol. Chem.* **2012**, *10*, 9137-9141.

⁵⁸ a) S. Wiese, Y. M. Badieli, R. T. Gephart, S. Mossin, M. S. Varonka, M. M. Melzer, K. Meyer, T. R. Cundari, T. H. Warren, *Angew. Chem. Int. Ed.* **2010**, *49*, 8850-8855. b) R. T. Gephart III, D. L. Huang, M. J. B. Aguila, G. Schmidt, A. Shahu, T. H. Warren, *Angew. Chem. Int. Ed.* **2012**, *51*, 6488-6492.

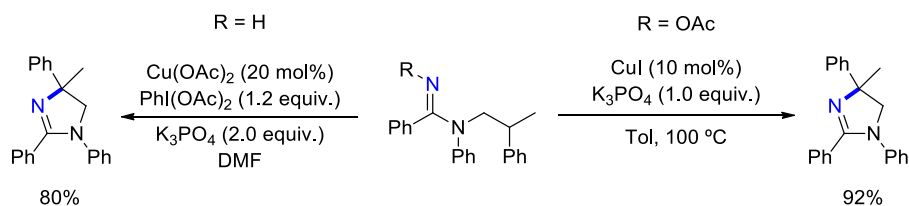
⁵⁹ B. L. Tran, B. Li, M. Driess, J. F. Hartwig, *J. Am. Chem. Soc.* **2014**, *136*, 2555-2563.

⁶⁰ Q. Michaudel, D. Thevenet, P. S. Baran, *J. Am. Chem. Soc.* **2012**, *134*, 2547-2550.



Scheme 1.12: Copper promoted Ritter-type amination of aliphatic tertiary C-H bonds.

A different approach was studied by Liu, who reported a copper-catalyzed protocol employing a pre-oxidized nitrogen source such as N-fluorobenzenesulfonimide (NFSI), thus performing a global redox-neutral amination reaction.⁶¹ In an intramolecular context, Chiba worked on directed intramolecular amination catalyzed by copper for the synthesis of imidazolines (Scheme 1.13).⁶² The authors described two complementary protocols that employ amidines for the direct intramolecular functionalization using hypervalent iodine(III) reagent PhI(OAc)₂ as terminal oxidant or activated amidoximes which did not require the use of any external oxidant (redox neutral process). The authors proposed the generation of imidyl radicals by either the oxidation of an amidine by in situ formed high valent Cu^{III} species or via activation of the amidoxime by reduction of the N-O bond promoted by Cu^I. In both cases selective 1,5-Hydrogen Atom Transfer (1,5-HAT) followed by oxidation by copper to the corresponding tertiary carbocation enables nucleophilic attack of the former nitrogen atom. With these methodologies, site-selectivity is dictated by the 1,5-HAT performed by the nitrogen-centered amidyl radical. Finally, Yu and Nevado investigated the use of iridium-based photoredox catalysts for the cyclization of activated nitrogen species.⁶³ While Yu reported a smooth pyrrolidine formation from the corresponding chloramines, Nevado identified photochemical conditions for the cyclization of oximes to the resultant cyclic imines.



Scheme 1.13: Chiba's synthesis of imidazolines.

⁶¹ Z. Ni, Q. Zhang, T. Xiang, Y. Zheng, Y. Li, H. Zhang, J. Zhang, Q. Liu, *Angew. Chem. Int. Ed.* **2012**, *51*, 1244-1247.

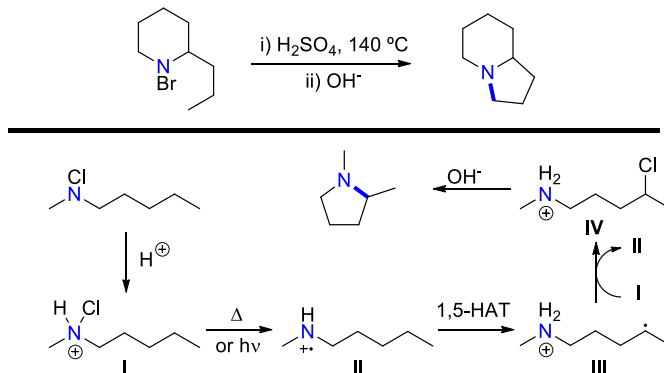
⁶² a) H. Chen, S. Sanjaya, Y.-F. Wang, S. Chiba, *Org. Lett.* **2013**, *15*, 212-215. b) H. Chen, S. Chiba, *Org. Biomol. Chem.* **2014**, *12*, 42-46.

⁶³ a) Q. Qin, S. Yu *Org. Lett.* **2015**, *17*, 1894-1897. b) W. Shu, C. Nevado, *Angew. Chem. Int. Ed.* **2017**, *56*, 1881-1884.

Chapter I. Introduction on C(sp³)-H Functionalization

1.3.2. Metal free C(sp³)-H amination

During the last two decades, the synthetic chemistry community explored alternative pathways from what previously discussed above to promote amination reactions avoiding the use of transition metal catalysts. Generally, these metal free strategies rely on the use of radical intermediates to promote inter or intramolecular hydrogen atom transfer (HAT) processes, thus generating active radical intermediate species from the corresponding inert aliphatic C-H bonds. Therefore, these methodologies often represent an orthogonal and complementary approach to aminated molecules when compared with available transition metal catalysis. Historically, the first reported metal free C(sp³)-H amination reaction is the so-called Hofmann-Löffler reaction. August Von Hofmann reported in 1880s that brominated aliphatic amines, when treated in neat sulphuric acid at high temperatures followed by basic aqueous work up, gave rise to pyrrolidine formation in a selective cyclization event (Scheme 1.14, top).⁶⁴ Few decades later, Löffler continued with the pioneering work of Hofmann and applied such reaction for the synthesis of different molecules such as nicotine, demonstrating its generality and robustness.⁶⁵ Almost one hundred years had to pass from Hofmann's initial observations until the mechanism was effectively understood. Corey studied the transformation in 1960 and postulated what is nowadays the accepted mechanism (Scheme 1.14, bottom).⁶⁶



Scheme 1.14: Top: Hofmann's initial observations. Bottom: Mechanism postulated by Corey.

The reaction starts with the protonation of the halogenated amine starting material. Species I undergo homolytical cleavage of the N-halogen bond under thermal conditions or by light exposure thus generating nitrogen-centered radical cation II.

⁶⁴ A. W. Hofmann, *Ber. Dtsch. Chem. Ges.* **1883**, *16*, 558-560.

⁶⁵ a) K. Löffler, C. Freytag, *Ber. Dtsch. Chem. Ges.* **1909**, *42*, 3427. b) K. Löffler, H. Kaim, *Ber. Dtsch. Chem. Ges.* **1909**, *42*, 94. c) K. Löffler, *S. Ber. Dtsch. Chem. Ges.* **1909**, *42*, 3431.

⁶⁶ E. J. Corey, W. R. Hertler, *J. Am. Chem. Soc.* **1960**, *82*, 1657-1668.

Selective 1,5-Hydrogen Atom Transfer (1,5-HAT) delivers carbon-centered radical **III** which engages halogen abstraction from **I** to form **IV** and regenerate **II** in a radical chain propagation mechanism. Finally, intramolecular nucleophilic displacement by the free amine delivers the final pyrrolidine.

The rather harsh reaction conditions used in this technology made this protocol inconvenient for synthetic applications. Still, however, Doll employed a modification of the Hofmann-Löffler reaction for the synthesis of natural product gelsedine which involved the use of *tert*-butyl hypochlorite as promoter.⁶⁷ In this regard, the group of Suárez reported a modification of such reaction conditions which implies the generation in situ of active iodinated amine species which later on follows the conventional mechanism. This modification involved the use of stoichiometric amounts of molecular iodine with overstoichiometric amounts of hypervalent iodine(III) as oxidant. By means of this strategy, they reported the effective cyclisation of a wide variety of amine derivatives such as nitroamides, cyanamides and phosphoramidates.⁶⁸

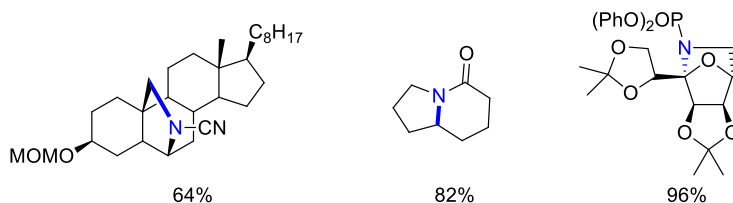


Figure 1.6: Selected examples accessed employing Suárez's modification.

Further work in the context of Suárez's modification was carried out by the groups of Wu, Herrera and Muñiz, who reported stoichiometric procedures based on electrophilic iodine promoters as active species for the selective preparation of pyrrolidine derivatives.⁶⁹ It is worth noting that the authors designed a protocol to promote the functionalization under relatively mild conditions, thus expanding the application profile of these technologies. In 2015, Muñiz reported the first catalytic Hofmann-Löffler reaction. Employing a combination of hypervalent iodine(III) oxidant PhI(*m*CBA)₂ and molecular iodine in catalytic amounts, it was possible to achieve the cyclization of a wide variety of sulfonamides, affording pyrrolidine formation not only

⁶⁷ S. W. Baldwin, R. J. Doll, *Tetrahedron Lett.* **1979**, *20*, 3275-3278.

⁶⁸ a) R. Carrau, R. Hernández, E. Suárez, C. Betancor, *J. Chem. Soc. Perkins. 1*, **1987**, 937-943. b) R. L. Dorta, C. G. Francisco, E. Suárez, *J. Chem. Soc. Chem. Commun.* **1989**, 1168-1169. c) C. G. Francisco, A. J. Herrera, E. Suárez, *J. Org. Chem.* **2003**, *68*, 1012-1017.

⁶⁹ a) R. Fan, D. Pu, F. Wen, J. Wu, *J. Org. Chem.* **2007**, *72*, 8994-8997. b) N. R. Paz, D. Rodríguez-Sosa, H. Valdés, R. Marticorena, D. Melián, M. B. Copano, C. C. González, A. J. Herrera, *Org. Lett.* **2015**, *17*, 2370-2373. c) C. Q. O'Broin, P. Fernández, C. Martínez, K. Muñiz, *Org. Lett.* **2016**, *18*, 436-439.

Chapter I. Introduction on C(sp³)-H Functionalization

over activated benzylic positions, but also over tertiary, secondary and primary positions (Figure 1.7, bottom).⁷⁰

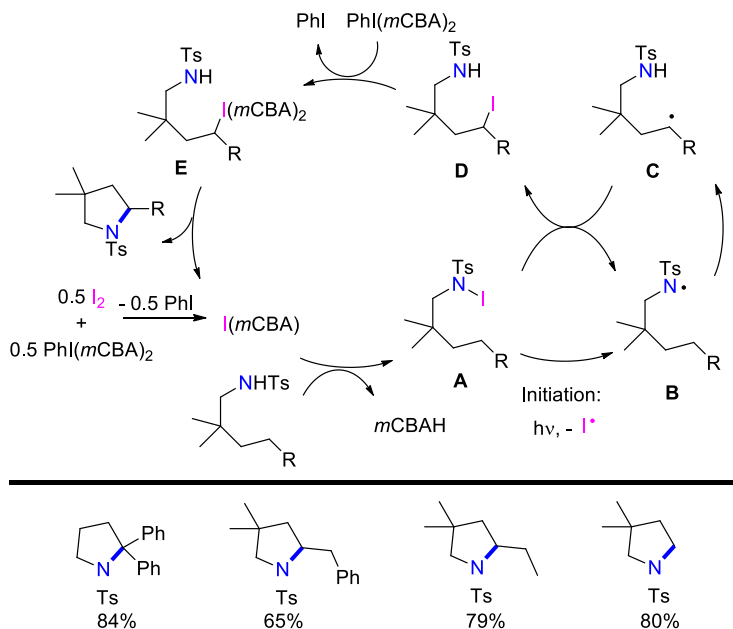


Figure 1.7: Top: Iodine-catalyzed Hofmann-Löffler reaction mechanism. Bottom: Selected examples accessed through this method.

Active electrophilic iodine(I) *ImCBA* catalyst is believed to be generated from the comproportionation of molecular iodine and hypervalent iodine(III) oxidant (Figure 1.7, top). This active catalyst enables the iodination of the starting material to form halogenated sulfonamide **A**. Homolytic cleavage of the N-I bond upon light irradiation generates nitrogen-centered radical **B** which performs a 1,5-HAT to afford carbon-centered radical **C**. Intermediate **C** then triggers a chain-propagation by abstracting an iodine atom from **A** to generate alkyl-iodide **D** and nitrogen-centered radical **B** simultaneously. Such a pathway was corroborated by a quantum yield of 44. At this point, a direct intramolecular nucleophilic displacement could be envisioned via oxidation to I(III) reagents. The installation of this alkyl iodine(III) supernucleophile species remains crucial for the kinetics adjustment in this rather complex mechanism thus ensuring the high performance of the reaction and allowing the functionalization at non-activated positions.⁷¹ Intramolecular nucleophilic displacement at **E** yields the final product and regenerates the active iodine(I) catalyst.

⁷⁰ C. Martínez, K. Muñiz, *Angew. Chem. Int. Ed.* **2015**, *54*, 8287-8291.

⁷¹ A. Bosnidou, K. Muñiz, *Chem. Eur. J.* **2019**, 13654-13664.

Taking into consideration the mechanistic rationale depicted in Figure 1.7, Muñiz and coworkers developed a series of amination reactions via catalytic Hofmann-Löffler reactions (Scheme 1.15). Additional modifications allowed them to perform the reaction using simple *m*CPBA as terminal oxidant, avoiding the use of chlorinated solvents and showing exquisite selectivity for the cyclization even at non-activated primary positions.⁷² They also reported a double catalytic approach employing molecular iodine in catalytic amounts together with photoredox catalyst TPT (2,4,6-Triphenylpyrylium tetrafluoroborate). In such process, the catalytic scenario consists of iodine(-I/I) cycle, limiting the scope of the reaction to the functionalization of activated benzylic positions due to the absence of the key alkyl-iodine(III) intermediate mentioned before. The photoredox catalyst triggers the oxidation of the iodide that is extruded in the cyclization step to hypoiodite, which is the active catalyst in the reaction. The blue LED light source have a dual role, acting both as activator of the photoredox catalyst and as promoter of the homolytic cleavage of the in situ formed N-I bond.⁷³ Parallel to this work, the authors reported a protocol for the selective cyclization of sulfonamides affording piperidine formation.⁷⁴ In this case, however, the authors did not propose an intramolecular HAT event, since amidyl 1,6-HAT is known to be outperformed by 1,5-HAT due to enthalpic reasons.⁷⁵ The combination of molecular iodine with NBS terminal oxidant allows for a free-radical process involving intermolecular HAT that enables selective piperidine formation over the Hofmann-Löffler pyrrolidine product. Additionally, the group of Muñiz reported an unprecedented bromine-based catalytic system that effectively promotes selective C(sp³)-H amination toward pyrrolidines employing a combination of tetrabutylammonium bromide and *m*CPBA.⁷⁶

⁷² T. Duhamel, C. J. Stein, C. Martínez, M. Reiher, K. Muñiz, *ACS Catal.* **2018**, *8*, 3918-3925.

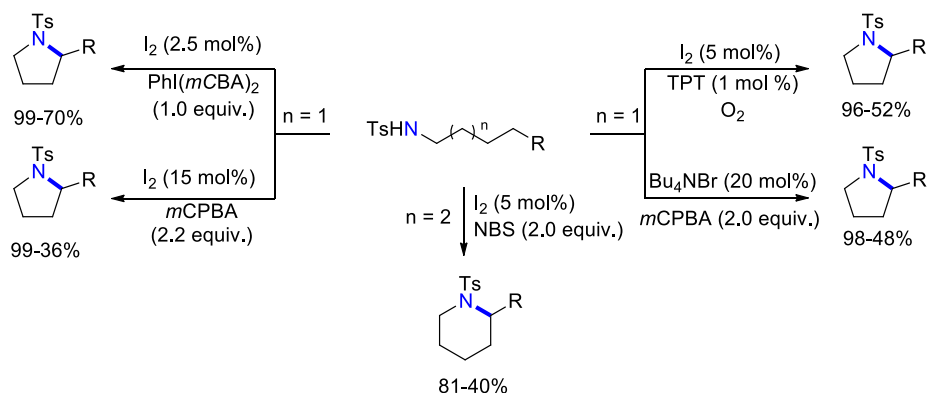
⁷³ P. Becker, T. Duhamel, C. J. Stein, M. Reiher, K. Muñiz, *Angew. Chem. Int. Ed.* **2017**, *56*, 8004-8008.

⁷⁴ H. Zhang, K. Muñiz, *ACS Catal.* **2017**, *7*, 4122-4125.

⁷⁵ D. Săkić, H. Zipse, *Adv. Synth. Catal.* **2016**, *358*, 3983-3991.

⁷⁶ P. Becker, T. Duhamel, C. Martínez, K. Muñiz, *Angew. Chem. Int. Ed.* **2018**, *57*, 5166-5170.

Chapter I. Introduction on C(sp³)-H Functionalization



Scheme 1.15: Recent advances of halogen catalysis for pyrrolidines and piperidines synthesis developed by the group of Muñiz.

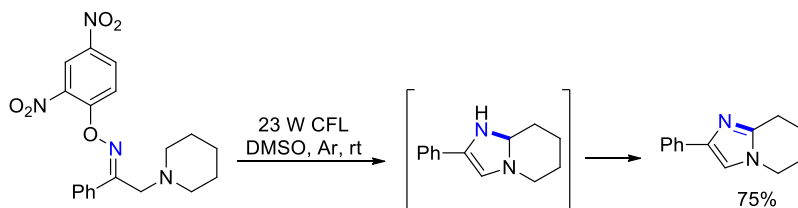
During last years, Nagib developed iodine-promoted amination reactions within the context of Hofmann-Löffler reactions. These authors reported in 2016 a variation which employs simple sodium iodide as iodine source and commercial PhI(OAc)₂ as terminal oxidant.⁷⁷ The authors suggest the in situ formation of triiodide as a molecular iodine reservoir, which prevents overoxidation byproducts formation associated with its presence. Additionally, Minakata recently reported a similar stoichiometric procedure for the cyclization of sulfamate esters and sulfamides employing NIS or *tert*-butyl hypoiodite.⁷⁸ Fu reported in 2017 a completely different strategy for the preparation of nitrogen-centered radicals and its use in C(sp³)-H amination (Scheme 1.16). They identified an oxime derivative bearing a labile group as suitable source for the generation of imidyl radicals. Imidyl radicals have been used in the past because of their known propensity to add over sp² carbon centers, albeit its use for sp³ functionalization was neglected.⁷⁹ Simple light irradiation triggered homolysis of the N-O bond at the oxime, thus generating the corresponding imidyl radical which selectively functionalized an activated position through 1,5-HAT. Latter cyclization and aromatization allowed for the preparation of a wide variety of imidazoles.⁸⁰

⁷⁷ E. A. Wappes, S. C. Fosu, T. C. Chopko, D. A. Nagib, *Angew. Chem. Int. Ed.* **2016**, *55*, 9974-9978.

⁷⁸ K. Kiyokawa, S. Nakamura, K. Jou, K. Iwaida, S. Minakata, *Chem. Commun.* **2019**, *55*, 11782-11785.

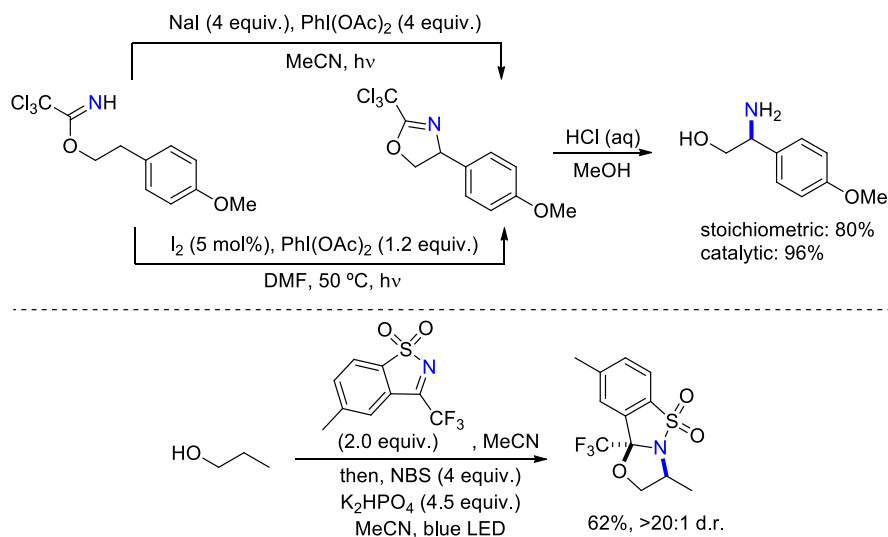
⁷⁹ J. Davies, S. P. Morcillo, J. J. Douglas, D. Leonori, *Chem. Eur. J.* **2018**, *24*, 12154-12163.

⁸⁰ J. Li, P. Zhang, M. Jiang, H. Yang, Y. Zhao, H. Fu, *Org. Lett.* **2017**, *19*, 1994-1997.



Scheme 1.16: Fu's photochemical imidazole synthesis.

In an elegant approach, Nagib reported that simple imidates deriving from the addition of alcohols to nitriles could act as suitable imidyl-radical precursors through the use of electrophilic iodine reagents (Scheme 1.17, top).⁸¹ Subsequently, a 1,5-HAT followed by selective iodination of the carbon centered radical and nucleophilic substitution gives rise to the corresponding cyclized oxazoline products, which could be deprotected in situ to afford free 1,2-aminoalcohols. This concept was later on improved for the direct amination of non-functionalized alcohols (Scheme 1.17, bottom).⁸² In situ formation of the active sulfonamide accounted from the addition of an alcohol to a suitable imine precursor. The amination event was effectively performed by the use of superstoichiometrical amounts of NBS, thus affording the final oxazolidine with high level of diastereoselectivity.



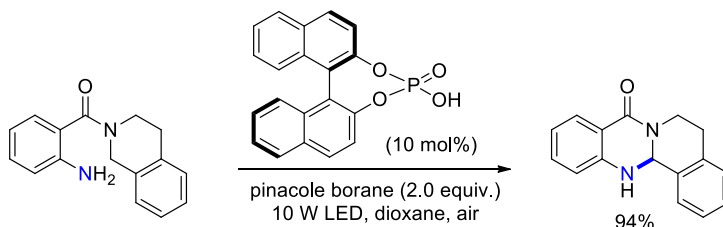
⁸¹ a) E. A. Wappes, K. M. Nakafuku, D. A. Nagib, *J. Am. Chem. Soc.* **2017**, *139*, 10204-10207. b) L. M. Stateman, E. A. Wappes, K. M. Nakafuku, K. M. Edwards, D. A. Nagib, *Chem. Sci.* **2019**, *10*, 2693-2699.

⁸² K. M. Nakafuku, R. K. Twumasi, A. Vanitcha, E. A. Wappes, K. Namitharan, M. Bekkaye, D. A. Nagib, *J. Org. Chem.* **2019**, *84*, 13065-13072.

Chapter I. Introduction on C(sp³)-H Functionalization

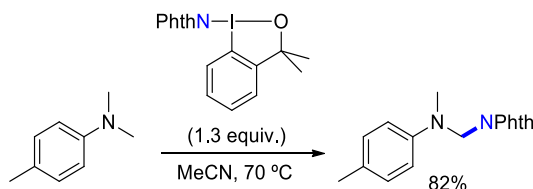
Scheme 1.17: Top: Imidyl radical mediated vicinal aminoalcohols synthesis. Bottom: Direct amination of free alcohols.

The group of Zheng reported in 2019 a different approach for C(sp³)-H amination employing a hydrogen bond catalyst for the formation of a transient electron donor acceptor (EDA) complex which starts the radical process under aerobic oxidation conditions (Scheme 1.18).⁸³ The authors were able to cyclize over activated benzylic positions for the smooth preparation of a wide variety of quinazolinone derivatives.



Scheme 1.18: Zheng's photochemical quinazolinone derivatives synthesis.

In the following section, we discuss recent advances on metal free intramolecular C(sp³)-H amination. Based on the precedents of Section 3.2.1 via iminoiodane intermediates, it is not particularly surprising that metal free methodologies for intermolecular aliphatic amination have relied on the use of electrophilic halogen species as activators to trigger such transformations. In 1997, Zhdankin identified hypervalent iodine(III) reagents containing nitrogen ligand groups which could perform oxidative amination of adamantane.⁸⁴ Minakata further investigated this concept introducing a new class of aminoiodanes bearing a transferable phthalimide ligand for successful α -amination of tertiary amines (Scheme 1.19).⁸⁵



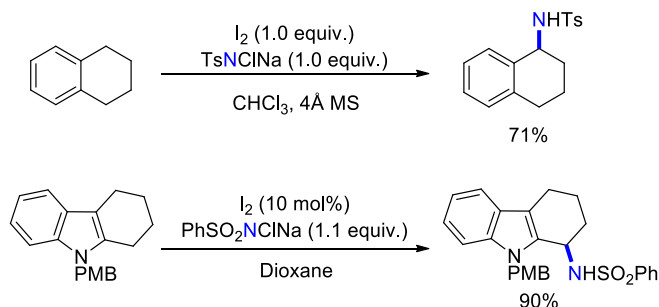
Scheme 1.19: Amination of tertiary amines promoted by hypervalent iodine(III) reagent bearing transferable phthalimide ligand.

⁸³ D. Jing, C. Lu, Z. Chen, S. Jin, L. Xie, Z. Meng, Z. Su, K. Zheng, *Angew. Chem. Int. Ed.* **2019**, *58*, 14666-14672.

⁸⁴ V. V. Zhdankin, M. McSherry, B. Mismash, J. T. Bolz, J. K. Woodward, R. M. Arbit, S. Erickson, *Tetrahedron Lett.* **1997**, *38*, 21-24.

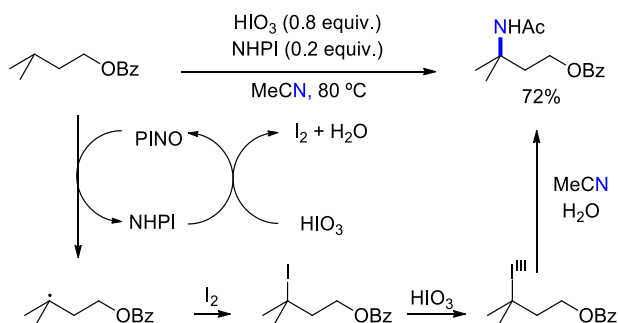
⁸⁵ K. Kiyokawa, T. Kosaka, T. Kojima, S. Minakata, *Angew. Chem. Int. Ed.* **2015**, *54*, 13719-13723.

Activated amines such as Chloramine-T and Chloramine-B have been employed as nitrogen sources in combination with molecular iodine both in stoichiometric and catalytic amounts for the amination of benzylic aliphatic positions (Scheme 1.20).⁸⁶ Crabtree and Gunnoe reported an α -amination of ethers through the use of non-activated sulphonamides in combination with hypervalent PhI(OAc)₂ as oxidant.⁸⁷



Scheme 1.20: Activated chloramide salts as nitrogen source for aliphatic C-H amination.

Current methodologies include the development of intermolecular amination reactions at non-activated aliphatic positions. Specifically, Minakata reported a Ritter-type amination over tertiary positions employing iodic acid as oxidant and N-hydroxyphthalimide (NHPI) as radical mediator (Scheme 1.21).⁸⁸ The authors postulated an HIO₃ driven oxidation of the NHPI to its corresponding N-oxide (PINO), which performs a selective intermolecular HAT over the starting material to generate a *tert*-alkyl radical. Iodination of such radical followed by oxidation to the key alkyl iodine(III) supernucleofuge sets the scenario for the nucleophilic displacement by the acetonitrile solvent, which upon hydrolysis release the corresponding Ritter-type aminated product. Unfortunately, however, the process is limited to the amination of *tert*-alkyl aliphatic C-H bonds.



⁸⁶ a) Y. Takeda, J. Hayakawa, K. Yano, S. Minakata, *Chem. Lett.* **2012**, *41*, 1672-1674. b) X. Liu, Y. Zhou, Z. Yang, Q. Li, L. Zhao, P. Liu, *J. Org. Chem.* **2018**, *83*, 4665-4673.

⁸⁷ J. Campos, S. K. Goforth, R. H. Crabtree, T. B. Gunnoe, *RSC Adv.* **2014**, *4*, 47951.

⁸⁸ K. Kiyokawa, K. Takemoto, S. Minakata, *Chem. Commun* **2016**, *52*, 13082-13085.

Chapter I. Introduction on C(sp³)-H Functionalization

Scheme 1.21: Iodic acid promoted Minakata's Ritter type amination.

In 2019, Muñiz reported the first iodine catalyzed intermolecular C(sp³)-H amination with the use of non-activated nitrogen sources.⁸⁹ Amination was effectively achieved by the use of molecular iodine in catalytic amounts, with hypervalent iodine(III) reagent (di-4-bromobenzyloxyiodio)benzene (PhI(*p*BBA)₂) as terminal oxidant and triflamide as nitrogen source under blue LED irradiation.

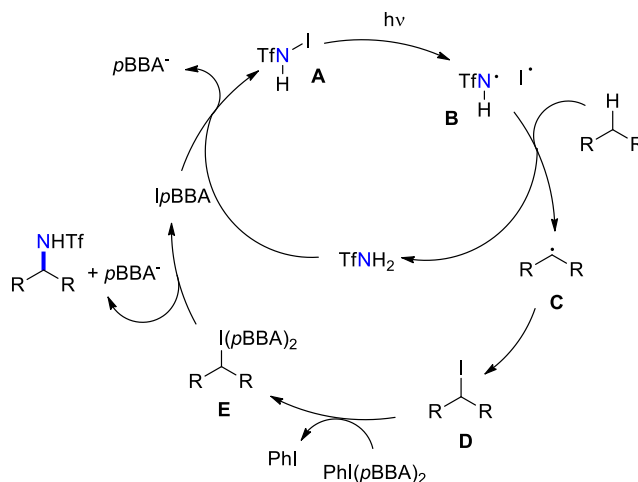
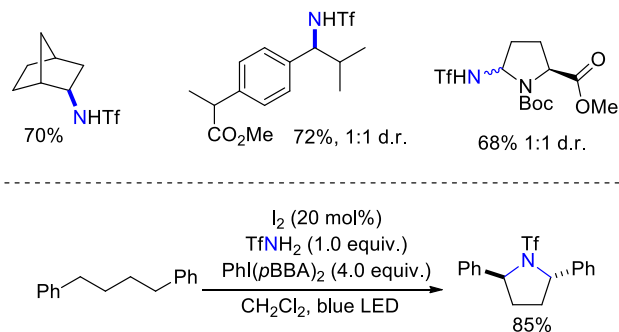


Figure 1.8: Catalytic cycle of molecular iodine catalyzed photochemical intermolecular amination reported by Muñiz.

The reaction starts by the comproportionation of molecular iodine and the hypervalent iodine(III) to form the active iodine(I) catalyst. Such species iodinate the amine source to form intermediate **A** (Figure 1.8). Homolytic cleavage to **B** and selective intermolecular hydrogen abstraction generates carbon centered radical **C**. Alkyl iodide **D** arises from the iodination of **C** (which could occur by radical recombination or radical chain reaction with **A**). Oxidation to alkyl-iodine(III) species **E** bearing the supernucleophile leaving group allows for the nucleophilic displacement by the triflamide group, which liberates the final product and regenerates the active catalyst. In this catalytic process, the triflamide acts with dual roles, acting as the radical carrier for the selective C-H abstraction, and performing the final nucleophilic substitution. With this protocol, the authors reported smooth amination of a wide variety of hydrocarbons, observing a general preference for secondary over tertiary positions, which is in sharp contrast to all methodologies discussed before (specially for nitrene insertion analogous procedures). Even amino acids could be successfully aminated (Scheme 1.22, top). Furthermore, the authors combined this method with iodine-

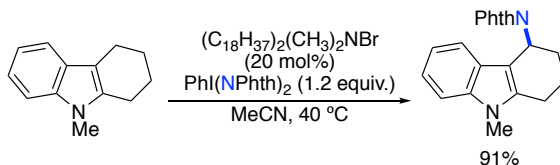
⁸⁹ A. E. Bosnidou, K. Muñiz, *Angew. Chem. Int. Ed.* **2019**, *58*, 7485-7489.

catalyzed Hofmann-Löffler reaction, thus affording direct pyrrolidine formation starting from a simple alkane and triflamide via a tandem intermolecular/intramolecular amination within a one-pot operation (Scheme 1.22, bottom).



Scheme 1.22: Top: Selected scope examples. Bottom: One-pot tandem inter-intramolecular amination for pyrrolidine synthesis.

Additionally, Muñiz developed an unprecedented bromine catalytic system for the selective amination of tetrahydrocarbazoles at the 4-position (Scheme 1.23).⁹⁰ The authors employed an ammonium bromide salt as catalyst in combination with an hypervalent iodine(III) oxidant bearing transferable phthalimide ligands that acted as nitrogen source. Furthermore, the authors applied such methodology for the preparation of important alkaloid natural compound *Aspidospermidine*. Finally, in the context of intermolecular aliphatic C-H amination, the potential of rather exotic hypervalent bromine(III) species bearing transferable amine ligands have been demonstrated by Ochiai. However, its implementation to efficient synthetic protocols has been barely explored.⁹¹



Scheme 1.23: Bromine-catalyzed 4-amination of tetrahydrocarbazoles.

⁹⁰ J. Bergès, B. García, K. Muñiz, *Angew. Chem. Int. Ed.* **2018**, *57*, 15891-15895.

⁹¹ a) M. Ochiai, K. Miyamoto, T. Kaneaki, S. Hayashi, W. Nakanishi, *Science* **2011**, *332*, 448-451.

b) M. Ochiai, T. Kaneaki, N. Tada, K. Miyamoto, H. Chuman, M. Shiro, S. Hayashi, W. Nakanishi, *J. Am. Chem. Soc.* **2007**, *129*, 12938-12939.

Chapter I. Introduction on C(sp³)-H Functionalization

1.4. Importance on C(sp³)-F bonds in bioactive molecules.

Fluorine represents the 13th most abundant element on Earth's crust, however, its presence on naturally occurring organic compounds does not seem to correlate with this observation. This can be rationalized because of its chemical properties. Biochemical halogen incorporation into organic molecules usually takes place through in situ formation of hypohalous species for electrophilic reactions or through nucleophilic halogenation of electrophiles such as epoxides. Fluorine remains a challenging halogen for its involvement in these synthetic strategies. Its high electronegativity (which consequently confers a high oxidation potential) and low nucleophilicity led for many years to the idea that naturally occurring fluorinated molecules do not exist. Sodium monofluoroacetate, the first fluorinated naturally appearing compound discovered in the 1940s showed high toxic properties, so even though it was demonstrated that nature could synthesize such molecules, they were thought to have no beneficial potential for medicinal chemistry. In 1955, the first fluorine-containing drug, Fludrocortisone, was approved by the FDA (Figure 1.9). Since then, the number of marketed drugs containing at least one fluorine atom dramatically increased, representing around 25% of current pharmaceuticals. Drugs like antidepressant Fluoxetine (Prozac), gastric acid regulator Lansprazole (Prevacid) or anti-diabetic Sitagliptin (Januvia) are among top sold pharmaceuticals, and exemplify the wide variety of action fields that bioactive fluorine-containing molecules afford.⁹² Analogously, fluorinated molecules account for nearly 25% of commercial herbicides. Penoxsultam, an acetolactate synthase inhibitor or Trifluralin, a mitosis inhibitor are just two examples of fluorine-containing agrochemicals employed for plague control.⁹³

The presence of fluorine atoms in bioactive molecules confer them with unique physicochemical properties.⁹⁴ His small size and high electronegativity allow for the formation of halogen-halogen and halogen-hydrogen bonds, thus introducing important conformational changes when interacting at the active target biological site. In addition, carbon-fluorine bonds are non-polarizable. These key aspect together with his slightly enhance lipophilicity when compared with other polar functional groups often result on an improved pharmacokinetics and ADME (absorption, distribution, metabolism and excretion) properties when introducing fluorine atoms in drug candidate molecules. Finally, the plethora of weak interactions arising from fluorine also propitiated his application to material science, where it has been successfully

⁹² a) J. Wang, M. Sánchez-Roselló, J. L. Aceña, C. del Pozo, A. E. Sorochinsky, S. Fustero, V. A. Soloshonok, H. Liu, *Chem. Rev.* **2014**, *114*, 2432-2506. b) Y. Zhou, J. Wang, Z. Gu, S. Wang, W. Zhu, J. L. Aceña, V. A. Soloshonok, K. Izawa, H. Liu, *Chem. Rev.* **2016**, *116*, 422-518.

⁹³ T. Fujiwara, D. O'Hagan, *J. Fluor. Chem.* **2014**, *167*, 16-29.

⁹⁴ a) E. P. Gillis, K. J. Eastman, M. D. Hill, D. J. Donnelly, N. A. Meanwell, *J. Med. Chem.* **2015**, *58*, 8315-8359. b) N. A. Meanwell, *J. Med. Chem.* **2018**, *61*, 5822-5880.

employed for the preparation of advanced materials such as liquid crystals, polymers or dendrimers.⁹⁵

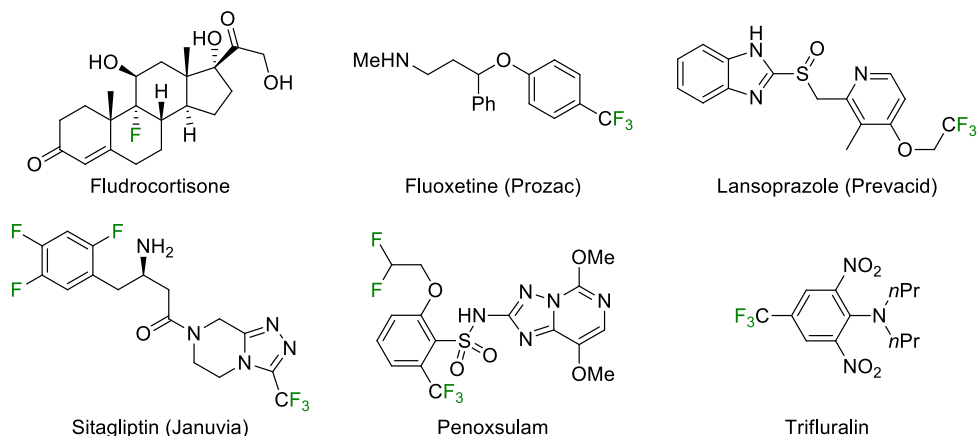


Figure 1.9: Selected commercial pharmaceuticals and agrochemicals bearing fluorine atoms.

1.5. C(sp³)-H fluorination

Because of the high importance of fluorinated molecules just discussed, fluorination chemistry has emerged as an exciting new field in synthetic organic endeavors.⁹⁶ Herein, we will discuss current aliphatic fluorination methodologies distinguishing between transition metal and metal free fluorination technologies.

1.5.1. Transition metal-mediated C(sp³)-H fluorination

In an analogous scenario with what discussed in section 3.1, we can distinguish regarding the activation mechanism in fluorination via C(sp³)-H metallation and radical-mediated processes.

1.5.1.1. Fluorination via C(sp³)-H metallation

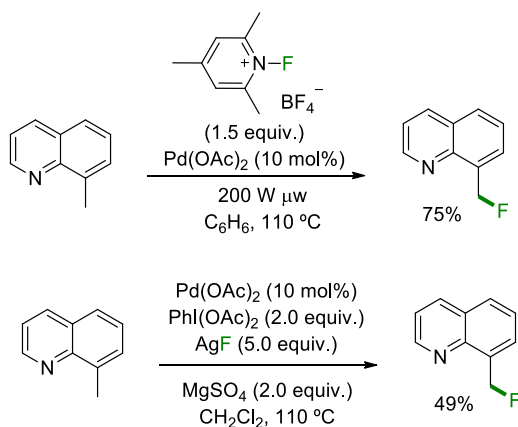
The formation of metallated intermediates from metal insertion on C-H bonds represents the first historical approach for C-H fluorination. Fluorination of sp² C-H centers have been extensively studied through last decades mainly in the context of palladium catalysis. Generally, described methodologies involved high oxidation state palladium catalytic scenarios (Pd^{II}/Pd^{IV}), since C-F bond forming reductive elimination was discovered to easily take place via Pd^{IV} intermediates. Common mechanistic picture

⁹⁵ R. Berger, G. Resnati, P. Metrangolo, E. Weberd, J. Hulliger, *Chem. Soc. Rev.* **2011**, *40*, 3496-3508.

⁹⁶ a) A. Lin, C. B. Huehls, J. Yang, *Org. Chem. Front.* **2014**, *1*, 434-438. b) R. Szpera, D. F. J. Moseley, L. B. Smith, A. J. Sterling, V. Gouverneur, *Angew. Chem. Int. Ed.* **2019**, *58*, 14824-14848.

Chapter I. Introduction on C(sp³)-H Functionalization

for these methodologies then involved insertion of palladium on aliphatic C-H bonds affording the corresponding Pd^{II} metallated intermediates. Oxidation to analogous high oxidation Pd^{IV} intermediates bearing a fluorine atom followed by reductive elimination afford final fluorinated products and regenerate Pd^{II} catalysts. In a seminal work by Sanford, it was demonstrated the utilization of quinolines as directing chelating groups for benzylic C-H fluorination under palladium catalysis (Scheme 1.24, top). The use of electrophilic fluorine reagents remained crucial, possessing a double role since they act both as oxidant and as fluorine source.⁹⁷ Some years later, they developed a modification which involved the use of hypervalent iodine(III) reagent as oxidant for the oxidation to the key Pd^{IV} intermediate species, thus allowing the use of simple fluoride salts like silver fluoride as fluorine source (Scheme 1.24, bottom).⁹⁸



Scheme 1.24: Sanford's pioneer work on palladium catalyzed aliphatic C-H fluorination.

Further contributions rapidly appeared in the field following Sanford's initial concept. The groups of Shi, Yu and Ge reported palladium catalyzed diastereoselective directed fluorination of aminoacids employing different nitrogen directing groups in an amide anchor (Scheme 1.25).⁹⁹ For all the cases, the authors employed commercially available electrophilic reagent Selectfluor as oxidant and fluorine source. The groups of Xu (Y.) and Xu (D.-Q.) described related transformations for directed fluorination of amide and

⁹⁷ K. L. Hull, W. Q. Anani, M. S. Sanford, *J. Am. Chem. Soc.* **2006**, *128*, 7134-7135.

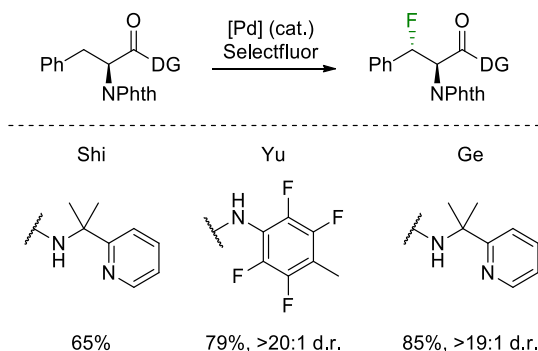
⁹⁸ K. B. McMurtrey, J. M. Racowski, M. S. Sanford, *Org. Lett.* **2012**, *14*, 4094-4097.

⁹⁹ a) Q. Zhang, X.-S. Yin, K. Chen, S.-Q. Zhang, B.-F. Shi, *J. Am. Chem. Soc.* **2015**, *137*, 8219-8226.

b) R.-Y. Zhu, K. Tanaka, G.-C. Li, J. He, H.-Y. Fu, S.-H. Li, J.-Q. Yu, *J. Am. Chem. Soc.* **2015**, *137*,

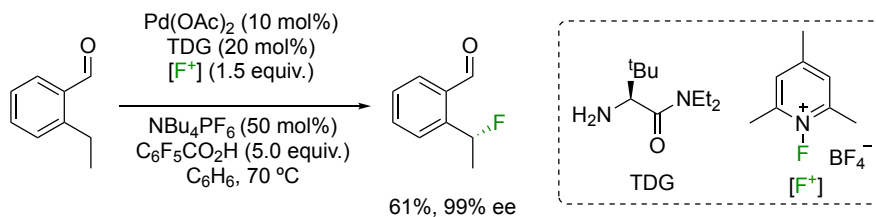
7067-7070. c) J. Miao, K. Yang, M. Kurek, H. Ge, *Org. Lett.* **2015**, *17*, 3738-3741.

alcohol derivatives bearing bidentate chelating groups respectively. In these cases, the authors used electrophilic NFSI as fluorine source.¹⁰⁰



Scheme 1.25: Palladium catalyzed directed fluorination of amioacids.

Recently, Yu reported an elegant approach for enantioselective aliphatic C-H fluorination at benzylic positions with aldehydes as transient directing groups (Scheme 1.26). In this scenario, the reductive elimination from palladium takes place in a diastereoselective manner, thus obtaining the optically active fluorinated product upon hydrolysis of the imine.¹⁰¹



Scheme 1.26: Yu's palladium-catalyzed enantioselective fluorination.

1.5.1.2. Radical-mediated C(sp³)-H fluorination

A different complementary approach for aliphatic fluorination comprises formation of radical intermediates, since common electrophilic fluorine sources like NFSY, Selectfluor or NFPY (N-fluoropyridinium salts) were found to be involved in fluorine atom transfer reactions.¹⁰² Generally, the synthetic strategies herein rely on inter or intramolecular hydrogen abstraction processes or single electron oxidations to generate carbon centered radicals which will be trapped by the fluorine source. The

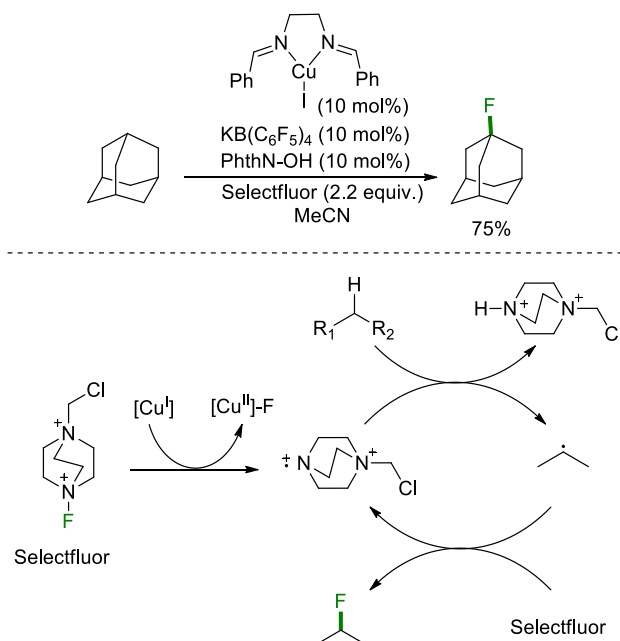
¹⁰⁰ a) Q. Zhu, D. Ji, T. Liang, X. Wang, Y. Xu, *Org. Lett.* **2015**, *17*, 3798-3801. b) Y.-J. Mao, S.-J. Lou, H.-Y. Hao, D.-Q. Xu, *Angew. Chem. Int. Ed.* **2018**, *57*, 14085-14089.

¹⁰¹ H. Park, P. Verma, K. Hong, J. Yu, *Nat. Chem.* **2018**, *10*, 755-762.

¹⁰² M. Rueda-Becerril, C. C. Sazepin, J. C. T. Leung, T. Okbinoglu, P. Kennepohl, J.-F. Paquin, G. M. Sammis, *J. Am. Chem. Soc.* **2012**, *134*, 4026-4029.

Chapter I. Introduction on C(sp³)-H Functionalization

group of Leckta reported in 2012 a copper catalytic system for fluorination of both activated and non-activated sp³ C-H bonds (Scheme 1.27). The authors discussed that Cu^I initiates the reaction by reducing fluorine source Selectfluor, generating a nitrogen-centered radical cation, which performs a hydrogen atom abstraction of the starting material. The corresponding carbon centered radical triggers a C-F bond-formation, regenerating a Selectfluor-derived radical cation. In line with this notion, Selectfluor plays with dual roles, enabling both a radical chain propagation and as fluorine source.¹⁰³



Scheme 1.27: Leckta's protocol for copper catalyzed aliphatic C-H fluorination.

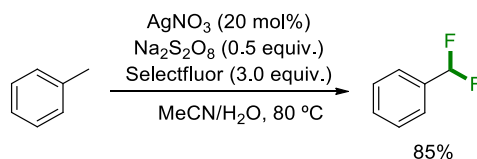
Some years later, Baxter reported a related Ag-catalyzed fluorination employing glycine as radical mediator for the hydrogen abstraction step.¹⁰⁴ In this case, the authors discussed in situ formation of Ag^{II} species from the oxidation with Selectfluor, which oxidize glycine to the active radical mediator species. Hydrogen abstraction of the starting material followed by radical quench by Selectfluor affords the final fluorinated product. Additionally, Tang reported a benzylic double fluorination procedure that operates in aqueous media.¹⁰⁵ Within the combination of Ag^I catalyst and sodium

¹⁰³ a) S. Bloom, C. R. Pitts, D. C. Miller, N. Haselton, M. G. Holl, E. Urheim, T. Leckta, *Angew. Chem. Int. Ed.* **2012**, *51*, 10580-10583. b) C. R. Pitts, S. Bloom, R. Woltornist, D. J. Auvenshine, L. R. Ryzhkov, M. A. Siegler, T. Leckta, *J. Am. Chem. Soc.* **2014**, *136*, 9780-9791.

¹⁰⁴ A. M. Hua, D. N. Mai, R. Martinez, R. D. Baxter, *Org. Lett.* **2017**, *19*, 2949-2952.

¹⁰⁵ P. Xu, S. Guo, L. Wang, P. Tang, *Angew. Chem. Int. Ed.* **2014**, *53*, 5955-5958.

persulfate oxidant, the authors proposed an in situ generation of high oxidation Ag^{II} which directly oxidize the substrate to the analogous benzylic radical that will be trapped by the fluorine source.



Scheme 1.28: Tang's double fluorination of benzylic C-H bonds.

Similar contributions were made from the groups of Leckta and Chen, who showed the feasibility of iron and vanadium catalysis for effective aliphatic C-H fluorination respectively, even though few mechanistic discussions were performed in that regard.¹⁰⁶ Britton made use of decatungstate clusters (W₁₀O₃₂⁴⁻) for photochemical fluorination at activated and non-activated aliphatic positions, including fluorination of aminoacids (Figure 1.10).¹⁰⁷ Decatungstate is known to act as photoredox catalyst, so upon light irradiation and excitation, proton coupled single electron transfer (hydrogen atom abstraction) directly affords carbon centered radical formation at the substrate. As for previous cases, fluorine atom transfer from the fluorine source (NFSY in this case) yields final fluorinated product. The catalytic cycle is terminated by reaction of NFSY-derived nitrogen centered radical with reduced tungstate intermediate, regenerating the active photocatalyst. Furthermore, the authors applied this methodology for C-H ¹⁸F labeling of aminoacids and peptides, aimed at the preparation of imaging agents for Positron Emission Tomography (PET).¹⁰⁸ In a more exotic variation of the discussed method, Sorensen reported a similar photocatalytic procedure for the fluorination of simple alkanes mediated by uranium species.¹⁰⁹

¹⁰⁶ a) S. Bloom, C. R. Pitts, R. Woltornist, A. Griswold, M. G. Holl, T. Lectka, *Org. Lett.* **2013**, *15*, 1722-1724. b) J.-B. Xia, Y. Ma, C. Chen, *Org. Chem. Front.* **2014**, *1*, 468-472.

¹⁰⁷ a) S. D. Halperin, H. Fan, S. Chang, R. E. Martin, R. Britton, *Angew. Chem. Int. Ed.* **2014**, *53*, 4690-4693. b) M. B. Nodwell, A. Bagai, S. D. Halperin, R. E. Martin, H. Knust, R. Britton, *Chem. Commun.* **2015**, *51*, 11783-11786S. c) D. Halperin, D. Kwon, M. Holmes, E. L. Regalado, L. C. Campeau, D. A. Dirocco, R. Britton, *Org. Lett.* **2015**, *17*, 5200-5203.

¹⁰⁸ a) M. B. Nodwell, H. Yang, M. Čolović, Z. Yuan, H. Merckens, R. E. Martin, F. Bénard, P. Schaffer, R. Britton, *J. Am. Chem. Soc.* **2017**, *139*, 3595-3598. b) R. Britton, Z. Yuan, M. Nodwell, H. Yang, N. Malik, H. Merckens, F. Benard, R. Martin, P. Schaffer, *Angew. Chem. Int. Ed.* **2018**, *57*, 12733-12736.

¹⁰⁹ J. G. West, T. A. Bedell, E. J. Sorensen, *Angew. Chem. Int. Ed.* **2016**, *55*, 8923-8927.

Chapter I. Introduction on C(sp³)-H Functionalization

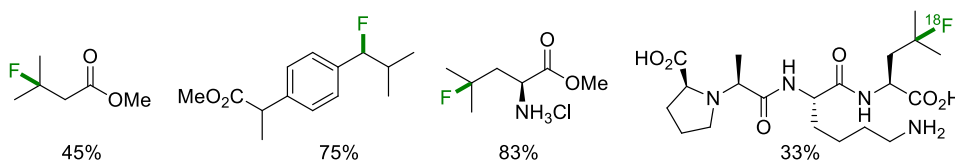


Figure 1.10: Selected examples accessed through decatungstate catalysis developed by Britton.

A very important contribution came from the group of Groves, who disclosed the use of manganese complexes for the fluorination of alkanes employing nucleophilic fluoride ions as fluorine source (Figure 1.11). The key performance of such system includes the use of an external oxidant (iodosobenzene, PhIO) to afford oxidized Mn^V species, which operate in a Mn^{III}/Mn^V catalytic cycle thus enabling the use of fluoride as fluorinating agent. The high valent Mn^V oxidize the substrate to key carbon centered radical in a one-electron process that renders a Mn^{IV} intermediary species bearing fluorine atoms in the coordination sphere. Fluorine atom transfer from the Mn^{IV} to the carbon centered radical yields the final fluorinated product and regenerates Mn^{III} catalyst. Their initial contribution involved the use of a porphyrin-based manganese catalyst, however, they shortly after described the use of rather less intricate catalytic systems like manganese-Salem salts complexes. Fine-tuning of the ligands substitution (both porphyrins and Salem) allow them to apply this methodology for fluorination of non-activated and activated aliphatic C-H positions.¹¹⁰ Moreover, they adapted both catalytic systems for ¹⁸F fluorination for PET imaging.¹¹¹

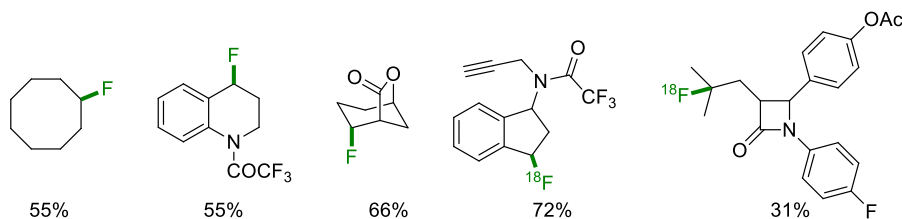


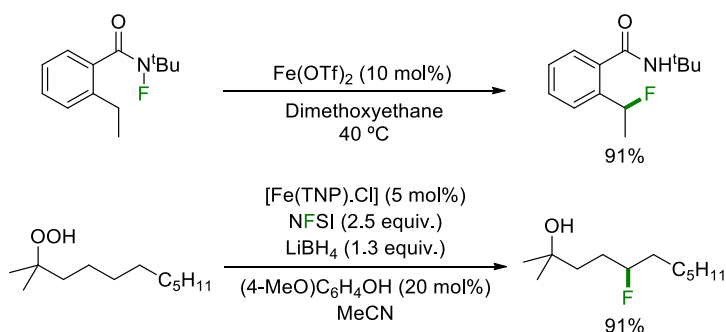
Figure 1.11: Selected examples accessed through manganese catalysis developed by Grooves.

All the methods discussed so far in this section correspond to direct C-H activation. In these procedures, the position selectivity is usually controlled by the bond dissociation energy (BDE) of the functionalized C-H bond. Inherently to this approach, selectivity

¹¹⁰ a) W. Liu, X. Huang, M.-J. Cheng, R. J. Nielsen, W. A. Goddard, J. T. Groves, *Science* **2012**, *337*, 1322-1325. b) W. Liu, J. T. Groves, *Angew. Chem. Int. Ed.* **2013**, *52*, 6024-6027. c) G. Li, A. K. Dilger, P. T. Cheng, W. R. Ewing, J. T. Groves, *Angew. Chem. Int. Ed.* **2018**, *57*, 1251-1255.

¹¹¹ a) X. Huang, W. Liu, H. Ren, R. Neelamegam, J. M. Hooker, J. T. Groves, *J. Am. Chem. Soc.* **2014**, *136*, 6842-6845. b) W. Liu, X. Huang, M. S. Placzek, S. W. Krska, P. McQuade, J. M. Hooker, J. T. Groves, *Chem. Sci.* **2018**, *9*, 1168-1172.

problems may be encountered when substrates offer aliphatic bonds with similar energy. An elegant solution to this problem implies the use of directing functionalities that will selectively afford one predictable position for its functionalization. This concept was applied by the group of Cook for iron catalyzed intramolecular directed benzylic fluorination employing fluoroamides both as fluorinating agent and as directing group (Scheme 1.29, top). The position selectivity is perfectly controlled by the intramolecular 1,5-HAT performed by the amidyl radical generated after fluoroamide activation with the iron catalyst.¹¹² The reaction does not require the use of an external oxidant, as it is a global redox neutral process (the fluoroamide acts as oxidant of the aliphatic C-H bond). Subsequently, Liu reported the use of hydroperoxides as active species for directed fluorination of non-activated aliphatic C-H bonds under iron catalysis (Scheme 1.29, bottom).¹¹³ In this reaction, the hydroperoxide moiety gets activated by the iron catalyst affording the corresponding oxygen-centered radical, which in this case performs the 1,5-HAT to generate the key carbon centered radical. Quenching of this radical with NFSI affords final fluorinated product formation.



Scheme 1.29: Directed radical-mediated fluorination procedures developed by Cook (top) and Liu (bottom).

Finally, the group Io Leonori explored in 2018 two photochemical approaches for the directed fluorination of oximes and amides (Scheme 1.30). For the first case, the authors developed an aliphatic fluorination method employing 9-mesityl-10-methylacridinium perchlorate as photoredox catalyst in combination with a silver co-catalyst.¹¹⁴ Homolytic cleavage of the oxime promoted by the catalytic mixture generates the analogous imidyl radical. Selective 1,5-HAT followed by Selectfluor quenching affords the final fluorinated product. For the amide series, an iridium based

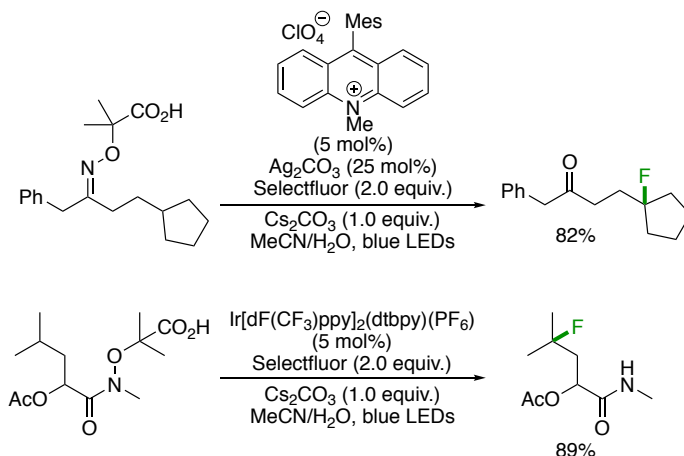
¹¹² B. J. Groendyke, D. I. Abusalim, S. P. Cook, *J. Am. Chem. Soc.* **2016**, *138*, 12771-12774.

¹¹³ H. Guan, S. Sun, Y. Mao, L. Chen, R. Lu, J. Huang, L. Liu, *Angew. Chem. Int. Ed.* **2018**, *57*, 11413-11417.

¹¹⁴ E. M. Dauncey, S. P. Morcillo, J. J. Douglas, N. S. Sheikh, D. Leonori, *Angew. Chem. Int. Ed.* **2018**, *57*, 744-748.

Chapter I. Introduction on C(sp³)-H Functionalization

photocatalyst was employed for generation of amidyl radicals, which engaged in the discussed selective 1,5-HAT.¹¹⁵ Quenching the carbon-centered radical with Selectfluor gave rise to a wide variety of fluorine-containing molecules. The later protocol could be effectively extended for directed fluorination of carbamates and even simple protected amines.



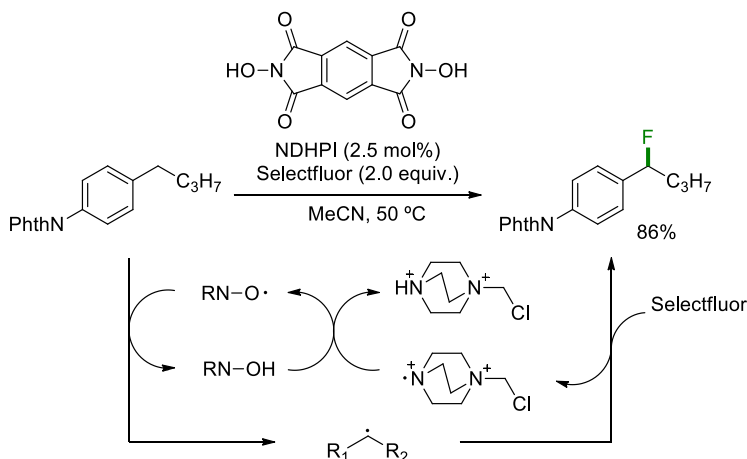
Scheme 1.30: Leonori's photochemical directed C(sp³)-H fluorination of oximes and amides.

1.5.2. Metal free C(sp³)-H fluorination

In parallel to procedures described above, the synthetic community explored novel fluorination technologies that avoid the use of transition metals. In this regard, the methodology described in this section follows the concept introduced in section 1.5.1.2. relying on the generation of carbon-centered radicals via intra- or intermolecular hydrogen abstraction events to further intercept these key aliphatic radical intermediates with a suitable fluorine source. The first example in these series was reported by Inoue in 2013 employing catalytic N,N-dihydroxypyromellitimide (NDHPI) as radical mediators in combination with Selectfluor (Scheme 1.31).¹¹⁶ The authors proposed that Selectfluor activates NDHPI to its corresponding N-oxyl radical which performs the intermolecular hydrogen abstraction at the substrate. Fluorine atom transfer to the carbon centered radical intermediate yields the final fluorinated product and Selectfluor-derived radical cation, which closes the catalytic cycle by one electron oxidation of the NDHPI to regenerate the N-oxyl radical species.

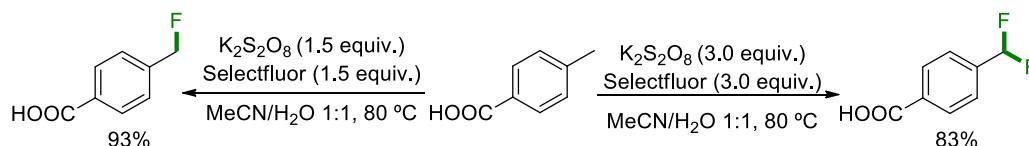
¹¹⁵ S. P. Morcillo, E. M. Dauncey, J. H. Kim, J. J. Douglas, N. S. Sheikh, D. Leonori, *Angew. Chem. Int. Ed.* **2018**, *57*, 12945-12949.

¹¹⁶ Y. Amaoka, M. Nagatomo, M. Inoue, *Org. Lett.* **2013**, *15*, 2160-2163.



Scheme 1.31: Inoue's metal free benzylic fluorination catalyzed by NDHPI.

A similar approach was developed by Lectka, who reported the use of catalytic Lewis acid BEt₃ as radical initiator in aerobic conditions for the fluorination of non-activated and activated aliphatic positions employing Selectfluor as fluorine source.¹¹⁷ The group of Tang reported a different approach that does not rely on the use of chemical mediators. The authors described a direct C-H fluorination employing Selectfluor in combination with potassium persulfate as oxidant.¹¹⁸ We can consider this work a metal free version of the silver-catalytic system reported by Tang that was discussed in the section 1.5.1.2 (Scheme 1.28).¹⁰⁷ The groups of Cai and Liang further expanded this protocol for the selective mono- and di-fluorination of benzylic positions (Scheme 1.32) and for ¹⁸F labeling respectively.¹¹⁹



Scheme 1.32: Cai's procedure for mono and di-fluorination of benzylic positions.

Photochemical processes were also explored in the context of metal free aliphatic fluorination. The pioneering work of Chen demonstrated the capacity of simple organic photosensitizer such as 9-fluorenone and xanthone for selective mono- and di-fluorination of benzylic C-H bonds respectively (Scheme 1.33).¹²⁰ Photoexcitation of the

¹¹⁷ C. R. Pitts, B. Ling, R. Woltornist, R. Liu, T. Lectka, *J. Org. Chem.* **2014**, *79*, 8895-8899.

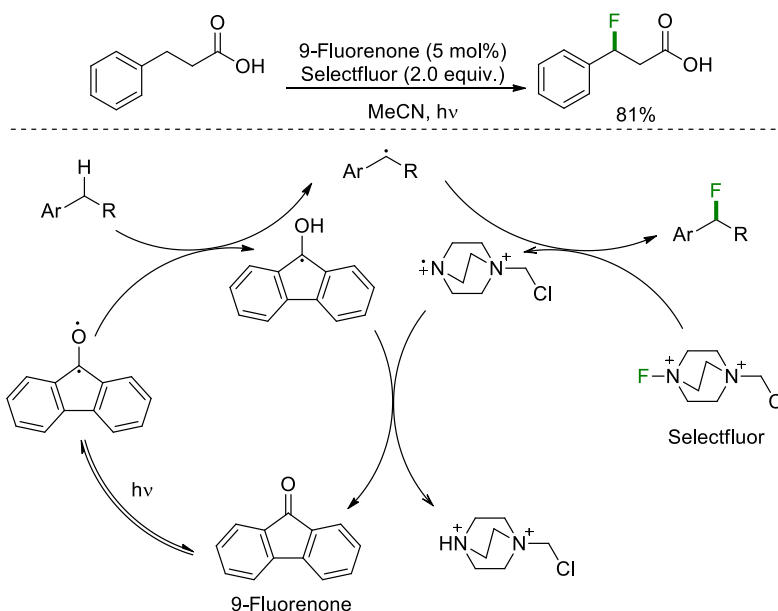
¹¹⁸ X. Zhang, S. Guo, P. Tang, *Org. Chem. Front.* **2015**, *2*, 806-810.

¹¹⁹ a) J. J. Ma, W. Bin Yi, G. P. Lu, C. Cai, *Org. Biomol. Chem.* **2015**, *13*, 2890-2894. b) G. Yuan, F. Wang, N. A. Stephenson, L. Wang, B. H. Rotstein, N. Vasdev, P. Tang, S. H. Liang, *Chem. Commun.* **2017**, *53*, 126-129.

¹²⁰ J. B. Xia, C. Zhu, C. Chen, *J. Am. Chem. Soc.* **2013**, *135*, 17494-17500.

Chapter I. Introduction on C(sp³)-H Functionalization

catalyst generates an active unpaired double radical species that performs hydrogen abstraction of the substrate affording the analogous carbon-centered benzylic radical. Radical quenching by Selectfluor gives rise to the final product and generates a nitrogen centered radical cation as byproduct. The catalytic cycle closes by reaction of this radical cation with the reduced form of the photocatalyst, thus regenerating the 9-fluorenone and allowing catalyst turnover.



Scheme 1.33: First metal free photochemical aliphatic fluorination.

Numerous contributions were developed in this respect by various groups, employing a plethora of photosensitizers such as dibenzosuberone,¹²¹ tetracyanobenzene,¹²² xanthone,¹²³ anthraquinone¹²⁴ or acetophenone.¹²⁵ In an interesting approach, the group of Hamashima also reported a fluorination method of molecules bearing a phthalimide moiety already installed which acts as internal photosensitizer.¹²⁶

¹²¹ D. D. Bume, C. R. Pitts, R. T. Jokhai, T. Lectka, *Tetrahedron* **2016**, *72*, 6031-6036.

¹²² a) S. Bloom, J. L. Knippel, T. Lectka, *Chem. Sci.* **2014**, *5*, 1175-1178. b) S. Bloom, M. McCann, T. Lectka, *Org. Lett.* **2014**, *16*, 6338-6341.

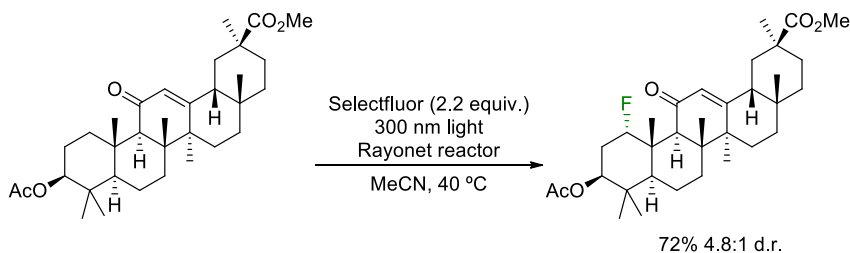
¹²³ D. Cantillo, O. de Frutos, J. A. Rincln, C. Mateos, C. O. Kappe, *J. Org. Chem.* **2014**, *79*, 8486-8490.

¹²⁴ C. W. Kee, K. F. Chin, M. W. Wong, C.-H. Tan, *Chem. Commun.* **2014**, *50*, 8211-8214.

¹²⁵ J.-B. Xia, C. Zhu, C. Chen, *Chem. Commun.* **2014**, *50*, 11701-11704.

¹²⁶ H. Egami, S. Masuda, Y. Kawato, Y. Hamashima, *Org. Lett.* **2018**, *20*, 1367-1370.

Finally, the group of Lectka performed some investigations in directed C-H aliphatic fluorination, in an attempt to completely control the position selectivity of the fluorination event. Specifically, the authors found that it was possible to use α,β -unsaturated ketones as both internal sensitizers and directing groups for aliphatic fluorination of a wide variety of complex polycyclic terpenoids (Scheme 1.34).¹²⁷ Furthermore, they developed a modification of this rather simple conditions by introducing an external photosensitizer, which allowed for directed fluorination of simple ketones or α,β -unsaturated ketones employing a milder light source.¹²⁸



Scheme 1.34: Photochemical fluorination of cyclic terpenoids.

¹²⁷ C. R. Pitts, D. D. Bume, S. A. Harry, M. A. Siegler, T. Lectka, *J. Am. Chem. Soc.* **2017**, *139*, 2208-2211.

¹²⁸ a) D. D. Bume, C. R. Pitts, F. Ghorbani, S. A. Harry, J. N. Capilato, M. A. Siegler, T. Lectka, *Chem. Sci.* **2017**, *8*, 6918-6923. b) D. D. Bume, S. A. Harry, C. R. Pitts, T. Lectka, *J. Org. Chem.* **2018**, *83*, 1565-1575.

Chapter I. Introduction on C(sp³)-H Functionalization

1.6. Global objectives

The present doctoral Thesis is focused on the development of novel C-H functionalization methods of sp³ carbon centers, with a particular insight in C-H amination and C-H fluorination reactions. Considering the current performance of state-of-the-art C(sp³)-H functionalization reactions and the experience in our group on the Hofmann-Löffler reaction, we devised to apply the conceptual working mode of such reaction for the development of innovative synthetic procedures. In this sense, we envisioned to use the Hofmann-Löffler reaction as scaffold for the development of more sustainable and atom economic methods for preparation of biologically interesting compounds. Additionally, we intended to identify unexplored functionalities as suitable groups for its activation toward directed aliphatic C-H functionalization.

First, we aimed to develop a sustainable electrochemical Hofmann-Löffler reaction, since this overall cyclization reaction is a formal two electron oxidation of an open-chain substrate. Even though the inherent benefits of electrochemical processes, intramolecular aliphatic C-H amination was not previously realized. The Hofmann-Löffler reaction appeared as the suitable scenario for an anodic oxidation which will avoid the use of catalysts and stoichiometric chemical oxidants. Furthermore, the two protons that are generated as sole byproduct of the cyclization reaction could be reduced at the cathode to close the electrochemical circuit.

Subsequently we directed our efforts to study an unprecedented activation of N-fluorosulfonamides toward intramolecular amination for the synthesis of saturated N-heterocycles. In the Hofmann-Löffler reaction context, a wide variety of preformed or in situ generated haloamines can be employed to promote the reaction. While haloamine derivatives where the halogen atom is iodine, bromine or chlorine have been extensively studied, the corresponding fluorinated series has been neglected. Consequently, we envisioned a copper catalytic system for activation of N-F bonds, which could be utilized as effective amidyl-radical precursors, suitable aminating groups and internal oxidants in the Hofmann-Löffler reaction.

Finally, we planned to exploit the concept of 'interrupted Hofmann-Löffler' for the directed fluorination of tertiary C-H bonds. On that regard, it was designed an iodine catalytic system that would perform selective aliphatic iodination following the classical Hofmann-Löffler reaction pathway. At this stage, a second oxidation event could be engaged to afford an hypervalent alkyl-iodine(III) intermediate. At conditions which intramolecular amination is not kinetically competent, such intermediate bearing a supernucleophile group could be nucleophilically displaced by a fluoride anion. This intended approach would afford a mild metal free protocol for C-H fluorination employing simple nucleophilic fluoride as fluorine source.

Chapter II: Anodic Benzylic C(sp³)-H Amination: A Unified Access to Pyrrolidines and Piperidines

Chapter II: Anodic Benzylic C(sp³)-H Amination:
A Unified Access to pyrrolidines and Piperidines

2.1. Introduction: Electrochemical amination.

Electrochemical processes have been applied for the preparation of valuable chemicals on an industrial scale for more than 100 years. However, its use in small scale preparation of fine chemicals and in basic research has been neglected by the synthetic community. From an environmental perspective, electrochemistry represents the most economical and ecological strategy to accomplish redox transformations. In this sense, it fulfils most of the principles of green chemistry.¹²⁹ From the atom economy point of view, electrochemical transformations avoid the use of stoichiometric oxidants or reductants, since only electrons are used as reagent, thus avoiding the generation of chemical waste. This aspect is even more sustainable if we take into account the current trend of developed societies to use more and more renewable resources for electricity generation (even though hydrocarbon combustion is still the first electricity source worldwide). In most of the cases, electrochemical setups are relatively simple, and operate under mild conditions like room temperature or non-anhydrous conditions. Inherently to the electrochemical setup, scale-up of small-scale processes are usually simpler when compared with traditional non-electrochemical methods. Even though stoichiometric amounts of byproducts are generated in all electrochemical reactions to close the cell circuit, paired electrolysis can be performed in order to obtain two valuable compounds out of the same process. In fact, in the vast majority of electrochemical oxidative processes, the byproduct generated at the cathode is molecular hydrogen. Furthermore, redox mediators may be introduced in particular challenging electrochemical procedures to improve efficiency and reduce byproduct formation (Figure 2.1).¹³⁰

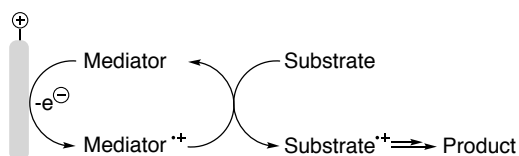


Figure 2.1: Anodic oxidation employing a chemical mediator.

Prompted by the increasing awareness of the environmental impact of chemical processes, electroorganic synthesis is experiencing a renaissance which started roughly two decades ago.¹³¹ The availability of standardized electrochemical kits and screening

¹²⁹ B. A. Frontana-Urbe, R. D. Little, J. G. Ibanez, A. Palma, R. Vasquez-Medrano, *Green Chem.* **2010**, *12*, 2099-2119.

¹³⁰ R. Francke, R. D. Little, *Chem. Soc. Rev.* **2014**, *43*, 2492-2521.

¹³¹ a) M. Yan, Y. Kawamata, P. S. Baran, *Chem. Rev.* **2017**, *117*, 13230-13319. b) E. J. Horn, B. R. Rosen, P. S. Baran, *ACS Cent. Sci.* **2016**, *2*, 302-308. c) A. Wiebe, T. Gieshoff, S. Möhle, E. Rodrigo,

Chapter II: Anodic Benzylic C(sp³)-H Amination:
A Unified Access to pyrrolidines and Piperidines

systems fully implemented increased its applicability.¹³² In this sense, it exhibited an increased use in synthetic research laboratories that were not exclusively focused on electrochemistry. As a consequence, electrochemical methods have been used for a wide variety of transformations, including late stage functionalization and synthesis of natural product, even outperforming in some cases the classical non-electrochemical analogous reactions.¹³³

Particularly, electrochemical reactions for C-N bond forming have been extensively studied and applied for the synthesis of nitrogen-containing heterocycles when performed in an intramolecular manner.¹³⁴ In this context, electrochemical generation of nitrogen-centered radicals and their potential use in amination reactions was known since late 1970. However, its study was reduced to few examples, since high reactive deprotonated amides or amines had to be employed as nitrogen-centered radical precursors.¹³⁵ It was in 2008 when the group of Moeller reported an effective pyrrolidine synthesis through intramolecular sulfonamide addition to electron-rich alkenes by means of electrochemically generated amidyl radicals (Scheme 2.1).¹³⁶ The authors discussed that this oxidative alkene functionalization reaction starts with deprotonation of the tosylamide to the corresponding amidate, which is oxidized at the glassy carbon anode to the resultant nitrogen-centered amidyl radical. Radical addition to the alkene renders a carbon centered-radical that engages in a second anodic SET oxidation yielding a carbocation intermediate. Final carbocation trapping by the methanol solvent yields the corresponding pyrrolidine. To close the electrochemical circuit, hydrogen evolution takes place at the platinum cathode.

M. Zirbes, S. R. Waldvogel, *Angew. Chem. Int. Ed.* **2018**, *57*, 5594-5619. d) S. Möhle, M. Zirbes, E. Rodrigo, T. Gieshoff, A. Wiebe, S. R. Waldvogel, *Angew. Chem. Int. Ed.* **2018**, *57*, 6018-6041.

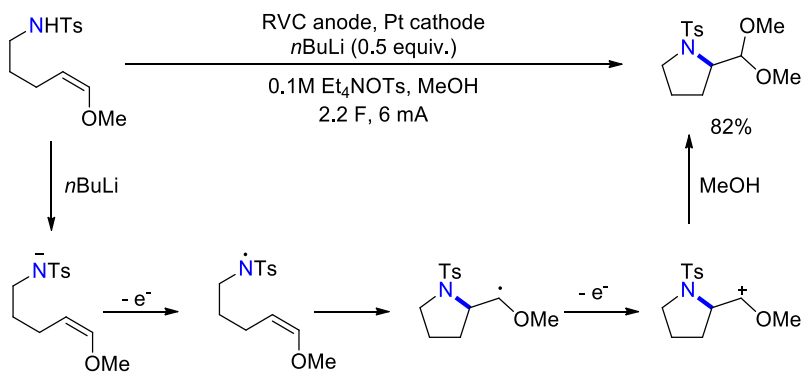
¹³² For example, IKA offers lab-scale electrochemical kits: <https://www.ika.com/en/Products-Lab-Eq/Electrochemistry-Kit-csp-516/>

¹³³ a) J. Mihelcic, K. Moeller, *J. Am. Chem. Soc.* **2004**, *126*, 9106-9111. b) B. R. Rosen, E. W. Werner, A. G. O'Brien, P. S. Baran, *J. Am. Chem. Soc.* **2014**, *136*, 5571-5574. c) A. Lipp, D. Ferenc, C. Gütz, M. Geffe, N. Vierengel, D. Schollmeyer, H. J. Schäfer, S. R. Waldvogel, T. Opatz, *Angew. Chem. Int. Ed.* **2018**, *57*, 11055-11059. d) R. R. Merchant, K. M. Oberg, Y. Lin, A. J. E. Novak, J. Felding, P. S. Baran, *J. Am. Chem. Soc.* **2018**, *140*, 7462-7465.

¹³⁴ Y. Jiang, K. Xu, C. Zeng, *Chem. Rev.* **2018**, *118*, 4485-4540.

¹³⁵ a) R. Bauer, H. Wendt, *Angew. Chem. Int. Ed.* **1978**, *17*, 202-203. b) M. Tokuda, T. Miyamoto, H. Fujita, H. Sugimoto, *Tetrahedron*, **1991**, *47*, 747-756. d) T. Fuchigami, T. Sato, T. Nonaka, *J. Org. Chem.* **1986**, *51*, 366-369.

¹³⁶ H.-C. Xu, K. D. Moeller, *J. Am. Chem. Soc.* **2008**, *130*, 13542-13543.



Scheme 2.1: Moeller's anodic electron-rich alkene difunctionalization for pyrrolidine synthesis.
RVC = reticulated vitreous carbon.

The same authors reported modifications of the initial reaction conditions to avoid the inconvenient use of *n*BuLi, expanding the reaction to the cyclization of simple free primary amines. In addition, access to piperidine products was achieved when substrates bearing the alkene functionality at the 6-position were employed (in general, a poorer performance was observed for piperidine formation compared with the corresponding pyrrolidine series).¹³⁷

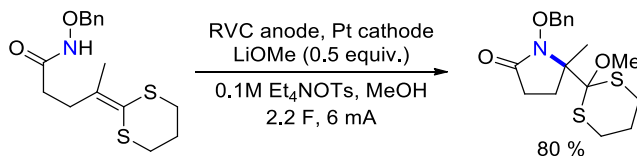
Moreover, the authors performed extended mechanistic studies in order to corroborate what was previously postulated (Scheme 2.1). It was envisioned that the first SET oxidation could take place at the alkene functionality rather than at the amide, thus generating an alkene radical cation that will be attacked by the sulfonamide in an intramolecular fashion. In that putative mechanism, the sulfonamide acts as a nucleophile rather than as a radical generator. A series of experiments involving the presence of a competing nucleophilic group at the substrate allowed to conclude that these two pathways might compete in this reaction. However, the authors reported that one pathway could be selectively chosen over the other by modification of the electrolyte composition of the media.¹³⁸ Furthermore, they reported a similar protocol of γ -lactam synthesis via difunctionalization of unsaturated amides initiated by an electrochemical amidyl-radical (Scheme 2.2).¹³⁹ In this case, the authors discussed an analogous mechanism from what had been disclosed for the previous examples.

¹³⁷ a) H.-C. Xu, K. D. Moeller, *J. Am. Chem. Soc.* **2010**, *132*, 2839-2844. b) H.-C. Xu, K. D. Moeller, *Angew. Chem. Int. Ed.* **2010**, *49*, 8004-8007.

¹³⁸ J. M. Campbell, H.-C. Xu, K. D. Moeller, *J. Am. Chem. Soc.* **2012**, *134*, 18338-18344.

¹³⁹ H.-C. Xu, J. M. Campbell, K. D. Moeller, *J. Org. Chem.* **2014**, *79*, 379-391.

Chapter II: Anodic Benzylic C(sp³)-H Amination:
A Unified Access to pyrrolidines and Piperidines



Scheme 2.2: Electrochemical amidyl-radical generation for γ -lactam synthesis. RVC = reticulated vitreous carbon.

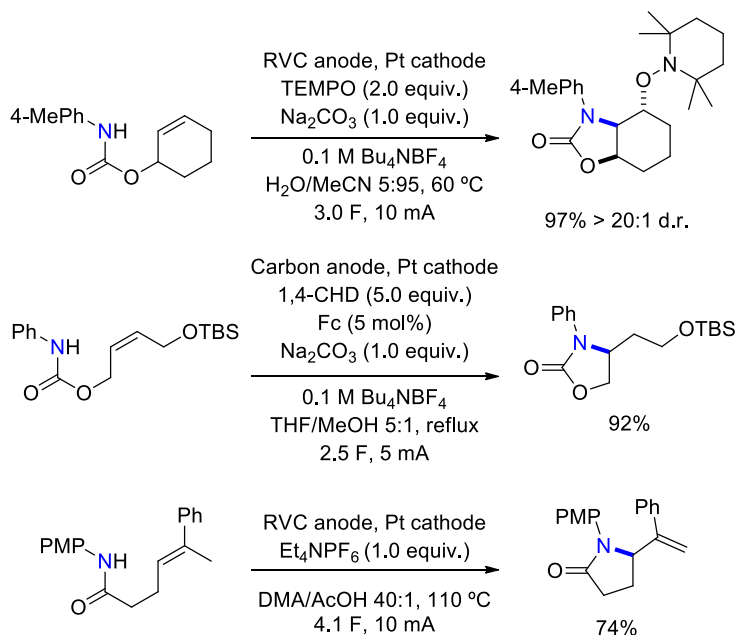
The group of Xu extensively worked in related electrochemical amination reactions involving nitrogen-centered radical intermediates. They reported different conditions for the cyclization of amides and carbamates (Scheme 2.3). Following Moeller's alkene functionalization,¹³⁷⁻¹³⁹ they described an amino-oxygenation protocol that employs TEMPO as radical trap for the carbon-centered radical generated after amidyl radical addition to the double bond (Scheme 2.3, top).¹⁴⁰ The group of Wirth engineered a microreactor for this electrochemical process that allowed its use in flow, improving the performance.¹⁴¹ In a different approach, Xu described an anodic reaction performed in presence of 1,4-cyclohexadiene (1,4-CHD) as reductant and employing ferrocene as electrochemical mediator, resulting in a formal alkene hydroamination reaction (Scheme 2.3, middle).¹⁴² In addition, they reported that unsaturated amides and carbamates could be involved in elimination reactions at the carbocation intermediate state, thus yielding the corresponding allylic aminated products (Scheme 2.3, bottom).¹⁴³

¹⁴⁰ F. Xu, L. Zhu, S. Zhu, X. Yan, H.-C. Xu, *Chem. Eur. J.* **2014**, *20*, 12740-12744.

¹⁴¹ A. A. Folguez-Amador, K. Philipps, S. Guilbaud, J. Poelakker, T. Wirth, *Angew. Chem. Int. Ed.* **2017**, *56*, 15446-15450.

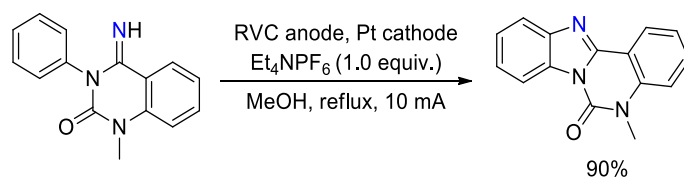
¹⁴² L. Zhu, P. Xiong, Z.-Y. Mao, Y.-H. Wang, X. Yan, X. Lu, H.-C. Xu, *Angew. Chem. Int. Ed.* **2016**, *55*, 2226-2229.

¹⁴³ P. Xiong, H.-H. Xu, H.-C. Xu, *J. Am. Chem. Soc.* **2017**, *139*, 2956-2959.



Scheme 2.3: Electrochemical amidyl radical-driven amino-oxygenation (top), hydroamination (middle) and amination (bottom) of alkenes. RVC = reticulated vitreous carbon.

The same group reported an elegant indole synthesis through intramolecular electrochemical amino-arylation of triple bonds employing ferrocene as redox mediator.¹⁴⁴ A similar cascade amino-arylation of alkynes protocol was applied for the synthesis of extended polycyclic heteroaromatic compounds.¹⁴⁵ Furthermore, they explored electrochemical generation of imidyl radicals for benzimidazole synthesis via radical addition to aryl rings (Scheme 2.4).¹⁴⁶



Scheme 2.4: Xu's electrochemical benzimidazole synthesis.

¹⁴⁴ Z.-W. Hou, Z.-Y. Mao, H.-B. Zhao, Y. Y. Melcamu, X. Lu, J. Song, H.-C. Xu, *Angew. Chem. Int. Ed.* **2016**, *55*, 9168-9172.

¹⁴⁵ Z.-W. Hou, Z.-Y. Mao, J. Song, H.-C. Xu, *ACS Catal.* **2017**, *7*, 5810-5813.

¹⁴⁶ H.-B. Zhao, Z.-W. Hou, Z.-J. Liu, Z.-F. Zhou, J. Song, H.-C. Xu, *Angew. Chem. Int. Ed.* **2017**, *56*, 587-590.

Chapter II: Anodic Benzylic C(sp³)-H Amination:
A Unified Access to pyrrolidines and Piperidines

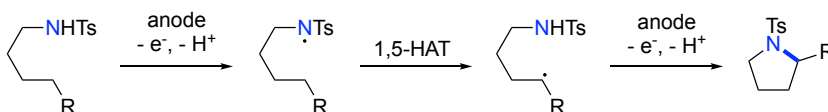
The group of Yoshida reported another electrochemical amino-oxygenation of double bonds for the synthesis of pyrrolidines bearing exo-cyclic ketones.¹⁴⁷ However, this protocol involves stepwise generation and accumulation of reactive intermediates at low temperatures and quenching those by suitable nucleophiles in a working mode known as the 'cation pool method'.¹⁴⁸ Additional methods for electrochemical amination of arenes were reported by Yoshida and Xu, however, these rely on direct arene oxidation and nucleophilic attack by nitrogen nucleophiles rather than radical nitrogen intermediate species generation.¹⁴⁹ Taking all these literature precedents into consideration, it can be concluded that electrochemical amination methods are feasible, even involving the utilization of amidyl-radical intermediates. However, these technologies have been applied only for the functionalization of sp² C-H bonds. In sharp contrast, electrochemical aliphatic C-H amination has been overlooked. Undoubtedly, electrochemical C(sp³)-H amination would be of mayor interest, especially in the context of saturated heterocycle formation for the synthesis of pharmaceutically important molecules such as pyrrolidines or piperidines.

Our group worked extensively on intramolecular aliphatic C-H amination over the past years for pyrrolidine synthesis involving the exploitation of amidyl radicals within the Hofmann-Löffler reaction.^{71c,72,74,75,78} Specifically, we reported a double catalytic system which employs molecular oxygen as terminal oxidant to generate nitrogen-centered radicals in an environmentally benign manner.⁷⁵ However, we envisioned an even more sustainable method for pyrrolidine synthesis dealing with a direct electrochemical oxidation of an aliphatic amine substrate to render cyclized pyrrolidine formation, since that cyclization step formally represents just a two electron oxidation. In this simple electrochemical approach, a sulfonamide substrate would be anodically oxidized to its corresponding amidyl radical. Selective 1,5-HAT would deliver a carbon centered radical that could be engaged in a second single electron oxidation at the anode surface generating a carbocation that would be immediately intramolecularly trapped by the sulfonamide that drove the transformation. The two protons generated as reaction byproduct could be reduced at the cathode thus affording hydrogen evolution and closing the electrochemical circuit. With this conceptual design in mind, we started our investigations in order to achieve the first electrochemical intramolecular C(sp³)-H amination protocol.

¹⁴⁷ Y. Ashikari, T. Nokami, J.-I. Yoshida, *Org. Biomol. Chem.* **2013**, *11*, 3322-3331.

¹⁴⁸ Y.-I. Yoshida, A. Shimizu, R. Hayashi, *Chem. Rev.* **2018**, *118*, 4702-4730.

¹⁴⁹ a) T. Morofuji, A. Shimizu, J.-I. Yoshida, *J. Am. Chem. Soc.* **2014**, *136*, 4496-4499. b) T. Morofuji, A. Shimizu, J.-I. Yoshida, *Chem. Eur. J.* **2015**, *21*, 3211-3214. c) H.-B. Zhao, Z.-J. Liu, J. Song, H.-C. Xu, *Angew. Chem. Int. Ed.* **2017**, *56*, 12732-12735.



Scheme 2.5: Envisioned concept for amidyl radical directed electrochemical pyrrolidine synthesis.

2.2. Results and discussion

We started our studies by building a rather simple electrochemical set-up (Figure 2.2). We employed a multimeter as current display, connected to an in-house build DC-power supply. For the electrochemical reactor we employed a simple Schlenk flask (undivided cell) with a Teflon cap that held the electrodes. A graphite rod was used as anode while platinum mesh acted as cathode.

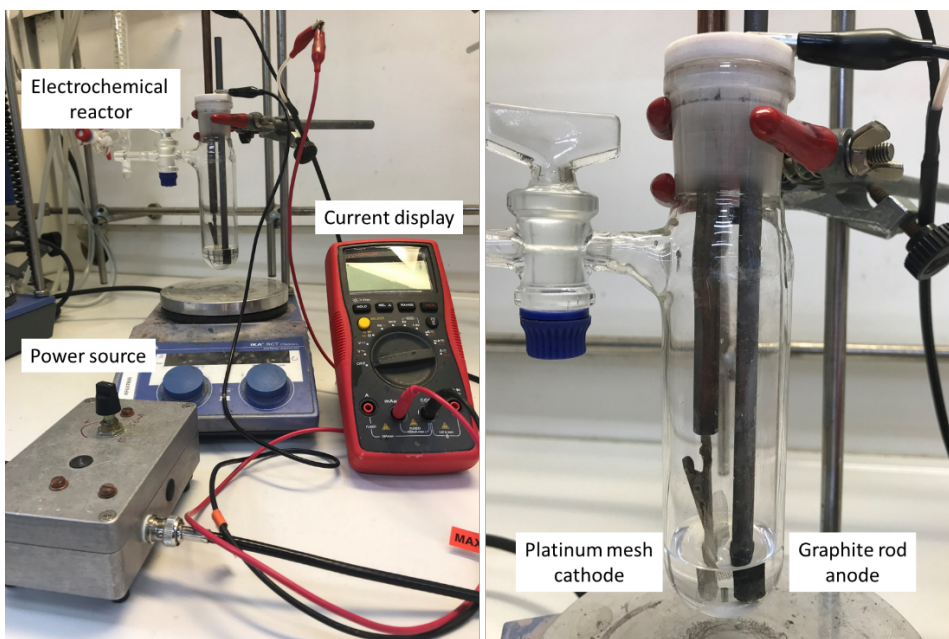


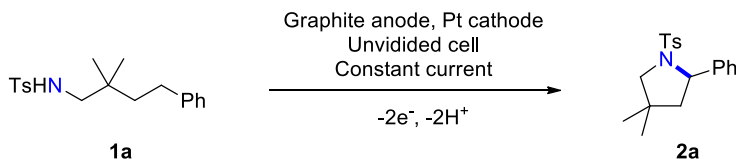
Figure 2.2: Electrochemical set-up.

In this simple set-up we started our optimization studies. We chose sulfonamide **1a** as standard substrate since it was successfully used in the past for our halogen-catalyzed Hofmann-Löffler reaction studies. Initial anodic oxidation of **1a** was performed in an undivided cell under constant current conditions. First experiments involved the use of similar conditions to those reported in the literature for electrochemical amidyl radical generation toward alkene functionalization, with a 5 mA current and an amount of charge of 2.2F.¹³⁶⁻¹³⁸ Electrochemical oxidation employing LiClO₄ in methanol or methanol/THF in the presence of sodium methoxide led to low yields of pyrrolidine **2a** (Table 2.1, entries 1 and 2). Change of the supporting electrolyte to Et₄NOTs or Bu₄NPF₆

Chapter II: Anodic Benzylic C(sp³)-H Amination:
A Unified Access to pyrrolidines and Piperidines

did not improve the reaction performance (entries 3 and 4). However, when changing the solvent to HFIP (1,1,1,3,3,3-Hexafluoro-2-propanol or hexafluoroisopropanol) keeping Bu₄NPF₆ as electrolyte we observed a dramatic improvement of product formation to 67% isolated yield of **2a** (entry 5). HFIP has proven to be a unique solvent for a plethora of organic transformations because of its distinctive physicochemical properties. Among these properties, particularly illustrative is its enhanced acidity (pK_a = 9.3), thermal and redox stability, low nucleophilicity and high hydrogen bonding ability. Because of these properties, HFIP possesses a stabilization ability of short-lived reactive organic intermediates such as radical cations. In consequence, it has been the key to success for numerous works in the fields of transition metal catalysis, photochemistry, hypervalent iodine chemistry, polymer synthesis or electrochemistry among others.¹⁵⁰

Once HFIP was established as the optimum solvent, the amount of charge was briefly evaluated, obtaining the best results with 2.2 F (entries 6 and 7). Increasing or decreasing the amount of charge did not improve the reaction outcome. A superior 77% isolated yield of **2a** was obtained when the current was reduced to 2.5 mA, albeit further current reduction proved to be counterproductive (entries 8 and 9). As mentioned, the use of HFIP remained crucial since the presence of a cosolvent such as acetonitrile resulted in a clear drop of **2a** yield (entry 10). Supporting electrolyte screening let us afford the best yield of **2a** formation, corresponding to 85% when Bu₄NBF₄ was employed (entries 12 and 13). 0.1 M concentration of the supporting electrolyte was proven to be the best one since neither increasing nor reducing its concentration showed a beneficial effect in cyclization yield (entries 14 and 15). Finally, with optimized conditions in hand, we demonstrated the robustness of the method by a single run of 1.0 mmol and 3.0 mmol of substrate, obtaining in both cases a comparable excellent performance (entries 16 and 17). It is worth to mention that these scaled-up experiments were performed within the same solvent and supporting electrolyte amounts, just adapting the amount of charge. This exemplifies how, in general, electrochemical processes are easily scaled-up when compared with its non-electrochemical methods analogues. Generation of reactive intermediate species only takes place at the electrodes surface, thus usually avoiding unproductive side reactions when working in high substrate concentrations.



¹⁵⁰ a) A. Berkessel, J. A. Adrio, D. Hüttenhain, J. M. Neudörfl, *J. Am. Chem. Soc.* **2006**, *128*, 8421-8426. b) I. Colomer, A. Chamberlain, M. Haughey, T. J. Donohoe, *Nat. Rev. Chem.* **2017**, *1*, 0088.

Entry	Electrolyte	Additive	Current (mA)	Amount of Charge (F)	2a yield (%)
1	0.1 M LiClO ₄ /MeOH	0.5 eq. NaOMe	5	2.2	23
2	0.1 M LiClO ₄ , 60% MeOH/THF	0.5 eq. NaOMe	5	2.2	25
3	0.1 M Et ₄ NOTs/MeOH	0.5 eq. NaOMe	5	2.2	traces
4	0.1 M Bu ₄ NPF ₆ /MeOH	0.5 eq. NaOMe	5	2.2	traces
5	0.1 M Bu ₄ NPF ₆ /HFIP	-	5	2.2	67
6	0.1 M Bu ₄ NPF ₆ /HFIP	-	5	2.0	61
7	0.1 M Bu ₄ NPF ₆ /HFIP	-	5	2.4	52
8	0.1 M Bu ₄ NPF ₆ /HFIP	-	2.5	2.2	77
9	0.1 M Bu ₄ NPF ₆ /HFIP	-	1.5	2.2	70
10	0.1 M Bu ₄ NPF ₆ , 50% CH ₃ CN/HFIP	-	2.5	2.2	24
11	0.05 M Bu ₄ NPF ₆ /HFIP	-	2.5	2.2	65
12	0.1 M Et ₄ NOTs/HFIP	-	2.5	2.2	53
13	0.1 M Bu ₄ NBF ₄ /HFIP	-	2.5	2.2	85
14	0.05 M Bu ₄ NBF ₄ /HFIP	-	2.5	2.2	68
15	0.2 M Bu ₄ NBF ₄ /HFIP	-	2.5	2.2	70
16 ^[a]	0.1 M Bu ₄ NBF ₄ /HFIP	-	2.5	2.2	80
17 ^[b]	0.1 M Bu ₄ NBF ₄ /HFIP	-	2.5	2.2	73

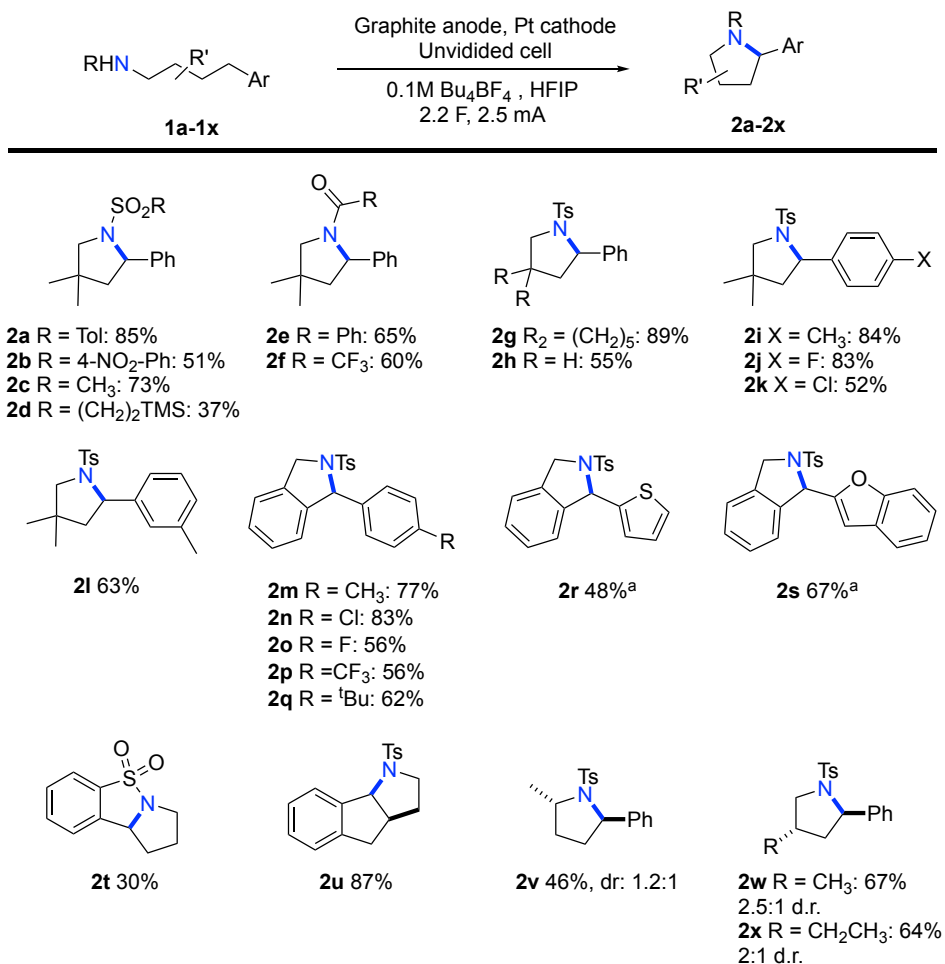
Table 2.1: Optimization studies for electrochemical pyrrolidine formation. Isolated yields. 0.2 mmol substrate scale. [a] 1.0 mmol of substrate. [b] 3.0 mmol of substrate.

Once we obtained optimized conditions for this novel electrochemical intramolecular aliphatic C-H amination, we studied the scope of the reaction for pyrrolidine formation (Scheme 2.6). Different sulfonamides like nosylamide and mesylamide could be effectively employed for pyrrolidine formation as demonstrated by **2b-2c**. In this sense, even labile protecting group such as 2-(Trimethylsilyl)ethanesulfonyl could be successfully employed (**2d**), facilitating a further deprotection step in order to access

Chapter II: Anodic Benzylic C(sp³)-H Amination:
A Unified Access to pyrrolidines and Piperidines

the free pyrrolidines. Carbonyl protecting groups were tolerated under the oxidative conditions, offering an alternative to sulfonyl protecting groups since compounds **1e** and **1f** afforded pyrrolidine formation in 65% and 60% isolated yield, respectively. Compound **1g** bearing a cyclohexyl group at the carbon backbone cyclized to pyrrolidine **2g** in an excellent 89% yield because of its increased Thorpe-Ingold effect. However, a Thorpe-Ingold effect is not required as demonstrated by compound **2h**, which was successfully synthesized, albeit in a lower yield of 55%. Para-substitution at the phenyl ring was tolerated including mild electron-donating and electron-withdrawing groups (**2i-2k**) as well as meta-substitution (**2l**). The present electrochemical transformation was applied for the synthesis of a wide variety of isoindolines, tolerating substitution patterns such as methyl, *tert*-butyl, chloro, fluoro and even trifluoromethyl at the 4-position of the aryl moiety as demonstrated by compounds **2m-2q**. Furthermore, it was possible to access isoindolines **2r** and **2s** bearing electron-rich aromatics such as thiophene and benzofurane in decent yields of 48% and 67%, respectively. Yet, a reduced current of 1 mA had to be employed for the preparation of such low oxidation potential compounds to prevent overoxidation. Transannular cyclization was also feasible for the preparation of [6,5,5]-fused ring compound **2t**. As expected, when compound **1u** was submitted to anodic oxidation, **2u** was obtained as a single *syn*-diastereoisomer in an excellent 87% yield. On the other hand, when compounds bearing mono-substitution at the carbon backbone were employed, still a remarkable acyclic stereocontrol was achieved. Compound **2v** bearing a methyl group alpha to the nitrogen functionality afforded a modest 1.2:1 diastereomeric ratio in favor of the *anti*- product, while compounds **2w** and **2x** achieved 2.5:1 and 2:1 diastereomeric ratio respectively in favor of the *anti*- compound as well in good yields.

In view of these results, we wondered whether the reaction could be applied for substrates bearing an extra methylene group at the carbon backbone. A priori, these substrates might trigger a cyclization either at the homobenzylic position en route to a pyrrolidine backbone following a Hofmann-Löffler-type reaction, or at the benzylic position, thus delivering a piperidine framework.

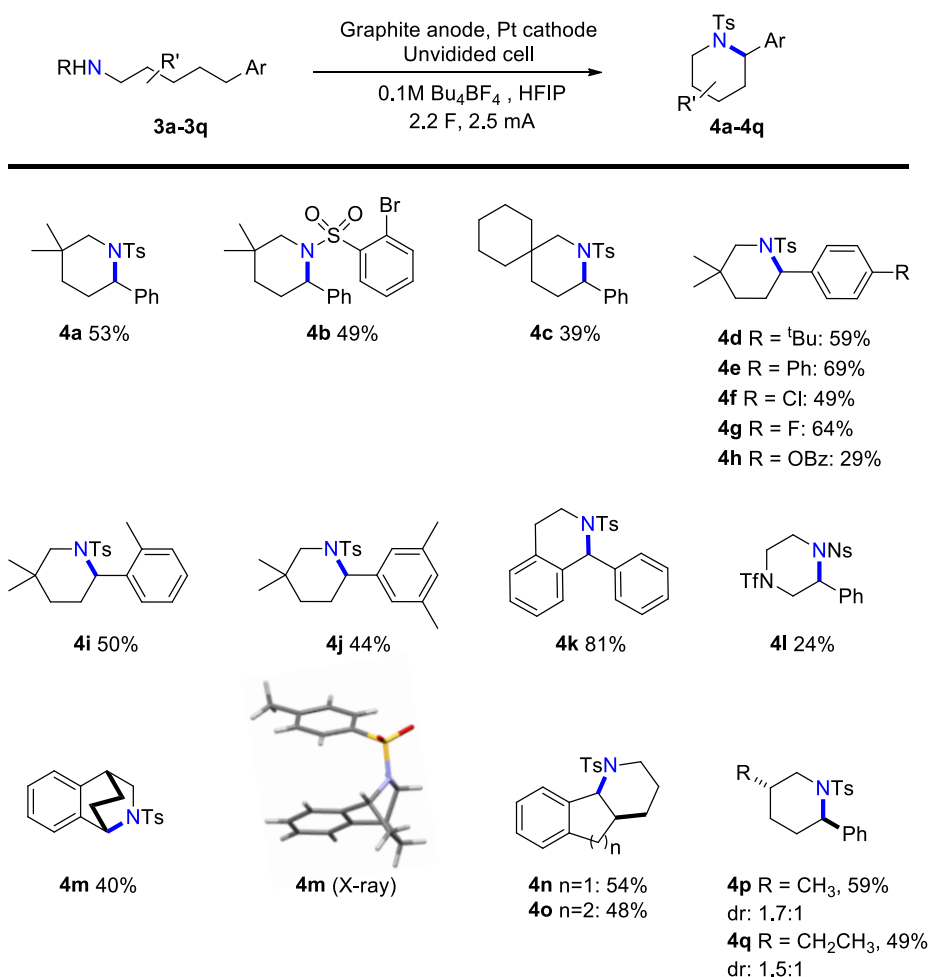


Scheme 2.6: Electrochemical pyrrolidine formation scope. ^a1 mA of current.

To our delight, we observed a smooth cyclization to the corresponding piperidine products, which represents a new entry for this class of saturated heterocycles. We subsequently investigated the scope for piperidine formation (Scheme 2.7). Cyclization could be performed using not only tosylamides, but also substrates bearing different sulfonyl protecting groups like **3b** bearing 2-bromophenyl-sulfonyl protecting group, which afforded **4b** in 49% yield. A modified backbone substitution was tolerated to access spirocyclic compound **4c**. Analogously to the pyrrolidine series, *para*-substitution at the phenyl ring was tolerated for a wide variety of functionalities like alkyl and aryl groups, electron-withdrawing groups such as chlorine and fluorine or benzoate (**4d-4h**). Further sterically demanding substitution patterns at the phenyl ring were equally suitable for piperidine formation as demonstrated by compound **4i** bearing an *ortho*-methyl group. Additionally, piperidine **4j** bearing *meta*, *meta*-bismethyl groups could be prepared. Compound **3k** bearing an accessible double

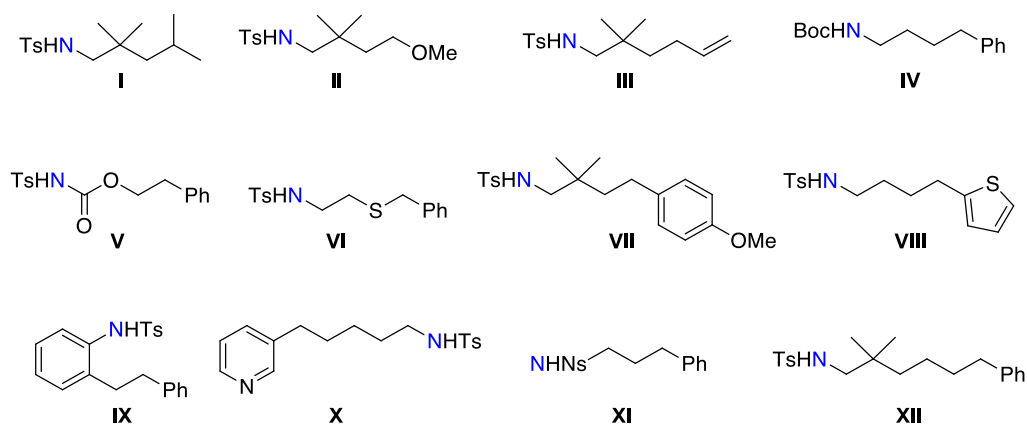
Chapter II: Anodic Benzylic C(sp³)-H Amination:
 A Unified Access to pyrrolidines and Piperidines

activated position was employed for successful preparation of tetrahydroisoquinoline **4k** in excellent 81% isolated yield. Heteroatoms such as nitrogen could be present at the carbon backbone, albeit in lower yields. In this case, the introduction of an electron-withdrawing group at the nitrogen was crucial to achieve productive cyclization. Anodic oxidation was used to prepare bicyclo[2.2.2]-compound **4m**, the structure of which was unambiguously confirmed by single crystal X-ray analysis. As for the pyrrolidine series, full cyclic diastereocontrol occurred in the preparation of [6,5,5]-fused and [6,6,5]-fused compounds **4n** and **4o**, that were obtained as single *syn*- diastereoisomers. Finally, partial acyclic diastereocontrol was exercised for compounds bearing mono-substitution at the carbon backbone, as exemplified by compounds **4p** and **4q**, that were prepared in 59% and 49% yield in a 1.7:1 and 1.5:1 diastereomeric ratio in favor of the *anti*- products.



Scheme 2.7: Electrochemical piperidine formation scope.

At this point it is worth mentioning the limitations of our protocol (Scheme 2.8). The main restriction of the present electrochemical amination method is that an activated benzylic position is required. Compound **I** with a tertiary aliphatic position remained unreactive when submitted to anodic oxidation. Compounds **II** and **III** bearing activated α -heteroatom and allylic positions suffered from overoxidation problems, resulting in complex reaction mixtures in both cases. Boc-protected amine **IV** and carbamate **V** did not lead to productive amination, since overoxidation was observed, demonstrating that sulfonamides and amides are the optimum amine source functionalities for the present protocol. A common limitation in electroorganic synthetic procedures involves overoxidation when electron rich functionalities with a low oxidation potential are present in the substrates. This limitation also affected our system, as exemplified by thioether **VI**, anisole **VII**, thiophene **VIII** or aniline **IX**, from which starting material degradation was obtained in all the cases. Even at reduced current of 1 mA, only 10% of cyclization from compound **VII** was observed. Additionally, highly electron-deficient arene moieties such as pyridines did not yield productive amination (**X**). Finally, although this protocol represents the first homogeneous approach for pyrrolidine and piperidine synthesis in the context of aliphatic amination, smaller ring size products like azetidines or larger cycles like azacycloheptanes could not be accessed by the present methodology (**XI** and **XII**).



Scheme 2.8: Scope limitation: Selected non-productive substrates.

Once we explored the reaction scope, we performed some mechanistic studies in order to get more insight on the discussed limitations and to gain a full understanding on the individual steps. Intrigued by the fact that the reaction only worked with substrates bearing activated benzylic positions, we wondered whether initial oxidation takes place at the nitrogen functionality to generate an amidyl radical (following the designed pathway showed in Scheme 2.5), or whether it takes place at the arene moiety in a different approach from what we envisioned.

Chapter II: Anodic Benzylic C(sp³)-H Amination:
A Unified Access to pyrrolidines and Piperidines

To address this point, we compared the oxidation potentials of model compounds **5** (Figure 2.3, pink), **6** (Figure 2.3, blue) and **1h** (Figure 2.3, red) by means of cyclic voltammetric studies. We first studied the electrochemical robustness of our electrolyte mixture (Figure 2.3, black) of 0.1 M Bu₄NBF₄ in HFIP. With a defined cut-off current of $j_{lim} = 0.1 \text{ mA.cm}^{-2}$, it was observed that oxidation of electrolyte mixture started at a potential of 2.80 V versus a Ag/AgNO₃ reference electrode. The presented observation demonstrated the robustness of HFIP-based electrolyte systems toward its use in anodic oxidation processes, which was already evidenced by the electrochemical community.¹⁵¹ Oxidation of model compound **5** bearing only an aromatic functionality as electrophore exhibited an oxidation potential of 1.77 V versus Ag/AgNO₃. Subsequently, sulfonamide **6** was studied to evaluate the oxidation potential of such a nitrogen functionality to generate the corresponding amidyl radical-cation. A potential of 2.02 V versus Ag/AgNO₃ was obtained, which is significantly higher when compared to oxidation of the phenyl ring in **5** (250 mV difference). Finally, oxidation of compound **1h** was determined to take place irreversibly at 1.79 V versus Ag/AgNO₃, in a similar potential value to hydrocarbon **5** and in a significant 230 mV lower potential than tosylamide **6**.

¹⁵¹ F. Francke, D. Cericola, D. Weingarth, R. Kötz, S. R. Waldvogel, *Electrochim. Acta* **2012**, 62, 372-380.

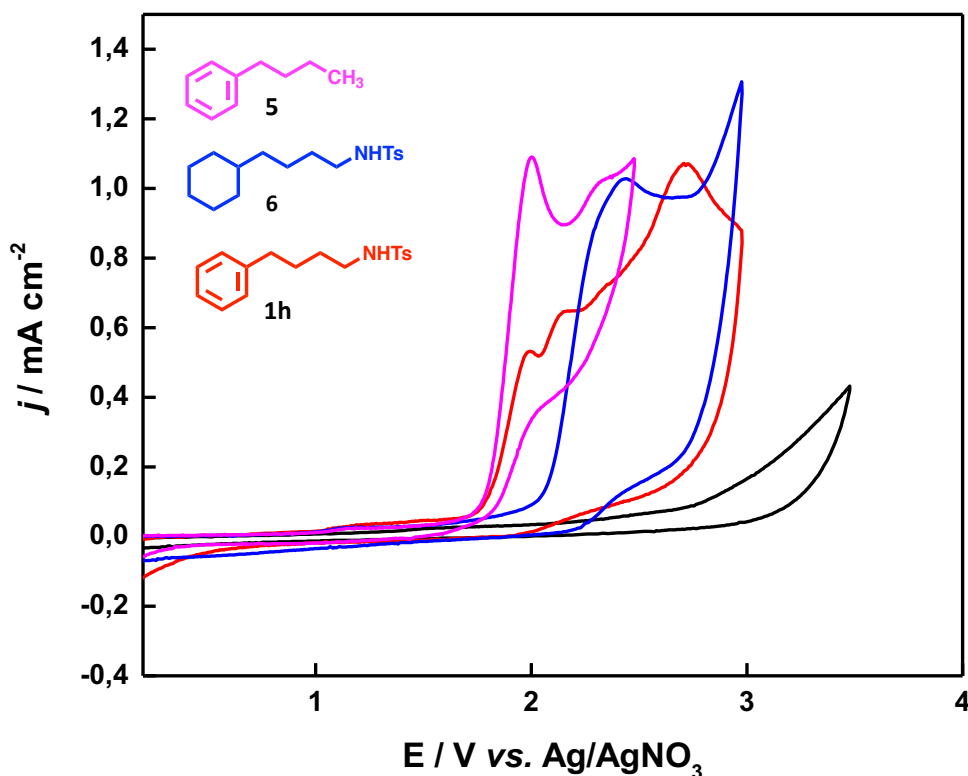


Figure 2.3: Cyclic voltammetry of **5** (pink), **6** (blue), **1h** (red) and blank electrolyte (black). Concentration: 3 mM substrate; working electrode: glassy carbon; counter electrode: platinum wire; reference electrode: Ag/0.01 M AgNO₃ in 0.1 M Bu₄NClO₄; scan rate: 50 mV s⁻¹.

Additional cyclic voltammetric studies were performed to compare the oxidation potential of selected starting material **1h** (Figure 2.4, red) with its corresponding cyclized product **2h** (Figure 2.4, brown). Oxidation of pyrrolidine **2h** was observed to take place at 1.88 V versus Ag/AgNO₃, at a significant 90 mV higher potential than **1h**. This difference gets directly translated in clean product formation because of the absence of selectivity problems owing to product oxidation.

Chapter II: Anodic Benzylic C(sp³)-H Amination:
A Unified Access to pyrrolidines and Piperidines

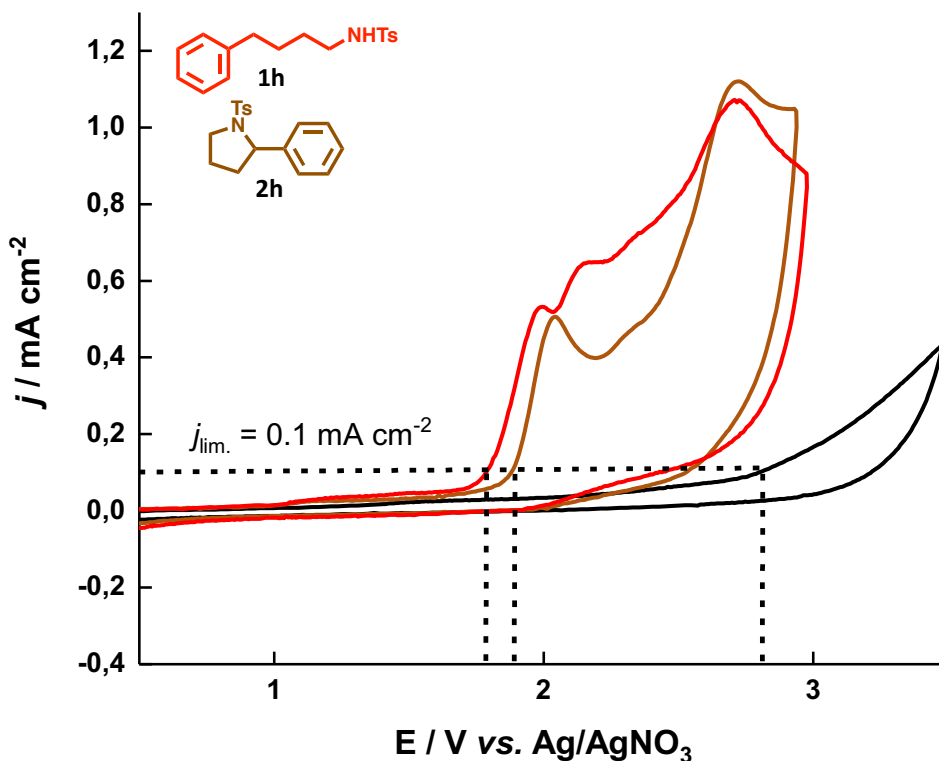


Figure 2.4: Cyclic voltammetry of **1h** (red), **2h** (brown), and blank electrolyte (black). Concentration: 3 mM substrate; working electrode: glassy carbon; counter electrode: platinum wire; reference electrode: Ag/0.01 M AgNO₃ in 0.1M Bu₄NClO₄; scan rate: 50 mVs⁻¹.

With all this data in hand, we conclude that the active functionality engaged in the electrochemical process is the aromatic group and not the sulfonamide moiety (oxidation potential of **1h** is similar to **5** while both of them are lower than **6**), contrary to what we initially expected. A full mechanistic proposal is depicted in Figure 2.5. Single electron oxidation at the anode of **1a** generates an aromatic radical-cation **A**. Radical cation such as **A** exhibit an increased acidity at the benzylic C-H bonds, indeed, a *p*K_a value between -9 and -13 have been estimated for a toluene radical-cation.¹⁵² Fast deprotonation of **A** yields benzylic carbon-centered radical **B**. As a general trend, benzylic radicals such as **B** exhibit a lower oxidation potential than the analogous neutral compounds.¹⁵³ Second oxidative SET over **B** generates carbocation **C** which gets immediately trapped in an intramolecular nucleophilic attack by the nitrogen group to

¹⁵² A. M. P. Nicholas, D. R. Arnold, *Can. J. Chem.* **1982**, *60*, 2165-2179.

¹⁵³ a) D. D. M. Wayner, D. J. McPhee, D. Griller, *J. Am. Chem. Soc.* **1988**, *110*, 132-137. b) O. Hammerich, in *Organic Electrochemistry*, ed. O. Hammerich, B. Speiser, CRC Press, Boca Raton, 5th edn, 2016, pp. 892-894 and 907-909.

afford pyrrolidine product **2a**. To close the electrochemical circuit, hydrogen evolution takes place at the platinum cathode by two electron reduction of two protons.

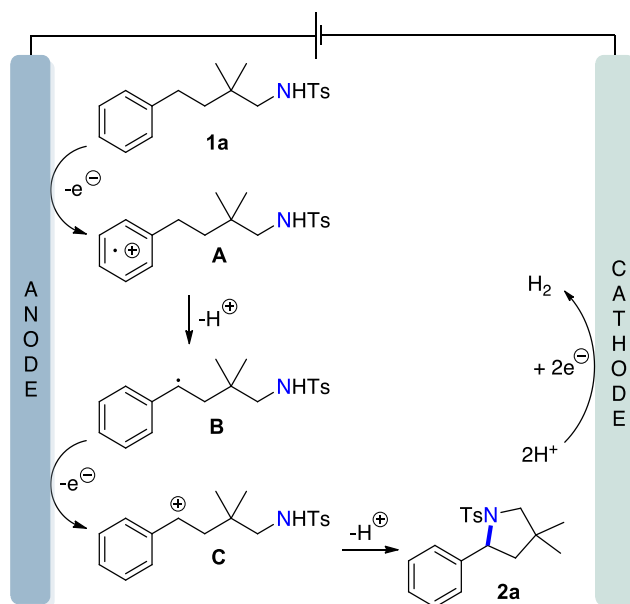


Figure 2.5: Proposed mechanism for electrochemical intramolecular C(sp³)-H amination.

The discussed mechanistic proposal is completely consistent with the observed limitations of the developed protocol, especially with the main limitation to activated benzylic positions. Furthermore, this pathway explains why electron-deficient aromatic compounds such as pyridine **X** with a high oxidation potential did not work. We further investigated this effect in another cyclic voltammetric experiment (Figure 2.6). By comparison of the oxidation potentials of pyridine-containing sulfonamide **8** (purple) and 3-ethylpyridine (**7**, orange) as model compound, it is obvious that sulfonamide oxidation occurs prior to oxidation of the electron-poor arene core (Figure 2.6). Sulfonamide oxidation seems to lead to side reactions that do not afford pyrrolidine formation. That sulfonamide oxidation is not a productive pathway for product formation was demonstrated by anodic oxidation of **8**, which led to complete degradation of starting material.

Chapter II: Anodic Benzylic C(sp³)-H Amination:
A Unified Access to pyrrolidines and Piperidines

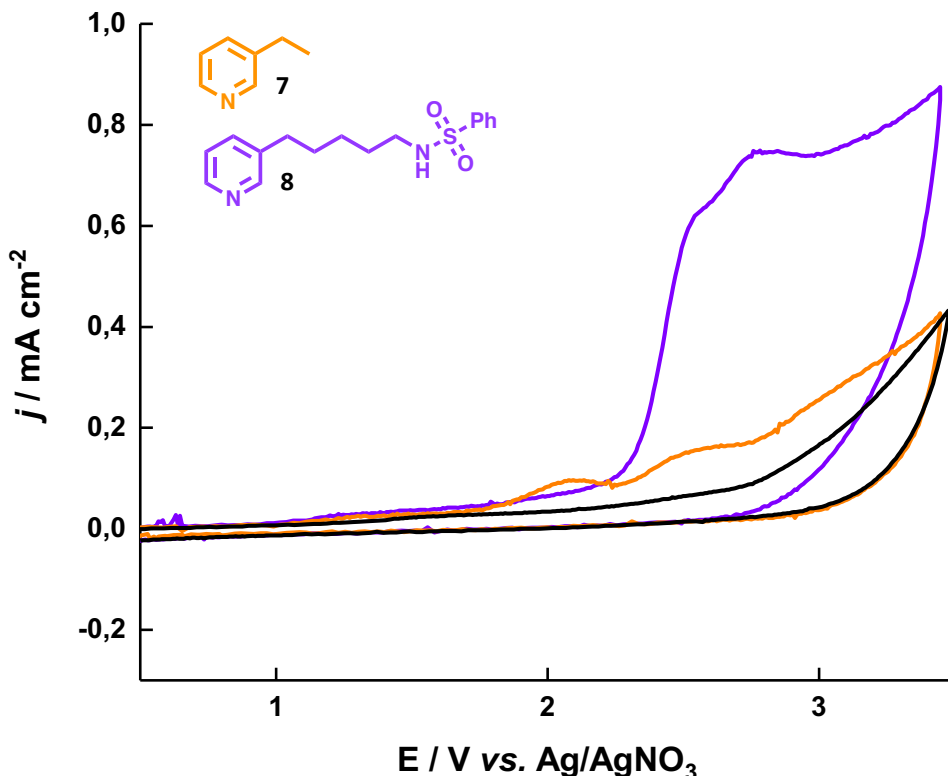
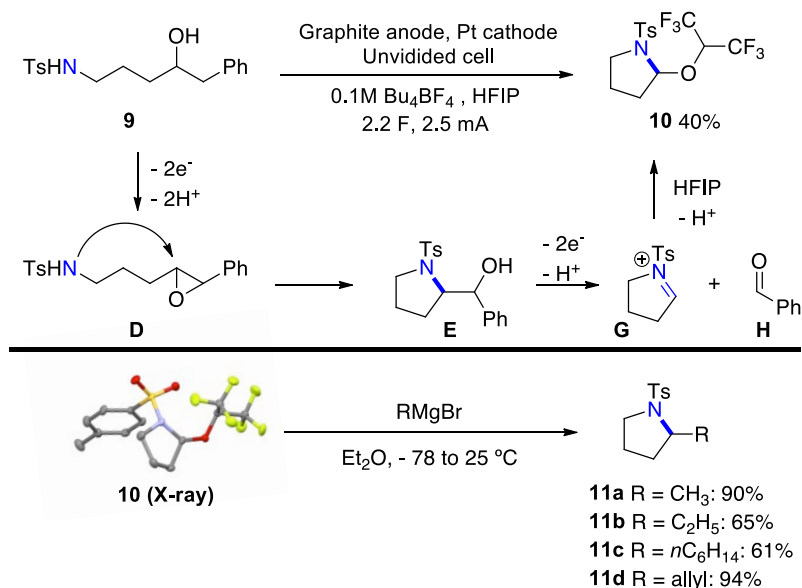


Figure 2.6: Cyclic voltammetry of **8** (purple), **7** (orange), and blank electrolyte (black). Concentration: 3 mM; working electrode: glassy carbon; counter electrode: platinum wire; reference electrode: Ag/0.01 M AgNO₃ in 0.1 M Bu₄NClO₄; scan rate: 50 mVs⁻¹.

An interesting reactivity was observed when homo-benzylic alcohol **9** was submitted to electrochemical reaction conditions (Scheme 2.9). Pyrrolidine **10** incorporating HFIP - the structure of which was unambiguously confirmed by X-ray analysis - was obtained in 40% yield. Following two electron oxidation of **9**, the intermediate benzylic carbocation gets intramolecularly trapped by the adjacent hydroxyl group, leading to epoxide **D**. Epoxide opening through intramolecular nucleophilic attack by the sulfonamide functionality generates pyrrolidine **E**. At this stage, aminoalcohol **E** undergoes a second two electron oxidation process resulting in carbon-carbon bond cleavage¹⁵⁴ to generate benzaldehyde **H** together with iminium species **G**, which is rapidly trapped by the HFIP solvent to afford **10**. In fact, the benzaldehyde byproduct could be observed by NMR analysis of the crude reaction mixture. The same product

¹⁵⁴ a) T. Shono, Y. Matsumura, T. Hasimoto, K. Hibino, H. Hamaguchi, T. Aoki, *J. Am. Chem. Soc.* **1975**, *97*, 2546-2548. b) T. Shono, H. Hamaguchi, Y. Matsumura, K. Yoshida, *Tetrahedron Lett.* **1977**, *18*, 3625-3628.

10 could also be obtained by Shono-type oxidation¹⁵⁵ of tosyl-protected pyrrolidine when employing HFIP as solvent (52% yield). Shono-type oxidation products have been used as synthetic platforms for carbon-carbon bond formation reactions.¹⁵⁶ Consequently, we employed pyrrolidine **10** as precursor in a series of diversification experiments through Grignard addition. Along these lines, a series of 2-alkyl pyrrolidines could be obtained in good to excellent yields, thus opening alternative venues from the limitation of our protocol to 2-aryl pyrrolidine synthesis.



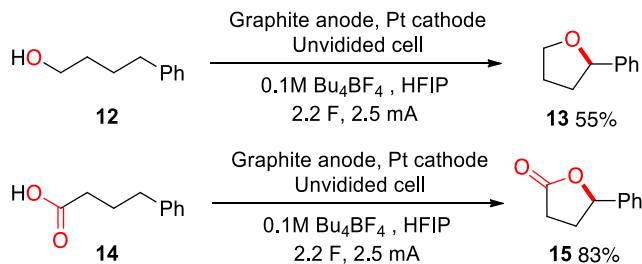
Scheme 2.9: Anodic carbon-carbon fragmentation toward **10** (top) and product derivatization to access 2-alkyl pyrrolidines (bottom).

Taking into consideration that the sulfonamide does merely act as a nucleophile and does not play a key role in the C-H functionalization event, we wondered whether other internal nucleophiles might be used for intramolecular C(sp³)-H functionalization. In this regard, we submitted linear alcohol **12** and carboxylic acid **14** to our developed electrochemical conditions, which afforded tetrahydrofuran **13** and lactone **15** in good 55% and excellent 83% yield, respectively.

¹⁵⁵ T. Shono, *Tetrahedron*, **1984**, *40*, 811-850.

¹⁵⁶ a) T. Shono, Y. Matsumura, K. Tsubata, *J. Am. Chem. Soc.* **1981**, *103*, 1172-1176. b) A. M. Jones, C. E. Banks, *Beilstein J. Org. Chem.* **2014**, *10*, 3056-3072.

Chapter II: Anodic Benzylic C(sp³)-H Amination:
A Unified Access to pyrrolidines and Piperidines



Scheme 2.10: Tetrahydrofuran and γ -butyrolactone synthesis by electrochemical C(sp³)-H oxidation.

The present methodology opens new synthetic applications and shows untapped potential for further application on anodic aliphatic C-H bond functionalization. It is particularly noteworthy that during the course of our studies, a report on electrochemical lactonization was published by the group of Zeng.¹⁵⁷ In this work, the authors reported that **15** can be obtained from **14** in 62% yield under their reaction conditions

2.3. Conclusions

In summary, we developed an unprecedented atom-economic electrochemical procedure for intramolecular aliphatic C-H amination. A total number of 25 different pyrrolidines were synthesized in good to excellent yields displaying a wide variety of functionalities and structural diversity, including challenging electron-rich heterocycles. The same mild experimental conditions could be extended to the synthesis of a total of 17 piperidines, demonstrating a functional and structural diversity tolerance similar to the pyrrolidine series. In this sense, the present works represents the first unified reaction conditions that can afford pyrrolidine and piperidine formation in the context of intramolecular aliphatic C-H amination. A series of mechanistic investigations were carried out in order to elucidate the reaction mechanism and to contextualize and rationalize its limitations.

2.4. Experimental section

General Remarks: All solvents and reagents employed were purchased from Aldrich, Acros, TCI and Fluorochem. Column chromatography was performed on silica gel (PanReac AppliChem, Silica Gel 60, 0.063-0.2 mm). NMR spectroscopy was performed on a Bruker Avance 300 MHz, 400 MHz or 500 MHz, respectively. The chemical shifts are given in ppm normalized to the shift of residual chloroform in the deuterated chloroform ($\delta_{\text{H}} = 7.26$ ppm and $\delta_{\text{C}} = 77.16$ ppm). The multiplicities are stated as follows: s = singlet, bs = broad singlet, d = doublet, t = triplet, q = quartet, m = multiplet. HRMS measurements were performed on a UHPLC-MS-QqTOF (MaXis Impact, Bruker

¹⁵⁷ S. Zhang, L. Li, H. Wang, Q. Li, W. Liu, K. Xu, C. Zeng, *Org. Lett.* **2018**, 20, 252-255.

Daltonics) or HPLC-MS-TOF (MicroTOF II, Bruker Daltonics) within the ICIQ service department. IR spectroscopy was performed using a Bruker Alpha instrument in the solid state. Melting points were determined employing a Büchi B-540 instrument. Cyclic voltammetry studies were carried out in a three-electrode cell using a Parstat 2273 potentiostat (Princeton Applied Research). As working electrode a glassy carbon disk (diameter: 3 mm) and as counter electrode a platinum wire were used. The working electrode was polished using alumina (0.05 µm) prior to each experiment. As reference served a Ag/AgNO₃ electrode (silver wire in 0.1 M Bu₄NClO₄/CH₃CN; 0.01 M AgNO₃).¹⁵⁸ The reference electrode was separated from the cell with a Vycor frit. 1,1,1,3,3,3-Hexafluoroisopropanol (99%, Fluorochem) was used as received. As supporting electrolyte served Bu₄NBF₄ (99%, Aldrich). The electrolyte was purged with Argon (5 min) prior to each experiment.

General protocol (GP 1) for the synthesis of the substrates for 5-membered ring formation: Compounds **1a-1x** were synthesized in a 3 steps synthetic sequence according to described procedures reported in literature.^{72,75}

Variation of General Protocol 1 (GP 1.1): For the synthesis of the required nitriles the first step of **GP 1** was replaced by a Suzuki coupling. Pd(OAc)₂ (6.9 mg, 0.031 mmol, 1 mol%), PPh₃ (16.0 mg, 0.061 mmol, 2 mol%), arylboronic acid (4.59 mmol, 1.5 equiv.) and K₃PO₄ (2.6 g, 12.24 mmol, 4 equiv.) were added to a flame-dried Schlenk tube. Dry toluene (10 mL) was added followed by addition of 2-(bromomethyl)benzotrile (0.6 g, 3.06 mmol, 1 equiv.). The reaction mixture was stirred overnight at 80 °C and then quenched by addition of water. The mixture was extracted with Et₂O and the combined organic phases were washed with water, aqueous NaOH solution (1M), brine and dried over Na₂SO₄. After filtration, the solvent was removed under reduced pressure and the crude product was directly used for the reduction of the nitrile (Step 2, **GP 1**).

General protocol (GP 2) for the synthesis of the substrates for 6-membered ring formation: Compounds **3a-3q** were synthesized in a 7 steps synthetic sequence according to described procedures reported in literature.⁷⁶


General protocol (GP 3) for the electrochemical cyclization reaction: The corresponding substrate (0.2 mmol) and Bu₄NBF₄ (0.1 M) were dissolved in 10 mL 1,1,1,3,3,3-Hexafluoroisopropanol (HFIP) in an undivided cell. As cathode material, a platinum mesh (Alfa Aesar, 25 x 25 mm) was employed. A graphite rod (Alfa Aesar, d = 6.3 mm, immersion depth: 10 mm) served as anode material. The electrolysis was performed under constant current conditions (2.5 mA) and a charge of 2.2 F was applied. After completion of the electrolysis, the solvent was evaporated under reduced pressure and the crude product was purified by column chromatography on silica gel using *n*-hexane/ethyl acetate as eluents.

¹⁵⁸ V. V. Pavlishchuk, A. W. Addison, *Inorg. Chim. Acta* **2000**, 298, 97-102.

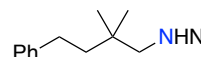
Chapter II: Anodic Benzylic C(sp³)-H Amination:
A Unified Access to pyrrolidines and Piperidines

General protocol (GP 4) for carbon-carbon bond formation with 2-hexafluoroisopropoxy pyrrolidine 10: A flame-dried Schlenk flask was charged with 2-hexafluoroisopropoxy pyrrolidine **10** (0.1 mmol, 1 equiv.) and dry diethyl ether (1 mL) under an argon atmosphere. The resulting solution was then cooled to -78 °C and the corresponding alkyl magnesium bromide reagent (1.2 equiv.) was added slowly at that temperature. The reaction mixture was stirred for 5 min at -78 °C, warmed to room temperature and stirred for 12 h at room temperature. The reaction was quenched by addition of a saturated aqueous NH₄Cl solution and the layers were separated. The aqueous phase was extracted three times with dichloromethane and the combined organic layers were dried over Na₂SO₄, filtered and the solvent was removed under reduced pressure. The crude product was further purified by column chromatography (hexane/ethyl acetate).


***N*-(2,2-dimethyl-4-phenylbutyl)-4-methylbenzenesulfonamide (1a)**

 **1a** was synthesized according to **GP 1**. The NMR data match those previously reported in literature.⁷² ¹H NMR (400 MHz, CDCl₃): δ = 7.79-7.74 (m, 2H), 7.35-7.25 (m, 4H), 7.22-7.13 (m, 3H), 4.65 (bs, 1H), 2.76 (d, *J* = 6.9 Hz, 2H), 2.57-2.48 (m, 2H), 2.44 (s, 3H), 1.56-1.49 (m, 2H), 0.95 (s, 6H). ¹³C NMR (100 MHz, CDCl₃): δ = 143.4, 142.7, 137.1, 129.8, 128.5, 128.4, 127.2, 125.9, 53.0, 41.6, 34.2, 30.4, 25.1, 21.6.

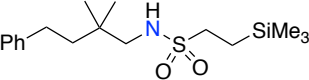
***N*-(2,2-dimethyl-4-phenylbutyl)-4-nitrobenzenesulfonamide (1b)**

 **1b** was synthesized according to **GP 1**. The NMR data match those previously reported in literature.⁷² ¹H NMR (300 MHz, CDCl₃): δ = 8.40-8.27 (m, 2H), 8.03-7.97 (m, 2H), 7.41-7.04 (m, 5H), 4.58 (bs, 1H), 2.89-2.76 (m, 2H), 2.56-2.45 (m, 2H), 1.56-1.41 (m, 2H), 0.94 (s, 6H). ¹³C NMR (75 MHz, CDCl₃): δ = 150.1, 146.0, 142.4, 128.6, 128.4, 128.3, 126.1, 124.5, 53.3, 41.5, 34.4, 30.4, 25.0.

***N*-(2,2-dimethyl-4-phenylbutyl)methanesulfonamide (1c)**

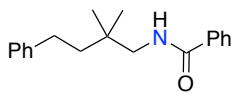
 **1c** was synthesized according to **GP 1**. The NMR data match those previously reported in literature.⁷⁵ ¹H NMR (400 MHz, CDCl₃): δ = 7.34-7.28 (m, 2H), 7.24-7.17 (m, 3H), 4.42 (bs, 1H), 2.98 (d, *J* = 6.9 Hz, 2H), 2.95 (s, 3H), 2.65-2.54 (m, 2H), 1.66-1.54 (m, 2H), 1.03 (s, 6H). ¹³C NMR (100 MHz, CDCl₃): δ = 142.6, 128.6, 128.4, 126.0, 53.1, 41.7, 40.1, 34.3, 30.5, 25.0.

***N*-(2,2-Dimethyl-4-phenylbutyl)-2-(trimethylsilyl)ethane-1-sulfonamide (1d)**

 **1d** was synthesized according to **GP 1**. The NMR data match those previously reported in literature.⁷² ¹H NMR (500 MHz, CDCl₃): δ = 7.35-7.27 (m, 2H), 7.23-7.18 (m, 3H), 4.26 (t, *J* = 6.9 Hz, 1H), 3.02-2.90 (m, 4H), 2.66-2.57 (m, 2H), 1.62-1.52 (m, 2H), 1.06-0.98 (m, 8H),

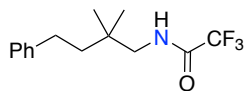
0.07 (s, 9H). ¹³C NMR (100 MHz, CDCl₃): δ = 142.7, 128.6, 128.4, 126.0, 53.3, 48.6, 41.7, 34.4, 30.5, 25.0, 10.8, -1.9.

***N*-(2,2-Dimethyl-4-phenylbutyl)benzamide (1e)**



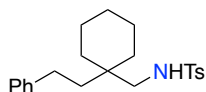
1e was synthesized according to **GP 1** applying the first two steps. Then, the crude amine (1 equiv.) and pyridine (1.5 equiv.) were dissolved in dry CH₂Cl₂ and cooled to 0 °C. Subsequently, benzoyl chloride (1.5 equiv.) was slowly added at 0 °C. The reaction mixture was then warmed to room temperature and stirred overnight at room temperature. The solvent was evaporated under reduced pressure. The thus obtained crude product was further purified by column chromatography on silica gel using *n*-hexane and ethyl acetate as eluents. The product was obtained as a white solid (69%). The NMR data match those previously reported in literature.⁷⁵ ¹H NMR (300 MHz, CDCl₃): δ = 7.78-7.71 (m, 2H), 7.54-7.40 (m, 3H), 7.32-7.24 (m, 2H), 7.22-7.14 (m, 3H), 6.13 (bs, 1H), 3.38 (d, *J* = 6.4 Hz, 2H), 2.72-2.59 (m, 2H), 1.66-1.54 (m, 2H), 1.04 (s, 6H). ¹³C NMR (75 MHz, CDCl₃): δ = 167.7, 142.9, 135.0, 131.4, 128.6, 128.5, 128.4, 126.8, 125.8, 49.3, 42.2, 34.9, 30.6, 25.1.

***N*-(2,2-Dimethyl-4-phenylbutyl)-2,2,2-trifluoroacetamide (1f)**



1f was synthesized according to **GP 1** applying the first two steps. Then, the crude amine (1 equiv.) and pyridine (1.2 equiv.) were dissolved in dry CH₂Cl₂ and cooled to 0 °C. Subsequently, trifluoroacetic anhydride (1.2 equiv.) was slowly added at 0 °C. The reaction mixture was then warmed to room temperature and stirred overnight at room temperature. The solvent was evaporated under reduced pressure. The thus obtained crude product was further purified by column chromatography on silica gel using *n*-hexane and ethyl acetate as eluents. The product was obtained as a white solid (44%). The NMR data match those previously reported in literature.⁷⁵ ¹H NMR (400 MHz, CDCl₃): δ = 7.32-7.27 (m, 2H), 7.22-7.16 (m, 3H), 6.19 (bs, 1H), 3.25 (d, *J* = 6.5 Hz, 2H), 2.65-2.58 (m, 2H), 1.58-1.52 (m, 2H), 1.00 (s, 6H). ¹³C NMR (100 MHz, CDCl₃): δ = 157.6 (q, *J* = 36.6 Hz), 142.5, 128.7, 128.4, 126.1, 116.1 (d, *J* = 288.1 Hz), 49.4, 42.0, 34.9, 30.6, 25.0. ¹⁹F NMR (375 MHz, CDCl₃): δ = -75.9.

4-methyl-*N*-((1-phenethylcyclohexyl)methyl)benzenesulfonamide (1g)

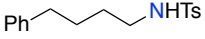


1g was synthesized according to **GP 1**. The NMR data match those previously reported in literature.⁷² ¹H NMR (300 MHz, CDCl₃): δ = 7.78-7.72 (m, 2H), 7.37-7.22 (m, 4H), 7.20-7.10 (m, 3H), 2.82 (s, 2H), 2.41-2.36 (m, 5H), 1.65-1.52 (m, 2H), 1.46-1.18 (m, 10H). ¹³C NMR (75 MHz, CDCl₃):

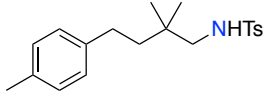
Chapter II: Anodic Benzylic C(sp³)-H Amination:
A Unified Access to pyrrolidines and Piperidines

$\delta = 143.5, 142.9, 137.1, 129.9, 128.5, 128.5, 127.2, 125.9, 49.3, 37.5, 36.2, 33.6, 29.3, 26.2, 21.7, 21.4.$

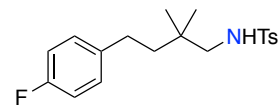
4-Methyl-N-(4-phenylbutyl)benzenesulfonamide (**1h**)

 **1h** was synthesized according to **GP 1**. The NMR data match those previously reported in literature.⁷² ¹H NMR (300 MHz, CDCl₃): $\delta = 7.75$ (dd, $J = 8.4, 1.9$ Hz, 2H), 7.33-7.22 (m, 4H), 7.21-7.14 (m, 1H), 7.13-7.08 (m, 2H), 4.67 (bs, 1H), 2.95 (q, $J = 6.6$ Hz, 2H), 2.55 (t, $J = 7.4$ Hz, 2H), 2.43 (s, 3H), 1.70-1.43 (m, 4H). ¹³C NMR (75 MHz, CDCl₃): $\delta = 143.5, 141.9, 137.1, 129.8, 128.5, 127.2, 126.0, 43.2, 35.4, 29.2, 28.3, 21.6.$

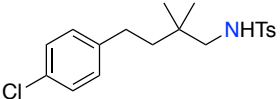
N-(2,2-dimethyl-4-(p-tolyl)butyl)-4-methylbenzenesulfonamide (**1i**)

 **1i** was synthesized according to **GP 1**. The NMR data match those previously reported in literature.⁷² ¹H NMR (300 MHz, CDCl₃): $\delta = 7.74$ (d, $J = 8.3$ Hz, 2H), 7.29 (d, $J = 8.0$ Hz, 2H), 7.04 (q, $J = 8.1$ Hz, 4H), 4.56 (t, $J = 6.7$ Hz, 1H), 2.73 (d, $J = 6.9$ Hz, 2H), 2.50-2.43 (m, 2H), 2.42 (s, 3H), 2.31 (s, 3H), 1.53-1.42 (m, 2H), 0.92 (s, 6H). ¹³C NMR (75 MHz, CDCl₃): $\delta = 143.4, 139.6, 137.1, 135.3, 129.8, 129.2, 128.3, 127.2, 53.0, 41.8, 34.1, 29.9, 25.1, 21.6, 21.1.$

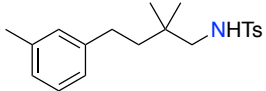
N-(4-(4-Fluorophenyl)-2,2-dimethylbutyl)-4-methylbenzenesulfonamide (**1j**)

 **1j** was synthesized according to **GP 1**. The NMR data match those previously reported in literature.⁷² ¹H NMR (400 MHz, CDCl₃): $\delta = 7.77$ -7.73 (m, 2H), 7.32-7.26 (m, 2H), 7.10-7.03 (m, 2H), 6.92 (t, $J = 8.1$ Hz, 2H), 2.73 (s, 2H), 2.54-2.43 (m, 2H), 2.41 (s, 3H), 1.51-1.42 (m, 2H), 0.91 (s, 6H). ¹³C NMR (100 MHz, CDCl₃): $\delta = 161.3$ (d, $J = 243.2$ Hz), 143.5, 138.3, 137.1, 129.8, 129.7 (d, $J = 7.7$ Hz), 127.2, 115.2 (d, $J = 21.2$ Hz), 52.9, 41.7, 34.1, 29.6, 25.1, 21.6. ¹⁹F NMR (375 MHz, CDCl₃): $\delta = -118.1.$

N-(4-(4-chlorophenyl)-2,2-dimethylbutyl)-4-methylbenzenesulfonamide (**1k**)

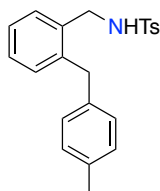
 **1k** was synthesized according to **GP 1**. The NMR data match those previously reported in literature.⁷² ¹H NMR (300 MHz, CDCl₃): $\delta = 7.74$ (d, $J = 8.3$ Hz, 2H), 7.32-7.27 (m, 2H), 7.23-7.17 (m, 2H), 7.10-7.03 (m, 2H), 4.66 (t, $J = 6.9$ Hz, 1H), 2.72 (d, $J = 6.9$ Hz, 2H), 2.52-2.43 (m, 2H), 2.42 (s, 3H), 1.53-1.40 (m, 2H), 0.91 (s, 6H). ¹³C NMR (75 MHz, CDCl₃): $\delta = 143.5, 141.1, 137.1, 131.5, 129.9, 129.8, 128.5, 127.2, 52.9, 41.4, 34.2, 29.8, 25.1, 21.7.$

N-(2,2-dimethyl-4-(m-tolyl)butyl)-4-methylbenzenesulfonamide (**1l**)

 **1l** was synthesized according to **GP 1**. The NMR data match those previously reported in literature.⁷⁵ ¹H NMR (300 MHz, CDCl₃): $\delta = 7.74$ (d, $J = 7.9$ Hz, 2H), 7.30 (d, $J = 8.0$ Hz, 2H), 7.15

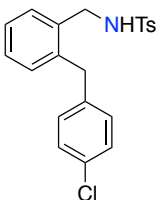
(t, $J = 7.4$ Hz, 1H), 7.01-6.91 (m, 3H), 4.57 (bs, 1H), 2.73 (s, 2H), 2.50-2.43 (m, 2H), 2.42 (s, 3H), 2.32 (s, 3H), 1.56-1.43 (m, 2H), 0.92 (s, 6H). ¹³C NMR (75 MHz, CDCl₃): $\delta = 143.4, 142.6, 138.1, 137.1, 129.8, 129.2, 128.4, 127.2, 126.6, 125.4, 53.0, 41.7, 34.2, 30.3, 25.1, 21.6, 21.5$.

4-Methyl-N-(2-(4-methylbenzyl)benzyl)benzenesulfonamide (1m)



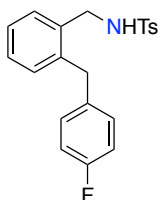
1m was synthesized according to **GP 1.1**. The NMR data match those previously reported in literature.⁷⁵ ¹H NMR (400 MHz, CDCl₃): $\delta = 7.76-7.70$ (m, 2H), 7.35-7.30 (m, 2H), 7.30-7.24 (m, 2H), 7.23-7.15 (m, 2H), 7.10 (d, $J = 7.8$ Hz, 2H), 6.97-6.92 (m, 2H), 4.83 (t, $J = 6.2$ Hz, 1H), 4.08 (d, $J = 6.0$ Hz, 2H), 3.95 (s, 2H), 2.49 (s, 3H), 2.38 (s, 3H). ¹³C NMR (100 MHz, CDCl₃): $\delta = 143.4, 139.3, 137.1, 136.6, 135.6, 134.3, 130.7, 129.7, 129.6, 129.2, 128.5, 128.2, 127.2, 126.8, 44.9, 38.1, 21.5, 21.0$.

4-Methyl-N-(2-(4-chlorobenzyl)benzyl)benzenesulfonamide (1n)



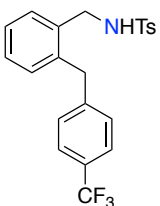
1n was synthesized according to **GP 1.1**. White solid, 66%. ¹H NMR (300 MHz, CDCl₃): $\delta = 7.68$ (d, $J = 8.3$ Hz, 2H), 7.30 (d, $J = 8.2$ Hz, 2H), 7.28-7.15 (m, 5H), 7.11 (d, $J = 7.1$ Hz, 1H), 6.92 (d, $J = 8.3$ Hz, 2H), 4.33 (t, $J = 6.1$ Hz, 1H), 3.99 (d, $J = 6.0$ Hz, 2H), 3.92 (s, 2H), 2.45 (s, 3H). ¹³C NMR (75 MHz, CDCl₃): $\delta = 143.8, 138.9, 138.7, 136.5, 134.2, 132.2, 131.0, 130.0, 129.9, 129.9, 128.8, 128.7, 127.4, 45.2, 37.9, 21.7$. IR ν (cm⁻¹): 3280, 1598. mp: 119-120 °C. HRMS: Mass calculated for C₂₁H₂₀NNaO₂S: 408.0795, found: 408.0795.

4-Methyl-N-(2-(4-fluorobenzyl)benzyl)benzenesulfonamide (1o)



1o was synthesized according to **GP 1.1**. White solid, 67%. ¹H NMR (400 MHz, CDCl₃): $\delta = 7.75-7.60$ (m, 2H), 7.32-7.22 (m, 3H), 7.21-7.18 (m, 2H), 7.11 (d, $J = 7.3$ Hz, 1H), 6.99-6.85 (m, 4H), 4.38 (bs, 1H), 4.00 (d, $J = 4.1$ Hz, 2H), 3.92 (s, 2H), 2.44 (s, 3H). ¹³C NMR (100 MHz, CDCl₃): $\delta = 161.5$ (d, $J = 244.6$ Hz), 143.7, 139.2, 136.6, 135.8, 135.8, 134.2, 130.9, 130.1, 130.0, 129.9, 129.9, 128.6, 127.4, 127.3, 115.4 (d, $J = 21.2$ Hz), 45.2, 37.8, 21.7. ¹⁹F NMR (375 MHz, CDCl₃): $\delta = -116.93$. IR ν (cm⁻¹): 3247, 1598, 1505. mp: 115-117 °C. HRMS: Mass calculated for C₂₁H₂₀FNNaO₂S: 392.1091, found: 392.1088.

4-Methyl-N-(2-(4-(trifluoromethyl)benzyl)benzyl)benzenesulfonamide (1p)

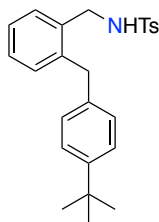


1p was synthesized according to **GP 1.1**. White solid, 50%. ¹H NMR (300 MHz, CDCl₃): $\delta = 7.68$ (d, $J = 8.3$ Hz, 2H), 7.48 (d, $J = 8.1$ Hz, 2H), 7.32-7.24 (m, 3H), 7.24-7.17 (m, 2H), 7.16-7.08 (m, 3H), 4.38 (bs, 1H), 4.03 (s, 2H), 3.99 (d, $J = 6.1$ Hz, 2H), 2.44 (s, 3H). ¹³C NMR (75 MHz, CDCl₃): $\delta = 144.4, 143.8, 138.4, 136.5, 134.2, 131.1, 130.0, 129.9, 129.0, 128.9, 128.8, 128.5, 127.5, 127.3, 126.1, 125.5$ (q, $J = 3.7$ Hz),

Chapter II: Anodic Benzylic C(sp³)-H Amination:
A Unified Access to pyrrolidines and Piperidines

122.5, 45.3, 38.3, 21.7. ¹⁹F NMR (375 MHz, CDCl₃): δ = -62.5. IR ν (cm⁻¹): 3285, 1617, 1598. mp: 133-134 °C. HRMS: Mass calculated for C₂₂H₂₀F₃NNaO₂S: 442.1059, found: 442.1059.

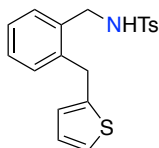
4-Methyl-N-(2-(4-(*tert*-butyl)benzyl)benzyl)benzenesulfonamide (1q)



1q was synthesized according to **GP 1.1**. White solid, 62%. ¹H NMR (500 MHz, CDCl₃): δ = 7.68 (d, *J* = 8.3 Hz, 2H), 7.33-7.30 (m, 2H), 7.30-7.27 (m, 3H), 7.26-7.24 (m, 1H), 7.23-7.22 (m, 2H), 7.21-7.17 (m, 2H), 6.96-6.90 (m, 2H), 4.17 (t, *J* = 6.1 Hz, 1H), 4.06 (d, *J* = 6.0 Hz, 2H), 3.93 (s, 2H), 2.47 (s, 3H), 1.33 (s, 9H). ¹³C NMR (125 MHz, CDCl₃): δ = 149.4, 143.6, 139.5, 137.2, 136.8, 134.4, 131.1, 130.1, 129.8, 128.5, 128.3, 127.4, 127.1, 125.6, 45.2, 38.3, 34.5, 31.5, 21.7. IR ν (cm⁻¹): 2385, 2958, 1596.

mp: 114-116 °C. HRMS: Mass calculated for C₂₅H₂₉NNaO₂S: 430.1811, found: 430.1808.

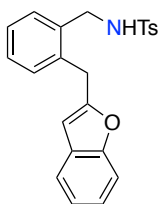
4-Methyl-N-(2-(thiophen-2-ylmethyl)benzyl)benzenesulfonamide (1r)



1r was synthesized according to **GP 1.1**. The NMR data match those previously reported in literature.⁷⁵ ¹H NMR (300 MHz, CDCl₃): δ = 7.69 (d, *J* = 8.3 Hz, 2H), 7.34-7.18 (m, 6H), 7.13 (dd, *J* = 5.2, 1.2 Hz, 1H), 6.88 (dd, *J* = 5.2, 3.4 Hz, 1H), 6.62-6.58 (m, 1H), 4.25 (bs, 1H), 4.10 (s, 2H), 4.07 (s, 2H), 2.44 (s, 3H). ¹³C NMR (75 MHz, CDCl₃): δ = 143.7, 143.6,

138.9, 136.6, 134.1, 130.6, 130.1, 129.9, 128.8, 127.6, 127.4, 127.0, 125.3, 124.3, 45.1, 33.1, 21.7.

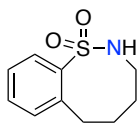
N-(2-(benzofuran-2-ylmethyl)benzyl)-4-methylbenzenesulfonamide (1s)



1s was synthesized according to **GP 1.1**. ¹H NMR (500 MHz, CDCl₃): δ = 7.71-7.65 (m, 2H), 7.46-7.43 (m, 1H), 7.40-7.35 (m, 1H), 7.25-7.19 (m, 7H), 7.19-7.15 (m, 1H), 6.25 (d, *J* = 1.0 Hz, 1H), 4.71 (bs, 1H), 4.16 (d, *J* = 4.3 Hz, 2H), 4.02 (s, 2H), 2.40 (s, 3H). ¹³C NMR (125 MHz, CDCl₃): δ =

156.9, 155.0, 143.7, 136.5, 135.9, 134.2, 130.9, 130.1, 129.8, 128.8, 128.7, 127.7, 127.3, 123.8, 122.8, 120.6, 111.0, 103.6, 45.2, 31.8, 21.7. IR ν (cm⁻¹): 3267, 3063, 2855, 1599. mp: 100-101 °C. HRMS: Mass calculated for C₂₃H₂₁NNaO₃S: 414.1134, found: 414.1149.

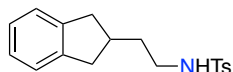
3,4,5,6-tetrahydro-2H-benzo[*g*][1,2]thiazocine 1,1-dioxide (1t)



1t was synthesized according to the literature and the NMR data match those previously reported.⁷² ¹H NMR (500 MHz, CDCl₃): δ = 7.99 (d, *J* = 7.9 Hz, 1H), 7.47 (t, *J* = 7.5 Hz, 1H), 7.32-7.28 (m, 2H), 4.54 (bs, 1H), 3.44-3.39 (m, 2H), 3.34 (t, *J* = 6.7 Hz, 2H), 1.87 (p, *J* = 6.6 Hz, 2H), 1.55-1.48 (m, 2H).

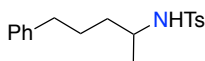
¹³C NMR (125 MHz, CDCl₃): δ = 142.2, 140.0, 132.8, 132.1, 128.0, 126.6, 41.8, 30.7, 29.5, 27.4.

***N*-2-(2,3-Dihydro-1*H*-inden-2-yl)ethyl-4-methylbenzenesulfonamide (1u)**



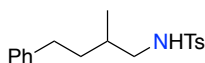
1u was synthesized according to **GP 1** starting from the known amine¹⁵⁹ applying step 3. The NMR data match those previously reported in literature.⁷² ¹H NMR (300 MHz, CDCl₃): δ = 7.84-7.72 (m, 2H), 7.33 (d, *J* = 8.1 Hz, 2H), 7.21-7.07 (m, 4H), 4.52 (bs, 1H), 3.13-2.91 (m, 4H), 2.60-2.40 (m, 6H), 1.69 (q, *J* = 7.1 Hz, 2H). ¹³C NMR (75 MHz, CDCl₃): δ = 143.6, 142.9, 137.0, 129.9, 127.3, 126.4, 124.5, 42.3, 39.0, 37.4, 35.6, 21.7.

4-Methyl-*N*-(1-methyl-4-phenylbutyl)benzenesulfonamide (1v)



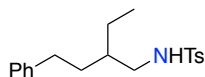
1v was synthesized according to **GP 1** starting from the known amine¹⁶⁰ applying step 3. Brown oil, 9%. ¹H NMR (300 MHz, CDCl₃): δ = 7.76 (d, *J* = 8.3 Hz, 2H), 7.31-7.23 (m, 4H), 7.23-7.15 (m, 1H), 7.11-7.07 (m, 2H), 4.32 (d, *J* = 8.3 Hz, 1H), 3.42-3.29 (m, 1H), 2.51 (t, *J* = 7.5 Hz, 2H), 2.42 (s, 3H), 1.64-1.47 (m, 2H), 1.47-1.34 (m, 2H), 1.02 (d, *J* = 6.6 Hz, 3H). ¹³C NMR (75 MHz, CDCl₃): δ = 143.3, 142.0, 138.4, 129.8, 128.5, 128.4, 127.2, 125.9, 50.0, 37.2, 35.5, 27.4, 22.0, 21.7. HRMS: Mass calculated for C₁₈H₂₃NNaO₂S: 340.1342, found: 340.1332. IR ν (cm⁻¹): 3278, 2930, 1598.

4-Methyl-*N*-(2-methyl-4-phenylbutyl)benzenesulfonamide (1w)



1w was synthesized according to **GP 1**. The NMR data match those previously reported in literature.⁷² ¹H NMR (300 MHz, CDCl₃): δ = 7.82-7.70 (m, 2H), 7.34-7.24 (m, 4H), 7.22-7.17 (m, 1H), 7.15-7.10 (m, 2H), 2.89 (dd, *J* = 12.5, 5.7 Hz, 1H), 2.80 (dd, *J* = 12.5, 6.5 Hz, 1H), 2.69-2.47 (m, 2H), 2.44 (s, 3H), 1.76-1.54 (m, 2H), 1.49-1.34 (m, 1H), 0.94 (d, *J* = 6.6 Hz, 3H). ¹³C NMR (75 MHz, CDCl₃): δ = 143.3, 142.0, 137.0, 129.7, 128.4, 128.3, 127.1, 125.8, 48.9, 35.7, 33.0, 32.8, 21.5, 17.4.

4-Methyl-*N*-(2-ethyl-4-phenylbutyl)benzenesulfonamide (1x)



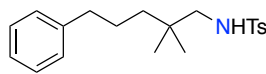
1x was synthesized according to **GP 1**. Colorless oil, 51%. ¹H NMR (300 MHz, CDCl₃): δ = 7.74 (d, *J* = 8.3 Hz, 2H), 7.33-7.22 (m, 4H), 7.21-7.14 (m, 1H), 7.14-7.08 (m, 2H), 4.34 (bs, 1H), 2.90 (t, *J* = 6.0 Hz, 2H), 2.57-2.47 (m, 2H), 2.42 (s, 3H), 1.62-1.50 (m, 2H), 1.49-1.24 (m, 3H), 0.82 (t, *J* = 7.3 Hz, 3H). ¹³C NMR (75 MHz, CDCl₃): δ = 143.5, 142.2, 137.1, 129.8, 128.5, 128.4, 127.2, 126.0, 45.7, 38.9, 32.9, 32.9, 24.0, 21.7, 10.8. HRMS: Mass calculated for C₁₉H₂₆NO₂S: 332.1679, found: 332.1673. IR ν (cm⁻¹): 3280, 2928, 1603.

¹⁵⁹ G. M. Ksander, R. deJesus, A. Yuan, C. Fink, M. Moskal, E. Carlson, P. Kukkola, N. Bilci, E. Wallace, A. Neubert, A. Feldman, T. Moselesky, K. Poirier, M. Jeune, R. Steele, J. Wasvery, Z. Stephan, E. Cahill, R. Webb, A. Navarrete, W. Lee, J. Gibson, N. Alexander, H. Sharif, A. Hospattankar, *J. Med. Chem.* **2001**, *44*, 4677-4687.

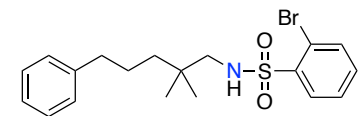
¹⁶⁰ F. Poulh.s, R. Sylvain, P. Perfetti, M. P. Bertrand, G. Gil, S. Gastaldi, *Synthesis* **2010**, *8*, 1334-1338.

Chapter II: Anodic Benzylic C(sp³)-H Amination:
A Unified Access to pyrrolidines and Piperidines

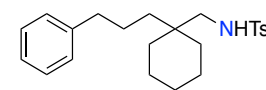
***N*-(2,2-Dimethyl-5-phenylpentyl)-4-methylbenzenesulfonamide (3a)**

 **3a** was synthesized according to **GP 1** using (3-Bromopropyl)benzene as starting material. The NMR data match those previously reported in literature.⁷⁶ ¹H NMR (400 MHz, CDCl₃): δ = 7.75 (d, *J* = 8.3 Hz, 2H), 7.34-7.31 (m, 2H), 7.31-7.27 (m, 2H), 7.23-7.15 (m, 3H), 4.38 (s, 1H), 2.69 (d, *J* = 6.8 Hz, 2H), 2.55 (t, *J* = 7.7 Hz, 2H), 2.44 (s, 3H), 1.56-1.45 (m, 2H), 1.29-1.21 (m, 2H), 0.85 (s, 6H). ¹³C NMR (100 MHz, CDCl₃): δ = 143.4, 142.5, 137.2, 129.8, 128.5, 128.4, 127.2, 125.9, 53.0, 39.2, 36.6, 33.9, 25.9, 25.0, 21.6.

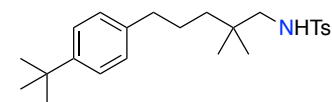
2-Bromo-*N*-(2,2-dimethyl-5-phenylpentyl)benzenesulfonamide (3b)

 **3b** was synthesized according to **GP 2**. The NMR data match those previously reported in literature.⁷⁶ ¹H NMR (300 MHz, CDCl₃): δ = 8.14 (dd, *J* = 7.6, 1.9 Hz, 1H), 7.74 (dd, *J* = 7.7, 1.4 Hz, 1H), 7.52-7.38 (m, 2H), 7.33-7.25 (m, 2H), 7.24-7.14 (m, 3H), 5.07 (t, *J* = 6.8 Hz, 1H), 2.62 (d, *J* = 6.8 Hz, 2H), 2.56 (t, *J* = 7.7 Hz, 2H), 1.65-1.45 (m, 2H), 1.34-1.22 (m, 2H), 0.87 (s, 6H). ¹³C NMR (125 MHz, CDCl₃): δ = 142.4, 138.8, 135.1, 133.8, 131.8, 128.5, 128.5, 128.0, 126.0, 119.7, 53.1, 39.2, 36.6, 33.9, 25.9, 25.1.

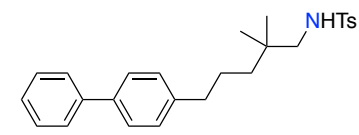
4-Methyl-*N*-((3-Phenylpropyl)cyclohexyl)methyl)benzenesulfonamide (3c)

 **3c** was synthesized according to **GP 2**. The NMR data match those previously reported in literature.⁷⁶ ¹H NMR (300 MHz, CDCl₃): δ = 7.76 (d, *J* = 8.4 Hz, 2H), 7.35-7.24 (m, 4H), 7.24-7.19 (m, 1H), 7.18-7.12 (m, 2H), 4.37 (bs, 1H), 2.75 (d, *J* = 6.4 Hz, 2H), 2.53 (t, *J* = 7.3 Hz, 2H), 2.43 (s, 3H), 1.49-1.16 (m, 14H). ¹³C NMR (75 MHz, CDCl₃): δ = 143.4, 142.6, 137.1, 129.8, 128.4, 128.5, 127.2, 125.9, 49.1, 36.6, 35.9, 34.9, 33.6, 26.2, 24.7, 21.7, 21.4.

***N*-(5-(4-(*tert*-Butyl)phenyl)-2,2-dimethylpentyl)-4-methylbenzenesulfonamide (3d)**

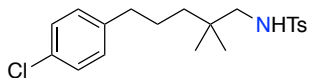
 **3d** was synthesized according to **GP 2**. The NMR data match those previously reported in literature.⁷⁶ ¹H NMR (300 MHz, CDCl₃): δ = 7.72 (d, *J* = 8.1 Hz, 2H), 7.30 (d, *J* = 8.2 Hz, 4H), 7.08 (d, *J* = 8.3 Hz, 2H), 4.26 (bs, 1H), 2.67 (d, *J* = 6.9 Hz, 2H), 2.49 (t, *J* = 7.7 Hz, 2H), 2.42 (s, 3H), 1.56-1.54 (m, 2H), 1.54-1.41 (m, 2H), 1.31 (s, 9H), 1.28-1.19 (m, 2H), 0.83 (s, 6H). ¹³C NMR (75 MHz, CDCl₃): δ = 148.7, 143.5, 139.4, 137.2, 129.8, 128.1, 127.2, 125.4, 53.1, 39.3, 36.1, 34.5, 33.9, 31.6, 25.9, 25.0, 21.7.

***N*-(5-([1,1'-Biphenyl]-4-yl)-2,2-dimethylpentyl)-4-methylbenzenesulfonamide (3e)**

 **3e** was synthesized according to **GP 2**. The NMR data match those previously reported in literature.⁷⁶ ¹H NMR (300 MHz, CDCl₃): δ = 7.73 (d, *J* = 8.3 Hz, 2H), 7.61-7.57 (m, 2H), 7.51 (d, *J* = 8.1 Hz, 2H), 7.47-7.40 (m, 2H),

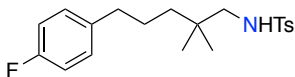
7.36-7.27 (m, 3H), 7.22 (d, $J = 8.2$ Hz, 2H), 4.41 (t, $J = 6.8$ Hz, 1H), 2.69 (d, $J = 6.8$ Hz, 2H), 2.58 (t, $J = 7.6$ Hz, 2H), 2.41 (s, 3H), 1.59-1.45 (m, 2H), 1.31-1.21 (m, 2H), 0.85 (s, 6H). ¹³C NMR (75 MHz, CDCl₃): $\delta = 143.5, 141.6, 141.2, 138.9, 137.2, 129.8, 128.9, 128.9, 127.2, 127.2, 127.1, 53.0, 39.2, 36.3, 33.9, 25.8, 25.1, 21.7$.

***N*-(5-(4-Chlorophenyl)-2,2-dimethylpentyl)-4-methylbenzenesulfonamide (3f)**



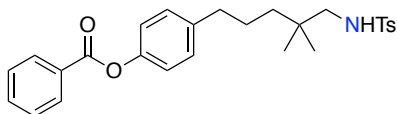
3f was synthesized according to **GP 2**. The NMR data match those previously reported in literature.⁷⁶ ¹H NMR (300 MHz, CDCl₃): $\delta = 7.74$ (d, $J = 8.3$ Hz, 2H), 7.32-7.27 (m, 2H), 7.26-7.20 (m, 2H), 7.06 (d, $J = 8.4$ Hz, 2H), 4.56 (bs, 1H), 2.66 (d, $J = 6.7$ Hz, 2H), 2.50 (t, $J = 7.6$ Hz, 2H), 2.42 (s, 3H), 1.55-1.39 (m, 2H), 1.27-1.15 (m, 2H), 0.82 (s, 6H). ¹³C NMR (75 MHz, CDCl₃): $\delta = 143.5, 140.9, 137.1, 131.6, 129.8, 128.5, 127.2, 53.0, 39.0, 35.9, 33.9, 25.7, 25.0, 21.7$.

***N*-(5-(4-Fluorophenyl)-2,2-dimethylpentyl)-4-methylbenzenesulfonamide (3g)**



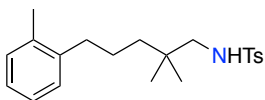
3g was synthesized according to **GP 2**. The NMR data match those previously reported in literature.⁷⁶ ¹H NMR (300 MHz, CDCl₃): $\delta = 7.73$ (d, $J = 8.3$ Hz, 2H), 7.30 (d, $J = 8.0$ Hz, 2H), 7.12-7.05 (m, 2H), 6.99-6.91 (m, 2H), 4.49 (bs, 1H), 2.71-2.62 (m, 2H), 2.50 (t, $J = 7.6$ Hz, 2H), 2.42 (s, 3H), 1.54-1.38 (m, 2H), 1.29-1.16 (m, 2H), 0.82 (s, 6H). ¹³C NMR (75 MHz, CDCl₃): $\delta = 161.3$ (d, $J = 243.3$ Hz), 143.5, 138.1 (d, $J = 3.1$ Hz), 137.2, 129.8, 129.8 (d, $J = 9.3$ Hz), 127.2, 115.1 (d, $J = 20.9$ Hz), 53.0, 39.0, 35.8, 33.9, 25.9, 25.0, 21.7. ¹⁹F NMR (375 MHz, CDCl₃): $\delta = -117.97$ (ddd, $J = 14.2, 8.8, 5.4$ Hz).

4-(4,4-Dimethyl-5-((4-methylphenyl)sulfonamido)pentyl)phenyl benzoate (3h)



3h was synthesized according to **GP 2**. The NMR data match those previously reported in literature.⁷⁶ ¹H NMR (300 MHz, CDCl₃): $\delta = 8.21$ (dd, $J = 8.4, 1.4$ Hz, 2H), 7.74 (d, $J = 8.3$ Hz, 2H), 7.68-7.60 (m, 1H), 7.55-7.46 (m, 2H), 7.34-7.29 (m, 2H), 7.20 (d, $J = 8.6$ Hz, 2H), 7.12 (d, $J = 8.5$ Hz, 2H), 4.46 (t, $J = 6.9$ Hz, 1H), 2.68 (d, $J = 6.7$ Hz, 2H), 2.56 (t, $J = 7.6$ Hz, 2H), 2.42 (s, 3H), 1.57-1.43 (m, 2H), 1.30-1.21 (m, 2H), 0.84 (s, 6H). ¹³C NMR (75 MHz, CDCl₃): $\delta = 165.5, 149.1, 143.5, 140.1, 137.1, 133.7, 130.3, 129.9, 129.8, 129.4, 128.7, 127.2, 121.6, 53.0, 39.1, 36.1, 33.9, 25.8, 25.0, 21.7$.

***N*-(2,2-dimethyl-5-(*o*-tolyl)pentyl)-4-methylbenzenesulfonamide (3i)**

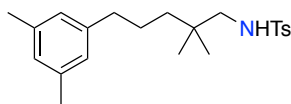


3i was synthesized according to **GP 2**. The NMR data match those previously reported in literature.⁷⁶ ¹H NMR (300 MHz, CDCl₃): $\delta = 7.74$ (d, $J = 8.3$ Hz, 2H), 7.32-7.28 (m, 2H), 7.16-7.05 (m, 4H), 4.50 (bs, 1H), 2.67 (d, $J = 6.8$ Hz, 2H), 2.56-2.47 (m, 2H), 2.42 (s, 3H), 2.28 (s, 3H), 1.54-1.35 (m, 2H), 1.34-1.22 (m, 2H), 0.84 (s, 6H). ¹³C NMR (75 MHz, CDCl₃): $\delta =$

Chapter II: Anodic Benzylic C(sp³)-H Amination:
A Unified Access to pyrrolidines and Piperidines

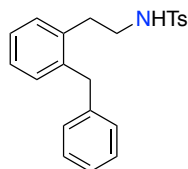
143.4, 140.7, 137.2, 135.9, 130.3, 129.8, 128.8, 127.2, 126.0, 53.1, 39.5, 33.9, 25.0, 24.6, 21.6, 19.4.

***N*-(5-(3,5-dimethylphenyl)-2,2-dimethylpentyl)-4-methylbenzenesulfonamide (3j)**



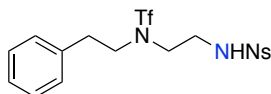
3j was synthesized according to **GP 2**. Obtained as a white solid. ¹H NMR (400 MHz, CDCl₃): δ = 7.79-7.72 (m, 2H), 7.33-7.28 (m, 2H), 6.87-6.75 (m, 3H), 4.60 (t, *J* = 6.8 Hz, 1H), 2.67 (d, *J* = 6.8 Hz, 2H), 2.48-2.41 (m, 5H), 2.30 (s, 6H), 1.51-1.42 (m, 2H), 1.28-1.18 (m, 2H), 0.84 (s, 6H). ¹³C NMR (100 MHz, CDCl₃): δ = 143.4, 142.5, 137.9, 137.2, 129.8, 127.6, 127.2, 126.3, 53.0, 39.3, 36.5, 33.9, 26.0, 25.0, 21.6, 21.4. IR ν (cm⁻¹): 3273, 2958, 2933, 2868, 1603. mp: 86-88 °C. HRMS: Mass calculated for C₂₂H₃₂NO₂S: 374.2148, found: 374.2143.

***N*-(2-Benzylphenethyl)-4-methylbenzenesulfonamide (3k)**



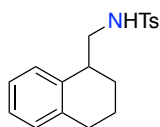
3k was synthesized according to the literature and the NMR data match those previously reported.⁷⁶ ¹H NMR (300 MHz, CDCl₃): δ = 7.66 (d, *J* = 8.2 Hz, 2H), 7.30-7.24 (m, 3H), 7.24-7.11 (m, 5H), 7.11-7.02 (m, 3H), 4.32 (bs, 1H), 3.95 (s, 2H), 3.09-2.99 (m, 2H), 2.77 (t, *J* = 7.3 Hz, 2H), 2.43 (s, 3H). ¹³C NMR (75 MHz, CDCl₃): δ = 143.5, 140.6, 139.0, 137.0, 136.3, 131.2, 129.9, 129.8, 128.7, 128.6, 127.2, 127.1, 126.3, 43.5, 39.1, 33.0, 21.7.

4-Nitro-*N*-(2-((1,1,1-trifluoro-*N*-phenethylmethyl)sulfonamido)ethyl)benzenesulfonamide (3l)



3l was synthesized according to a literature known procedure and the NMR data match those previously reported.⁷⁶ ¹H NMR (300 MHz, CDCl₃): δ = 8.37 (d, *J* = 8.9 Hz, 2H), 8.03 (d, *J* = 8.8 Hz, 2H), 7.38-7.23 (m, 3H), 7.22-7.16 (m, 2H), 4.94 (t, *J* = 6.1 Hz, 1H), 3.63-3.46 (m, 4H), 3.17 (q, *J* = 6.3 Hz, 2H), 2.99-2.89 (m, 2H). ¹³C NMR (75 MHz, CDCl₃): δ = 150.4, 145.5, 136.8, 129.1, 128.9, 128.4, 127.4, 124.7, 51.7, 49.1, 41.9, 35.5. ¹⁹F NMR (375 MHz, CDCl₃): δ = -75.0.

4-methyl-*N*-((1,2,3,4-tetrahydronaphthalen-1-yl)methyl)benzenesulfonamide (3m)

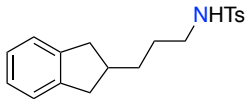


3m was synthesized from the corresponding known amine¹⁶¹ by applying the last step of **GP1**. ¹H NMR (500 MHz, CDCl₃): δ = 7.78 (d, *J* = 8.4 Hz, 2H), 7.31 (d, *J* = 8.1 Hz, 2H), 7.13-7.04 (m, 4H), 5.12-5.07 (m, 1H), 3.23-3.17 (m, 1H), 3.16-3.08 (m, 1H), 3.00-2.91 (m, 1H), 2.75-2.69 (m, 2H), 2.44 (s, 3H), 1.93-1.86 (m, 1H), 1.86-1.81 (m, 1H), 1.81-1.74 (m, 1H), 1.72-1.65

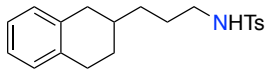
¹⁶¹ B. K. Trivedi, C. J. Blankley, J. A. Bristol, H. W. Hamilton, W. C. Patt, W. J. Kramer, S. A. Johnson, R. F. Bruns, D. M. Cohen, M. J. Ryan, *J. Med. Chem.* **1991**, *34*, 1043-1049.

(m, 1H). ¹³C NMR (125 MHz, CDCl₃): δ = 143.4, 137.9, 137.0, 136.5, 129.7, 129.4, 128.6, 127.1, 126.4, 125.8, 48.2, 37.6, 29.5, 25.4, 21.5, 19.3. IR ν (cm⁻¹): 3286, 2929, 1598. mp: 107-108 °C. HRMS: Mass calculated for C₁₈H₂₀NO₂S: 314.1220, found: 314.1219.

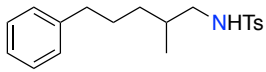
***N*-(3-(2,3-Dihydro-1*H*-inden-2-yl)propyl)-4-methylbenzenesulfonamide (3n)**

 The required amine was synthesized according to an adaption of a previously reported procedure¹⁵⁹ and was tosylated by applying the last step of **GP 1**. The NMR data match those previously reported in literature.⁷⁶ ¹H NMR (300 MHz, CDCl₃): δ = 7.75 (d, *J* = 8.3 Hz, 2H), 7.31 (d, *J* = 8.3 Hz, 2H), 7.19-7.08 (m, 4H), 4.33 (t, *J* = 6.2 Hz, 1H), 3.04-2.92 (m, 4H), 2.50 (dd, *J* = 15.4, 7.9 Hz, 2H), 2.43 (s, 3H), 2.41-2.28 (m, 1H), 1.64-1.41 (m, 4H). ¹³C NMR (75 MHz, CDCl₃): δ = 143.6, 143.3, 137.1, 129.9, 127.3, 126.3, 124.5, 43.5, 39.8, 39.3, 32.7, 28.6, 21.7.

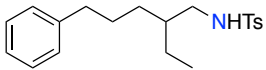
4-Methyl-*N*-(3-(1,2,3,4-tetrahydronaphthalen-2-yl)propyl)benzenesulfonamide (3o)

 The required amine was synthesized according to an adaption of a previously reported procedure¹⁵⁹ and was tosylated by applying the last step of **GP 1**. **XX** was obtained as a white solid. ¹H NMR (400 MHz, CDCl₃): δ = 7.77 (d, *J* = 8.3 Hz, 2H), 7.34-7.28 (m, 2H), 7.11-6.99 (m, 4H), 4.62 (bs, 1H), 3.00-2.93 (m, 2H), 2.83-2.68 (m, 3H), 2.42 (s, 3H), 2.37-2.27 (m, 1H), 1.89-1.79 (m, 1H), 1.68-1.51 (m, 3H), 1.39-1.25 (m, 3H). ¹³C NMR (100 MHz, CDCl₃): δ = 143.5, 137.2, 136.8, 136.4, 129.8, 129.2, 128.9, 127.2, 125.7, 125.6, 43.6, 36.1, 33.9, 33.3, 29.4, 29.1, 27.2, 21.6. IR ν (cm⁻¹): 3284, 2926, 2901, 2845, 1596. mp: 66-68 °C. HRMS: Mass calculated for C₂₀H₂₆NO₂S: 344.1679, found: 344.1676.

4-Methyl-*N*-(2-methyl-5-phenylpentyl)benzenesulfonamide (3p)

 **3p** was synthesized according to **GP 1** using (3-Bromopropyl)benzene as starting material. The NMR data match those previously reported in literature.⁷⁶ ¹H NMR (400 MHz, CDCl₃): δ = 7.77-7.68 (m, 2H), 7.33-7.24 (m, 4H), 7.20-7.15 (m, 1H), 7.15-7.11 (m, 2H), 4.52 (bs, 1H), 2.87-2.80 (m, 1H), 2.77-2.69 (m, 1H), 2.57-2.49 (m, 2H), 2.42 (s, 3H), 1.65-1.54 (m, 2H), 1.54-1.45 (m, 1H), 1.40-1.29 (m, 1H), 1.16-1.06 (m, 1H), 0.86 (d, *J* = 6.7 Hz, 3H). ¹³C NMR (100 MHz, CDCl₃): δ = 143.4, 142.4, 137.2, 129.8, 128.5, 128.4, 127.2, 125.9, 49.1, 36.1, 33.6, 33.2, 28.7, 21.6, 17.5.

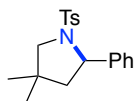
4-Methyl-*N*-(2-ethyl-5-phenylpentyl)benzenesulfonamide (3q)

 **3q** was synthesized according to **GP 1** using (3-Bromopropyl)benzene as starting material. The NMR data match those previously reported in literature.⁷⁶ ¹H NMR (300 MHz, CDCl₃): δ = 7.73 (d, *J* = 8.3 Hz, 2H), 7.32-7.23 (m, 4H), 7.22-7.16 (m, 1H), 7.16-7.10 (m, 2H), 4.30 (bs, 1H), 2.84 (t, *J* = 6.1 Hz, 2H), 2.53 (t, *J* = 7.7 Hz, 2H), 2.42 (s, 3H), 1.55-

Chapter II: Anodic Benzylic C(sp³)-H Amination:
A Unified Access to pyrrolidines and Piperidines

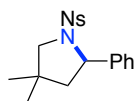
1.45 (m, 2H), 1.44-1.34 (m, 1H), 1.34-1.21 (m, 4H), 0.78 (t, $J = 7.3$ Hz, 3H). ¹³C NMR (75 MHz, CDCl₃): $\delta = 143.5, 142.4, 137.1, 129.8, 128.5, 128.4, 127.3, 125.9, 45.8, 39.3, 36.2, 30.7, 28.4, 24.0, 21.7, 10.8$.

4,4-Dimethyl-2-phenyl-1-tosylpyrrolidine (2a)



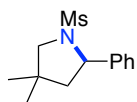
2a was obtained as a colorless oil (85%) by applying **GP 3**. The NMR data match those previously reported.⁷² ¹H NMR (400 MHz, CDCl₃): $\delta = 7.53$ (d, $J = 8.3$ Hz, 2H), 7.29-7.24 (m, 4H), 7.24-7.18 (m, 3H), 4.70 (dd, $J = 9.4, 7.3$ Hz, 1H), 3.44 (dd, $J = 10.4, 1.5$ Hz, 1H), 3.34 (dd, $J = 10.4, 0.8$ Hz, 1H), 2.39 (s, 3H), 2.02 (ddd, $J = 12.8, 7.3, 1.5$ Hz, 1H), 1.72 (dd, $J = 12.8, 9.4$ Hz, 1H), 1.05 (s, 3H), 0.76 (s, 3H). ¹³C NMR (75 MHz, CDCl₃): $\delta = 143.1, 143.0, 135.9, 129.4, 128.4, 127.5, 127.2, 126.6, 63.9, 62.0, 51.7, 38.3, 26.2, 25.8, 21.6$.

4,4-Dimethyl-1-((4-nitrophenyl)sulfonyl)-2-phenylpyrrolidine (2b)



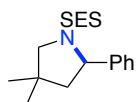
2b was obtained as a white solid (51%) by applying **GP 3**. The NMR data match those previously reported.⁷² ¹H NMR (500 MHz, CDCl₃): $\delta = 8.11$ (d, $J = 8.8$ Hz, 2H), 7.58 (d, $J = 8.8$ Hz, 2H), 7.20-7.14 (m, 3H), 7.12-7.09 (m, 2H), 4.86 (dd, $J = 9.8, 7.2$ Hz, 1H), 3.66 (dd, $J = 10.0, 1.7$ Hz, 1H), 3.30 (d, $J = 10.0$ Hz, 1H), 2.15 (ddd, $J = 12.9, 7.2, 1.7$ Hz, 1H), 1.79 (dd, $J = 12.9, 9.8$ Hz, 1H), 1.13 (s, 3H), 1.02 (s, 3H). ¹³C NMR (125 MHz, CDCl₃): $\delta = 149.6, 145.9, 141.4, 128.5, 128.1, 127.8, 127.2, 123.8, 64.1, 61.9, 51.3, 38.6, 25.7, 25.7$.

4,4-Dimethyl-1-(methylsulfonyl)-2-phenylpyrrolidine (2c)



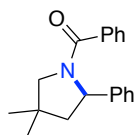
2c was obtained as a white solid (73%) by applying **GP 3**. The NMR data match those previously reported.⁷⁵ ¹H NMR (500 MHz, CDCl₃): $\delta = 7.39$ -7.35 (m, 4H), 7.31-7.26 (m, 1H), 4.92 (dd, $J = 9.8, 7.3$ Hz, 1H), 3.68 (dd, $J = 10.2, 1.7$ Hz, 1H), 3.30 (dd, $J = 10.2, 0.8$ Hz, 1H), 2.55 (s, 3H), 2.22 (ddd, $J = 12.8, 7.3, 1.7$ Hz, 1H), 1.85 (dd, $J = 12.8, 9.8$ Hz, 1H), 1.21 (s, 3H), 1.17 (s, 3H). ¹³C NMR (125 MHz, CDCl₃): $\delta = 142.6, 128.8, 127.8, 126.9, 63.5, 61.5, 51.6, 40.7, 38.4, 25.8, 25.7$.

4,4-Dimethyl-2-phenyl-1-((2-(trimethylsilyl)ethyl)sulfonyl)pyrrolidine (2d)



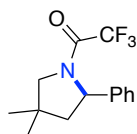
2d was obtained as a white solid (37%) by applying **GP 3**. The NMR data match those previously reported.⁷² ¹H NMR (400 MHz, CDCl₃): $\delta = 7.36$ -7.31 (m, 4H), 7.29-7.26 (m, 1H), 4.93 (dd, $J = 10.2, 7.2$ Hz, 1H), 3.75 (dd, $J = 10.2, 1.8$ Hz, 1H), 3.25 (d, $J = 10.2$ Hz, 1H), 2.47 (td, $J = 13.9, 4.1$ Hz, 1H), 2.28 (td, $J = 13.9, 4.5$ Hz, 1H), 2.22-2.15 (m, 1H), 1.89-1.78 (m, 1H), 1.19 (s, 3H), 1.15 (s, 3H), 0.82 (ddd, $J = 20.8, 13.7, 4.2$ Hz, 2H), -0.13 (s, 9H). ¹³C NMR (100 MHz, CDCl₃): $\delta = 142.8, 128.8, 127.9, 127.2, 63.4, 62.4, 51.6, 50.4, 38.8, 25.6, 25.5, 10.1, -1.9$.

(4,4-Dimethyl-2-phenylpyrrolidin-1-yl)(phenyl)methanone (2e)



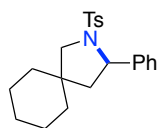
2e was obtained in 65% yield (NMR) by applying **GP 3**. Product could not be separated from starting material by column chromatography. The NMR data match those previously reported.⁷⁵ ¹H NMR (500 MHz, CDCl₃): δ = 7.66-7.60 (m, 2H), 7.45 (td, *J* = 7.7, 2.1 Hz, 3H), 7.39-7.33 (m, 4H), 5.36 (dd, *J* = 10.2, 7.7 Hz, 1H), 3.61 (d, *J* = 10.4 Hz, 1H), 3.42-3.37 (m, 1H), 2.26 (dd, *J* = 12.8, 7.7 Hz, 1H), 1.83-1.76 (m, 1H), 1.13 (s, 3H), 1.06 (s, 3H). ¹³C NMR (125 MHz, CDCl₃): δ = 170.3, 143.6, 136.8, 130.4, 128.5, 128.3, 127.9, 126.9, 125.8, 64.2, 60.9, 49.4, 39.1, 25.6, 25.4.

1-(4,4-Dimethyl-2-phenylpyrrolidin-1-yl)-2,2,2-trifluoroethan-1-one (**2f**)



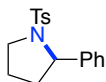
2f was obtained as a white solid (60%) by applying **GP 3**. The NMR data match those previously reported.⁷⁵ ¹H NMR (400 MHz, CDCl₃): δ = 7.38-7.32 (m, 2H), 7.29-7.26 (m, 1H), 7.24-7.19 (m, 2H), 5.13 (dd, *J* = 9.8, 7.8 Hz, 1H), 3.74 (dt, *J* = 10.9, 2.0 Hz, 1H), 3.53 (d, *J* = 10.9 Hz, 1H), 2.26 (ddd, *J* = 13.0, 7.8, 1.7 Hz, 1H), 1.76 (dd, *J* = 13.0, 9.8 Hz, 1H), 1.21 (s, 3H), 1.15 (s, 3H). ¹³C NMR (100 MHz, CDCl₃): δ = 155.9 (d, *J* = 36.5 Hz), 141.7, 128.9, 127.5, 125.7, 116.4 (q, *J* = 287.9 Hz), 62.7, 60.6 (d, *J* = 2.8 Hz), 48.6, 39.0, 25.6, 25.5. ¹⁹F NMR (375 MHz, CDCl₃): δ = -71.61.

3-Phenyl-2-tosyl-2-azaspiro[4.5]decane (**2g**)



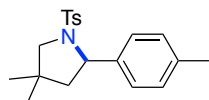
2g was obtained as a white solid (89%) by applying **GP 3**. The NMR data match those previously reported.⁷² ¹H NMR (400 MHz, CDCl₃): δ = 7.59 (d, *J* = 8.3 Hz, 2H), 7.31-7.28 (m, 4H), 7.26-7.22 (m, 3H), 4.64 (dd, *J* = 9.4, 7.3 Hz, 1H), 3.64 (d, *J* = 10.8 Hz, 1H), 3.33 (d, *J* = 10.7 Hz, 1H), 2.42 (s, 3H), 2.13 (dd, *J* = 12.9, 7.3 Hz, 1H), 1.67 (dd, *J* = 12.9, 9.4 Hz, 1H), 1.47-1.41 (m, 4H), 1.38-1.26 (m, 4H), 1.07-0.98 (m, 2H). ¹³C NMR (100 MHz, CDCl₃): δ = 143.2, 143.1, 135.6, 129.4, 128.4, 127.5, 127.2, 126.5, 63.2, 59.4, 49.7, 42.1, 36.5, 34.0, 26.0, 23.9, 22.9, 21.6.

2-Phenyl-1-tosylpyrrolidine (**2h**)



2h was obtained as a white solid (55%) by applying **GP 3**. The NMR data match those previously reported.⁷² ¹H NMR (300 MHz, CDCl₃): δ = 7.67 (d, *J* = 8.3 Hz, 2H), 7.34-7.17 (m, 7H), 4.78 (dd, *J* = 7.8, 3.6 Hz, 1H), 3.66-3.56 (m, 1H), 3.48-3.37 (m, 1H), 2.42 (s, 3H), 2.08-1.75 (m, 3H), 1.75-1.60 (m, 1H). ¹³C NMR (75 MHz, CDCl₃): δ = 143.4, 143.2, 135.2, 129.7, 128.4, 127.6, 127.1, 126.3, 63.4, 49.5, 35.9, 24.1, 21.6.

4,4-Dimethyl-2-(*p*-tolyl)-1-tosylpyrrolidine (**2i**)

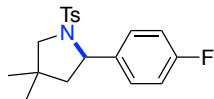


2i was obtained as a white solid (84%) by applying **GP 3**. The NMR data match those previously reported.⁷² ¹H NMR (300 MHz, CDCl₃): δ = 7.58-7.49 (m, 2H), 7.24-7.12 (m, 4H), 7.09-7.04 (m, 2H), 4.65

Chapter II: Anodic Benzylic C(sp³)-H Amination:
A Unified Access to pyrrolidines and Piperidines

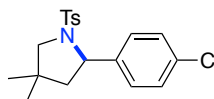
(dd, $J = 9.4, 7.2$ Hz, 1H), 3.45-3.30 (m, 2H), 2.40 (s, 3H), 2.32 (s, 3H), 1.99 (dd, $J = 12.8, 7.2$ Hz, 1H), 1.71 (dd, $J = 12.8, 9.4$ Hz, 1H), 1.05 (s, 3H), 0.74 (s, 3H). ¹³C NMR (75 MHz, CDCl₃): $\delta = 143.1, 140.0, 136.8, 135.9, 129.4, 129.1, 127.5, 126.6, 63.7, 62.0, 51.6, 38.1, 26.3, 25.8, 21.6, 21.2$.

2-(4-Fluorophenyl)-4,4-dimethyl-1-tosylpyrrolidine (2j)



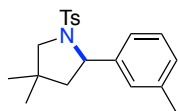
2j was obtained as a white solid (83%) by applying **GP 3**. The NMR data match those previously reported.⁷² ¹H NMR (400 MHz, CDCl₃): $\delta = 7.58-7.50$ (m, 2H), 7.27-7.20 (m, 4H), 6.97-6.90 (m, 2H), 4.67 (dd, $J = 9.4, 7.2$ Hz, 1H), 3.43 (dd, $J = 10.4, 1.5$ Hz, 1H), 3.33 (d, $J = 10.4$ Hz, 1H), 2.40 (s, 3H), 2.00 (ddd, $J = 12.8, 7.2, 1.5$ Hz, 1H), 1.68 (dd, $J = 12.8, 9.4$ Hz, 1H), 1.05 (s, 3H), 0.75 (s, 3H). ¹³C NMR (100 MHz, CDCl₃): $\delta = 162.0$ (d, $J = 245.1$ Hz), 143.3, 138.8 (d, $J = 3.1$ Hz), 135.8, 129.5, 128.2 (d, $J = 8.1$ Hz), 127.4, 115.2 (d, $J = 21.6$ Hz), 63.3, 61.9, 51.6, 38.2, 26.2, 25.7, 21.6. ¹⁹F NMR (375 MHz, CDCl₃): $\delta = -116.0$.

2-(4-Chlorophenyl)-4,4-dimethyl-1-tosylpyrrolidine (2k)



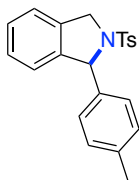
2k was obtained as a slightly brown solid (52%) by applying **GP 3**. The NMR data match those previously reported.⁷² ¹H NMR (300 MHz, CDCl₃): $\delta = 7.59$ (d, $J = 8.2$ Hz, 2H), 7.32-7.27 (m, 6H), 4.70 (dd, $J = 9.3, 7.3$ Hz, 1H), 3.47 (dd, $J = 10.4, 1.4$ Hz, 1H), 3.38 (d, $J = 10.5$ Hz, 1H), 2.45 (s, 3H), 2.04 (ddd, $J = 12.8, 7.2, 1.4$ Hz, 1H), 1.71 (dd, $J = 12.8, 9.3$ Hz, 1H), 1.09 (s, 3H), 0.78 (s, 3H). ¹³C NMR (75 MHz, CDCl₃): $\delta = 143.4, 141.6, 135.6, 132.8, 129.5, 128.5, 128.0, 127.5, 63.3, 62.0, 51.5, 38.2, 26.2, 25.8, 21.6$.

4,4-Dimethyl-2-(*m*-tolyl)-1-tosylpyrrolidine (2l)



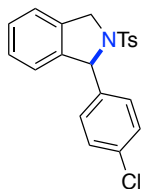
2l was obtained as a yellow oil (63%) by applying **GP 3**. The NMR data match those previously reported.⁷⁵ ¹H NMR (300 MHz, CDCl₃): $\delta = 7.57-7.48$ (m, 2H), 7.22-6.97 (m, 6H), 4.69 (dd, $J = 9.5, 7.2$ Hz, 1H), 3.48 (dd, $J = 10.4, 1.5$ Hz, 1H), 3.33 (d, $J = 10.3$ Hz, 1H), 2.39 (s, 3H), 2.27 (s, 3H), 2.01 (ddd, $J = 12.8, 7.2, 1.5$ Hz, 1H), 1.71 (dd, $J = 12.8, 9.5$ Hz, 1H), 1.06 (s, 3H), 0.78 (s, 3H). ¹³C NMR (75 MHz, CDCl₃): $\delta = 143.0, 142.8, 137.8, 136.1, 129.3, 128.2, 127.9, 127.4, 127.2, 123.8, 63.9, 61.9, 51.7, 38.2, 26.1, 25.8, 21.6, 21.5$.

1-(*p*-Tolyl)-2-tosylisoindoline (2m)



2m was obtained as a white solid (77%) by applying **GP 3**. The NMR data match those previously reported.⁷⁵ ¹H NMR (400 MHz, CDCl₃): $\delta = 7.58$ (d, $J = 8.3$ Hz, 2H), 7.24-7.21 (m, 2H), 7.20-7.15 (m, 3H), 7.13-7.05 (m, 4H), 6.88 (d, $J = 7.6$ Hz, 1H), 5.89-5.83 (m, 1H), 4.83-4.78 (m, 2H), 2.36 (s, 3H), 2.32 (s, 3H). ¹³C NMR (125 MHz, CDCl₃): $\delta = 143.3, 141.2, 139.1, 137.6, 135.4, 135.2, 129.5, 129.2, 128.1, 128.0, 127.6, 127.5, 123.7, 122.5, 69.4, 54.1, 21.6, 21.2$.

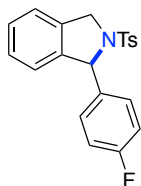
1-(4-Chlorophenyl)-2-tosylisoindoline (2n)



2n was obtained as a yellow oil (83%) by applying **GP 3**. ¹H NMR (300 MHz, CDCl₃): δ = 7.58 (d, *J* = 8.3 Hz, 2H), 7.28-7.15 (m, 9H), 6.87 (dd, *J* = 7.5, 1.1 Hz, 1H), 5.88 (s, 1H), 4.91-4.79 (m, 2H), 2.39 (s, 3H). ¹³C NMR (75 MHz, CDCl₃): δ = 143.7, 140.6, 140.5, 135.2, 135.1, 133.8, 129.7, 129.1, 128.7, 128.3, 128.2, 127.5, 123.7, 122.6, 68.8, 54.1, 21.6. IR ν (cm⁻¹): 2846, 1598. HRMS: Mass calculated for C₂₁H₁₈ClNNaO₂S: 406.0639,

found: 406.0647.

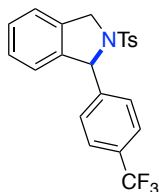
1-(4-Fluorophenyl)-2-tosylisoindoline (2o)



2o was obtained as a white solid (56%) by applying **GP 3**. ¹H NMR (400 MHz, CDCl₃): δ = 7.62-7.53 (m, 2H), 7.29-7.25 (m, 2H), 7.24-7.17 (m, 5H), 7.0-6.94 (m, 2H), 6.88 (d, *J* = 7.6 Hz, 1H), 5.92 (s, 1H), 4.85 (s, 2H), 2.39 (s, 3H). ¹³C NMR (100 MHz, CDCl₃): δ = 162.5 (d, *J* = 246.5 Hz), 143.6, 140.9, 137.9, 137.9, 135.4, 135.2, 129.7, 129.6, 129.5, 128.2 (d, *J* = 2.4 Hz), 127.5, 123.7, 122.6, 115.5 (d, *J* = 21.6 Hz), 68.8, 54.1, 21.6. ¹⁹F NMR (375

MHz, CDCl₃*d*): δ = -114.65. IR ν (cm⁻¹): 2923, 1603, 1508. mp: 154-156 °C. HRMS: Mass calculated for C₂₁H₁₈FNNaO₂S: 390.0934, found: 390.0928.

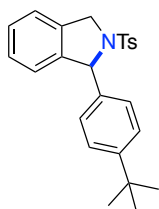
2-Tosyl-1-(4-(trifluoromethyl)phenyl)isoindoline (2p)



2p was obtained as a yellow oil (56%) by applying **GP 3**. ¹H NMR (300 MHz, CDCl₃): δ = 7.56 (d, *J* = 8.3 Hz, 2H), 7.52 (d, *J* = 8.2 Hz, 2H), 7.35 (d, *J* = 8.0 Hz, 2H), 7.31-7.26 (m, 2H), 7.23-7.16 (m, 3H), 6.87 (dd, *J* = 7.5, 1.1 Hz, 1H), 5.95 (s, 1H), 4.92-4.85 (m, 2H), 2.38 (s, 3H). ¹³C NMR (75 MHz, CDCl₃): δ = 145.9, 143.8, 140.2, 135.2, 130.3, 129.9, 129.7, 128.5, 128.3, 128.1, 127.5, 126.0, 125.6 (q, *J* = 3.8 Hz), 123.7, 122.8, 122.4,

68.9, 54.3, 21.6. ¹⁹F NMR (375 MHz, CDCl₃): δ = -62.6. IR ν (cm⁻¹): 2926, 1718, 1618, 1598. HRMS: Mass calculated for C₂₂H₁₈F₃NNaO₂S: 440.0903, found: 440.0905.

1-(4-(tert-Butyl)phenyl)-2-tosylisoindoline (2q)

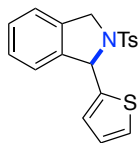


2q was obtained as an orange solid (62%) by applying **GP 3**. ¹H NMR (300 MHz, CDCl₃): δ = 7.47 (d, *J* = 8.3 Hz, 2H), 7.24-7.21 (m, 4H), 7.20-7.14 (m, 1H), 7.13-7.05 (m, 4H), 6.92 (d, *J* = 7.8 Hz, 1H), 5.93 (s, 1H), 4.93-4.78 (m, 2H), 2.33 (s, 3H), 1.29 (s, 9H). ¹³C NMR (75 MHz, CDCl₃): δ = 150.7, 143.1, 141.3, 138.6, 135.9, 135.3, 129.5, 128.1, 128.0, 127.5, 127.4, 125.4, 123.9, 122.5, 69.3, 54.0, 34.6, 31.5, 21.6. mp: 170-171 °C.

IR ν (cm⁻¹): 2959. HRMS: Mass calculated for C₂₅H₂₇NNaO₂S: 428.1655, found: 428.1656.

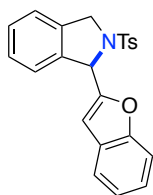
1-(Thiophen-2-yl)-2-tosylisoindoline (2r)

Chapter II: Anodic Benzylic C(sp³)-H Amination:
A Unified Access to pyrrolidines and Piperidines



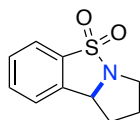
2r was obtained as a white solid (48%) by applying **GP 3** ($I = 1$ mA). The NMR data match those previously reported.⁷⁵ ¹H NMR (500 MHz, CDCl₃): $\delta = 7.60$ -7.56 (m, 2H), 7.30-7.28 (m, 1H), 7.27-7.22 (m, 2H), 7.22-7.17 (m, 3H), 7.13 (dd, $J = 3.4, 1.2$ Hz, 1H), 7.10-7.07 (m, 1H), 6.94 (dd, $J = 5.1, 3.5$ Hz, 1H), 6.35 (s, 1H), 4.84 (d, $J = 13.5$ Hz, 1H), 4.76 (dd, $J = 13.6, 2.6$ Hz, 1H), 2.38 (s, 3H). ¹³C NMR (125 MHz, CDCl₃): $\delta = 143.4, 140.4, 135.8, 135.3, 129.6, 128.5, 128.1, 127.4, 126.5, 126.5, 126.1, 123.8, 122.6, 64.7, 53.3, 21.6$.

1-(benzofuran-2-yl)-2-tosylisoindoline(2s)



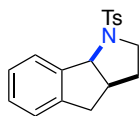
2s was obtained as a white solid (67%) by applying **GP 3** ($I = 1$ mA). ¹H NMR (500 MHz, CDCl₃): $\delta = 7.54$ -7.49 (m, 3H), 7.32-7.27 (m, 2H), 7.22 (td, $J = 7.1, 6.6, 1.9$ Hz, 1H), 7.19-7.15 (m, 2H), 7.15-7.10 (m, 2H), 6.96 (d, $J = 8.0$ Hz, 2H), 6.77 (s, 1H), 6.18 (d, $J = 2.7$ Hz, 1H), 4.95 (d, $J = 13.2$ Hz, 1H), 4.88 (dd, $J = 13.2, 2.8$ Hz, 1H), 2.22 (s, 3H). ¹³C NMR (125 MHz, CDCl₃): $\delta = 155.3, 155.1, 143.4, 137.6, 136.0, 135.5, 129.3, 128.6, 128.1, 127.9, 127.2, 124.3, 123.5, 122.8, 122.8, 121.3, 111.4, 105.6, 62.8, 53.8, 21.4$. IR ν (cm⁻¹): 3023, 2921, 1599. mp: 134-135 °C. HRMS: Mass calculated for C₂₃H₁₉NNaO₃S: 412.0978, found: 412.0968.

1,2,3,9b-Tetrahydrobenzo[1,2-b]isothiazole-5,5-dioxide (2t)



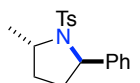
2t was obtained in 30% yield (NMR) by applying **GP 3**. The product could not be separated from the starting material by column chromatography. The NMR data match those previously reported.⁷² ¹H NMR (500 MHz, CDCl₃): $\delta = 7.74$ (d, $J = 7.8$ Hz, 1H), 7.60 (t, $J = 7.5$ Hz, 1H), 7.53-7.48 (m, 1H), 7.36 (d, $J = 7.8$ Hz, 1H), 4.99 (t, $J = 6.6$ Hz, 1H), 3.83-3.79 (m, 1H), 3.39-3.36 (m, 1H), 2.48-2.40 (m, 1H), 2.03-1.96 (m, 1H), 1.95-1.90 (m, 2H). ¹³C NMR (100 MHz, CDCl₃): $\delta = 140.1, 136.4, 133.3, 129.5, 124.0, 121.6, 65.2, 48.4, 32.6, 26.2$.

1-Tosyl-1,2,3,3a,4,8b-hexahydroindeno[1,2-b]pyrrole (2u)



2u was obtained as a white solid (87%) by applying **GP 3**. The NMR data match those previously reported.⁷² ¹H NMR (500 MHz, CDCl₃): $\delta = 7.88$ -7.78 (m, 3H), 7.36 (d, $J = 8.0$ Hz, 2H), 7.32-7.24 (m, 2H), 7.21-7.16 (m, 1H), 5.18 (d, $J = 7.8$ Hz, 1H), 3.40 (ddd, $J = 10.3, 7.2, 4.4$ Hz, 1H), 3.27 (ddd, $J = 10.3, 8.7, 6.7$ Hz, 1H), 3.05 (dd, $J = 16.3, 7.8$ Hz, 1H), 2.81-2.70 (m, 2H), 2.47 (s, 3H), 1.91-1.83 (m, 1H), 1.63-1.53 (m, 1H). ¹³C NMR (125 MHz, CDCl₃): $\delta = 143.6, 142.1, 141.0, 135.0, 129.8, 128.4, 127.8, 127.4, 126.9, 125.0, 68.8, 49.3, 41.9, 36.0, 31.5, 21.6$.

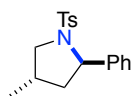
2-methyl-5-phenyl-1-tosylpyrrolidine (2v)



2v was obtained as a white solid (46%, d.r. = 1.2:1) by applying **GP 3**. The NMR data of the major diastereoisomer (*anti*) is given. ¹H NMR (300 MHz, CDCl₃): $\delta = 7.69$ (d, $J = 8.3$ Hz, 2H), 7.42-7.22 (m, 5H), 7.16-7.00 (m, 2H),

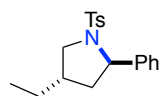
4.72 (t, $J = 6.5$ Hz, 1H), 3.92 (dq, $J = 12.8, 6.4$ Hz, 1H), 2.42 (s, 3H), 1.94-1.83 (m, 1H), 1.78-1.67 (m, 1H), 1.63-1.54 (m, 1H), 1.47 (d, $J = 6.4$ Hz, 3H). ¹³C NMR (75 MHz, CDCl₃): $\delta = 143.4, 143.0, 135.4, 129.7, 128.4, 127.1, 127.1, 126.4, 65.1, 57.4, 34.6, 32.3, 22.9, 21.7$. IR ν (cm⁻¹): 2928, 1596. HRMS: Mass calculated for C₁₈H₂₁NNaO₂S: 338.1185, found: 338.1180.

4-Methyl-2-phenyl-1-tosylpyrrolidine (2w)



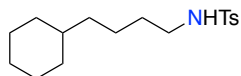
2w was obtained as a white foam (67%, d.r. = 2.5:1) by applying **GP 3**. The NMR data of the major diastereoisomer (*anti*) is given which match those previously reported.⁷² ¹H NMR (500 MHz, CDCl₃): $\delta = 7.65$ -7.61 (m, 2H), 7.37-7.18 (m, 7H), 4.67 (dd, $J = 9.5, 7.2$ Hz, 1H), 3.86 (ddd, $J = 11.2, 7.3, 1.4$ Hz, 1H), 3.11 (t, $J = 10.8$ Hz, 1H), 2.44 (s, 3H), 2.43-2.37 (m, 1H), 1.96-1.80 (m, 1H), 1.51 (ddd, $J = 12.7, 11.4, 9.5$ Hz, 1H), 0.98 (d, $J = 6.5$ Hz, 3H). ¹³C NMR (125 MHz, CDCl₃): $\delta = 143.3, 143.1, 135.7, 129.6, 128.4, 127.6, 127.2, 126.4, 64.8, 56.8, 45.8, 33.5, 21.6, 16.6$.

4-Ethyl-2-phenyl-1-tosylpyrrolidine (2x)



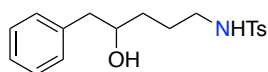
2x was obtained as a colorless oil (64%, d.r. 2:1) by applying **GP 3**. The NMR data of the major diastereoisomer (*anti*) is given. ¹H NMR (300 MHz, CDCl₃): $\delta = 7.62$ (d, $J = 8.3$ Hz, 2H), 7.34-7.20 (m, 6H), 4.64 (dd, $J = 9.5, 7.1$ Hz, 1H), 3.89 (ddd, $J = 11.1, 7.3, 1.3$ Hz, 1H), 3.13 (dd, $J = 11.1, 10.3$ Hz, 1H), 2.43 (s, 3H), 1.80-1.63 (m, 1H), 1.56-1.45 (m, 1H), 1.41-1.17 (m, 3H), 0.90-0.79 (m, 3H). ¹³C NMR (75 MHz, CDCl₃): $\delta = 143.3, 143.1, 135.7, 129.6, 128.4, 127.5, 127.2, 126.4, 64.6, 55.3, 43.8, 40.6, 25.4, 21.6, 12.6$. IR ν (cm⁻¹): 2961, 1598. HRMS: Mass calculated for C₁₉H₂₃NNaO₂S: 352.1342, found: 352.1338.

N-(4-Cyclohexylbutyl)-4-methylbenzenesulfonamide (6)



6 was prepared from the corresponding nitrile following **GP 1**. ¹H NMR (300 MHz, CDCl₃): $\delta = 7.75$ (d, $J = 8.2$ Hz, 2H), 7.30 (d, $J = 8.0$ Hz, 2H), 4.48 (bs, 1H), 2.92 (t, $J = 7.0$ Hz, 2H), 2.42 (s, 3H), 1.69-1.57 (m, 5H), 1.48-1.35 (m, 2H), 1.30-1.01 (m, 8H), 0.89-0.71 (m, 2H). ¹³C NMR (75 MHz, CDCl₃): $\delta = 143.4, 137.2, 129.8, 127.2, 43.4, 37.6, 37.0, 33.4, 30.0, 26.8, 26.48, 23.9, 21.7$. mp: 76-77 °C. IR ν (cm⁻¹): 3288, 2918, 2845, 1597. HRMS: Mass calculated for C₁₇H₂₈NO₂S: 310.1835, found: 310.1843.

N-(4-hydroxy-5-phenylpentyl)-4-methylbenzenesulfonamide (9)

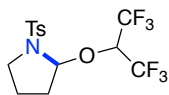


¹H NMR (500 MHz, CDCl₃): $\delta = 7.76$ -7.71 (m, 2H), 7.34-7.28 (m, 4H), 7.25-7.21 (m, 1H), 7.18-7.14 (m, 2H), 3.82-3.71 (m, 1H), 3.02-2.91 (m, 2H), 2.76 (dd, $J = 13.5, 4.3$ Hz, 1H), 2.61 (dd, $J = 13.5, 8.5$ Hz, 1H), 2.42 (s, 3H), 1.70-1.53 (m, 3H), 1.49-1.38 (m, 1H). ¹³C NMR (125 MHz, CDCl₃): $\delta = 143.4, 138.2, 137.2, 129.8, 129.5, 128.8, 127.2, 126.8, 72.4, 44.4, 43.3, 33.7,$

Chapter II: Anodic Benzylic C(sp³)-H Amination:
A Unified Access to pyrrolidines and Piperidines

26.1, 21.6. IR ν (cm⁻¹): 3465, 3146, 2914, 1598. HRMS: Mass calculated for C₁₈H₂₂NO₃S: 332.1326, found: 332.1329.

2-((1,1,1,3,3,3-hexafluoropropan-2-yl)oxy)-1-tosylpyrrolidine (10)



10 was obtained as a white solid (40%) by applying **GP 3**. **10** can also be obtained by a Shono oxidation from tosylated pyrrolidine. The electrolysis conditions are the following: graphite rod anode (d = 6.3 mm, immersion depth: 10 mm), platinum mesh cathode, 5 mA, 2.2 F, 10 mL 0.1 M HFIP/Bu₄NBF₄, 0.2 g (0.89 mmol) *N*-tosyl pyrrolidine. After the electrolysis, the solvent was evaporated under reduced pressure and the resulting crude product was further purified by column chromatography (hexane/ethyl acetate). **9** was obtained as a white solid (52%). ¹H NMR (400 MHz, CDCl₃): δ = 7.71-7.65 (m, 2H), 7.37-7.32 (m, 2H), 5.42 (d, *J* = 4.9 Hz, 1H), 5.13 (hept, *J* = 6.2 Hz, 1H), 3.57-3.51 (m, 1H), 3.11 (td, *J* = 10.0, 7.5 Hz, 1H), 2.44 (s, 3H), 2.18-1.98 (m, 2H), 1.88-1.75 (m, 1H), 1.38-1.20 (m, 1H). ¹³C NMR (100 MHz, CDCl₃): δ = 144.6, 134.5, 130.2, 127.5, 91.7, 70.6 (p, *J* = 32.5 Hz), 48.2, 33.1, 22.8, 21.7. ¹⁹F NMR (375 MHz, Chloroform-*d*): δ = -73.57 (q, *J* = 8.9 Hz), -74.12 (q, *J* = 8.8 Hz), -75.79 (s). mp: 95-96 °C. IR ν (cm⁻¹): 2955, 1597. HRMS: Mass calculated for C₁₄H₁₅F₆NNaO₃S: 414.0569, found: 414.0571.

X-Ray Analytical Data for Compound 10

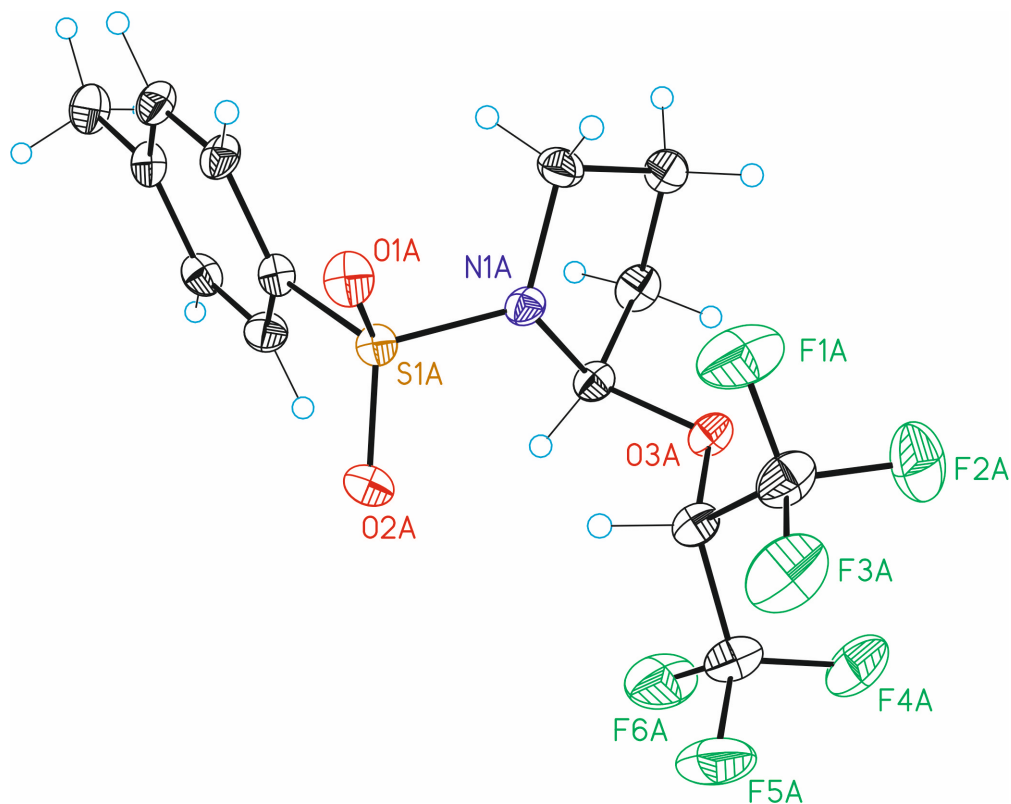


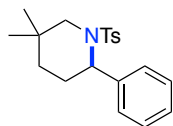
Table S-1. Crystal data and structure refinement for compound **10**.

Identification code	CCDC 1841280	
Empirical formula	C ₁₄ H ₁₅ F ₆ N O ₃ S	
Formula weight	391.33	
Temperature	100(2) K	
Wavelength	0.71073 Å	
Crystal system	Monoclinic	
Space group	C2/c	
Unit cell dimensions	a = 39.756(4) Å	α = 90°.
	b = 6.2412(7) Å	β = 123.261(2)°.
	c = 31.125(3) Å	γ = 90°.
Volume	6457.8(12) Å ³	

Chapter II: Anodic Benzylic C(sp³)-H Amination:
A Unified Access to pyrrolidines and Piperidines

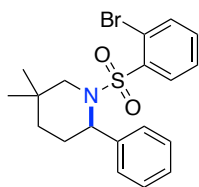
Z	16
Density (calculated)	1.610 Mg/m ³
Absorption coefficient	0.280 mm ⁻¹
F(000)	3200
Crystal size	0.25 x 0.05 x 0.01 mm ³
Theta range for data collection	1.565 to 30.686°
Index ranges	-37<=h<=56,-8<=k<=8,-44<=l<=42
Reflections collected	45043
Independent reflections	9922[R(int) = 0.0627]
Completeness to theta =30.686°	99.4%
Absorption correction	Multi-scan
Max. and min. transmission	0.997 and 0.767
Refinement method	Full-matrix least-squares on F ²
Data / restraints / parameters	9922/ 0/ 453
Goodness-of-fit on F ²	1.071
Final R indices [>2sigma(I)]	R1 = 0.0641, wR2 = 0.1453
R indices (all data)	R1 = 0.1017, wR2 = 0.1599
Largest diff. peak and hole	0.522 and -0.629 e. ⁻³

5,5-Dimethyl-2-phenyl-1-tosylpiperidine (4a)



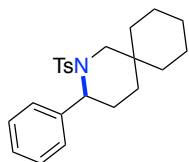
4a was obtained as a colorless oil (53%) by applying **GP 3**. The NMR data match those previously reported.⁷⁶ ¹H NMR (400 MHz, CDCl₃): δ = 7.65 (d, *J* = 8.3 Hz, 2H), 7.25-1.19 (m, 4H), 7.19-7.13 (m, 3H), 5.23 (t, *J* = 4.1 Hz, 1H), 3.41 (d, *J* = 13.5 Hz, 1H), 2.86 (d, *J* = 13.5 Hz, 1H), 2.40 (s, 3H), 2.13-2.05 (m, 2H), 1.30-1.17 (m, 2H), 0.80 (s, 3H), 0.79 (s, 3H). ¹³C NMR (100 MHz, CDCl₃): δ = 142.9, 139.0, 138.7, 129.5, 128.5, 127.1, 127.1, 126.8, 55.5, 52.7, 32.6, 30.4, 28.7, 25.9, 24.2, 21.6.

1-((2-Bromophenyl)sulfonyl)-5,5-dimethyl-2-phenylpiperidine (4b)



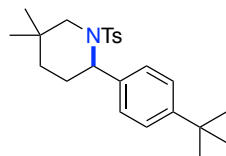
4b was obtained as a white solid (49%) by applying **GP 3**. The NMR data match those previously reported.⁷⁶ ¹H NMR (300 MHz, CDCl₃): δ = 8.12-8.08 (m, 1H), 7.75-7.70 (m, 1H), 7.40-7.24 (m, 6H), 7.22-7.15 (m, 1H), 5.32 (dd, J = 5.4, 2.9 Hz, 1H), 3.30 (d, J = 13.6 Hz, 1H), 3.01 (d, J = 13.6 Hz, 1H), 2.46-2.29 (m, 1H), 2.24-2.12 (m, 1H), 1.32-1.24 (m, 2H), 0.79 (s, 3H), 0.74 (s, 3H). ¹³C NMR (125 MHz, CDCl₃): δ = 139.9, 139.0, 135.5, 133.3, 132.4, 128.6, 127.6, 127.0, 126.9, 120.5, 56.4, 53.3, 32.8, 30.7, 28.6, 25.5, 23.9.

3-Phenyl-2-tosyl-2-azaspiro[5.5]undecane (**4c**)



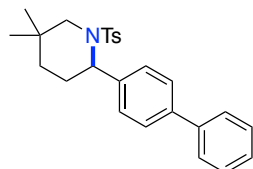
4c was obtained as a colorless oil (39%) by applying **GP 3**. The NMR data match those previously reported.⁷⁶ ¹H NMR (300 MHz, CDCl₃): δ = 7.65 (d, J = 8.3 Hz, 2H), 7.25-7.14 (m, 7H), 5.21 (t, J = 4.2 Hz, 1H), 3.73 (d, J = 13.6 Hz, 1H), 2.78 (d, J = 13.7 Hz, 1H), 2.39 (s, 3H), 2.10-2.01 (m, 2H), 1.47-1.24 (m, 8H), 1.22-1.03 (m, 4H). ¹³C NMR (75 MHz, CDCl₃): δ = 142.8, 139.1, 138.6, 129.5, 128.5, 127.1, 127.0, 126.8, 56.1, 50.3, 37.9, 32.7, 31.9, 30.9, 26.6, 25.1, 21.7, 21.6, 21.5.

2-(4-(*tert*-Butyl)phenyl)-5,5-dimethyl-1-tosylpiperidine (**4d**)



4d was obtained as a brownish oil (59%) by applying **GP 3**. The NMR data match those previously reported.⁷⁶ ¹H NMR (300 MHz, CDCl₃): δ = 7.61 (d, J = 8.3 Hz, 2H), 7.25-7.16 (m, 4H), 7.07 (d, J = 7.9 Hz, 2H), 5.17 (t, J = 4.2 Hz, 1H), 3.40 (d, J = 13.4 Hz, 1H), 2.88 (d, J = 13.3 Hz, 1H), 2.39 (s, 3H), 2.11-2.03 (m, 2H), 1.31-1.19 (m, 11H), 0.81 (s, 6H). ¹³C NMR (75 MHz, CDCl₃): δ = 149.7, 142.7, 138.6, 136.0, 129.5, 127.1, 126.8, 125.4, 55.4, 52.7, 34.5, 32.6, 31.5, 30.5, 28.7, 25.9, 24.3, 21.6.

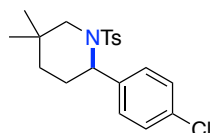
2-([1,1'-Biphenyl]-4-yl)-5,5-dimethyl-1-tosylpiperidine (**4e**)



4e was obtained as a white solid (69%) by applying **GP 3**. The NMR data match those previously reported.⁷⁶ ¹H NMR (300 MHz, CDCl₃): δ = 7.70 (dd, J = 8.3, 1.7 Hz, 2H), 7.58 (d, J = 8.5 Hz, 2H), 7.49 (dd, J = 8.4, 1.6 Hz, 2H), 7.44 (d, J = 7.6 Hz, 2H), 7.39-7.32 (m, 1H), 7.25-7.22 (m, 4H), 5.30 (d, J = 4.1 Hz, 1H), 3.47 (d, J = 13.4 Hz, 1H), 2.94 (d, J = 13.4 Hz, 1H), 2.42 (s, 3H), 2.20-2.11 (m, 2H), 1.41-1.21 (m, 3H), 0.84 (s, 6H). ¹³C NMR (75 MHz, CDCl₃): δ = 142.9, 140.7, 139.7, 138.6, 138.1, 129.5, 128.9, 127.5, 127.4, 127.2, 127.1, 127.1, 55.4, 52.7, 32.7, 30.5, 28.7, 25.8, 24.2, 21.6.

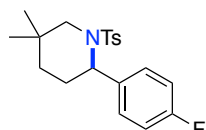
2-(4-Chlorophenyl)-5,5-dimethyl-1-tosylpiperidine (**4f**)

Chapter II: Anodic Benzylic C(sp³)-H Amination:
A Unified Access to pyrrolidines and Piperidines



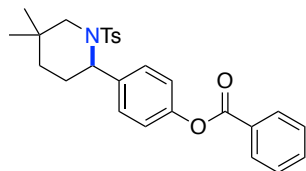
4f was obtained as a white solid (49%) by applying **GP 3**. The NMR data match those previously reported.⁷⁶ ¹H NMR (300 MHz, CDCl₃): δ = 7.65 (d, *J* = 8.3 Hz, 2H), 7.26-7.18 (m, 4H), 7.09 (dd, *J* = 8.8, 1.0 Hz, 2H), 5.17 (t, *J* = 4.3 Hz, 1H), 3.39 (d, *J* = 13.5 Hz, 1H), 2.80 (d, *J* = 13.8 Hz, 1H), 2.41 (s, 3H), 2.11-2.00 (m, 2H), 1.27-1.16 (m, 2H), 0.79 (s, 3H), 0.77 (s, 3H). ¹³C NMR (75 MHz, CDCl₃): δ = 143.1, 138.5, 137.6, 132.7, 129.6, 128.7, 128.5, 127.1, 55.1, 52.6, 32.6, 30.4, 28.6, 25.8, 24.2, 21.6.

2-(4-Fluorophenyl)-5,5-dimethyl-1-tosylpiperidine (4g)



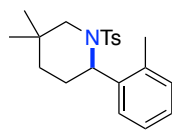
4g was obtained as a white solid (64%) by applying **GP 3**. The NMR data match those previously reported.⁷⁶ ¹H NMR (300 MHz, CDCl₃): δ = 7.64 (d, *J* = 8.3 Hz, 2H), 7.26-7.21 (m, 2H), 7.17-7.09 (m, 2H), 6.96-6.88 (m, 2H), 5.20-5.15 (m, 1H), 3.38 (d, *J* = 13.5 Hz, 1H), 2.82 (d, *J* = 13.5 Hz, 1H), 2.40 (s, 3H), 2.10-2.00 (m, 2H), 1.27-1.17 (m, 2H), 0.80 (s, 3H), 0.77 (s, 3H). ¹³C NMR (75 MHz, CDCl₃): δ = 161.8 (d, *J* = 245.5 Hz), 143.0, 138.5, 134.7 (d, *J* = 3.2 Hz), 129.6, 128.8 (d, *J* = 8.0 Hz), 127.1, 115.4 (d, *J* = 21.2 Hz), 55.1, 52.6, 32.6, 30.5, 28.7, 26.0, 24.3, 21.6. ¹⁹F NMR (375 MHz, CDCl₃): δ = -116.46 – -116.55 (m).

4-(5,5-Dimethyl-1-tosylpiperidin-2-yl)phenyl benzoate (4h)



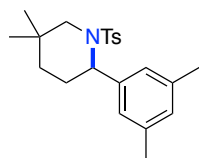
4h was obtained as a white solid (29%) by applying **GP 3**. The NMR data match those previously reported.⁷⁶ ¹H NMR (300 MHz, CDCl₃): δ = 8.21-8.17 (m, 2H), 7.69-7.60 (m, 3H), 7.55-7.48 (m, 2H), 7.25-7.18 (m, 3H), 7.10 (d, *J* = 8.7 Hz, 2H), 5.24 (t, *J* = 4.0 Hz, 1H), 3.43 (d, *J* = 13.8 Hz, 1H), 2.86 (d, *J* = 13.5 Hz, 1H), 2.40 (s, 3H), 2.17-2.06 (m, 2H), 1.39-1.16 (m, 2H), 0.81 (s, 6H). ¹³C NMR (75 MHz, CDCl₃): δ = 165.2, 149.8, 143.0, 138.6, 136.6, 133.8, 130.3, 129.6, 128.7, 128.2, 127.1, 121.7, 55.1, 52.6, 32.6, 30.5, 28.7, 25.8, 24.2, 21.6.

5,5-Dimethyl-2-(*o*-tolyl)-1-tosylpiperidine (4i)



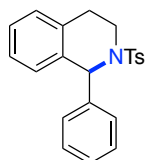
4i was obtained as a slightly yellow oil (50%) by applying **GP 3**. The NMR data match those previously reported.⁷⁶ ¹H NMR (300 MHz, CDCl₃): δ = 7.33-7.22 (m, 2H), 7.08-6.98 (m, 4H), 6.89 (dd, *J* = 7.8, 1.4 Hz, 1H), 6.81-6.74 (m, 1H), 5.08 (t, *J* = 5.8 Hz, 1H), 3.40-3.26 (m, 2H), 2.35 (s, 3H), 2.32 (s, 3H), 2.10-1.96 (m, 1H), 1.76-1.60 (m, 1H), 1.50-1.37 (m, 1H), 1.34-1.21 (m, 1H), 1.04 (s, 3H), 1.03 (s, 3H). ¹³C NMR (75 MHz, CDCl₃): δ = 142.5, 140.1, 137.4, 134.9, 130.7, 129.0, 127.2, 126.9, 126.7, 125.4, 55.2, 54.0, 33.3, 30.7, 27.9, 25.8, 21.5, 19.7.

2-(3,5-dimethylphenyl)-5,5-dimethyl-1-tosylpiperidine (4j)



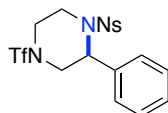
4j was obtained as a colorless oil (44%) by applying **GP 3**. ¹H NMR (500 MHz, CDCl₃): δ = 7.65-7.61 (m, 2H), 7.22 (d, *J* = 8.0 Hz, 2H), 6.78 (s, 1H), 6.58 (s, 2H), 5.16 (t, *J* = 4.1 Hz, 1H), 3.45 (d, *J* = 13.2 Hz, 1H), 2.83 (d, *J* = 13.3 Hz, 1H), 2.40 (s, 3H), 2.16 (s, 6H), 2.11-2.07 (m, 2H), 1.28-1.20 (m, 2H), 0.91 (s, 3H), 0.81 (s, 3H). ¹³C NMR (125 MHz, CDCl₃): δ = 142.7, 138.9, 138.8, 137.9, 129.5, 128.4, 127.1, 124.8, 55.4, 52.7, 32.8, 30.5, 28.7, 26.0, 24.2, 21.6, 21.5. IR ν (cm⁻¹): 2952, 2919, 2865, 1601. HRMS: Mass calculated for C₂₂H₂₉NNaO₂S: 394.1811, found: 294.1815.

1-Phenyl-2-tosyl-1,2,3,4-tetrahydroisoquinoline (**4k**)



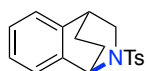
4k was obtained as a white solid (81%) by applying **GP 3**. The NMR data match those previously reported.⁷⁶ ¹H NMR (300 MHz, CDCl₃): δ = 7.55 (d, *J* = 8.3 Hz, 2H), 7.30-7.17 (m, 5H), 7.16-7.11 (m, 2H), 7.08 (d, *J* = 8.1 Hz, 2H), 7.02-6.96 (m, 2H), 6.24 (s, 1H), 3.77 (dddd, *J* = 14.1, 6.5, 2.9, 1.2 Hz, 1H), 3.32 (ddd, *J* = 14.1, 10.9, 5.4 Hz, 1H), 2.76-2.52 (m, 2H), 2.32 (s, 3H). ¹³C NMR (75 MHz, CDCl₃): δ = 143.1, 141.7, 137.8, 134.1, 133.9, 129.4, 129.1, 128.8, 128.5, 128.4, 127.7, 127.2, 127.2, 126.2, 59.3, 39.2, 26.8, 21.5.

1-((4-Nitrophenyl)sulfonyl)-2-phenyl-4-((trifluoromethyl)sulfonyl)piperazine (**4l**)



4l was obtained as a white solid (24%) by applying **GP 3**. The NMR data match those previously reported.⁷⁶ ¹H NMR (300 MHz, CDCl₃): δ = 8.28 (d, *J* = 8.9 Hz, 2H), 7.86 (d, *J* = 8.9 Hz, 2H), 7.30-7.25 (m, 3H), 7.21-7.16 (m, 2H), 5.22 (s, 1H), 4.29 (d, *J* = 13.3 Hz, 1H), 3.93-3.78 (m, 2H), 3.63-3.53 (m, 1H), 3.48-3.24 (m, 2H). ¹³C NMR (75 MHz, CDCl₃): δ = 150.3, 145.4, 134.8, 129.2, 128.8, 128.5, 127.4, 124.6, 49.2, 46.3, 41.8. ¹⁹F NMR (375 MHz, CDCl₃): δ = -74.1.

10-tosyl-1,2,3,4-tetrahydro-1,4-(epiminomethano)naphthalene (**4m**)



4m was obtained as a white solid (40%) by applying **GP 3**. ¹H NMR (500 MHz, CDCl₃): δ = 7.48-7.44 (m, 2H), 7.12 (td, *J* = 7.4, 1.3 Hz, 1H), 7.08-7.02 (m, 4H), 6.95 (d, *J* = 7.3 Hz, 1H), 4.93-4.90 (m, 1H), 3.61 (dd, *J* = 9.5 Hz, 2.3, 1H), 3.17-3.14 (m, 1H), 2.93 (dt, *J* = 9.4, 2.5 Hz, 1H), 2.34-2.27 (m, 4H), 1.88-1.82 (m, 1H), 1.50-1.40 (m, 2H). ¹³C NMR (125 MHz, CDCl₃): δ = 142.9, 140.1, 139.0, 135.8, 129.3, 127.6, 127.4, 126.2, 123.7, 123.1, 52.5, 49.8, 34.8, 28.4, 22.9, 21.5. mp: 118-120 °C. IR ν (cm⁻¹): 2933, 2872, 1598. HRMS: Mass calculated for C₁₈H₂₀NO₂S: 314.1209, found: 314.1206.

X-Ray Analytical Data for Compound **4m**

Chapter II: Anodic Benzylic C(sp³)-H Amination:
A Unified Access to pyrrolidines and Piperidines

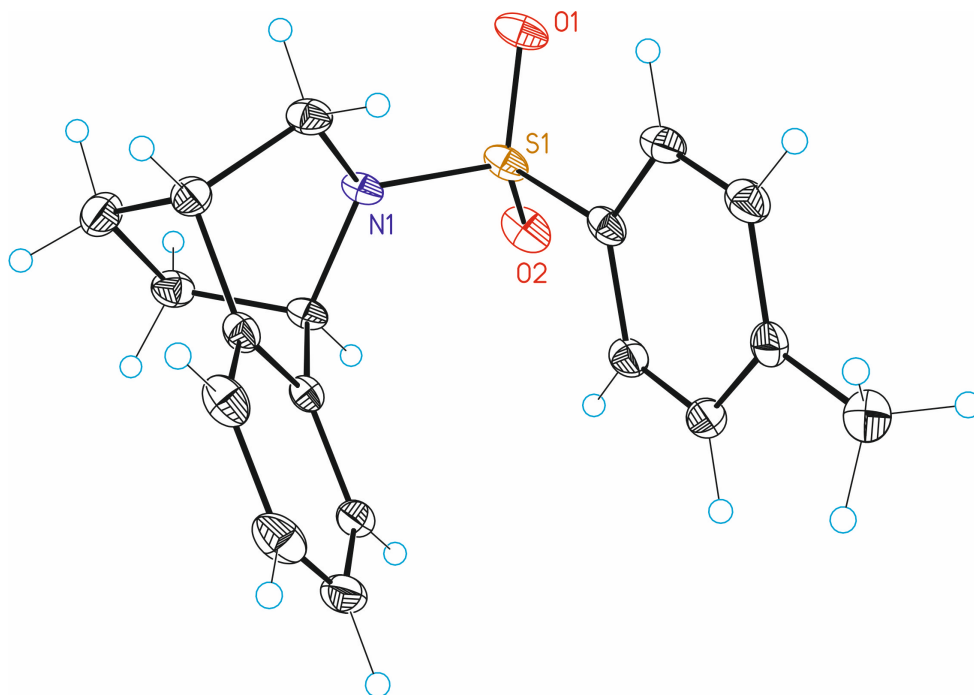
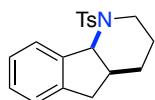


Table S-2. Crystal data and structure refinement for **4m**.

Identification code	CCDC 1841279	
Empirical formula	C ₁₈ H ₁₉ N O ₂ S	
Formula weight	313.40	
Temperature	100(2) K	
Wavelength	0.71073 \approx	
Crystal system	Triclinic	
Space group	P-1	
Unit cell dimensions	a = 8.9159(18) \approx b = 9.2280(19) \approx c = 10.159(2) \approx	$\alpha = 105.035(5)^\circ$. $\beta = 98.430(5)^\circ$. $\gamma = 102.959(5)^\circ$.
Volume	767.9(3) \approx^3	
Z	2	
Density (calculated)	1.356 Mg/m ³	

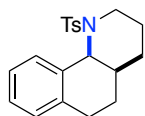
Absorption coefficient	0.218 mm ⁻¹
F(000)	332
Crystal size	0.20 x 0.10 x 0.05 mm ³
Theta range for data collection	2.127 to 30.608°
Index ranges	-12<=h<=10,-9<=k<=13,-14<=l<=14
Reflections collected	7780
Independent reflections	4257[R(int) = 0.0218]
Completeness to theta =30.608°	90.200005%
Absorption correction	Multi-scan
Max. and min. transmission	0.989 and 0.761
Refinement method	Full-matrix least-squares on F ²
Data / restraints / parameters	4257/ 0/ 200
Goodness-of-fit on F ²	1.066
Final R indices [I>2sigma(I)]	R1 = 0.0389, wR2 = 0.1008
R indices (all data)	R1 = 0.0476, wR2 = 0.1063
Largest diff. peak and hole	0.429 and -0.415 e. ⁻³

1-Tosyl-2,3,4,4a,5,9b-hexahydro-1H-indeno[1,2-b]pyridine (4n)



4n was obtained as a white solid (54%) by applying **GP 3**. The NMR data match those previously reported.⁷⁶ ¹H NMR (300 MHz, CDCl₃): δ = 7.82 (d, *J* = 8.3 Hz, 2H), 7.33 (d, *J* = 8.0 Hz, 2H), 7.20 (s, 4H), 5.40 (d, *J* = 6.3 Hz, 1H), 3.91-3.78 (m, 1H), 2.95 (dd, *J* = 15.3, 6.0 Hz, 1H), 2.81 (ddd, *J* = 14.4, 12.2, 2.8 Hz, 1H), 2.50-2.40 (m, 4H), 2.41-2.26 (m, 1H), 1.67-1.52 (m, 1H), 1.35-1.23 (m, 1H), 1.23-1.15 (m, 1H), 1.15-0.96 (m, 1H). ¹³C NMR (75 MHz, CDCl₃): δ = 143.2, 141.2, 139.9, 138.8, 129.9, 127.6, 127.1, 126.9, 125.7, 124.0, 61.1, 41.4, 37.2, 37.1, 26.2, 23.3, 21.7.

1-Tosyl-1,2,3,4,4a,5,6,10b-octahydrobenzo[*h*]quinolone (4o)

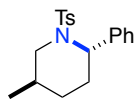


4o was obtained as a white solid (48%) by applying **GP 3**. ¹H NMR (400 MHz, CDCl₃): δ = 7.87-7.74 (m, 2H), 7.50-7.44 (m, 1H), 7.37-7.31 (m, 2H), 7.23-7.14 (m, 2H), 7.13-7.04 (m, 1H), 5.21 (d, *J* = 5.2 Hz, 1H), 3.90-3.77 (m, 1H), 2.90-2.66 (m, 3H), 2.45 (s, 3H), 2.02-1.92 (m, 1H), 1.91-1.84 (m, 1H), 1.80-1.72 (m, 1H), 1.46-1.37 (m, 3H), 1.33-1.25 (m, 1H). ¹³C NMR (125 MHz, CDCl₃):

Chapter II: Anodic Benzylic C(sp³)-H Amination:
A Unified Access to pyrrolidines and Piperidines

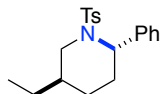
δ = 143.1, 139.3, 137.1, 134.0, 129.9, 129.0, 127.4, 127.1, 127.0, 126.8, 56.4, 41.0, 32.6, 27.6, 24.5, 24.4, 23.7, 21.7. mp: 117-122 °C. IR ν (cm⁻¹): 2926, 2852. HRMS: Mass calculated for C₂₀H₂₃NNaO₂S: 364.1342, found: 364.1344.

5-Methyl-2-phenyl-1-tosylpiperidine (4p)



4p was obtained as a white solid (59%, d.r. = 1.7:1) by applying **GP 3**. The NMR data of the major diastereoisomer (*anti*) is given which match those previously reported.⁷⁶ ¹H NMR (500 MHz, CDCl₃): δ = 7.61 (d, *J* = 7.9 Hz, 2H), 7.35 (d, *J* = 4.4 Hz, 2H), 7.28-7.21 (m, 5H), 4.80 (t, *J* = 5.1 Hz, 1H), 3.55 (dd, *J* = 13.0, 3.8 Hz, 1H), 3.15 (dd, *J* = 12.9, 5.1 Hz, 1H), 2.43 (s, 3H), 2.06-1.96 (m, 2H), 1.87-1.81 (m, 1H), 1.54-1.48 (m, 1H), 1.22-1.15 (m, 1H), 0.89 (d, *J* = 6.9 Hz, 3H). ¹³C NMR (125 MHz, CDCl₃): δ = 142.8, 140.0, 138.7, 129.3, 128.2, 127.3, 127.2, 126.8, 57.8, 49.2, 28.3, 27.4, 26.8, 21.5, 18.0.

5-Ethyl-2-phenyl-1-tosylpiperidine (4q)



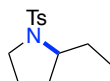
4q was obtained as a colorless oil (49%, d.r. = 1.5:1) by applying **GP 3**. The NMR data of the major diastereoisomer (*anti*) is given which match those previously reported.⁷⁶ ¹H NMR (300 MHz, CDCl₃): δ = 7.58 (d, *J* = 8.3 Hz, 2H), 7.34-7.19 (m, 7H), 4.82 (t, *J* = 5.0 Hz, 1H), 3.49 (dd, *J* = 13.0, 3.8 Hz, 1H), 3.25 (dd, *J* = 13.1, 4.8 Hz, 1H), 2.40 (s, 3H), 2.00-1.91 (m, 2H), 1.73-1.56 (m, 2H), 1.55-1.45 (m, 1H), 1.40-1.10 (m, 3H), 1.09-0.91 (m, 2H), 0.89-0.75 (m, 3H). ¹³C NMR (75 MHz, CDCl₃): δ = 142.9, 140.2, 138.9, 129.4, 128.4, 127.3, 127.0, 126.9, 57.9, 47.0, 35.6, 27.7, 26.7, 24.8, 21.6, 11.9.

2-Methyl-1-tosylpyrrolidine (11a)



11a was obtained as a white solid (90%) by applying **GP 4**. The NMR data match those previously reported.¹⁶² ¹H NMR (400 MHz, CDCl₃): δ = 7.74-7.70 (m, 2H), 7.32-7.28 (m, 2H), 3.76-3.65 (m, 1H), 3.46-3.40 (m, 1H), 3.18-3.11 (m, 1H), 2.42 (s, 3H), 1.89-1.76 (m, 1H), 1.72-1.64 (m, 1H), 1.57-1.44 (m, 2H), 1.31 (d, *J* = 6.4 Hz, 3H). ¹³C NMR (100 MHz, CDCl₃): δ = 143.3, 135.1, 129.7, 127.6, 56.2, 49.2, 33.6, 24.0, 23.0, 21.6.

2-Ethyl-1-tosylpyrrolidine (11b)



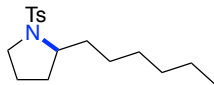
11b was obtained as an inseparable mixture with the SM (65%) by applying **GP 4**. The NMR data match those previously reported.¹⁶³ ¹H NMR (500 MHz, CDCl₃): δ = 7.74-7.70 (m, 2H), 7.32-7.28 (m, 2H), 3.57-3.49 (m, 1H), 3.37 (ddd, *J* = 10.4 Hz, 7.1 Hz, 5.2 Hz, 1H), 3.19 (dt, *J* = 10.4 Hz, 7.3 Hz, 1H), 2.43 (s, 3H), 1.89-1.82 (m, 1H), 1.76 (dt, *J* = 12.1 Hz, 7.4 Hz, 1H), 1.58-1.54 (m, 2H), 1.51-1.45 (m, 2H),

¹⁶² Y. Kato, D. H. Yen, Y. Fukudome, T. Hata, H. Urabe, *Org. Lett.* **2010**, *12*, 4137-4139.

¹⁶³ R. Fan, D. Pu, F. Wen, J. Wu, *J. Org. Chem.* **2007**, *72*, 8994-8997.

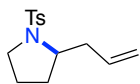
0.91-0.87 (m, 3H). ¹³C NMR (125 MHz, CDCl₃): δ = 143.3, 135.3, 129.7, 127.6, 62.0, 49.1, 30.3, 29.3, 24.3, 21.6, 10.5.

2-Hexyl-1-tosylpyrrolidine (**11c**)



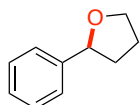
11c was obtained as a colorless oil (61%) by applying **GP 4**. The NMR data match those previously reported. ¹H NMR (500 MHz, CDCl₃): δ = 7.73-7.70 (m, 2H), 7.32-7.28 (m, 2H), 3.62-3.56 (m, 1H), 3.37 (ddd, *J* = 10.4 Hz, 7.1 Hz, 5.1 Hz, 1H), 3.19 (dt, *J* = 10.4 Hz, 7.2 Hz, 1H), 2.43 (s, 3H), 1.87-1.72 (m, 2H), 1.61-1.53 (m, 3H), 1.51-1.44 (m, 1H), 1.32-1.27 (m, 8H), 0.92-0.85 (m, 3H). ¹³C NMR (125 MHz, CDCl₃): δ = 143.2, 135.3, 129.7, 127.7, 60.8, 49.0, 36.6, 32.0, 30.8, 29.4, 26.3, 24.3, 22.8, 21.6, 14.2. IR ν (cm⁻¹): 2926, 2857. HRMS: Mass calculated for C₁₇H₂₇NNaO₂S: 332.1655, found: 332.1665.

2-Allyl-1-tosylpyrrolidine (**11d**)



11d was obtained as a colorless oil (94%) by applying **GP 4**. The NMR data match those previously reported.¹⁶⁴ ¹H NMR (500 MHz, CDCl₃): δ = 7.75-7.71 (m, 2H), 7.32-7.29 (m, 2H), 5.79 (ddt, *J* = 17.2 Hz, 10.2 Hz, 7.1 Hz, 1H), 5.11-5.04 (m, 2H), 3.66 (ddd, *J* = 12.9 Hz, 8.0 Hz, 3.9 Hz, 1H), 3.39 (ddd, *J* = 10.1 Hz, 7.0 Hz, 4.8 Hz, 1H), 3.17 (dt, *J* = 10.3 Hz, 7.3 Hz, 1H), 2.63-2.56 (m, 1H), 2.43 (s, 3H), 2.34-2.26 (m, 1H), 1.81-1.73 (m, 1H), 1.68-1.61 (m, 1H), 1.60-1.53 (m, 1H), 1.53-1.46 (m, 1H). ¹³C NMR (125 MHz, CDCl₃): δ = 143.4, 135.1, 134.8, 129.8, 127.7, 117.7, 59.8, 49.3, 41.0, 30.2, 24.1, 21.6.

2-Phenyltetrahydrofuran (**13**)



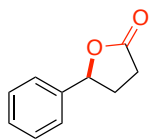
13 was obtained in 55% yield (NMR) by applying **GP 3**. The yield was determined by NMR using 1,3,5-trimethoxybenzene as internal standard due to the volatility of the compound. The NMR data match those reported in literature.¹⁶⁵ ¹H NMR (500 MHz, CDCl₃): δ = 7.36-7.33 (m, 4H), 7.28-7.25 (m, 1H), 4.91 (t, *J* = 7.2 Hz, 1H), 4.11 (ddd, *J* = 8.5, 7.3, 6.4 Hz, 1H), 3.95 (td, *J* = 7.8, 6.3 Hz, 1H), 2.38-2.30 (m, 1H), 2.07-1.98 (m, 2H), 1.87-1.78 (m, 1H). ¹³C NMR (125 MHz, CDCl₃): δ = 143.6, 128.4, 127.2, 125.8, 80.8, 68.8, 34.7, 26.2.

5-Phenyldihydrofuran-2(3H)-one (**15**)

¹⁶⁴ J. M. Pierson, E. L. Ingalls, R. D. Vo, F. E. Michael, *Angew. Chem. Int. Ed.* **2013**, *52*, 13311-13313.

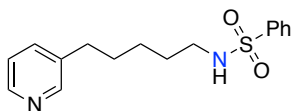
¹⁶⁵ F. Zhu, J. Rodriguez, T. Yang, I. Kevlishvili, E. Miller, D. Yi, S. O'Neill, M. J. Rourke, P. Liu, M. A. Walczak, *J. Am. Chem. Soc.* **2017**, *139*, 17908-17922.

Chapter II: Anodic Benzylic C(sp³)-H Amination:
A Unified Access to pyrrolidines and Piperidines



15 was obtained in 73% yield by applying **GP 3**. The NMR data match those reported in literature.¹⁵⁷ ¹H NMR (500 MHz, CDCl₃): δ = 7.42-7.37 (m, 2H), 7.36-7.32 (m, 3H), 5.55-5.49 (m, 1H), 2.72-2.62 (m, 3H), 2.25-2.13 (m, 1H). ¹³C NMR (125 MHz, CDCl₃): δ = 177.0, 139.5, 128.9, 128.6, 125.4, 81.4, 31.1, 29.1.

***N*-(5-(Pyridin-3-yl)pentyl)benzenesulfonamide (8)**



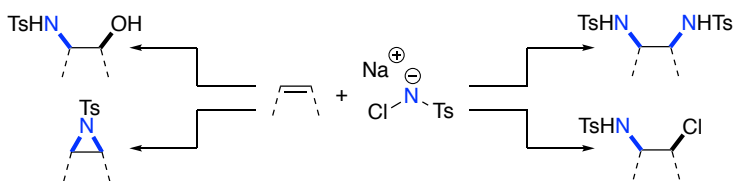
¹H NMR (400 MHz, CDCl₃): δ = 8.42 (dd, *J* = 4.8, 1.7 Hz, 1H), 8.39 (d, *J* = 2.3 Hz, 1H), 7.87-7.84 (m, 2H), 7.60-7.43 (m, 4H), 7.20 (ddd, *J* = 7.8, 4.8, 0.9 Hz, 1H), 4.85 (bs, 1H), 2.97-2.91 (m, 2H), 2.55 (t, *J* = 7.7 Hz, 2H), 1.60-1.45 (m, 4H), 1.35-1.24 (m, 2H). ¹³C NMR (75 MHz, CDCl₃): δ = 149.8, 147.3, 140.2, 137.6, 136.0, 132.6, 129.2, 127.1, 123.4, 43.13, 32.8, 30.6, 29.5, 26.1. mp: 70-71 °C. IR ν (cm⁻¹): 3059, 2933, 2859. HRMS: Mass calculated for C₁₆H₂₁N₂O₂S: 305.1318, found: 305.1324.

Chapter III. Copper-Catalyzed N-F Bond Activation for Uniform Intramolecular C-H Amination Yielding Pyrrolidines and Piperidines

Chapter III. Copper-Catalyzed N-F Bond Activation for Uniform
Intramolecular C-H Amination Yielding Pyrrolidines and Piperidines

3.1. Introduction: N-fluorosulfonamide activation.

Halogenated amine derivatives have demonstrated to be useful aminating agents in a plethora of organic transformations. Their use has not only been limited to act as reactive species for intramolecular aliphatic amination reactions (Hofmann-Löffler reaction), but also as nitrogen sources for multiple functionalization reactions including sp² and sp³ carbon centers. In this regard, probably the most exploited haloamine for synthetic purposes have been commercially available Chloramine-T (N-chloro tosylamide sodium salt).¹⁶⁶ As an example, Chloramine-T have been widely studied for alkene functionalization reactions comprising amino-hydroxylations,¹⁶⁷ aziridinations,¹⁶⁸ amino-chlorinations¹⁶⁹ or diaminations¹⁷⁰ (Figure 3.1) among other valuable transformations.



Scheme 3.1: Selected synthetic applications of Chloramine-T for alkene functionalization.

Chloramines' synthetic applications go beyond alkene functionalization, since they have been greatly used as transferable electrophilic nitrogen groups for aromatic C-H amination as well.¹⁷¹ Among other recent contributions,¹⁷² the group of Leonori reported an elegant photochemical approach for intermolecular aromatic C-H amination (Scheme 3.2).¹⁷³ This protocol involved in situ generation of N-chlorinated

¹⁶⁶ M. M. Campbell, G. Johnson, *Chem. Rev.* **1978**, *78*, 65-79.

¹⁶⁷ a) M. Bruncko, G. Schlingloff, K. B. Sharpless, *Angew. Chem. Int. Ed.* **1996**, *35*, 451-454. b) J. A. Bodkin, M. D. Mcleod, *J. Chem. Soc., Perkin Trans. 1*, **2002**, 2733-2746.

¹⁶⁸ A) T. Ando, S. Minakata, I. Ryu, M. Komatsu, *Tetrahedron Lett.* **1998**, *39*, 309-312. b) D. P. Albone, P. S. Aujla, P. C. Taylor, *J. Org. Chem.* **1998**, *63*, 9569-9571. c) S. I. Ali, M. D. Nikalje, A. Sudalai, *Org. Lett.* **1999**, *1*, 705-707. d) D. Caine, P. O'Brien, C. M. Rosser, *Org. Lett.* **2002**, *4*, 1923-1926. e) S. C. Coote, P. O'Brien, A. C. Whitwood, *Org. Biomol. Chem.* **2008**, *6*, 4299-4314.

¹⁶⁹ C. Martínez, K. Muñiz, *Adv. Synth. Catal.* **2014**, *356*, 205-211.

¹⁷⁰ a) V. Kumar, N. G. Ramesh, *Chem. Commun.* **2006**, 4952-4954. b) V. Kumar, N. G. Ramesh, *Org. Biomol. Chem.* **2007**, *5*, 3847-3858.

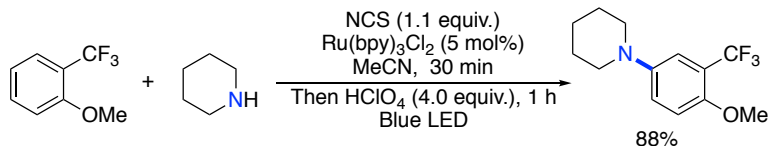
¹⁷¹ J. Jiao, K. Murakami, K. Itami, *ACS Catal.* **2016**, *6*, 610-633.

¹⁷² Selected examples of aromatic C-H amination employing chloramine derivatives as nitrogen source: a) H. Kim, T. Kim, D. G. Lee, S. W. Roh, C. Lee, *Chem. Commun.* **2014**, *50*, 9273-9276. b) W. Xie, J. H. Yoon, S. Chang, *J. Am. Chem. Soc.* **2016**, *138*, 12605-12614. c) S. C. Cosgrove, J. M. C. Plane, S. P. Marsden, *Chem. Sci.* **2018**, *9*, 6647-6652. d) X.-D. An, S. Yu, *Tetrahedron Lett.* **2018**, *59*, 1605-1613.

¹⁷³ A. Ruffoni, F. Juliá, T. D. Svejstrup, A. J. McMillan, J. J. Douglas, D. Leonori, *Nat. Chem.* **2019**, *11*, 426-433.

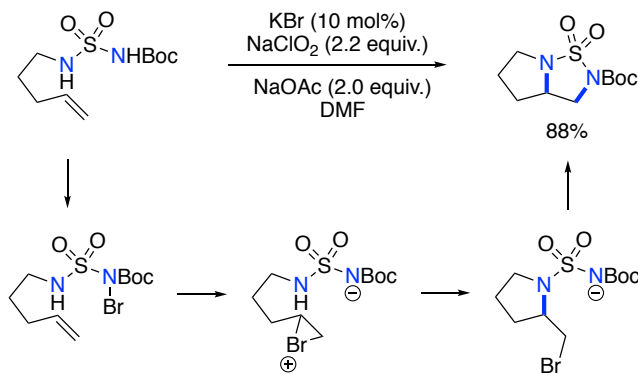
Chapter III. Copper-Catalyzed N-F Bond Activation for Uniform Intramolecular C-H Amination Yielding Pyrrolidines and Piperidines

amines by reaction of N-chlorosuccinimide with the corresponding nitrogen source. The active aminating species generated in situ can be engaged in a photochemical activation to deliver nitrogen-centered radical-cations that ultimately delivers the targeted aniline by radical addition and final rearomatization.



Scheme 3.2: Leonori's photochemical C(sp²)-H amination procedure employing chloramines as nitrogen source.

Along these lines, analogous brominated amines have been explored as convenient activated nitrogen source. In this regard, classical Sharpless amino-hydroxylation of alkenes employed brominated acetamides exploiting its dual role as amine source and oxidant.¹⁷⁴ Alkene aziridination,¹⁷⁵ arene amination¹⁷⁶ or alkene diamination¹⁷⁷ are additional accessible transformations employing bromoamines as aminating agents. As for the latter case, our group developed a bromide catalytic procedure which involved in situ generation of N-brominated species, which acted as intramolecular diaminating agent for vicinal diamination of a wide variety of alkenes (Scheme 3.3).



Scheme 3.3: Bromine catalysis toward vicinal alkene diamination involving transient formation of bromoamine derivatives.

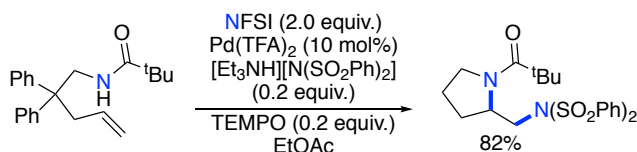
¹⁷⁴ a) M. Bruncko, G. Schlingloff, K. B. Sharpless, *Angew. Chem. Int. Ed.* **1997**, *36*, 1483-1486. b) Z. P. Demko, M. Bartsch, K. B. Sharpless, *Org. Lett.* **2000**, *2*, 2221-2223.

¹⁷⁵ a) R. Vyas, B. M. Chanda, A. V. Bedekar, *Tetrahedron Lett.* **1998**, *39*, 4715-4716. b) V. V. Thakur, A. Sudalai, *Tetrahedron Lett.* **2003**, *44*, 989-992.

¹⁷⁶ L. Song, L. Zhang, S. Luo, J.-P. Cheng, *Chem. Eur. J.* **2014**, *20*, 14231-14234.

¹⁷⁷ P. Chávez, J. Kirsch, C. H. Hövelmann, J. Streuff, M. Martínez-Belmonte, E. C. Escudero-Adán, E. Martina, K. Muñiz, *Chem. Sci.* **2012**, *3*, 2375-2382.

Following the halogen series, its corresponding fluorinated-amine counterparts have been substantially less studied for amination reactions. Given the electrophilic character of the nitrogen atom adjacent to the fluorine atom, N-fluorinated analogues have been used as electrophilic fluorinating reagents of carbon nucleophiles.¹⁷⁸ In addition, the pioneering work of Sammis has demonstrated the involvement of fluoroamides in radical pathways of fluorine atom abstraction¹⁰³ (Section 1.5, introductory chapter). Furthermore, diversification of N-fluorosulfonamides such as NFSI can be performed, tuning its reactivity and improving its application for preparation of fluorinated molecules.¹⁷⁹ Despite the extensive work on fluoroimide activation for fluorination reactions, few examples can be found in the literature where this haloamine species act as nitrogen source. In the context of palladium catalysis, the group of Michael reported in 2009 the use of NFSI as aminating agent for the preparation of vicinal 1,2-diamines through an intra/intermolecular alkene diamination reaction (Scheme 3.4).¹⁸⁰



Scheme 3.4: Palladium-catalyzed alkene diamination employing NFSI as oxidant and nitrogen source.

Along the same lines, Zhang reported two palladium catalytic systems for directed C-H amination of arenes employing simple NFSI as nitrogen source.¹⁸¹ Indeed, the authors could extend the catalytic protocol for directed benzylic C-H amination when suitable para-methylaniline derivatives are employed. However, it was in 2012 when the group of Liu reported a copper catalytic system for the activation of NFSI toward aliphatic amination of a wide variety of toluene derivatives (Scheme 3.5).¹⁸² Even if the mechanism of this transformation still remains ambiguous, the authors proposed a catalytic cycle involving formation of Cu^{III} species from reaction of CuCl with NFSI. Intermolecular hydrogen atom abstraction delivers a reduced Cu^{II} complex and the corresponding benzylic radical from the starting material. Further oxidative amination of the carbon-centered radical intermediate delivers final benzylic-aminated product

¹⁷⁸ a) S. T. Purrington, W. A. Jones, *J. Org. Chem.* **1983**, *48*, 761-762. b) N. Satyamurthy, G. T. Bida, M. E. Phelps, J. R. Barrio, *J. Org. Chem.* **1990**, *55*, 3373-3374. c) D. S. Timofeeva, A. R. Ofial, H. Mayr, *J. Am. Chem. Soc.* **2018**, *140*, 11474-11486.

¹⁷⁹ D. Meyer, H. Jangra, F. Walther, H. Zipse, P. Renaud, *Nat. Commun.* **2018**, *9*, 4888.

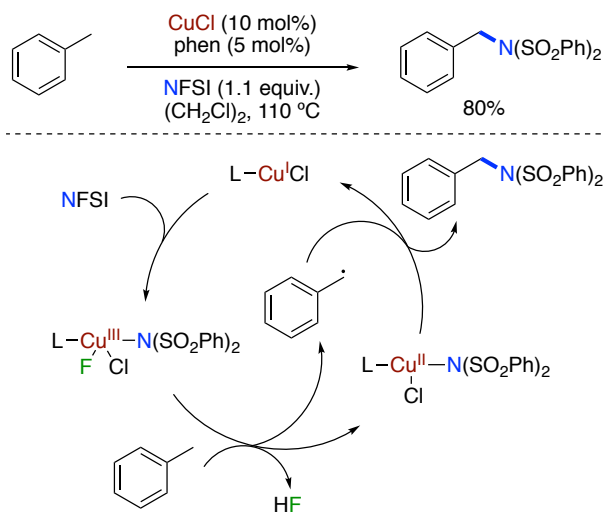
¹⁸⁰ P. A. Sibbald, F. E. Michael, *Org. Lett.* **2009**, *11*, 1147-1149.

¹⁸¹ a) T. Xiong, Y. Li, Y. Lv, Q. Zhang, *Chem. Commun.* **2010**, *46*, 6831-6833. b) K. Sun, Y. Li, T. Xiong, J. Zhang, Q. Zhang, *J. Am. Chem. Soc.* **2011**, *133*, 1694-1697.

¹⁸² Z. Ni, Q. Zhang, T. Xiong, Y. Zheng, Y. Li, H. Zhang, J. Zhang, Q. Liu, *Angew. Chem. Int. Ed.* **2012**, *51*, 1244-1247.

Chapter III. Copper-Catalyzed N-F Bond Activation for Uniform
Intramolecular C-H Amination Yielding Pyrrolidines and Piperidines

while regenerating the Cu^I catalyst. Interestingly, the amination was observed preferentially at primary benzylic carbon positions even in the presence of competing secondary benzylic ones.



Scheme 3.5: Intermolecular copper-catalyzed C(sp³)-H amination with NFSI.

The aforementioned report by Liu demonstrated the feasibility for copper to activate N-F bonds and the ability to functionalize distal aliphatic C-H bonds without recourse to directing groups. All the examples discussed so far concern the use of haloamines as reactive partners for amination reactions in an intermolecular manner. For the intramolecular scenario (Hofmann-Löffler reaction), chloramines, bromoamines and iodoamines have been identified as suitable intramolecular amination promoters (section 1.3.2 at the introductory chapter). However, study of the corresponding fluorinated series has received little echo. To exemplify this trend, Figure 3.1 displays the full halogenated series for a sulfonamide motif extensively employed at our group in the context of Hofmann-Löffler amination. In this context, the corresponding iodinated compound remains the most reactive and less stable derivative while the fluorinated sulfonamide represents the most stable and less reactive compound of the halogenated series. Iodinated derivative can be activated by simple ambient light irradiation, and such species were only detected by ¹H-NMR upon in situ formation. Brominated series shown an increased stability compared with its iodine counterpart, since isolation and full characterization was possible. Photochemical activation of the N-Br bond could similarly be performed upon ambient light irradiation, and the half-life of such derivative is around 30 min. For the chlorine series, on the other hand, an increased stability of few weeks was observed, while a higher energetic light source such as black LED or UV light is needed for N-Cl bond homolysis. Finally, the fluorinated derivative showed a full stability. Furthermore, its photochemical activation could not

be performed by means of direct irradiation, even when high intensity Xenon lamp was used.

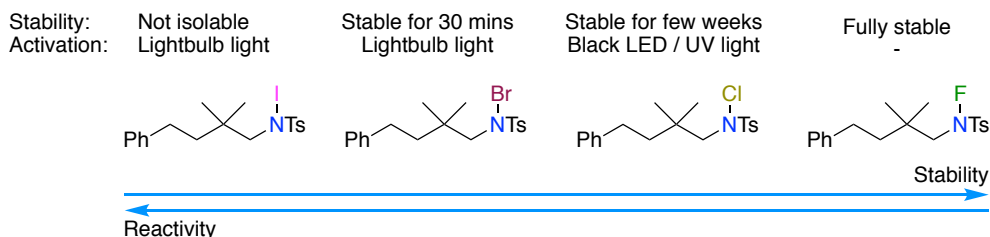
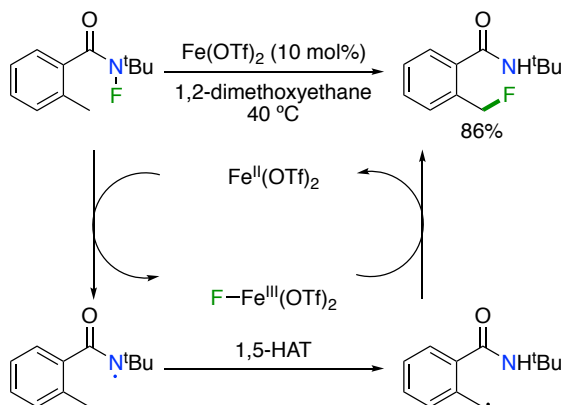


Figure 3.1: N-X bonds for the halogen series: reactivity vs. stability.

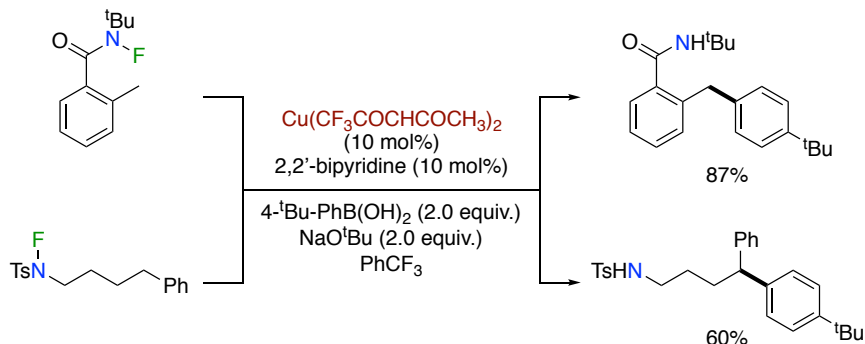
Since photochemical activation of N-fluoroamides remained elusive, transition metals such as iron and copper were employed for its activation employing such functionalities as intramolecular platforms for directed aliphatic C-H functionalization. Along these lines, the pioneering work of Cook¹¹³ reported the use of fluoroamides as intramolecular promoters for δ -C-H functionalization. In this particular case, the authors disclosed an Fe^{II}/Fe^{III} catalytic system for benzylic C-H bond fluorination (Scheme 3.6). Single electron reduction of the N-F bond by the Fe^{II} catalysts affords the corresponding nitrogen-centered radical at the amide functionality. Selective 1,5-HAT delivers benzylic carbon-centered radical, which gets fluorinated in a fluorine atom transfer step from the Fe^{III}-F intermediate. The authors state that the Fe^{III}-F intermediate is an active species for the C-F bond formation step, excluding the possibility of a free radical fluorination or a fluorine atom abstraction to fluoroimide starting material. In this sense, DFT calculations and crossover experiments support that statement.



Scheme 3.6: Iron-catalyzed N-F bond activation toward directed C-H fluorination.

Chapter III. Copper-Catalyzed N-F Bond Activation for Uniform
Intramolecular C-H Amination Yielding Pyrrolidines and Piperidines

Shortly after Cook's work, Zhu reported the application of copper catalysis for fluoroamide activation in directed aliphatic C-H arylation (Scheme 3.7).¹⁸³ By exploiting this rather simple copper catalytic system, the authors could promote C-C bond formation when trapping the carbon centered radical intermediate with aryl-boronic acids in a cross-coupling process. Not only activated benzylic C-H positions, but non-activated δ -aliphatic positions could be efficiently arylated. Furthermore, fluorotosylamides could be successfully employed as directing groups for such C-H functionalization reaction.

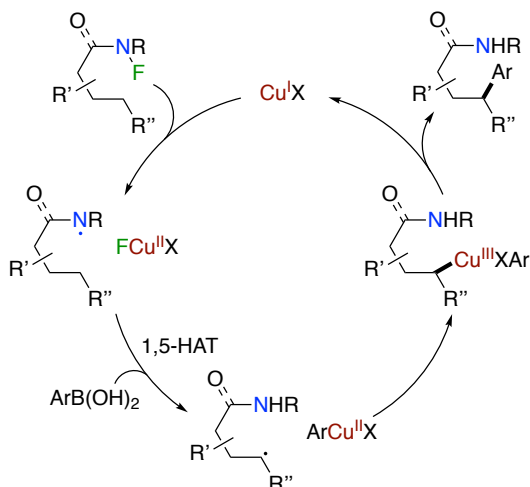


Scheme 3.7: Copper-catalyzed δ -arylation of N-fluoroamides.

From a mechanistic standpoint, the authors invoke a catalytic cycle involving Cu^I, Cu^{II} and Cu^{III} species (Scheme 3.8). In situ formed active Cu^I catalysts initiates the reaction by one electron reduction of the N-F bond, accessing the corresponding nitrogen-centered radical together with Cu^{II} fluoride. Subsequent 1,5-HAT delivers carbon-centered radical while transmetalation of aryl-boronic acid with Cu^{II} fluoride affords ArCu^{II}F species. At this stage a radical rebound to obtain an alkylCu^{III} intermediate was postulated. Final reductive elimination from such reactive intermediate delivers the final arylated product while regenerating the Cu^I catalyst.

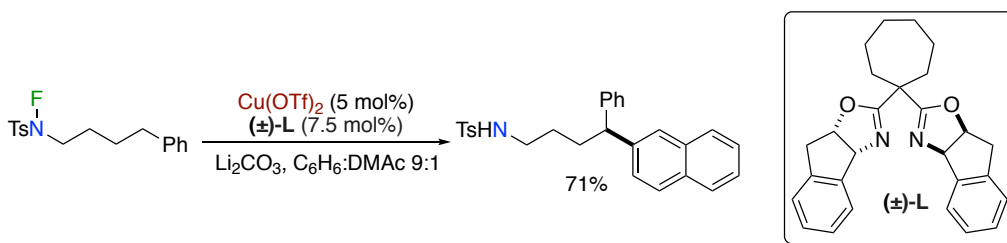
¹⁸³ Z. Li, Q. Wang, J. Zhu, *Angew. Chem. Int. Ed.* **2018**, *57*, 13288-13292.

Chapter III. Copper-Catalyzed N-F Bond Activation for Uniform
 Intramolecular C-H Amination Yielding Pyrrolidines and Piperidines



Scheme 3.8: Mechanistic context for copper-catalyzed N-F bond activation toward C-H arylation.

In 2019, the group of Nagib reported a similar copper catalytic system for directed arylation of fluorosulfonamides (Scheme 3.9).¹⁸⁴ In this case, N-fluorinated tosylamides were employed as the optimum substrates for directed C-H arylation employing simple Cu(OTf)₂ as catalyst and oxazoline-based ligands. Interestingly, the employment of a chiral oxazoline ligand resulted in an arylation with moderate enantioselectivities, thus demonstrating the potential of copper-catalyzed N-F activation in asymmetric synthesis.



Scheme 3.9: Nagib's approach for C-H arylation through a copper-oxazoline catalytic system.

In conclusion, haloamines have been identified and employed as active reagents for C-N bond formation, even in the fluoroamine series. In the intramolecular context (Hofmann-Löffler reaction), extensive work has been performed for N-I, N-Br and N-Cl bond activation toward intramolecular amination for the synthesis of pyrrolidines. However, the corresponding N-F series have remained less explored. The only examples reported at the outset of our investigations involved formation of C-F and C-C bonds, but no C-N bonds.

¹⁸⁴ Z. Zhang, L. H. Stateman, D. A. Nagib, *Chem. Sci.* **2019**, *10*, 1207-1211.

Chapter III. Copper-Catalyzed N-F Bond Activation for Uniform
Intramolecular C-H Amination Yielding Pyrrolidines and Piperidines

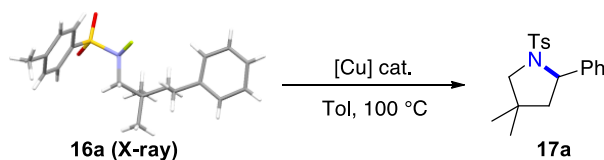
Based on these precedents, we started our investigations in order to achieve a reliable protocol for the activation of N-F bonds in the context of intramolecular C-H amination reactions. For such purpose, this project was conducted in collaboration with the group of Prof. Pedro J. Pérez from the University of Huelva due to his knowledge in organometallic chemistry and with the group of Prof. Feliu Maseras from the ICIQ for DFT calculations.

3.2. Results and discussion

We started our investigation with N-fluorosulfonamide **16a**, readily prepared by reaction of the corresponding free sulfonamide with NFSI and NaH.¹⁸⁵ X-ray crystallographic analysis unambiguously confirmed its structure. Copper-based salts were chosen for the initial exploration of suitable catalyst for N-F activation toward amination. We started our optimization by running a blank reaction, which demonstrated that thermal activation of the substrate did not lead to productive pyrrolidine **17a** formation (Table 3.1, entry 1). Screening of rather simple copper salts such as CuCl as catalyst already afforded good 76% conversion to **17a** (entry 2). Similar Cu^{II} precatalyst like CuCl₂ and CuBr₂ achieved similar conversions, while CuSO₄ appeared completely ineffective to promote cyclization. The aforementioned performances could be substantially improved by the use of chelating N-ligands such as TPMA (Tris(2-pyridylmethyl)amine), allowing to reduce the catalyst loading to just 1 mol% (entries 6 and 7). We subsequently explored the utilization of strongly chelating Tp (hydrotrispyrazolylborate) family of ligands (Figure 3.2). Reaction of fluorinated tosylamide **16a** with Cu^I complexes bearing Tp^{Br³} (hydrotris(3,4,5-tribromo-1-pyrazolyl)borate) and Tp^{*Br} (hydrotris(4-bromo-3,5-dimethyl-1-pyrazolyl)borate) as ligands led to cyclization product in 60% and 74% yield respectively (entries 8 and 9). However, when neutral Cu^I catalysts bearing Tp* (hydrotris(3,5-dimethyl-1-pyrazolyl)borate) and Tp^{iPr²} (hydrotris(3,5-diisopropyl-1-pyrazolyl)borate) were employed, full conversion to pyrrolidine product **17a** was obtained in both cases (entries 11 and 12). Although excellent performances results were achieved with both [Tp*Cu(NCMe)] and [Tp^{iPr²}Cu(NCMe)] as catalyst, [Tp^{iPr²}Cu(NCMe)] was selected as the optimum catalyst because of its improved stability toward aerobic oxidation (which translates in an increased long term stability) when compared with [Tp*Cu(NCMe)]. Importantly, catalyst loading could be reduced even to 0.1 mol% without significant loss of performance (entry 13). Reduction of temperature or reaction times resulted in lower cyclization yields (entries 14 and 15) whereas the solvent could be replaced by acetonitrile maintaining the excellent performance (entry 16). The cyclization reaction was completely shut-down upon addition of TEMPO radical trap (entry 17), which points toward involvement of radical species though the catalysis. On the other hand, only partial inhibition was observed when 1 equivalent of BHT was added or when the

¹⁸⁵ D. W. Taylor, G. P. Meier, *Tetrahedron Lett.* **2000**, *41*, 3291-3294.

reaction was performed under aerobic conditions (entries 18 and 19). Interestingly, the copper catalyzed amination reaction still proceeded with an excellent 84% yield even in the presence of 0.5 equivalents of water (entry 20). Finally, the robustness cyclization protocol was demonstrated by a 1 gram scale (2.95 mmol) single-run experiment, which achieved a reliable 79% isolated yield of pyrrolidine **17a**.



Entry	[Cu] (mol%)	Additive	17a yield (%) ^[a]
1	-	-	0
2	CuCl (10)	-	76
3	CuCl ₂ (10)	-	77
4	CuBr ₂ (10)	-	77
5	CuSO ₄ (10)	-	0
6	CuCl ₂ (1) / TPMA (1)	-	83
7	CuI (1) / TPMA (1)	-	90
8	Tp ^{Br₃} Cu(NCMe) (1)	-	60
9	Tp ^{*Br} Cu(NCMe) (1)	-	74
10	Tp ^{iPr₂} CuCl (1)	-	85
11	Tp ^{iPr₂} Cu(NCMe) (1)	-	99
12	Tp [*] Cu(NCMe) (1)	-	99
13	Tp ^{iPr₂} Cu(NCMe) (0.1)	-	93

Chapter III. Copper-Catalyzed N-F Bond Activation for Uniform
 Intramolecular C-H Amination Yielding Pyrrolidines and Piperidines

14 ^[b]	Tp ^{iPr₂} Cu(NCMe) (1)	-	traces
15 ^[c]	Tp ^{iPr₂} Cu(NCMe) (1)	-	62
16 ^[d]	Tp ^{iPr₂} Cu(NCMe) (1)	-	99
17	Tp ^{iPr₂} Cu(NCMe) (1)	TEMPO (1 equiv.)	8
18	Tp ^{iPr₂} Cu(NCMe) (1)	BHT (1 equiv.)	70
19	Tp ^{iPr₂} Cu(NCMe) (1)	air	61
20	Tp ^{iPr₂} Cu(NCMe) (1)	H ₂ O (0.5 equiv.)	84
21 ^[e]	Tp ^{iPr₂} Cu(NCMe) (1)	-	79 ^[f]

Table 3.1: Optimization studies for intramolecular amination. Isolated yields. 0.1 mmol substrate scale. [a] ¹H NMR yields versus diphenylmethane as internal standard. [b] Room temperature. [c] 8 h reaction time. [d] Acetonitrile as solvent at 80 °C. [e] 1 gram scale (2.95 mmol). [f] Isolated yield.

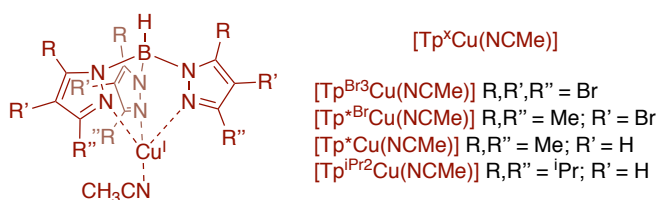
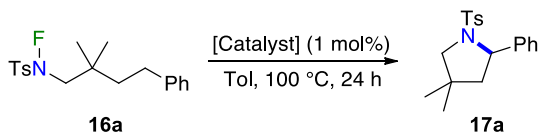


Figure 3.2: General structure of [Tp^XCu(NCMe)] complexes bearing different Tp ligands.

The choice of copper as catalyst proved to be particularly important, as the preliminary exploration of Fe, Ru, Au or Ni catalysts did not lead to effective cyclization, with traces, if any, of the corresponding pyrrolidine (Table 3.2).

Chapter III. Copper-Catalyzed N-F Bond Activation for Uniform
 Intramolecular C-H Amination Yielding Pyrrolidines and Piperidines



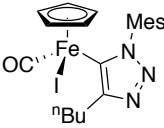
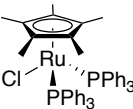
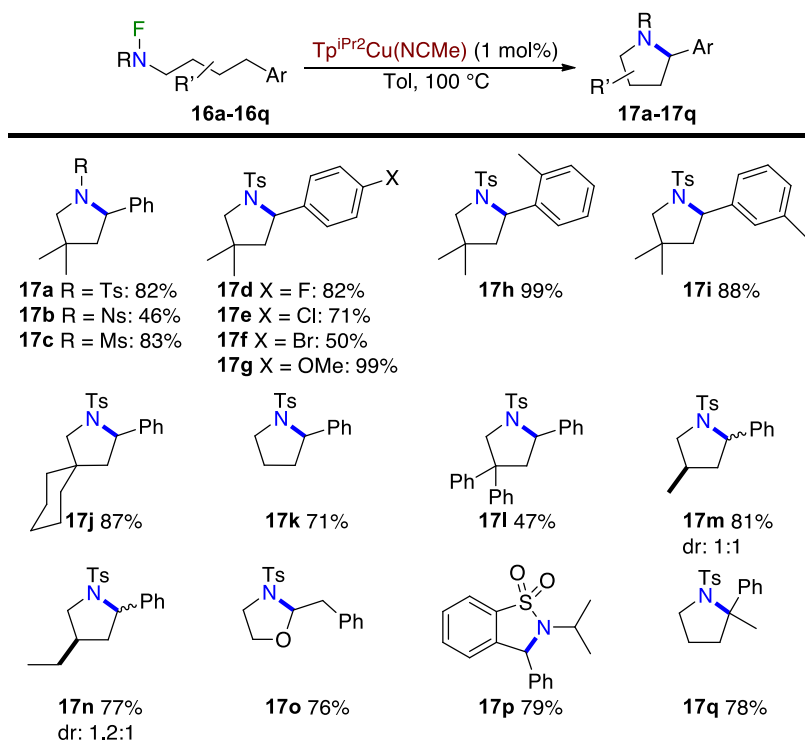
Entry	[Cu] (mol%)	17a yield (%)
1		0
2		0
3	Tp ^{*Br} Ag	0
4	IPrAuCl	0
5	IPrNi(sty) ₂	0

Table 3.2: Additional studies on intramolecular amination employing alternative transition metals as catalysts. 0.1 mmol substrate scale.

Once we determined the optimized conditions for fluorosulfonamide activation toward intramolecular amination, we proceeded to explore the reaction's applicability. The reaction proved to be general since a series of fluorinated sulfonamides **16a-16q** were successfully submitted to copper-catalyzed cyclization reaction (Scheme 3.10). Different sulfonamide protecting groups apart of *para*-toluenesulfonyl such as methylsulfonyl or *para*-nitrobenzenesulfonyl are well tolerated as demonstrated by pyrrolidine **17b** and **17c** formation in 46% and 83% isolated yield respectively. Cyclization could be achieved over substrates bearing different substitution at the arene core. In this context, pyrrolidine formation of substrates comprising *para*-substitution including electron-withdrawing and electron-donating groups was accomplished (**17d-17g**). Particularly, pyrrolidine **17g** displaying an electron-rich anisole moiety was obtained in an excellent 99% isolated yield. The presence of such low-oxidation potential functionalities often represents a limitation in similar halogen-catalyzed Hofmann-Löffler reaction catalytic systems. Increased steric hindrance at the phenyl ring did not substantially influence the excellent performances, as exemplified by pyrrolidine **17h** and **17i** formation bearing 2-methyl and 3-methyl substitution. Different substituents at the carbon backbone were explored for pyrrolidine formation

Chapter III. Copper-Catalyzed N-F Bond Activation for Uniform
Intramolecular C-H Amination Yielding Pyrrolidines and Piperidines

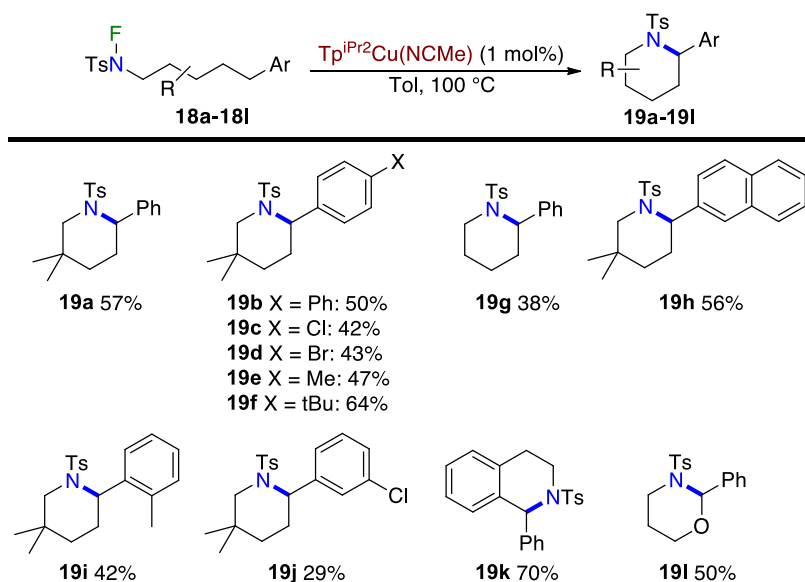
(**17j-17l**). It is worth noting that substrate **16k** bearing no substitution at the carbon backbone resulted in 71% yield of **17k**, thus indicating that Thorpe-Ingold effect was not required for the reaction to occur. Mono-substitution at the carbon backbone in substrate **16m** afforded cyclization to **17m**, which was obtained as an unseparable mixture of diastereoisomers in 81% isolated yield. On the other hand, subtle acyclic stereocontrol was observed though the cyclization to pyrrolidine **17n** bearing an ethyl group at the carbon backbone, which was obtained in 77% isolated yield an in a 1.2:1 diastereomeric ratio in favor of the anti-product. Smooth oxazolidine **17o** formation was achieved in 76% isolated yield when promoting the cyclization over an activated position alpha to heteroatom. Furthermore, dioxisothiazole **17p** could be efficiently synthesized employing the present methodology. Finally, cyclization over tertiary C-H bonds was studied with fluorosulfonamide **17q**, which was transformed into pyrrolidine **17q** in 78% yield.



Scheme 3.10: Copper-catalyzed pyrrolidine formation scope.

We subsequently explored the reactivity of N-fluorosulfonamides substrate bearing an extended alkyl backbone chain, thus offering an ϵ -benzylic position accessible though 1,6-HAT. We wondered whether the expected homo-benzylic cyclization would be achieved through selective 1,5-HAT process or the present protocol could tune the selectivity of nitrogen-centered radical for 1,5-HAT. To our delight, when fluorinated

amide **18a** was submitted to optimized reaction conditions, piperidine **19a** was obtained in 57% isolated yield (Scheme 3.11). Further exploration of the piperidine formation scope was conducted. In general, a similar structural diversity to the pyrrolidine series can be achieved, yet with moderate lower performances. In this sense, para-substitution at the phenyl ring including electron-withdrawing and electron-donating groups allowed for formation of piperidine derivatives **19b-19f** in decent yields. Different substitution at the arene moiety such as naphthyl, *ortho*-methylphenyl or *meta*-chlorophenyl were equally tolerated as demonstrated by cyclized products **19h-19j**. Finally, alternative heterocyclic scaffolds could be similarly accessed such as tetrahydroisoquinoline **19k**, which was obtained in 70% isolated yield from substrate **18k** offering a double activated benzylic position, or 1,3-oxazinane **19l**.



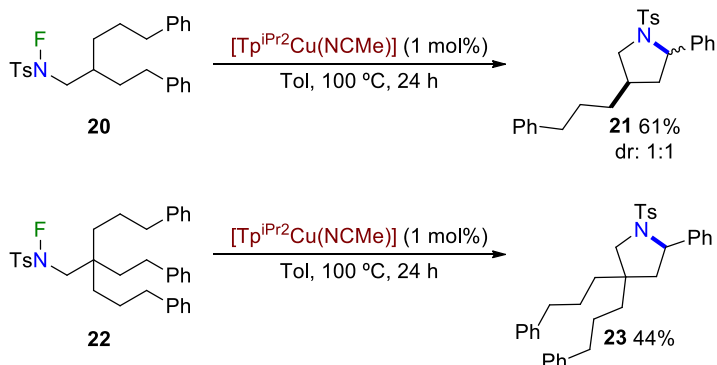
Scheme 3.11: Copper-catalyzed piperidine formation scope.

The ability to generate piperidines is particularly important, allowing to extend our protocol beyond the synthesis of pyrrolidines. This is certainly noteworthy, as amidyl-radicals show a thermodynamic preference for 1,5-HAT over 1,6-HAT processes,¹⁸⁶ particularly in the context of the Hofmann-Löffler reaction. However, the presence of the copper catalyst allows to override this inherent selectivity, achieving preferential 1,6-HAT when a benzylic position is present on the side chain. To further evaluate such selectivity, an intramolecular competition experiment was conducted. N-fluorosulfonamide **20** offering two competing benzylic positions accessible either by 1,5-HAT or 1,6-HAT was prepared for such purpose (Scheme 3.12). Interestingly, our copper catalytic conditions for intramolecular amination afforded pyrrolidine product

¹⁸⁶ M. Nechab, S. Mondal, M. P. Bertrand, *Chem. Eur. J.* **2014**, *20*, 16034-16059.

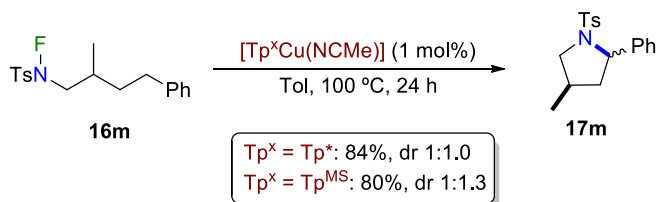
Chapter III. Copper-Catalyzed N-F Bond Activation for Uniform
Intramolecular C-H Amination Yielding Pyrrolidines and Piperidines

21 in 61% isolated yield as single product. Notably, **23** was uniquely obtained from **22**, indicating that the five-membered ring was obtained preferentially over statistically-favored six-membered ring analogues.



Scheme 3.12: Pyrrolidine formation vs. piperidine formation selectivity.

Additionally, the effect on the Tp^x ligand nature was evaluated for the cyclization of fluoroamide **16m** (Scheme 3.13). While Tp^{iPr_2} or Tp^* afforded pyrrolidine formation **17m** as an 1:1 mixture of diastereoisomers, the use of Tp^{MS} ligand (hydrotris(3-(2,4,6-trimethylphenyl)pyrazolyl)borate) with an increased steric impedance promoted partial acyclic stereocontrol. For the latter case, pyrrolidine **17m** was obtained in a diastereomeric mixture with a 1.3:1 ratio in favor of the anti-product. Even though a very modest effect was obtained on the reaction selectivity when tuning catalyst's bulkiness, the present observation points toward a subtle effect of the copper catalyst on the C-N forming step. In other words, it likely indicates that the catalyst is being at spatial proximity, if not coordinated, to the sulfonamide functionality in the cyclization step.



Scheme 3.13: Effect of Tp^x ligand.

In order to obtain a deep understanding on the individual steps of the reaction, a series of mechanistic experiments were conducted. We first focused our attention on the activation of the N-F bond by the copper catalyst. In this regard, Electronic Paramagnetic Resonance (EPR) studies were conducted (Figure 3.3). We first performed a blank measurement of the $[\text{Tp}^{\text{iPr}_2}\text{Cu}(\text{NCMe})]$ catalyst in toluene (orange

line). As expected, EPR silent Cu^I did not show any significant signal.¹⁸⁷ However, when mixed with fluorinated sulfonamide **16k**, a typical resonance band at 3260 Gauss corresponding to Cu^{II} appeared (yellow line).

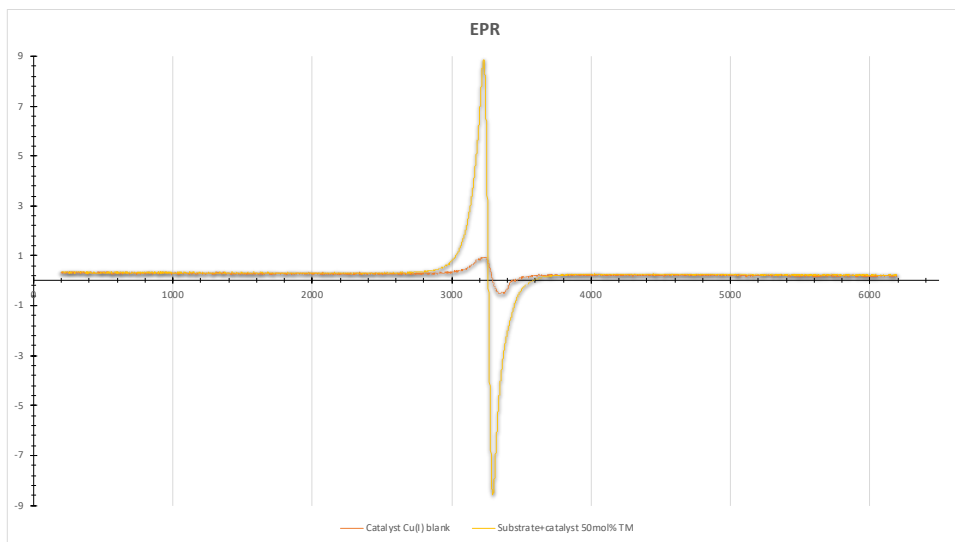


Figure 3.3: EPR studies at room temperature.

Furthermore, Cu^{II} hyperfine coupling pattern could be observed at 77K, (Figure 3.4). In this case, anisotropic effects due to the catalyst complex shape caused appearance of superimposed sets of signals. The parallel resonance signal ($g_{\parallel} = 2.31$) is overlapped with the perpendicular resonance ($g_{\perp} = 2.07$).¹⁸⁸

¹⁸⁷ A residual signal corresponding to Cu^{II} could be observed due to aerobic oxidation by adventitious air.

¹⁸⁸ P. S. Subramanian, E. Suresh, P. Dastidar, S. Waghmode, D. Srinivas, *Inorg. Chem.* **2001**, *40*, 4291-4301.

Chapter III. Copper-Catalyzed N-F Bond Activation for Uniform
Intramolecular C-H Amination Yielding Pyrrolidines and Piperidines

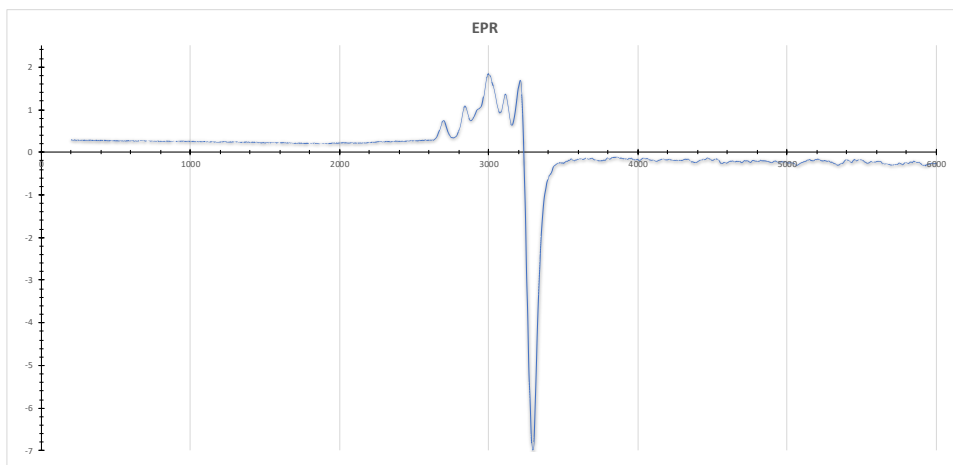
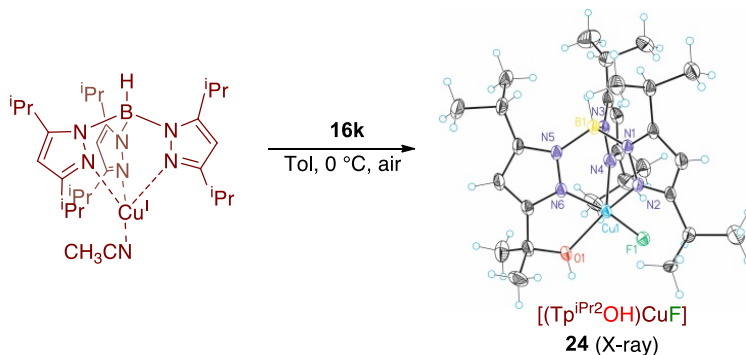


Figure 3.4: [Cu^{II}] EPR spectrum at 77K.

EPR investigations showed that N-fluorinated sulfonamides such as **16k** can efficiently promote single electron oxidation of [Tp^{iPr₂}Cu(NCMe)] to a Cu^{II} complex such as [Tp^{iPr₂}CuF(NCMe)], concomitantly delivering the corresponding amidyl radical. To further evaluate this oxidative process, a series of co-crystallization assays of fluoroimide **16k** and [Tp^{iPr₂}Cu(NCMe)] were performed. Unfortunately, when co-crystallization was attempted under inert atmosphere, no crystals were obtained. However, when such two substances were co-crystallized at open-air conditions from a toluene solution at 0 °C, copper-complex **24** was obtained. X-ray crystallographic analysis unambiguously confirmed its structure. Interestingly, this new complex **24** was structurally characterized as [(Tp^{iPr₂}OH)CuF], derived from the aerobic oxidation of one tertiary C-H bond of the *iso*-propyl groups at the Tp ligand. We hypothesize that **24** was formed through SET from the Cu^I species to the N-F bond, after which the corresponding Cu^{II}-F and nitrogen-centered radical were generated. Fragmentation of such species could involve intermolecular hydrogen atom abstraction from the amidyl radical to the tertiary C-H bond at the ligand, followed by copper-assisted aerobic oxidation to the final hydroxylated product. Alternatively, direct copper-promoted oxidation of the aliphatic C-H position by O₂ without amidyl radical involvement could lead to same product formation.¹⁸⁹

¹⁸⁹ M. Koddera, Y. Tachi, T. Kita, H. Kobushi, Y. Sumi, K. Kano, M. Shirao, M. Koikawa, T. Tokii, M. Ohba, H. Okawa, *Inorg. Chem.* **2000**, *39*, 226-234.



Scheme 3.14: Crystallization assay as evidence for the involvement of Cu^{II}-F species.

Indeed, mass spectrometric investigation identified the presence of species such as [Tp^{iPr}2CuF(NCMe)] (*m/z* = 588.34) in the reaction media of fluoro-sulfonamide **16k** cyclization. Further investigations aimed to determine the kinetic properties of the mechanism were performed to evaluate the kinetic performance of the putative 1,5-HAT event at the amidyl radical stage. First, we evaluated conversion rates of **16a** to **17a** at different catalyst concentrations, determining an order one with respect to the copper complex (Figure 3.5). This observation points toward involvement of discrete mononuclear copper species though the catalysis.

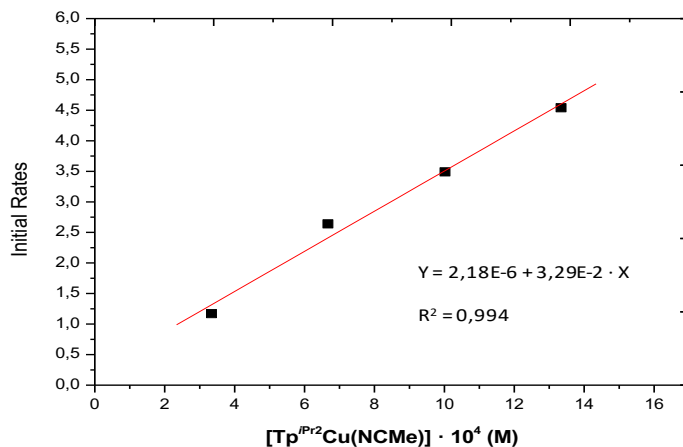
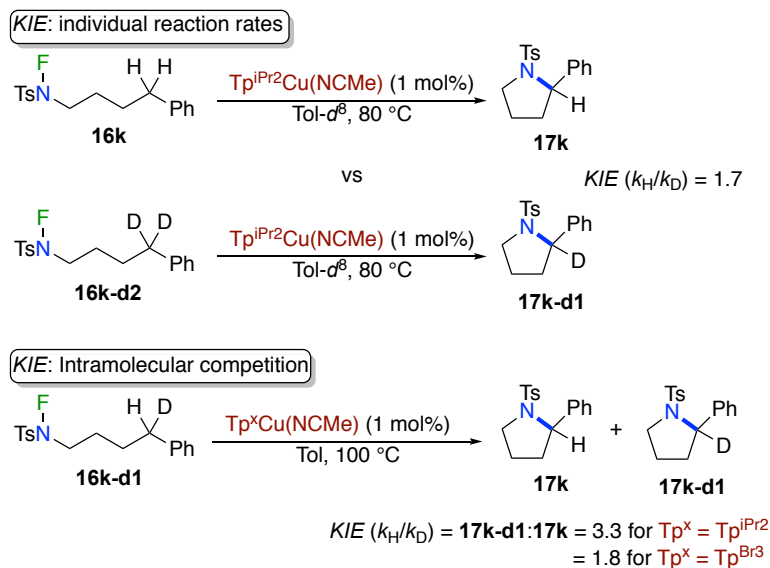


Figure 3.5: [Tp^{iPr}2Cu(NCMe)] reaction order determination.

Consecutively, we prepared **16k-d2** as a bis-deuterated analogue of fluoro-sulfonamide **16k** for Kinetic Isotope Effect (KIE) studies. Individual cyclization reaction rates for substrates **16k** and **16k-d2** were independently determined (Scheme 3.15, top). Simple initial rates comparison furnished a KIE value of 1.7. An intramolecular KIE experiment employing **16k-d1** afforded a value of 3.3 when using our optimized catalyst. This

Chapter III. Copper-Catalyzed N-F Bond Activation for Uniform
 Intramolecular C-H Amination Yielding Pyrrolidines and Piperidines

kinetic data is consistent with the 1,5-HAT process being the rate-limiting step for the cyclization reaction.¹⁹⁰ Interestingly, when employing a different copper catalyst bearing Tp^{Br3} as ligand, a reduced KIE value of 1.8 was obtained for the intramolecular competition experiment. Once again, this observation points toward an active involvement of the Tp^xCu core in the functionalization process.



Scheme 3.15: KIE experiments. Initial rates determination (top) and intramolecular competition (bottom) assays.

To further obtain a detailed picture on the reaction mechanism, DFT calculations were performed employing **16k** as model substrate and [Tp^xCu(NCMe)] as catalyst because of the more limited conformational flexibility and the comparable performance to [Tp^{iPr2}Cu(NCMe)]. All the structures were optimized employing B3LYP-D3 functional¹⁹¹ in toluene. Energies were refined with triple- ζ basis set plus polarization and diffusion shells. Free energies are reported in all the cases. A data set of all computed structures is available in the ioChem-BD repository and can be accessed via <https://doi.org/10.19061/iochem-bd-1-119>.¹⁹² The computed free energy profile of the reaction is shown in Figure 3.3. The reaction starts by acetonitrile ligand extrusion from the copper center followed by substrate **16k** coordination at the vacant position. This substrate can be coordinated via the nitrogen (**c1**) or the fluorine atom (**c1F**). The most favored activation of the N-F bond occurs through single electron transfer, either from

¹⁹⁰ E. M. Simmons, J. F. Hartwig, *Angew. Chem. Int. Ed.* **2012**, *51*, 3066-3072.

¹⁹¹ a) P. J. Stephens, F. J. Devlin, C. F. Chabalowski, M. J. Frisch, *J. Phys. Chem.* **1994**, *98*, 11623-11627. b) S. Grimme, J. Antony, S. Ehrlich, H. Krieg, *J. Chem. Phys.* **2010**, *132*, 154104-154119.

¹⁹² M. Álvarez-Moreno, C. de Graaf, N. López, F. Maseras, J. M. Poblet, C. Bo, *J. Chem. Inf. Model.* **2015**, *55*, 95- 103.

c1 (black path) or from **c1F** (red path). The transfer of one electron from the Cu^I center to the N-F σ* orbital results in cleavage of the N-F bond and formation of a new Cu-F bond in intermediate **c2** which contains a nitrogen centered radical coordinated to a Cu^{II} center. These reactions involve a change from singlet to triplet spin state, and are thus characterized by minimum energy crossing points (MECP) instead of transition states.¹⁹³ Intermediate **c1** is not a minimum in the triplet spin state. The processes from either **c1** or **c1F** have similar low barriers of 12.1 kcal/mol and 11.3 kcal/mol, so they are likely to coexist. In contrast, the oxidative addition pathway to yield the Cu^{III} intermediate **c2S** (blue path) is 6.4 kcal/mol higher in energy, and thus must be discarded. Intermediates **c2** and **c2F** have the same spin and are local minima, thus a transition state must exist between them, which should involve a low barrier.

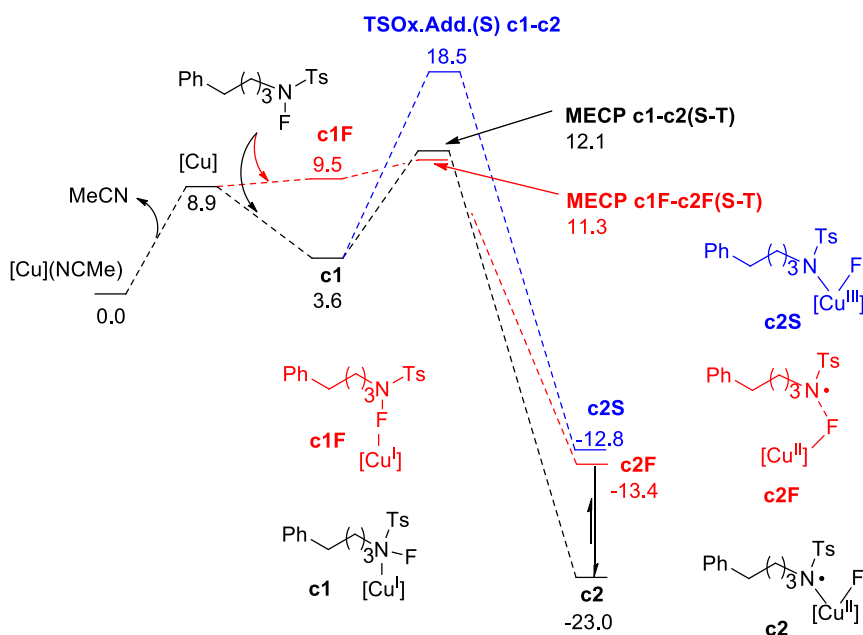


Figure 3.3: Free energy profile for copper-promoted N-F activation. [Cu] = Tp*Cu.

Alkyl-rotation of intermediate **c2** toward intermediate **c2'** ensures interaction of the fluorine atom with the benzyl C-H bond (Figure 3.4). Fluorine-assisted 1,5-HAT affords carbon-centered radical intermediate **c3** formation. According to the calculations, **TS c2'-c3** is the rate limiting barrier with an energy of 15.6 kcal/mol, which is in agreement with the results from the KIE studies (Scheme 3.15). The transition vector in **TS c2'-c3** is localized mainly in the F-H-C moiety. Once at the carbon-centered radical intermedia **c3**, the system undergoes a series of low-barrier rearrangements that results in C-N

¹⁹³ MECP were calculated using the software by J. N. Harvey, M. Aschi, H. Schwarz, W. Koch, *Theor. Chem. Acc.* **1998**, *99*, 95-99.

Chapter III. Copper-Catalyzed N-F Bond Activation for Uniform
 Intramolecular C-H Amination Yielding Pyrrolidines and Piperidines

bond formation concomitantly reducing Cu^{II} to Cu^I. Intermediate **c5** releases the corresponding pyrrolidine **16k** product together with HF byproduct. The overall process is highly exergonic by 56.5 kcal/mol. The DFT calculations confirmed the EPR and MS measurements that pointed toward formation of Cu^I species as well as radical ones. Furthermore, it matches with the measured KIE data and hints at the crucial role of the fluorine substituent. The present catalytic cycle was also computed for mesyl-containing substrate **Ms16k** as an analogue of fluorosulfonamide **16k** (see experimental section). For such case, an equivalent free energy profile to what just discussed was obtained. Additional calculations on [Tp^{Br3}Cu(NCMe)] as catalyst reproduce the experimental data of a more sluggish reaction in form of a higher barrier (see experimental section). Not surprisingly, the electronic properties of the substituents at the Tp^x ligand play an important role. They are known to affect the electronic density at copper,¹⁹⁴ and therefore also exert a certain influence in this reaction involving electron transfer from copper.

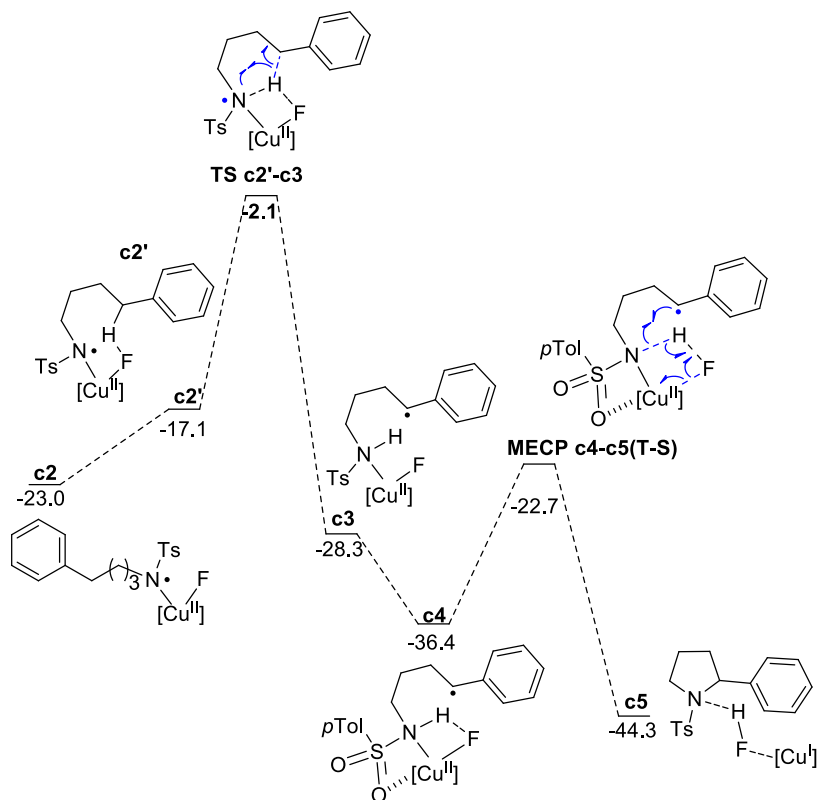


Figure 3.4: Free energy profile for C-H activation and cyclization steps. [Cu] = Tp^{*}Cu.

¹⁹⁴ A. Caballero, P. J. Pérez, *Isr. J. Chem.* **2017**, *57*, 1047-1052.

It is worth mentioning that putative formation of a benzylic carbocation derived by **c4** oxidation by Cu^{II} to concomitantly generate a high oxidation Cu^{III} species is not substantiated by theoretical calculation. In fact, the reductive pathway from **c4** is energetically straightforward (Figure 3.5). An intramolecular electron-transfer between the benzyl radical and the Cu^{II} center is indeed taking place, but it is coupled with C-N bond formation. This means that there is no formation of a detectable cationic state. The possibility of a Cu^I/Cu^{III} catalytic cycle involving the same fundamental steps from what just discussed for our Cu^I/Cu^{II} catalytic system was also computationally evaluated. However, calculations clearly discarded this possibility, since Cu^{II} was found unable to reduce the N-F bond at the initial step of the reaction (see experimental section). In that regard, the extensive mechanistic evaluation ultimately ruled out the intervention of high-oxidation state Cu^{III} intermediates. Its putative formation was discarded for each individual step, as indicated above. This conclusion is in sharp contrast with previously reported similar systems of copper-mediated N-F activation, which often postulate the involvement of such Cu^{III} species.¹⁸²⁻¹⁸⁴

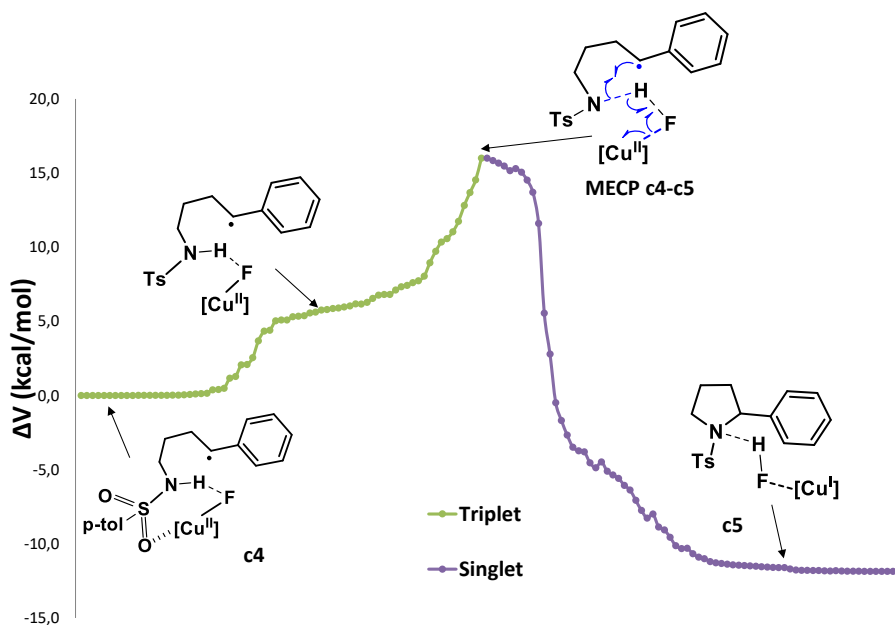
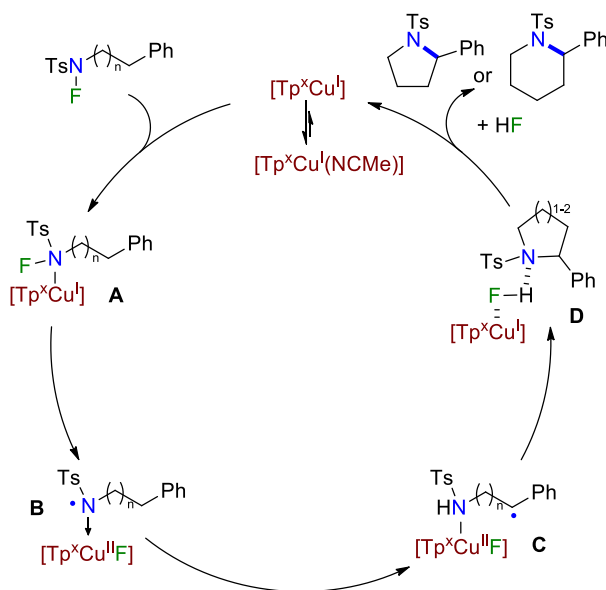


Figure 3.5: Evolution of potential energy between intermediates **c4** and **c5**.

Finally, the corresponding cyclization of model compound **18g** for the piperidine series was likewise computationally studied (see experimental section). In this case, the reaction mechanism discloses an analogous Cu^I/Cu^{II} catalytic system for what discussed for the pyrrolidine series. On the basis of all collected data from the extensive mechanistic studies, a full catalytic cycle could be depicted (Scheme 3.16). Initial acetonitrile release at the copper catalyst enable substrate N-coordination at intermediate **A**. Single electron reduction from the copper center to the N-F bond

Chapter III. Copper-Catalyzed N-F Bond Activation for Uniform
Intramolecular C-H Amination Yielding Pyrrolidines and Piperidines

generates the corresponding nitrogen-centered radical coordinated to Cu^{II}-F, affording organometallic complex **B**. Upon selective intramolecular hydrogen atom transfer, the organic radical relocates at benzylic position thus generating carbon-centered radical **C**. In the final amination step, the C-N bond formation occurs simultaneously with the HF byproduct generation and Cu^{II} reduction. This tandem process is a formal N-H-F shuttled SET from the benzylic radical to the copper catalyst that thus regenerate the active Cu^I catalyst.



Scheme 3.16: Final mechanistic proposal for copper-catalyzed intramolecular C-H amination.

3.3. Conclusions

In summary, we developed a Cu^I/Cu^{II} catalytic system for N-F bond activation toward intramolecular C(sp³)-H amination, resulting in a new methodology for obtaining pyrrolidine and piperidine scaffolds. This technique shows how copper is able to override the inherent reactivity of amidyl radicals, thus outperforming the traditional Hofmann-Löffler reaction in terms of ring-size limitation. In addition, a plethora of mechanistic studies were performed in order to obtain a deep understanding of each individual step of the reaction.

3.4. Experimental section

General Remarks: All solvents and reagents employed were purchased from Aldrich, Acros, TCI and Fluorochem. The complexes [Tp^{iPr₂}Cu(NCMe)],¹⁹⁵ [Tp^{Br₃}Cu(NCMe)],¹⁹⁶ [Tp^{*,Br}Cu(NCMe)]¹⁹⁷ and [Tp^{*}Cu(NCMe)]¹⁹⁸ were prepared according to literature. Column chromatography was performed on silica gel (PanReac AppliChem, Silica Gel 60, 0.063-0.2 mm). NMR spectroscopy was performed on a Bruker Avance 300 MHz, 400 MHz or 500 MHz, respectively. The chemical shifts are given in ppm normalized to the shift of residual chloroform in the deuterated chloroform ($\delta\text{H} = 7.26$ ppm and $\delta\text{C} = 77.16$ ppm). The multiplicities are stated as follows: s = singlet, bs = broad singlet, d = doublet, t = triplet, q = quartet, m = multiplet. HRMS measurements were performed on a UHPLC-MS-QqTOF (MaXis Impact, Bruker Daltonics) or HPLC-MS-TOF (MicroTOF II, Bruker Daltonics) within the ICIQ service department. Continuous wave (CW) EPR spectra were obtained at room temperature on a Bruker EMX Micro X-band spectrometer operating at 9.826e9 using a Bruker ER 1164 HS resonator. IR spectroscopy was performed using a Bruker Alpha instrument in the solid state. Melting points were determined employing a Büchi B-540 instrument.

General protocol (GP1) for the synthesis of N-fluoroamides: A solution of the corresponding sulfonamide^{72,75,76} (0.8 mmol) in dry CH₂Cl₂ (7 mL) was added to a stirred mixture of NaH (4.8 mmol) in dry CH₂Cl₂ (7 mL) at 25 °C. After 30 min, NFSI (2.4 mmol) in CH₂Cl₂ (7 mL) was added dropwise at 25 °C. The reaction was stirred for 24 h and monitored by TLC. After 24 h, the reaction was quenched with NH₃ (2%)/NaOH (6.5%) solution (20 mL) at 0 °C. The reaction mixture was extracted with Et₂O (3 x 15 mL) and the combined organic layers were washed with NH₃/NaOH solution (3 x 15 mL), NaOH (5%) (3 x 15 mL) and HCl (5%) (3 x 15 mL), dried over MgSO₄, filtered and the solvent was removed under reduced pressure. The residue was purified by column chromatography on silica gel using hexane/ethyl acetate.

General protocol (GP2) for synthesis of saturated N-heterocycles: A flame-dried schlenk tube was charged with the corresponding N-fluorotosylamide (0.1 mmol), [Tp^{iPr₂}Cu(NCMe)] (1 mol%) and dry toluene under an atmosphere of argon. The reaction mixture was stirred at 100 °C. After 24 h, the reaction mixture was cooled down to room temperature and the solvent was removed under reduced pressure. The thus

¹⁹⁵ K. Fujisawa, T. Ono, Y. Ishikawa, N. Amir, Y. Miyashita, K.-I. Okamoto, N. Lehnert, *Inorg. Chem.* **2006**, *45*, 1698-1713.

¹⁹⁶ A. Caballero, M. M. Díaz-Requejo, T. R. Belderraín, M. C. Nicasio, S. Trofimenko, P. J. Pérez, *J. Am. Chem. Soc.* **2003**, *125*, 1446-1447.

¹⁹⁷ M. A. Mairena, J. Urbano, J. Carbajo, J. J. Maraver, E. Alvarez, M. M. Díaz-Requejo, P. J. Pérez, *Inorg. Chem.* **2007**, *46*, 7428-7435.

¹⁹⁸ C. Mealli, C. S. Arcus, J. L. Wilkinson, T. J. Marks, J. A. Ibers, *J. Am. Chem. Soc.* **1976**, *98*, 711-718.

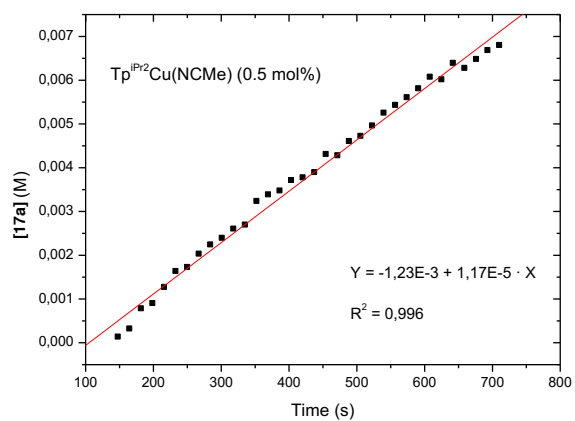
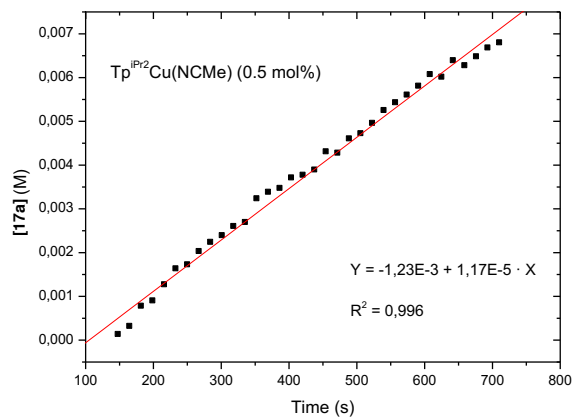
Chapter III. Copper-Catalyzed N-F Bond Activation for Uniform
Intramolecular C-H Amination Yielding Pyrrolidines and Piperidines

obtained crude product was further purified by column chromatography on silica gel using hexane/ethyl acetate.

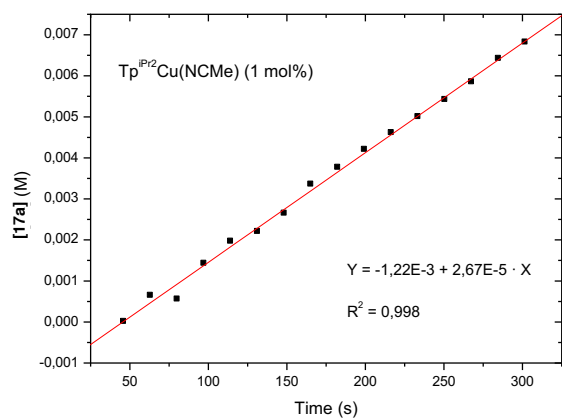
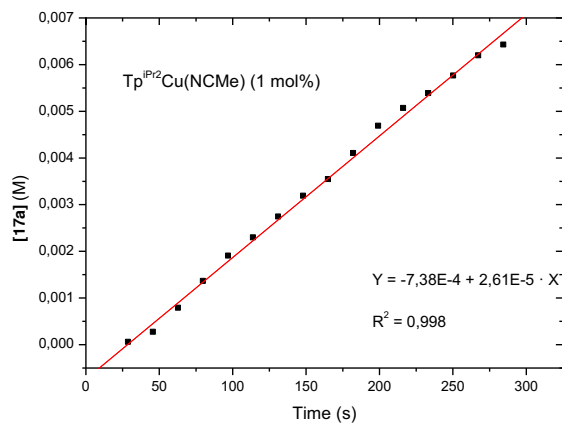
EPR measurements: The spectral data was collected at 298 K with the following spectrometer settings: microwave frequency = 9.826e9, g-factor = 2.000000, microwave power = 2.05 mW; center field = 3200.00 G, sweep width = 6000 G, sweep time = 60 s, modulation frequency = 100 KHz, modulation amplitude = 4 G, power attenuation = 20 dB, time constant = 0.01 ms, conversion time = 4 ms, gain = 20 dB. The spectral data was collected at 77 K with the following spectrometer settings: microwave frequency = 9.388e9, g-factor = 2.000000, microwave power = 1.76 mW; center field = 3200.00 G, sweep width = 6000 G, sweep time = 60 s, modulation frequency = 100 KHz, modulation amplitude = 4 G, power attenuation = 20 dB, time constant = 0.01 ms, conversion time = 4 ms, gain = 20 dB.

Determination of reaction order in copper-catalyst: In a glovebox, 14.0 mg (0.040 mmol) of **16a** were added to a vial. Then, the required amount of a stock solution of the complex [Tp^{Pr}2Cu(NCMe)] in toluene-*d*⁸ was added via syringe. Diphenylmethane was added via syringe as an internal standard. Finally, the required amount of toluene-*d*⁸ was added to reach a total volume of 0.6 mL ([**16a**]₀ = 0.067 M). The mixture was transferred to an NMR pressure tube and sealed with a Teflon screw cap. The reaction was then monitored by ¹H NMR spectroscopy at 100 °C, using a delay D1 = 10 s. The integration of the signals corresponding to **16a** and **17a** with respect to the internal standard indicated that no other byproducts are formed. The graphical representation of the extrapolated initial rate of formation of **17a** (M) vs time (s) for four different catalyst loadings (0.5, 1.0, 1.5, and 2.0 mol%) is shown below.

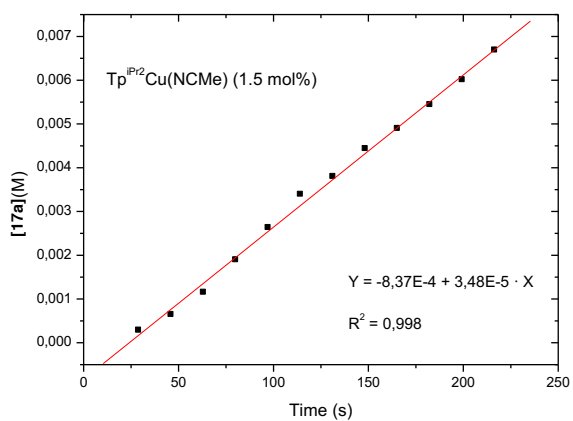
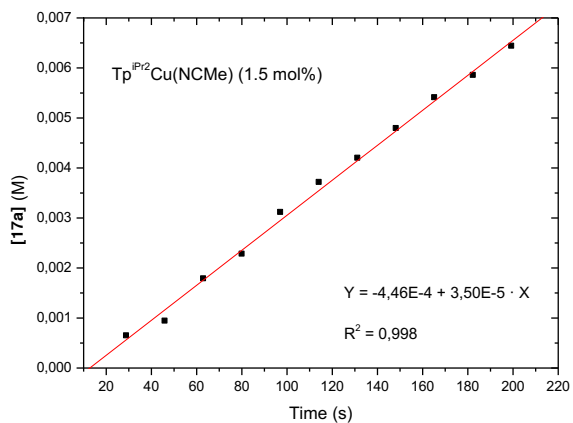
Chapter III. Copper-Catalyzed N-F Bond Activation for Uniform
Intramolecular C-H Amination Yielding Pyrrolidines and Piperidines



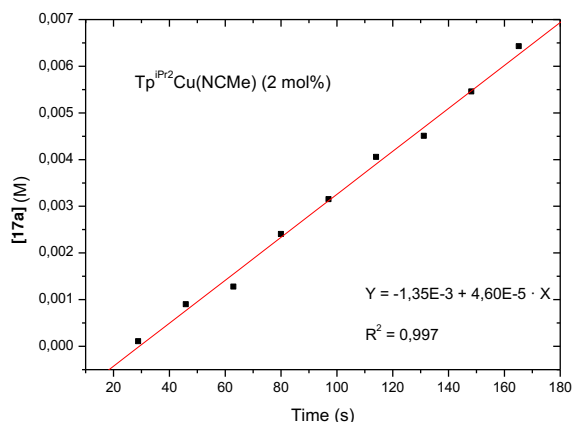
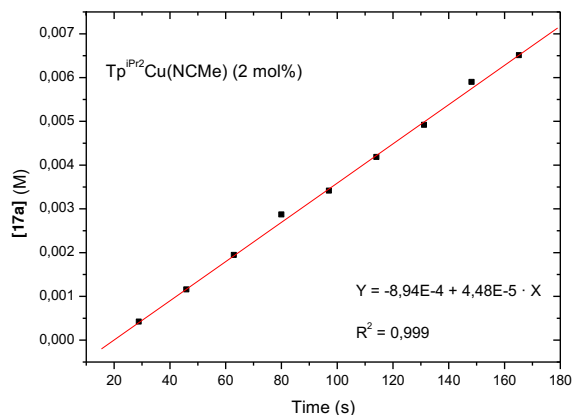
Chapter III. Copper-Catalyzed N-F Bond Activation for Uniform Intramolecular C-H Amination Yielding Pyrrolidines and Piperidines



Chapter III. Copper-Catalyzed N-F Bond Activation for Uniform
Intramolecular C-H Amination Yielding Pyrrolidines and Piperidines



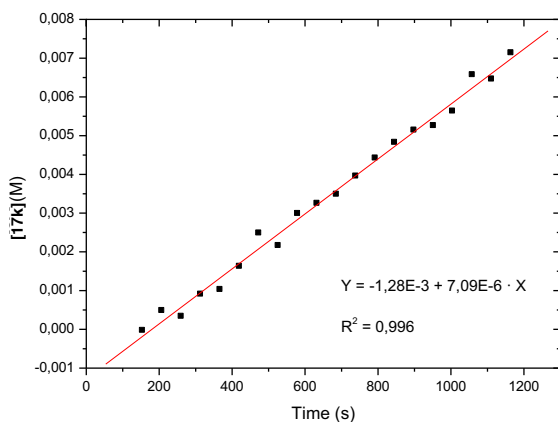
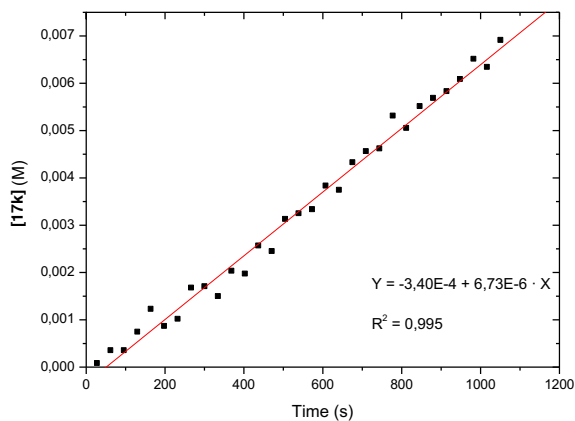
Chapter III. Copper-Catalyzed N-F Bond Activation for Uniform Intramolecular C-H Amination Yielding Pyrrolidines and Piperidines



Linear dependence of the cyclization initial rate with the concentration of the catalyst $[\text{Tp}^{\text{iPr}_2}\text{Cu}(\text{NCMe})]$ led us to conclude a reaction order of 1 for the copper-catalyst (Figure 3.5).

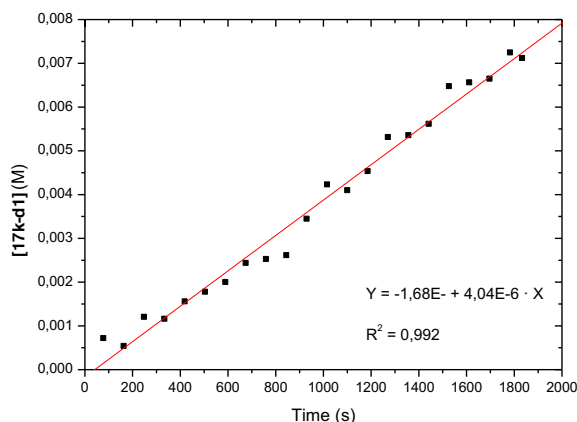
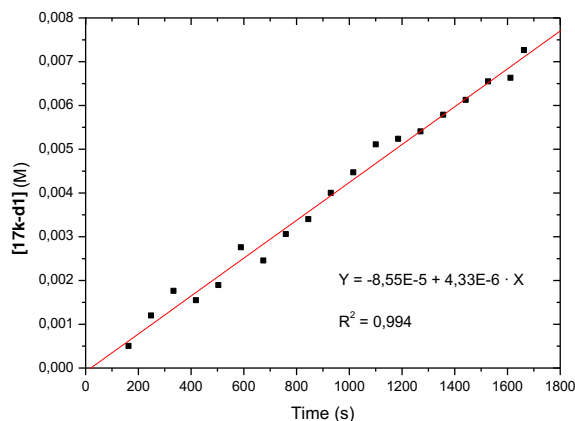
KIE studies: In a glovebox, 14.0 mg (0.043 mmol) of **16k** were added to a vial. Then, the required amount of a stock solution of the complex $[\text{Tp}^{\text{iPr}_2}\text{Cu}(\text{NCMe})]$ in toluene- d^8 was added via syringe. Diphenylmethane was added via syringe as an internal standard. Finally, the required amount of toluene- d^8 was added to reach a total volume of 0.6 mL ($[\mathbf{16k}]_0 = 0.072$ M). The mixture was transferred to an NMR pressure tube and sealed with a Teflon screw cap. The reaction was then monitored by ^1H NMR spectroscopy at 80 °C. The integration of the signals corresponding to **16k** and **17k** with respect to the internal standard indicated that no other byproducts are formed. The graphical

representation of the extrapolated initial rate of formation of **17k** (M) vs time (s) is shown below.



The same procedure was repeated for cyclization of substrate **16k-d2** to **17k-d1**. The graphical representation of the extrapolated initial rate of formation of **17k-d1** vs time (s) is shown below.

Chapter III. Copper-Catalyzed N-F Bond Activation for Uniform Intramolecular C-H Amination Yielding Pyrrolidines and Piperidines



Direct determination of the kinetic constants revealed an isotope effect $k_H/k_D = 1.7$.

Computational details: All the calculations were carried out using the Gaussian09 (V D.01)¹⁹⁹ program package and density functional theory as the method. B3LYP-

¹⁹⁹ Gaussian 09, Revision D.01, M. J. Frisch, G. W. Trucks, H. B. Schlegel, G. E. Scuseria, M. A. Robb, J. R. Cheeseman, G. Scalmani, V. Barone, G. A. Petersson, H. Nakatsuji, X. Li, M. Caricato, A. Marenich, J. Bloino, B. G. Janesko, R. Gomperts, B. Mennucci, H. P. Hratchian, J. V. Ortiz, A. F. Izmaylov, J. L. Sonnenberg, D. Williams-Young, F. Ding, F. Lipparini, F. Egidi, J. Goings, B. Peng, A. Petrone, T. Henderson, D. Ranasinghe, V. G. Zakrzewski, J. Gao, N. Rega, G. Zheng, W. Liang, M. Hada, M. Ehara, K. Toyota, R. Fukuda, J. Hasegawa, M. Ishida, T. Nakajima, Y. Honda, O. Kitao, H. Nakai, T. Vreven, K. Throssell, J. A. Montgomery, Jr., J. E. Peralta, F. Ogliaro, M. Bearpark, J. J. Heyd, E. Brothers, K. N. Kudin, V. N. Staroverov, T. Keith, R. Kobayashi, J. Normand, K. Raghavachari, A. Rendell, J. C. Burant, S. S. Iyengar, J. Tomasi, M. Cossi, J. M. Millam, M. Klene,

D3^{191,200} was used as the functional due to its good agreement in similar copper catalyzed reactions.²⁰¹ Optimizations and frequency calculations were calculated using the basis set I: 6-31G(d)²⁰² basis set for all atoms except for Cu, where LANL2TZ(f) and the associated pseudopotential was used.²⁰³ Potential energies were further refined using the larger basis set (basis set II) 6-311+G(d,p)²⁰⁴ for all atoms except for Cu, where we kept the same basis set. All the stationary points were characterized as minima (zero imaginary frequencies) or transition states (one imaginary frequency) using vibrational frequency analysis. Free energy corrections were applied at 298K and 1 atm. Solvation was implicitly considered in all the calculations using the SMD model and toluene as solvent ($\epsilon = 2.3741$).²⁰⁵ All the energies reported along the manuscript are free energies in kcal/mol calculated as the sum of the potential energy with the large basis set plus the free energy correction calculated with the low basis set. Minimum energy crossing points (MECP) between singlet and triplet states were located using the Harvey's software^{193,206} and the frequencies were calculated as the average of the projected frequencies at the MECP geometry. A data set collection of all computational data is available in the ioChem-BD repository.¹⁹²

Additional DFT studies: The free energy profile of the C-H activation and cyclization steps of reaction with **M^s16k** as the substrate is shown below. Energies in kcal/mol.

C. Adamo, R. Cammi, J. W. Ochterski, R. L. Martin, K. Morokuma, O. Farkas, J. B. Foresman, and D. J. Fox, Gaussian, Inc., Wallingford CT, **2016**.

²⁰⁰ a) A. D. Becke, *J. Chem. Phys.* **1993**, *98*, 5648-5652. b) C. Lee, W. Yang, R. G. Parr, *Phys. Rev. B.: Condens. Mater.* **1988**, *37*, 785-789.

²⁰¹ a) M. R. Rodríguez, A. Beltrán, A. L. Mudarra, E. Álvarez, F. Maseras, M. M. Díaz-Requejo, P. J. Pérez, *Angew. Chem. Int. Ed.* **2017**, *56*, 12842-12847. b) R. Gava, A. Olmos, B. Noverges, T. Varea, I. Funes-Ardoiz, T. R. Belderrain, A. Caballero, F. Maseras, G. Asensio, P. J. Pérez, *ChemCatChem* **2015**, *7*, 32543260.

²⁰² a) M. M. Francl, W. J. Pietro, W. J. Hehre, J. S. Binkley, M. S. Gordon, D. J. DeFrees, J. A. Pople, *J. Chem. Phys.* **1982**, *77*, 3654-3665. b) P. C. Hariharan, J. A. Pople, *Theoret. Chim. Acta* **1973**, *28*, 213-222. c) W. J. Hehre, R. Ditchfield, J. A. Pople, *J. Chem. Phys.* **1972**, *56*, 2257-2261.

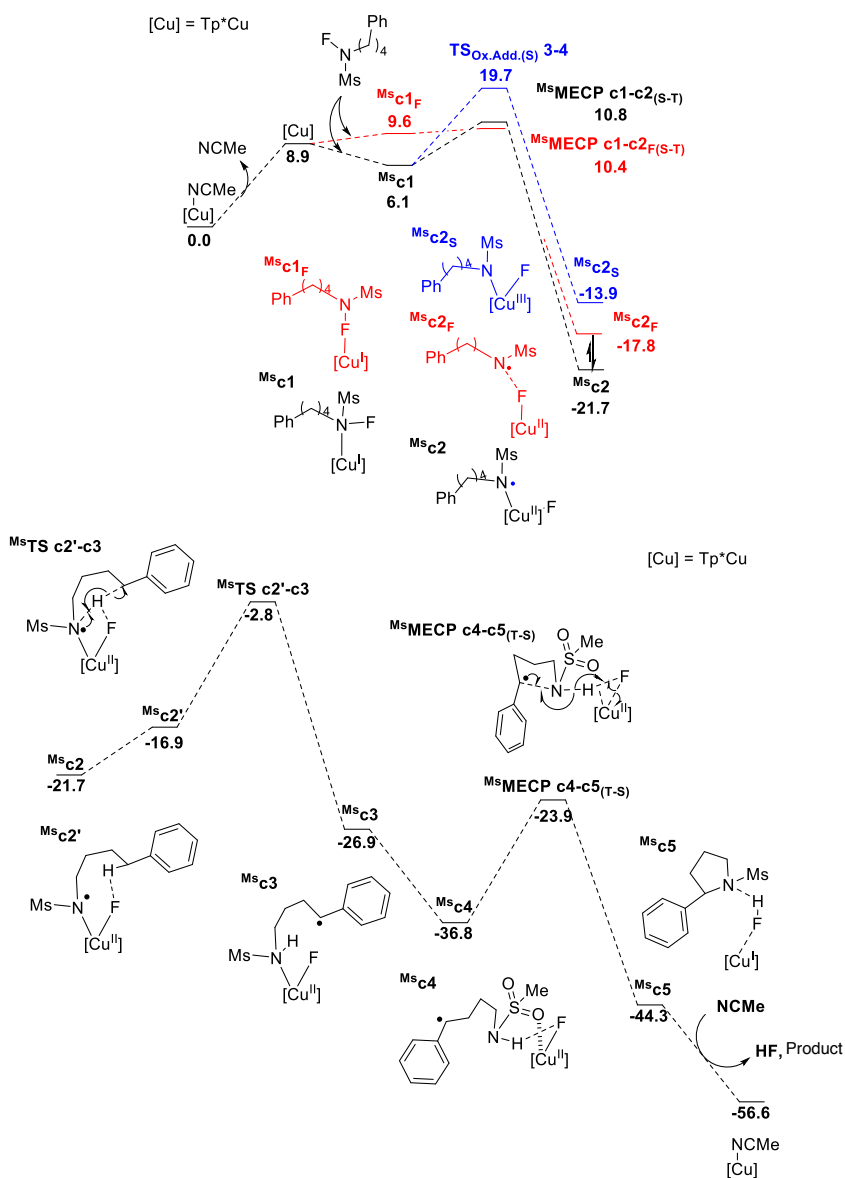
²⁰³ a) P. J. Hay, W. R. Wadt, *J. Chem. Phys.* **1985**, *82*, 270-283. b) L. E. Roy, P. J. Hay, R. L. Martin, *J. Chem. Theor. Comput.* **2008**, *4*, 1029-1031. c) A. W. Ehlers, M. Böhme, S. Dapprich, A. Gobbi, A. Höllwarth, V. Jonas, K. F. Köhler, R. Stegmann, A. Veldkamp, G. Frenking, *Chem. Phys. Lett.* **1993**, *208*, 111-114.

²⁰⁴ R. Krishnan, J. S. Binkley, R. Seeger, J. A. Pople, *J. Chem. Phys.* **1980**, *72*, 650-654.

²⁰⁵ A. V. Marenich, C. J. Cramer, D. G. Truhlar, *J. Phys. Chem. B* **2009**, *113*, 6378-6396.

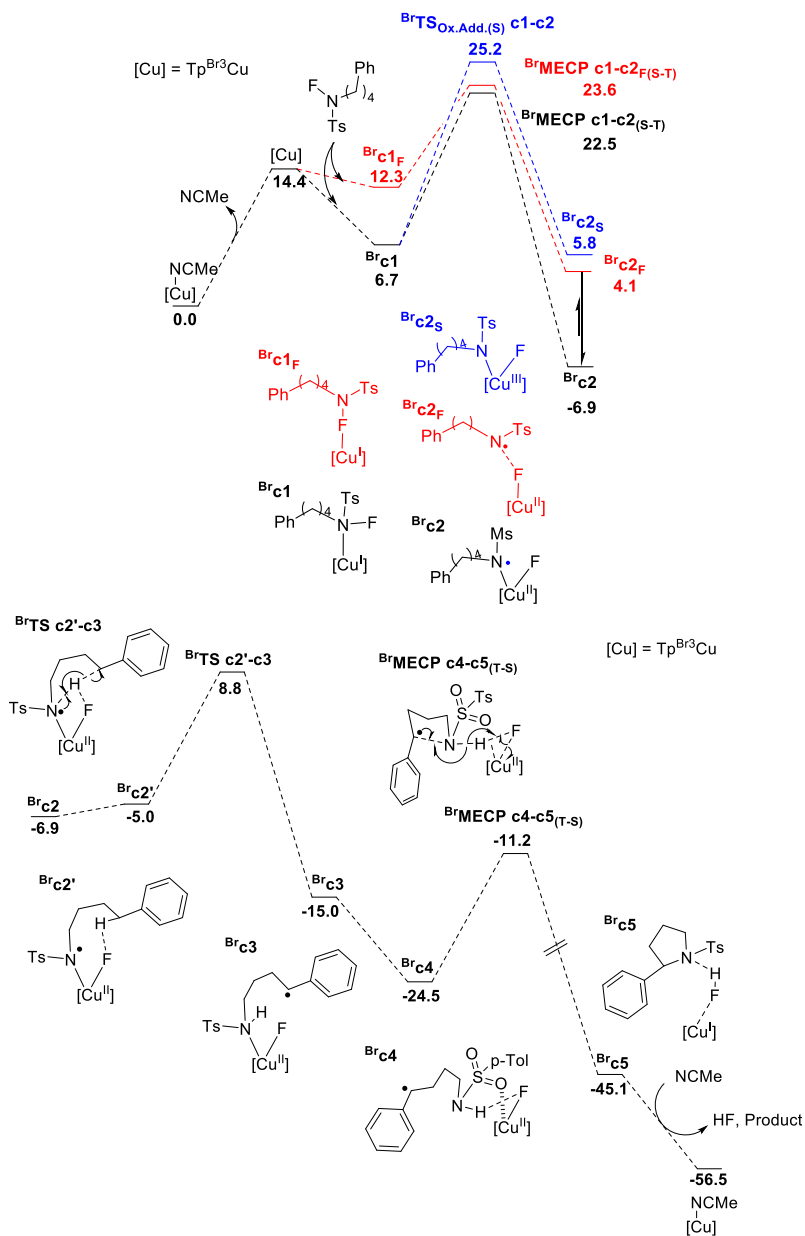
²⁰⁶ R. Poli, J. N. Harvey, *Chem. Soc. Rev.* **2003**, *32*, 1-8.

Chapter III. Copper-Catalyzed N-F Bond Activation for Uniform
 Intramolecular C-H Amination Yielding Pyrrolidines and Piperidines



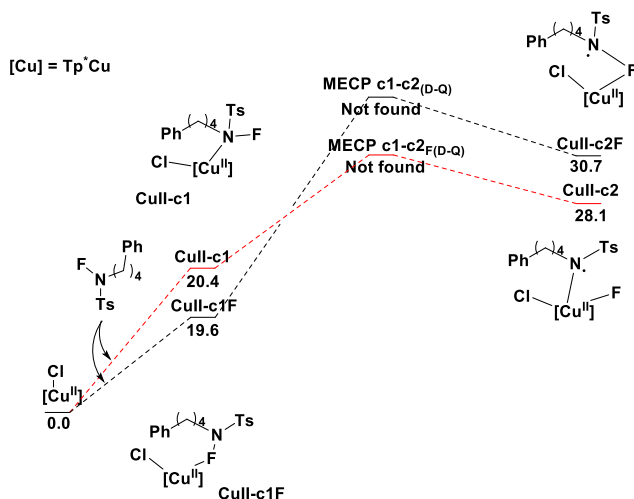
The free energy profile of the C-H activation and cyclization steps of reaction with $[\text{Tp}^{\text{Br}_3}\text{Cu}(\text{NCMe})]$ as catalyst is shown below. Energies in kcal/mol.

Chapter III. Copper-Catalyzed N-F Bond Activation for Uniform
 Intramolecular C-H Amination Yielding Pyrrolidines and Piperidines

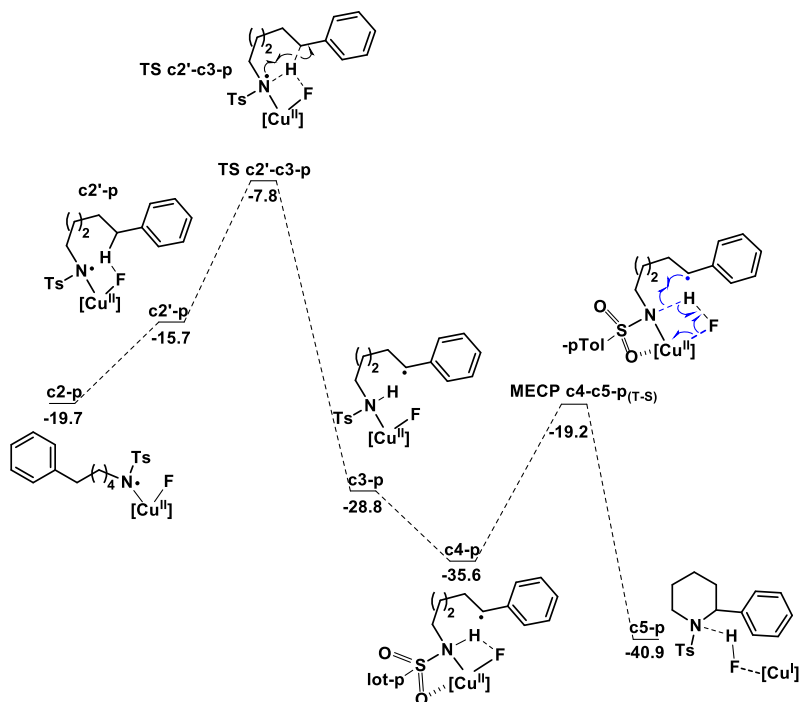


The free energy profile of the intramolecular C-H amination catalyzed by $[\text{Tp}^*\text{CuCl}]$ and the substrate **16k** is shown below. As observed, a productive pathway toward N-F activation involving oxidation of Cu^{II} to Cu^{III} could not be found. Energies in kcal/mol.

Chapter III. Copper-Catalyzed N-F Bond Activation for Uniform
 Intramolecular C-H Amination Yielding Pyrrolidines and Piperidines



We have calculated the C-H activation and cyclization steps for the reaction of substrate **19g**, which leads to a product containing a 6-member piperidine ring. The shape of the profile is similar to that depicted in the main text for substrate **16k**, leading to a 5-member pyrrolidine ring. There are however some quantitative differences. The rate-determining step is now in the cyclization (**MECP c4-c5-p(T-S)**). The overall barrier for **19g** (16.4 kcal/mol) is slightly higher than for **16k** (15.6 kcal/mol), in agreement with experiment, which indicates that the formation of piperidine rings is more sluggish. The difference between the systems seem to be associated to the change in ring strain for the different rate-determining steps. The free energy profile of the Intramolecular C-H amination catalyzed by [Tp*Cu(NCMe)] and the substrate **19g** is shown below. Energies in kcal/mol.



N-(2,2-Dimethyl-4-phenylbutyl)-N-fluoro-4-methylbenzenesulfonamide (16a)

16a was obtained as a white solid (65%) by applying GP1. ¹H NMR (400 MHz, CDCl₃): δ = 7.88-7.84 (m, 2H), 7.46-7.42 (m, 2H), 7.33-7.28 (m, 2H), 7.20-7.15 (m, 3H), 3.12 (d, J = 44.4 Hz, 2H), 2.63-2.55 (m, 2H), 2.52 (s, 3H), 1.73-1.63 (m, 2H), 1.08 (s, 6H). ¹³C NMR (100 MHz, CDCl₃): δ = 146.3, 142.7, 130.1, 129.9, 129.6, 128.5, 128.5, 125.9, 62.9 (d, J = 10.6 Hz), 42.4, 34.6, 30.4, 25.8, 21.9. ¹⁹F{¹H} NMR (375 MHz, CDCl₃): δ = -36.38. IR ν (cm⁻¹): 3028, 2958, 1954. mp: 72-73 °C. HRMS: Mass calculated for C₁₉H₂₄FNNaO₂S: 372.1404, found: 372.1402.

X-Ray Analytical Data for Compound 16a

Chapter III. Copper-Catalyzed N-F Bond Activation for Uniform
Intramolecular C-H Amination Yielding Pyrrolidines and Piperidines

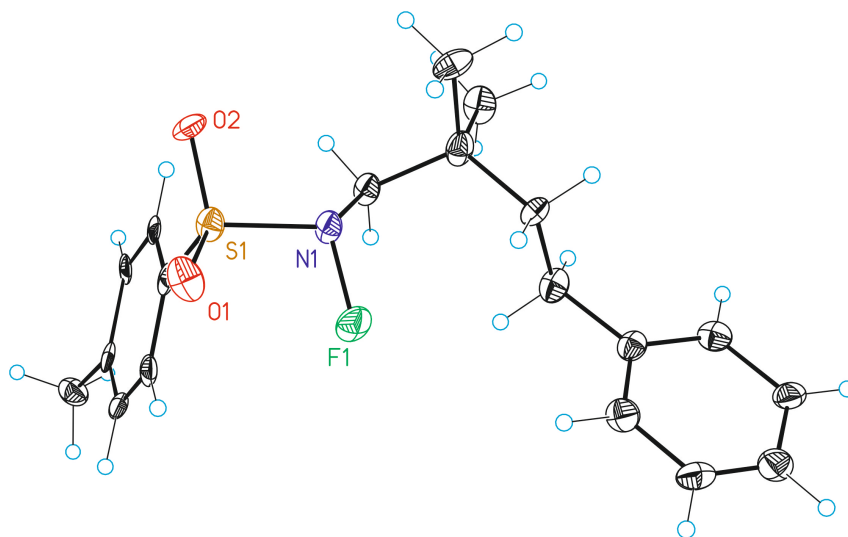
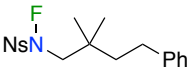


Table S-1. Crystal data and structure refinement for compound **16a**.

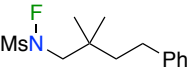
Identification code	16a	
Empirical formula	C ₁₉ H ₂₄ F N O ₂ S	
Formula weight	349.45	
Temperature	100(2) K	
Wavelength	null Å	
Crystal system	Orthorhombic	
Space group	Pbca	
Unit cell dimensions	a = 6.2239(9)Å	α = 90°.
	b = 16.8222(16)Å	β = 90°.
	c = 33.926(4)Å	γ = 90°.
Volume	3552.1(7) Å ³	
Z	8	
Density (calculated)	1.307 Mg/m ³	
Absorption coefficient	0.203 mm ⁻¹	
F(000)	1488	

Crystal size	0.35 x 0.35 x 0.10 mm ³
Theta range for data collection	2.401 to 28.627°.
Index ranges	-8<=h<=8,-22<=k<=21,-45<=l<=36
Reflections collected	33502
Independent reflections	4538[R(int) = 0.0768]
Completeness to theta =28.627°	99.4%
Absorption correction	Multi-scan
Max. and min. transmission	_exptl_absorpt_correction_T_max 0.7457 and _exptl_absorpt_correction_T_min 0.5510
Refinement method	Full-matrix least-squares on F ²
Data / restraints / parameters	4538/ 587/ 434
Goodness-of-fit on F ²	1.125
Final R indices [I>2sigma(I)]	R1 = 0.0576, wR2 = 0.1316
R indices (all data)	R1 = 0.0804, wR2 = 0.1433
Largest diff. peak and hole	0.226 and -0.388 e.Å ⁻³

N-(2,2-Dimethyl-4-phenylbutyl)-N-fluoro-4-nitrobenzenesulfonamide (16b)

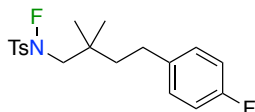
 **16b** was obtained as a white solid (34%) by applying GP1. ¹H NMR (400 MHz, CDCl₃): δ = 8.45 (d, J = 8.9 Hz, 2H), 8.15 (d, J = 8.8 Hz, 2H), 7.30-7.27 (m, 1H), 7.21-7.15 (m, 3H), 3.17 (d, J = 43.7 Hz, 2H), 2.61-2.53 (m, 2H), 1.70-1.61 (m, 2H), 1.06 (s, 6H). ¹³C NMR (125 MHz, CDCl₃): δ = 151.6, 142.5, 138.6, 131.3, 128.6, 128.4, 126.0, 124.6, 62.6 (d, J = 10.7 Hz), 42.3, 34.9, 30.4, 25.7. ¹⁹F{¹H} NMR (470 MHz, CDCl₃): δ = -35.7. IR ν (cm⁻¹): 3115, 3028, 2966, 2933, 2866, 1608, 1536. mp: 130-131 °C. HRMS: Mass calculated for C₁₈H₂₁FN₂NaO₄S: 403.1098, found: 403.1097.

N-(2,2-Dimethyl-4-phenylbutyl)-N-fluoromethanesulfonamide (16c)

 **16c** was obtained as a white solid (34%) by applying GP1. ¹H NMR (300 MHz, CDCl₃): δ = 7.34-7.26 (m, 2H), 7.23-7.17 (m, 3H), 3.37 (d, J = 45.4 Hz, 2H), 3.15 (d, J = 2.0 Hz, 3H), 2.66-2.58 (m, 2H), 1.74-1.65 (m, 2H), 1.11 (d, J = 1.1 Hz, 6H). ¹³C NMR (75 MHz, CDCl₃): δ = 142.7, 128.5, 128.4, 125.9, 60.2, 42.4, 35.7, 34.4, 30.4, 25.7, 25.7. ¹⁹F{¹H} NMR (375 MHz, CDCl₃): δ = -36.09. IR ν (cm⁻¹): 2963, 2938. HRMS: Mass calculated for C₁₃H₂₀FNNaO₂S: 296.1091, found: 296.1088.

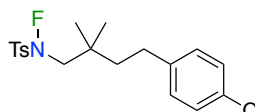
Chapter III. Copper-Catalyzed N-F Bond Activation for Uniform
Intramolecular C-H Amination Yielding Pyrrolidines and Piperidines

N-Fluoro-N-(4-(4-fluorophenyl)-2,2-dimethylbutyl)-4-methylbenzenesulfonamide (16d)



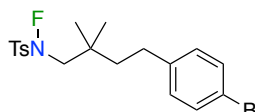
16d was obtained as a white solid (69%) by applying GP1. ¹H NMR (400 MHz, CDCl₃): δ = 7.82 (d, J = 8.3 Hz, 2H), 7.43-7.39 (m, 2H), 7.15-7.07 (m, 2H), 6.97-6.91 (m, 2H), 3.08 (d, J = 44.3 Hz, 2H), 2.57-2.50 (m, 2H), 2.49 (s, 3H), 1.66-1.58 (m, 2H), 1.03 (s, 6H). ¹³C NMR (100 MHz, CDCl₃): δ = 161.4 (d, J = 243.3 Hz), 146.3, 138.3 (d, J = 3.3 Hz), 130.1, 130.0, 129.8 (d, J = 7.8 Hz), 129.6, 115.2 (d, J = 21.1 Hz), 62.8 (d, J = 10.6 Hz), 42.5, 34.6, 29.7, 25.8, 21.9. ¹⁹F{¹H} NMR (375 MHz, CDCl₃): δ = -36.37, -118.03. IR ν (cm⁻¹): 2965, 2932, 2914, 2871, 1597, 1508. mp: 69-70 °C. HRMS: Mass calculated for C₁₉H₂₃F₂NNaO₂S: 390.1310, found: 390.1309.

N-(4-(4-Chlorophenyl)-2,2-dimethylbutyl)-N-fluoro-4-methylbenzenesulfonamide (16e)



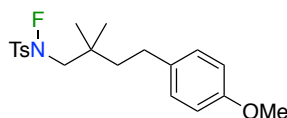
16e was obtained as a white solid (53%) by applying GP1. ¹H NMR (400 MHz, CDCl₃): δ = 7.82 (d, J = 8.4 Hz, 2H), 7.43-7.39 (m, 2H), 7.23 (d, J = 8.4 Hz, 2H), 7.09 (d, J = 8.4 Hz, 2H), 3.08 (d, J = 44.2 Hz, 2H), 2.56-2.50 (m, 2H), 2.49 (s, 3H), 1.65-1.58 (m, 2H), 1.03 (s, 6H). ¹³C NMR (100 MHz, CDCl₃): δ = 146.3, 141.2, 131.6, 130.1, 130.0, 129.8, 129.6, 128.6, 62.8 (d, J = 10.6 Hz), 42.2, 34.7, 29.9, 25.8, 21.9. ¹⁹F{¹H} NMR (375 MHz, CDCl₃): δ = -36.4. IR ν (cm⁻¹): 2966, 2909, 1597. mp: 101-102 °C. HRMS: Mass calculated for C₁₉H₂₃ClFNNaO₂S: 406.1014, found: 406.1015.

N-(4-(4-Bromophenyl)-2,2-dimethylbutyl)-N-fluoro-4-methylbenzenesulfonamide (16f)



16f was obtained as a white solid (45%) by applying GP1. ¹H NMR (400 MHz, CDCl₃): δ = 7.82 (d, J = 8.3 Hz, 2H), 7.41 (d, J = 8.2 Hz, 2H), 7.38 (d, J = 8.3 Hz, 2H), 7.04 (d, J = 8.3 Hz, 2H), 3.08 (d, J = 44.2 Hz, 2H), 2.54-2.50 (m, 2H), 2.49 (s, 3H), 1.64-1.58 (m, 2H), 1.03 (s, 6H). ¹³C NMR (100 MHz, CDCl₃): δ = 146.3, 141.7, 131.6, 130.3, 130.1, 130.0, 129.6, 119.6, 62.7 (d, J = 10.6 Hz), 42.2, 34.7, 29.9, 25.8, 21.9. ¹⁹F{¹H} NMR (375 MHz, CDCl₃): δ = -36.3. IR ν (cm⁻¹): 2966, 2909, 1597. mp: 118-119 °C. HRMS: Mass calculated for C₁₉H₂₃BrFNNaO₂S: 450.0509, found: 450.0513.

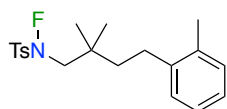
N-Fluoro-N-(4-(4-methoxyphenyl)-2,2-dimethylbutyl)-4-methylbenzenesulfonamide (16g)



16g was obtained as a white solid (64%) by applying GP1. ¹H NMR (400 MHz, CDCl₃): δ = 7.82 (d, J = 8.3 Hz, 2H), 7.43-7.39 (m, 2H), 7.08 (d, J = 8.6 Hz, 2H), 6.82 (d, J = 8.6 Hz, 2H), 3.78 (s, 3H), 3.08 (d, J = 44.4 Hz, 2H), 2.54-2.46 (m, 5H), 1.65-1.57 (m, 2H), 1.03 (s, 6H). ¹³C NMR (100 MHz, CDCl₃): δ = 157.9, 146.3, 134.8, 130.1, 130.0,

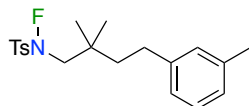
129.7, 129.3, 114.0, 63.0 (d, $J = 10.6$ Hz), 55.4, 42.7, 34.6, 29.5, 25.8, 21.9. $^{19}\text{F}\{^1\text{H}\}$ NMR (375 MHz, CDCl_3): $\delta = -36.4$. IR ν (cm^{-1}): 3057, 2968, 2945, 2837, 1611, 1596, 1511. mp: 75-76 °C. HRMS: Mass calculated for $\text{C}_{20}\text{H}_{26}\text{FNNaO}_3\text{S}$: 402.1510, found: 402.1510.

N-(2,2-Dimethyl-4-(*o*-tolyl)butyl)-N-fluoro-4-methylbenzenesulfonamide (16h)



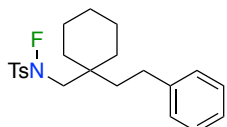
16h was obtained as a white solid (70%) by applying GP1. ^1H NMR (400 MHz, CDCl_3): $\delta = 7.83$ (d, $J = 8.2$ Hz, 2H), 7.43-7.39 (m, 2H), 7.15-7.08 (m, 4H), 3.11 (d, $J = 44.3$ Hz, 2H), 2.59-2.52 (m, 2H), 2.49 (s, 3H), 2.30 (s, 3H), 1.60-1.53 (m, 2H), 1.07 (s, 6H). ^{13}C NMR (125 MHz, CDCl_3): $\delta = 146.3$, 140.8, 135.8, 130.4, 130.1, 130.0, 129.6, 129.0, 126.2, 126.1, 62.9 (d, $J = 10.5$ Hz), 41.2, 34.7, 27.7, 25.7, 21.9, 19.3. $^{19}\text{F}\{^1\text{H}\}$ NMR (470 MHz, CDCl_3): $\delta = -36.59$. IR ν (cm^{-1}): 3068, 3018, 2968, 2926, 1595. mp: 58-60 °C. HRMS: Mass calculated for $\text{C}_{20}\text{H}_{26}\text{FNNaO}_2\text{S}$: 386.1560, found: 386.1579.

N-(2,2-Dimethyl-4-(*m*-tolyl)butyl)-N-fluoro-4-methylbenzenesulfonamide (16i)



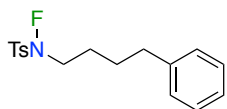
16i was obtained as a white solid (65%) by applying GP1. ^1H NMR (400 MHz, CDCl_3): $\delta = 7.85$ -7.81 (m, 2H), 7.44-7.40 (m, 2H), 7.17 (t, $J = 7.7$ Hz, 1H), 7.02-6.96 (m, 3H), 3.09 (d, $J = 44.4$ Hz, 2H), 2.57-2.50 (m, 2H), 2.49 (s, 3H), 2.33 (s, 3H), 1.68-1.61 (m, 2H), 1.05 (s, 6H). ^{13}C NMR (125 MHz, CDCl_3): $\delta = 146.2$, 142.7, 138.1, 130.1, 129.9, 129.6, 129.3, 128.4, 126.6, 125.5, 62.9 (d, $J = 10.5$ Hz), 42.5, 34.7, 30.4, 25.8, 21.9, 21.5. $^{19}\text{F}\{^1\text{H}\}$ NMR (375 MHz, CDCl_3): $\delta = -36.43$. IR ν (cm^{-1}): 3012, 2966, 2945, 2865, 1596. mp: 58-59 °C. HRMS: Mass calculated for $\text{C}_{20}\text{H}_{26}\text{FNNaO}_2\text{S}$: 386.1560, found: 386.1561.

N-Fluoro-4-methyl-N-((1-phenethylcyclohexyl)methyl)benzenesulfonamide (16j)



16j was obtained as a white solid (55%) by applying GP1. ^1H NMR (400 MHz, CDCl_3): $\delta = 7.85$ (d, $J = 8.3$ Hz, 2H), 7.44-7.40 (m, 2H), 7.30-7.24 (m, 2H), 7.21-7.14 (m, 3H), 3.23 (d, $J = 44.9$ Hz, 2H), 2.54-2.47 (m, 5H), 1.79-1.71 (m, 2H), 1.53-1.33 (m, 10H). ^{13}C NMR (100 MHz, CDCl_3): $\delta = 146.3$, 143.1, 130.1, 130.0, 128.6, 128.5, 125.8, 59.5 (d, $J = 11.0$ Hz), 38.3, 36.8, 34.2, 29.4, 26.1, 21.9, 21.4. $^{19}\text{F}\{^1\text{H}\}$ NMR (375 MHz, CDCl_3): $\delta = -36.3$. IR ν (cm^{-1}): 2931, 2850, 1596. mp: 79-80 °C. HRMS: Mass calculated for $\text{C}_{22}\text{H}_{28}\text{FNNaO}_2\text{S}$: 412.1717, found: 412.1730.

N-Fluoro-4-methyl-N-(4-phenylbutyl)benzenesulfonamide (16k)

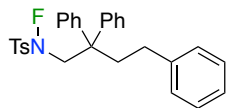


16k was obtained as a white solid (59%) by applying GP1. ^1H NMR (400 MHz, CDCl_3): $\delta = 7.81$ (d, $J = 8.3$ Hz, 2H), 7.40 (d, $J = 8.1$ Hz, 2H), 7.30-7.25 (m, 2H), 7.21-7.14 (m, 3H), 3.30-3.14 (m, 2H), 2.67-2.61 (m, 2H), 2.48 (s, 3H), 1.79-1.71 (m, 4H). ^{13}C NMR (100 MHz, CDCl_3): $\delta = 146.3$, 141.9, 130.1, 130.1, 129.1, 128.5, 126.0, 53.6 (d, 12.4 Hz), 35.4, 28.4, 26.0, 21.9. $^{19}\text{F}\{^1\text{H}\}$ NMR

Chapter III. Copper-Catalyzed N-F Bond Activation for Uniform
Intramolecular C-H Amination Yielding Pyrrolidines and Piperidines

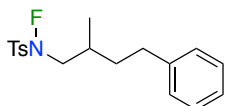
(375 MHz, CDCl₃): δ = -49.8. IR ν (cm⁻¹): 3027, 2917, 2862, 1593. mp: 67-69 °C. HRMS: Mass calculated for C₁₇H₂₀FNNaO₂S: 344.1091, found: 344.1088.

N-Fluoro-4-methyl-N-(2,2,4-triphenylbutyl)benzenesulfonamide (16l)



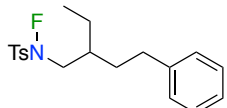
16l was obtained as a white solid (48%) by applying GP1. ¹H NMR (400 MHz, CDCl₃): δ = 7.87-7.83 (m, 2H), 7.51-7.46 (m, 2H), 7.40-7.35 (m, 5H), 7.35-7.30 (m, 3H), 7.29-7.23 (m, 5H), 7.22-7.17 (m, 2H), 4.25 (d, J = 40.3 Hz, 2H), 2.76-2.68 (m, 2H), 2.58 (s, 3H), 2.44-2.36 (m, 2H). ¹³C NMR (100 MHz, CDCl₃): δ = 146.4, 145.8, 142.5, 130.2, 129.9, 128.6, 128.3, 128.0, 126.6, 126.0, 59.6 (d, J = 10.2 Hz), 49.7, 39.7, 30.6, 22.0. ¹⁹F{¹H} NMR (375 MHz, CDCl₃): δ = -36.99. IR ν (cm⁻¹): 3057, 3027, 2925, 1595. mp: 141-142 °C. HRMS: Mass calculated for C₂₉H₂₈FNNaO₂S: 496.1717, found: 496.1721.

N-fluoro-4-methyl-N-(2-methyl-4-phenylbutyl)benzenesulfonamide (16m)



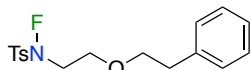
16m was obtained as a yellow oil (62%) by applying GP1. ¹H NMR (400 MHz, CDCl₃): δ = 7.81 (d, J = 8.4 Hz, 2H), 7.40 (d, J = 8.2 Hz, 2H), 7.30-7.24 (m, 2H), 7.21-7.13 (m, 3H), 3.10 (dt, J = 42.1 Hz, 6.4, 2H), 2.73-2.64 (m, 1H), 2.61-2.53 (m, 1H), 2.49 (s, 3H), 1.99-1.89 (m, 1H), 1.86-1.75 (m, 1H), 1.58-1.46 (m, 1H), 1.07 (d, J = 6.7 Hz, 3H). ¹³C NMR (100 MHz, CDCl₃): δ = 146.3, 142.1, 130.1, 128.5, 128.4, 126.0, 59.4 (d, J = 12.0 Hz), 36.2, 33.1, 30.8, 21.9, 17.8. ¹⁹F{¹H} NMR (375 MHz, CDCl₃): δ = -45.87. IR ν (cm⁻¹): 2965, 2926 1596. HRMS: Mass calculated for C₁₈H₂₂FNNaO₂S: 358.1247, found: 358.1242.

N-(2-Ethyl-4-phenylbutyl)-N-fluoro-4-methylbenzenesulfonamide (16n)



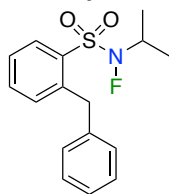
16n was obtained as a colorless oil (68%) by applying GP1. ¹H NMR (400 MHz, CDCl₃): δ = 7.85-7.80 (m, 2H), 7.44-7.39 (m, 2H), 7.30-7.24 (m, 2H), 7.20-7.12 (m, 3H), 3.17 (ddd, J = 42.4, 6.2, 1.3 Hz, 2H), 2.60 (t, J = 8.2 Hz, 2H), 2.49 (s, 3H), 1.84-1.65 (m, 3H), 1.55-1.46 (m, 2H), 0.89 (t, J = 7.5 Hz, 3H). ¹³C NMR (100 MHz, CDCl₃): δ = 146.3, 142.3, 130.1, 130.0, 129.3, 128.5, 128.4, 125.9, 56.6 (d, J = 11.9 Hz), 36.7, 33.2, 32.8, 24.2, 21.9, 10.6. ¹⁹F{¹H} NMR (375 MHz, CDCl₃): δ = -45.99. IR ν (cm⁻¹): 3027, 2962, 2927, 2863, 1596. HRMS: Mass calculated for C₁₉H₂₄FNNaO₂S: 372.1404, found: 372.1406.

N-Fluoro-4-methyl-N-(2-phenethoxyethyl)benzenesulfonamide (16o)



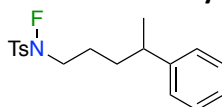
16o was obtained as a colorless oil (53%) by applying GP1. ¹H NMR (400 MHz, CDCl₃): δ = 7.85-7.81 (m, 2H), 7.42-7.38 (m, 2H), 7.30-7.26 (m, 1H), 7.21 (td, J = 5.4, 5.0, 2.8 Hz, 3H), 3.74 (t, J = 5.9 Hz, 2H), 3.69 (t, J = 7.1 Hz, 2H), 3.41 (dt, J = 40.0, 5.9 Hz, 2H), 2.88 (t, J = 7.1 Hz, 2H), 2.48 (s, 3H). ¹³C NMR (100 MHz, CDCl₃): δ = 146.5, 138.7, 130.2, 130.1, 129.0, 128.5, 126.4, 72.5, 66.6, 53.6 (d, J = 11.9 Hz), 36.3, 21.9. ¹⁹F{¹H} NMR (375 MHz, CDCl₃): δ = -46.75. IR ν (cm⁻¹): 30028, 2924, 1596. HRMS: Mass calculated for C₁₇H₂₀FNNaO₃S: 360.1040, found: 360.1036.

2-benzyl-N-fluoro-N-isopropylbenzenesulfonamide (16p)



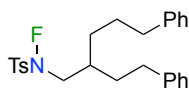
16p was obtained as a yellow oil (65%) by applying GP1. ¹H NMR (400 MHz, CDCl₃): δ = 8.20 (dd, J = 8.0, 1.5 Hz, 1H), 7.56 (td, J = 7.6, 1.5 Hz, 1H), 7.42 (td, J = 7.7, 1.3 Hz, 1H), 7.39-7.33 (m, 2H), 7.32-7.26 (m, 1H), 7.26-7.22 (m, 3H), 4.51 (s, 2H), 4.40 (dp, J = 37.6, 6.6 Hz, 1H), 1.43 (dd, J = 6.6, 1.0 Hz, 6H). ¹³C NMR (100 MHz, CDCl₃): δ = 142.6, 139.7, 134.6, 134.1, 132.5, 131.8, 129.5, 128.6, 126.6, 126.5, 54.8 (d, J = 13.5 Hz), 38.0, 19.4, 19.3. ¹⁹F{¹H} NMR (375 MHz, CDCl₃): δ = -78.46. IR ν (cm⁻¹): 2983, 2926. HRMS: Mass calculated for C₁₆H₁₈FNNaO₂S: 330.0934, found: 330.0929.

N-fluoro-4-methyl-N-(4-phenylpentyl)benzenesulfonamide (16q)



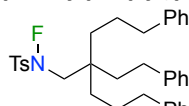
16q was obtained as a colorless oil (60%) by applying GP1. ¹H NMR (400 MHz, CDCl₃): δ = 7.82-7.76 (m, 2H), 7.41-7.37 (m, 2H), 7.31-7.25 (m, 2H), 7.21-7.12 (m, 3H), 3.14 (dt, J = 40.8, 5.9 Hz, 2H), 2.73-2.66 (m, 1H), 2.48 (s, 3H), 1.76-1.53 (m, 4H), 1.25 (d, J = 6.9 Hz, 3H). ¹³C NMR (100 MHz, CDCl₃): δ = 146.9, 146.3, 130.1, 130.0, 129.0, 128.6, 127.0, 126.2, 53.9 (d, J = 12.4 Hz), 39.7, 35.2, 24.7, 22.4, 21.9. ¹⁹F{¹H} NMR (375 MHz, CDCl₃): δ = -49.92. IR ν (cm⁻¹): 3027, 2959, 2926, 2872, 1596. HRMS: Mass calculated for C₁₈H₂₂FNNaO₂S: 358.1247, found: 358.1246.

N-fluoro-4-methyl-N-(2-phenethyl-5-phenylpentyl)benzenesulfonamide (20)



20 was obtained as a colorless oil (56%) by applying GP1. ¹H NMR (400 MHz, CDCl₃): δ = 7.85-7.79 (m, 2H), 7.44-7.37 (m, 2H), 7.31-7.23 (m, 4H), 7.21-7.11 (m, 6H), 3.17 (dd, J = 42.3, 6.3 Hz, 2H), 2.58 (q, J = 7.8, 7.4 Hz, 4H), 2.49 (s, 3H), 1.86 (p, J = 6.3 Hz, 1H), 1.77-1.67 (m, 2H), 1.67-1.57 (m, 2H), 1.57-1.44 (m, 2H). ¹³C NMR (100 MHz, CDCl₃): δ = 146.3, 142.4, 142.2, 130.1, 130.0, 129.3, 128.5, 128.5, 126.0, 125.9, 56.9 (d, J = 12.0 Hz), 36.1, 35.3, 33.6, 32.8, 31.3, 28.2. ¹⁹F{¹H} NMR (375 MHz, CDCl₃): δ = -45.65. IR ν (cm⁻¹): 3026, 2929, 2859, 1597. Mass calculated for C₂₆H₃₀FNNaO₂S: 462.1873, found: 462.1875.

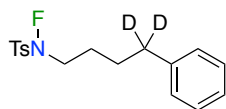
N-fluoro-4-methyl-N-(2-phenethyl-5-phenyl-2-(3-phenylpropyl)pentyl)benzenesulfonamide (22)



22 was obtained as a colorless oil (47%) by applying GP1. ¹H NMR (400 MHz, CDCl₃): δ = 7.81 (d, J = 8.3 Hz, 2H), 7.40 (d, J = 8.2 Hz, 2H), 7.32-7.23 (m, 7H), 7.23-7.13 (m, 6H), 7.13-7.08 (m, 2H), 3.14 (d, J = 44.4 Hz, 2H), 2.57 (t, J = 7.4 Hz, 4H), 2.49 (s, 3H), 2.45-2.32 (m, 2H), 1.61-1.47 (m, 6H), 1.42-1.35 (m, 4H). ¹³C NMR (100 MHz, CDCl₃): δ = 146.3, 142.7, 142.4, 130.1, 129.9, 129.8, 129.7, 128.6, 128.5, 128.5, 128.4, 127.9, 127.8, 126.0, 125.9, 57.8 (d, J = 10.7 Hz), 39.4, 37.5, 36.6, 34.4, 29.4, 24.8, 21.9. ¹⁹F{¹H} NMR (375 MHz, CDCl₃): δ = -37.76. IR ν (cm⁻¹): 3025, 2936, 2862, 1598. HRMS: Mass calculated for C₃₅H₄₀FNNaO₂S: 580.2656, found: 580.2654.

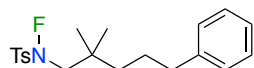
Chapter III. Copper-Catalyzed N-F Bond Activation for Uniform
Intramolecular C-H Amination Yielding Pyrrolidines and Piperidines

N-fluoro-4-methyl-N-(4-phenylbutyl-4,4-d₂)benzenesulfonamide (16k-d₂)



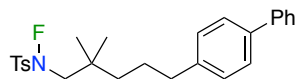
16k-d₂ was obtained as a red oil (50%) by applying GP1. ¹H NMR (400 MHz, CDCl₃): δ = 7.85-7.80 (m, 2H), 7.44-7.39 (m, 2H), 7.32-7.26 (m, 2H), 7.22-7.13 (m, 3H), 3.31-3.16 (m, 2H), 2.49 (s, 3H), 1.80-1.71 (m, 4H). ¹³C NMR (100 MHz, CDCl₃): δ = 146.3, 141.7, 130.0, 130.0, 128.4, 126.9, 53.7 (d, J = 12.4 Hz), 35.2-34.1 (m), 28.2, 25.9, 21.8. ¹⁹F{¹H} NMR (375 MHz, CDCl₃): δ = -49.77. IR ν (cm⁻¹): 2961, 2951, 2939, 2910, 2873, 1593. mp: 68-69 °C. HRMS: Mass calculated for C₁₇H₁₈D₂FNNaO₂S: 346.1222, found: 346.1218.

N-(2,2-dimethyl-5-phenylpentyl)-N-fluoro-4-methylbenzenesulfonamide (18a)



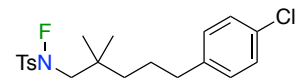
18a was obtained as a yellow oil (61%) by applying GP1. ¹H NMR (400 MHz, CDCl₃): δ = 7.81 (d, J = 8.3 Hz, 2H), 7.42-7.38 (m, 2H), 7.30-7.26 (m, 2H), 7.21-7.14 (m, 3H), 3.01 (d, J = 44.5 Hz, 2H), 2.57 (t, J = 7.7 Hz, 2H), 2.48 (s, 3H), 1.61-1.53 (m, 2H), 1.42-1.35 (m, 2H), 0.95 (s, 6H). ¹³C NMR (100 MHz, CDCl₃): δ = 146.2, 142.6, 130.1, 130.0, 128.5, 128.4, 125.9, 63.0 (d, J = 10.7 Hz), 40.0, 36.7, 34.5, 25.9, 21.9. ¹⁹F{¹H} NMR (375 MHz, CDCl₃): δ = -36.53. IR ν (cm⁻¹): 2931, 2858, 1597. HRMS: Mass calculated for C₂₀H₂₆FNNaO₂S: 386.1560, found: 386.1563.

N-(5-([1,1'-biphenyl]-4-yl)-2,2-dimethylpentyl)-N-fluoro-4-methylbenzenesulfonamide (18b)



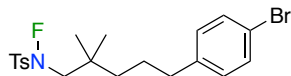
18b was obtained as a yellow oil (88%) by applying GP1. ¹H NMR (400 MHz, CDCl₃): δ = 7.88-7.83 (m, 2H), 7.66-7.62 (m, 2H), 7.59-7.55 (m, 2H), 7.50-7.45 (m, 2H), 7.43-7.40 (m, 2H), 7.39-7.34 (m, 1H), 7.32-7.28 (m, 2H), 3.09 (d, J = 44.4 Hz, 2H), 2.67 (t, J = 7.7 Hz, 2H), 2.49 (s, 3H), 1.73-1.61 (m, 2H), 1.51-1.43 (m, 2H), 1.02 (s, 6H). ¹³C NMR (100 MHz, CDCl₃): δ = 146.2, 141.6, 141.2, 138.8, 130.0, 129.9, 129.6, 128.9, 128.8, 127.1, 127.1, 127.0, 63.0 (d, J = 10.5 Hz), 39.9, 36.3, 34.4, 29.8, 25.8, 25.7, 21.8. ¹⁹F{¹H} NMR (375 MHz, CDCl₃): δ = -36.34. IR ν (cm⁻¹): 3026, 2960, 2946, 2910, 2874, 2848, 1596. mp: 87-88 °C. HRMS: Mass calculated for C₂₆H₃₀FNNaO₂S: 462.1873, found: 462.1872.

N-(5-(4-chlorophenyl)-2,2-dimethylpentyl)-N-fluoro-4-methylbenzenesulfonamide (18c)



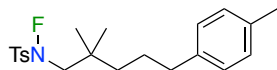
18c was obtained as a slightly yellow oil (85%) by applying GP1. ¹H NMR (400 MHz, CDCl₃): δ = 7.81 (d, J = 8.4 Hz, 2H), 7.44-7.39 (m, 2H), 7.28-7.23 (m, 2H), 7.11 (d, J = 8.4 Hz, 2H), 3.02 (d, J = 44.4 Hz, 2H), 2.56 (t, J = 7.6 Hz, 2H), 2.50 (s, 3H), 1.58-1.50 (m, 2H), 1.41-1.32 (m, 2H), 0.95 (s, 6H). ¹³C NMR (100 MHz, CDCl₃): δ = 146.3, 141.0, 131.6, 130.1, 129.9, 129.9, 129.7, 128.5, 62.9 (d, J = 10.6 Hz), 39.6, 36.0, 34.4, 25.8, 25.7, 21.9. ¹⁹F{¹H} NMR (375 MHz, CDCl₃): δ = -36.49. IR ν (cm⁻¹): 2962, 2938, 2866, 1597. HRMS: Mass calculated for C₂₀H₂₆ClFNO₂S: 398.1351, found: 398.1353.

N-(5-(4-bromophenyl)-2,2-dimethylpentyl)-N-fluoro-4-methylbenzenesulfonamide (18d)



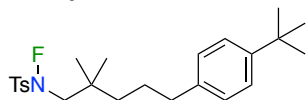
18d was obtained as a colorless oil (98%) by applying GP1. ¹H NMR (400 MHz, CDCl₃): δ = 7.81 (dd, J = 8.4, 2.7 Hz, 2H), 7.43-7.38 (m, 3H), 7.31-7.25 (m, 1H), 7.21-7.16 (m, 1H), 7.07-7.02 (m, 1H), 3.02 (dd, J = 44.4 Hz, 2H), 2.59 (t, J = 7.7 Hz, 1H), 2.54 (t, J = 7.6 Hz, 1H), 2.49 (s, 3H), 1.62-1.51 (m, 2H), 1.43-1.33 (m, 2H), 0.96 (s, 3H), 0.95 (s, 3H). ¹³C NMR (100 MHz, CDCl₃): δ = 146.2, 146.2, 142.5, 141.4, 131.4, 130.3, 130.1, 130.0, 129.9, 128.5, 128.4, 125.8, 119.5, 62.9 (d, J = 10.6 Hz), 39.9, 39.6, 36.7, 36.0, 34.4, 25.7, 25.7, 21.9. ¹⁹F{¹H} NMR (375 MHz, CDCl₃): δ = -36.05. IR ν (cm⁻¹): 2926, 2855, 1597. HRMS: Mass calculated for C₂₀H₂₅BrFNNaO₂S: 464.0666, found: 464.0661.

N-(2,2-dimethyl-5-(p-tolyl)pentyl)-N-fluoro-4-methylbenzenesulfonamide (18e)



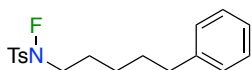
18e was obtained as a colorless oil (74%) by applying GP1. ¹H NMR (400 MHz, CDCl₃): δ = 7.81 (d, J = 8.3 Hz, 2H), 7.42-7.37 (m, 2H), 7.12-7.03 (m, 4H), 3.01 (d, J = 44.5 Hz, 2H), 2.53 (t, J = 7.7 Hz, 2H), 2.49 (s, 3H), 2.32 (s, 3H), 1.58-1.50 (m, 2H), 1.40-1.33 (m, 2H), 0.95 (s, 6H). ¹³C NMR (100 MHz, CDCl₃): δ = 146.2, 139.5, 135.3, 130.1, 130.0, 129.7, 129.1, 128.4, 63.1 (d, J = 10.5 Hz), 40.0, 36.3, 34.5, 26.0, 25.7, 21.9, 21.1. ¹⁹F{¹H} NMR (375 MHz, CDCl₃): δ = -36.52. IR ν (cm⁻¹): 2936, 2863, 1597, 1515. HRMS: Mass calculated for C₂₁H₂₈FNNaO₂S: 400.1717, found: 400.1719.

N-(5-(4-(tert-Butyl)phenyl)-2,2-dimethylpentyl)-N-fluoro-4-methylbenzenesulfonamide (18f)



18f was obtained as a yellow oil (29%) by applying GP1. ¹H NMR (300 MHz, CDCl₃): δ = 7.82 (d, J = 8.3 Hz, 2H), 7.40 (d, J = 8.0 Hz, 2H), 7.30 (d, J = 8.3 Hz, 2H), 7.11 (d, J = 8.3 Hz, 2H), 3.01 (d, J = 44.5 Hz, 2H), 2.58-2.51 (m, 2H), 2.49 (s, 3H), 1.63-1.49 (m, 2H), 1.43-1.35 (m, 2H), 1.31 (s, 9H), 0.95 (s, 6H). ¹³C NMR (75 MHz, CDCl₃): δ = 148.7, 146.2, 139.6, 130.1, 130.0, 129.7, 128.1, 125.3, 63.1 (d, J = 10.4 Hz), 40.2, 36.2, 34.5, 31.6, 25.9, 25.7, 21.9. ¹⁹F{¹H} NMR (375 MHz, CDCl₃): δ = -36.5. IR ν (cm⁻¹): 2961, 1596. HRMS: Mass calculated for C₂₄H₃₄FNNaO₂S: 442.2186, found: 442.2185.

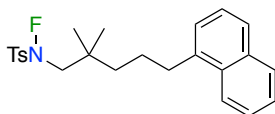
N-fluoro-4-methyl-N-(5-phenylpentyl)benzenesulfonamide (18g)



18g was obtained as a yellow oil (83%) by applying GP1. ¹H NMR (300 MHz, CDCl₃): δ = 7.82 (d, J = 8.3 Hz, 2H), 7.40 (d, J = 7.9 Hz, 2H), 7.31-7.24 (m, 2H), 7.21-7.13 (m, 3H), 3.20 (dt, J = 40.7, 7.0 Hz, 2H), 2.61 (t, J = 7.6 Hz, 2H), 2.48 (s, 3H), 1.80-1.58 (m, 4H), 1.51-1.39 (m, 2H). ¹³C NMR (100 MHz, CDCl₃): δ = 146.3, 142.4, 130.1, 130.1, 129.1, 128.5, 128.5, 125.9, 53.7 (d, J = 10.6 Hz), 35.8, 31.0, 26.3, 21.9. ¹⁹F{¹H} NMR (375 MHz, CDCl₃): δ = -49.54. IR ν (cm⁻¹): 2928, 2858, 1596. HRMS: Mass calculated for C₁₈H₂₂FNNaO₂S: 358.1247, found: 358.1241.

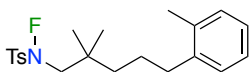
Chapter III. Copper-Catalyzed N-F Bond Activation for Uniform
Intramolecular C-H Amination Yielding Pyrrolidines and Piperidines

N-(2,2-dimethyl-5-(naphthalen-2-yl)pentyl)-N-fluoro-4-methylbenzenesulfonamide (18h)



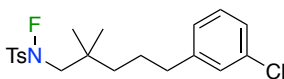
18h was obtained as a slightly orange oil (83%) by applying GP1. ¹H NMR (500 MHz, CDCl₃): δ = 7.82-7.75 (m, 5H), 7.60 (s, 1H), 7.47-7.39 (m, 2H), 7.39-7.36 (m, 2H), 7.32 (dd, J = 8.4, 1.8 Hz, 1H), 3.02 (d, J = 44.4 Hz, 2H), 2.75 (t, J = 7.6 Hz, 2H), 2.47 (s, 3H), 1.70-1.62 (m, 2H), 1.45-1.39 (m, 2H), 0.96 (s, 6H). ¹³C NMR (100 MHz, CDCl₃): δ = 146.2, 140.1, 133.8, 132.1, 130.1, 129.9, 129.7, 128.0, 127.7, 127.6, 127.5, 126.5, 126.0, 125.2, 62.9 (d, J = 10.6 Hz), 39.9, 36.8, 34.5, 25.7, 25.7, 21.9. ¹⁹F{¹H} NMR (375 MHz, CDCl₃): δ = -36.48. IR ν (cm⁻¹): 3051, 2960, 2938, 2865, 1597. HRMS: Mass calculated for C₂₄H₂₈FNNaO₂S: 436.1717, found: 436.1723.

N-(2,2-dimethyl-5-(o-tolyl)pentyl)-N-fluoro-4-methylbenzenesulfonamide (18i)



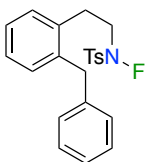
18i was obtained as a yellow oil (90%) by applying GP1. ¹H NMR (400 MHz, CDCl₃): δ = 7.86-7.82 (m, 2H), 7.45-7.40 (m, 2H), 7.19-7.11 (m, 4H), 3.05 (d, J = 44.4 Hz, 2H), 2.62-2.56 (m, 2H), 2.51 (s, 3H), 2.32 (s, 3H), 1.66-1.52 (m, 2H), 1.51-1.43 (m, 2H), 0.99 (s, 6H). ¹³C NMR (100 MHz, CDCl₃): δ = 146.2, 140.8, 135.9, 130.2, 130.0, 129.9, 129.5, 128.8, 126.0, 126.0, 63.0 (d, J = 10.4 Hz), 40.2, 34.4, 34.0, 25.7, 24.7, 21.8, 19.3. ¹⁹F{¹H} NMR (375 MHz, CDCl₃): δ = -36.54. IR ν (cm⁻¹): 2940, 2869, 1597. HRMS: Mass calculated for C₂₁H₂₈FNNaO₂S: 400.1717, found: 400.1721.

N-(5-(3-chlorophenyl)-2,2-dimethylpentyl)-N-fluoro-4-methylbenzenesulfonamide (18j)



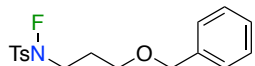
18j was obtained as a yellow oil (66%) by applying GP1. ¹H NMR (400 MHz, CDCl₃): δ = 7.83-7.79 (m, 2H), 7.43-7.38 (m, 2H), 7.23-7.13 (m, 3H), 7.05 (dt, J = 7.3, 1.6 Hz, 1H), 3.01 (d, J = 44.3 Hz, 2H), 2.55 (t, J = 7.7 Hz, 2H), 2.48 (s, 3H), 1.62-1.50 (m, 2H), 1.41-1.34 (m, 2H), 0.95 (s, 6H). ¹³C NMR (100 MHz, CDCl₃): δ = 146.3, 144.6, 134.1, 130.1, 129.9, 129.7, 129.6, 128.6, 126.7, 126.1, 63.0 (d, J = 10.6 Hz), 39.7, 36.3, 34.4, 25.7, 25.6, 21.9. ¹⁹F{¹H} NMR (375 MHz, CDCl₃): δ = -36.52. IR ν (cm⁻¹): 2940, 1597. HRMS: Mass calculated for C₂₀H₂₅ClFNNaO₂S: 420.1171, found: 420.1170.

N-(2-Benzylphenethyl)-N-fluoro-4-methylbenzenesulfonamide (18k)



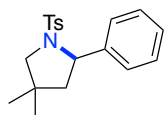
18k was obtained as a colorless oil (48%) by applying GP1. ¹H NMR (400 MHz, CDCl₃): δ = 7.73 (d, J = 8.2 Hz, 2H), 7.36 (d, J = 8.1 Hz, 2H), 7.29-7.23 (m, 1H), 7.23-7.13 (m, 6H), 7.08-7.03 (m, 2H), 3.99 (s, 2H), 3.28-3.12 (m, 2H), 3.06-2.99 (m, 2H), 2.48 (s, 3H). ¹³C NMR (100 MHz, CDCl₃): δ = 146.3, 140.5, 139.1, 136.0, 131.1, 130.4, 130.1, 128.8, 128.6, 127.3, 127.1, 126.2, 54.6 (d, J = 12.1 Hz), 39.2, 30.1, 21.9. ¹⁹F{¹H} NMR (375 MHz, CDCl₃): δ = -48.67. IR ν (cm⁻¹): 3026, 2922, 1596. HRMS: Mass calculated for C₂₂H₂₂FNNaO₂S: 406.1247, found: 406.1251.

N-(3-(Benzyloxy)propyl)-N-fluoro-4-methylbenzenesulfonamide (**18l**)



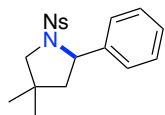
18l was obtained as a white solid (40%) by applying GP1. ¹H NMR (400 MHz, CDCl₃): δ = 7.83 (d, J = 8.3 Hz, 2H), 7.43-7.38 (m, 2H), 7.36-7.28 (m, 5H), 4.50 (s, 2H), 3.59 (t, J = 6.0 Hz, 2H), 3.36 (dt, J = 41.0, 6.7 Hz, 2H), 2.48 (s, 4H), 2.01 (p, J = 6.3 Hz, 2H). ¹³C NMR (100 MHz, CDCl₃): δ = 146.4, 138.3, 130.2, 130.1, 129.0, 128.6, 127.8, 127.8, 73.2, 66.8, 51.2 (d, J = 12.4 Hz), 27.0, 21.9. ¹⁹F{¹H} NMR (375 MHz, CDCl₃): δ = -49.47. IR ν (cm⁻¹): 2954, 2866, 1595. mp: 48-50 °C. HRMS: Mass calculated for C₁₇H₂₀FNNaO₃S: 360.1040, found: 360.1050.

4,4-Dimethyl-2-phenyl-1-tosylpyrrolidine (**17a**)



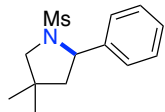
17a was obtained as a white solid (82%) by applying GP2. The NMR data match those reported in literature.⁷² ¹H NMR (400 MHz, CDCl₃): δ = 7.55-7.51 (m, 2H), 7.27-7.25 (m, 4H), 7.24-7.19 (m, 3H), 4.71 (dd, J = 9.4, 7.3 Hz, 1H), 3.45 (dd, J = 10.4, 1.5 Hz, 1H), 3.34 (d, J = 10.4 Hz, 1H), 2.40 (s, 3H), 2.02 (ddd, J = 12.8, 7.3, 1.5 Hz, 1H), 1.73 (dd, J = 12.8, 9.4 Hz, 1H), 1.05 (s, 3H), 0.77 (s, 3H). ¹³C NMR (100 MHz, CDCl₃): δ = 143.1, 143.0, 136.0, 129.4, 128.4, 127.5, 127.2, 126.6, 64.0, 62.0, 51.7, 38.3, 26.2, 25.8, 21.6.

4,4-Dimethyl-1-((4-nitrophenyl)sulfonyl)-2-phenylpyrrolidine (**17b**)



17b was obtained as a yellow solid (46%) by applying GP2. The NMR data match those reported in literature.⁷² ¹H NMR (300 MHz, CDCl₃): δ = 8.11 (d, J = 8.9 Hz, 2H), 7.57 (d, J = 8.8 Hz, 2H), 7.21-7.07 (m, 5H), 4.87 (dd, J = 9.8, 7.2 Hz, 1H), 3.66 (dd, J = 10.0, 1.7 Hz, 1H), 3.30 (d, J = 10.0 Hz, 1H), 2.15 (ddd, J = 12.9, 7.2, 1.7 Hz, 1H), 1.79 (dd, J = 12.9, 9.8 Hz, 1H), 1.13 (s, 3H), 1.03 (s, 3H). ¹³C NMR (75 MHz, CDCl₃): δ = 149.6, 145.9, 141.4, 128.5, 128.1, 127.8, 127.2, 123.8, 64.1, 61.9, 51.4, 38.6, 25.7, 25.7.

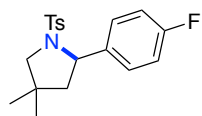
4,4-Dimethyl-1-(methylsulfonyl)-2-phenylpyrrolidine (**17c**)



17c was obtained as a white solid (83%) by applying GP2. The NMR data match those reported in literature.⁷⁵ ¹H NMR (300 MHz, CDCl₃): δ = 7.37-7.33 (m, 4H), 7.31-7.27 (m, 1H), 4.90 (dd, J = 9.8, 7.2 Hz, 1H), 3.67 (dd, J = 10.2, 1.7 Hz, 1H), 3.28 (d, J = 10.2 Hz, 1H), 2.52 (s, 3H), 2.20 (ddd, J = 12.7, 7.3, 1.7 Hz, 1H), 1.83 (dd, J = 12.8, 9.8 Hz, 1H), 1.19 (s, 3H), 1.15 (s, 3H). ¹³C NMR (125 MHz, CDCl₃): δ = 142.6, 128.8, 127.8, 127.0, 63.5, 61.6, 51.7, 40.8, 38.5, 25.8, 25.8.

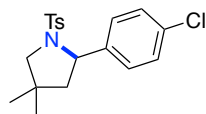
2-(4-Fluorophenyl)-4,4-dimethyl-1-tosylpyrrolidine (**17d**)

Chapter III. Copper-Catalyzed N-F Bond Activation for Uniform
Intramolecular C-H Amination Yielding Pyrrolidines and Piperidines



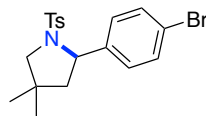
17d was obtained as a white solid (82%) by applying GP2. The NMR data match those reported in literature.⁷² ¹H NMR (300 MHz, CDCl₃): δ = 7.53 (d, J = 8.3 Hz, 2H), 7.27-7.19 (m, 4H), 6.98-6.89 (m, 2H), 4.67 (dd, J = 9.4, 7.2 Hz, 1H), 3.43 (dd, J = 10.4, 1.5 Hz, 1H), 3.33 (d, J = 10.4 Hz, 1H), 2.40 (s, 3H), 2.00 (ddd, J = 12.8, 7.2, 1.5 Hz, 1H), 1.68 (dd, J = 12.8, 9.4 Hz, 1H), 1.05 (s, 3H), 0.75 (s, 3H). ¹³C NMR (75 MHz, CDCl₃): δ = 162.1 (d, J = 245.1 Hz), 143.3, 138.8 (d, J = 3.2 Hz), 135.8, 129.5, 128.2 (d, J = 8.1 Hz), 127.5, 115.2 (d, J = 21.6 Hz), 63.3, 61.9, 51.6, 38.2, 26.2, 25.8, 21.6. ¹⁹F{¹H} NMR (375 MHz, CDCl₃): δ = -115.97.

2-(4-Chlorophenyl)-4,4-dimethyl-1-tosylpyrrolidine (17e)



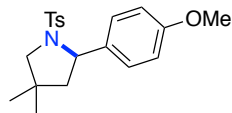
17e was obtained as a white solid (71%) by applying GP2. The NMR data match those reported in literature.⁷² ¹H NMR (300 MHz, CDCl₃): δ = 7.54 (d, J = 8.3 Hz, 2H), 7.25-7.16 (m, 6H), 4.65 (dd, J = 9.3, 7.2 Hz, 1H), 3.42 (dd, J = 10.4, 1.4 Hz, 1H), 3.33 (d, J = 10.4 Hz, 1H), 2.41 (s, 3H), 2.00 (ddd, J = 12.8, 7.2, 1.4 Hz, 1H), 1.66 (dd, J = 12.8, 9.3 Hz, 1H), 1.04 (s, 3H), 0.74 (s, 3H). ¹³C NMR (75 MHz, CDCl₃): δ = 143.4, 141.7, 135.6, 132.9, 129.5, 128.5, 128.0, 127.5, 63.3, 62.0, 51.5, 38.3, 26.2, 25.8, 21.6.

2-(4-Bromophenyl)-4,4-dimethyl-1-tosylpyrrolidine (17f)



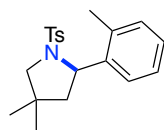
17f was obtained as a white solid (50%) by applying GP2. The NMR data match those reported in literature.⁷² ¹H NMR (300 MHz, CDCl₃): δ = 7.54 (d, J = 8.3 Hz, 2H), 7.39-7.34 (m, 2H), 7.25-7.20 (m, 2H), 7.14 (d, J = 8.5 Hz, 2H), 4.64 (dd, J = 9.3, 7.2 Hz, 1H), 3.42 (dd, J = 10.4, 1.4 Hz, 1H), 3.33 (d, J = 10.4 Hz, 1H), 2.41 (s, 3H), 2.00 (ddd, J = 12.7, 7.2, 1.4 Hz, 1H), 1.66 (dd, J = 12.8, 9.3 Hz, 1H), 1.04 (s, 3H), 0.74 (s, 3H). ¹³C NMR (75 MHz, CDCl₃): δ = 143.4, 142.2, 135.6, 131.5, 129.5, 128.4, 127.5, 121.0, 63.3, 62.0, 51.5, 38.3, 26.2, 25.8, 21.7.

2-(4-Methoxyphenyl)-4,4-dimethyl-1-tosylpyrrolidine (17g)



17g was obtained as a slightly yellow oil (99%) by applying GP2. The NMR data match those reported in literature.⁷² ¹H NMR (300 MHz, CDCl₃): δ = 7.51 (d, J = 8.3 Hz, 2H), 7.22-7.15 (m, 4H), 6.79 (d, J = 8.7 Hz, 2H), 4.66 (dd, J = 9.4, 7.2 Hz, 1H), 3.78 (s, 3H), 3.43 (dd, J = 10.3, 1.4 Hz, 1H), 3.32 (d, J = 10.4 Hz, 1H), 2.39 (s, 3H), 1.98 (ddd, J = 12.8, 7.2, 1.4 Hz, 1H), 1.71 (dd, J = 12.8, 9.5 Hz, 1H), 1.05 (s, 3H), 0.77 (s, 3H). ¹³C NMR (75 MHz, CDCl₃): δ = 158.8, 143.0, 136.1, 135.0, 129.4, 127.9, 127.5, 113.8, 63.4, 61.9, 55.4, 51.6, 38.1, 26.3, 25.8, 21.6.

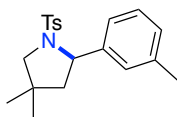
4,4-Dimethyl-2-(o-tolyl)-1-tosylpyrrolidine (17h)



17h was obtained as a white solid (99%) by applying GP2. The NMR data match those reported in literature.⁷⁵ ¹H NMR (300 MHz, CDCl₃): δ = 7.54 (d, J = 8.3 Hz, 2H), 7.32-7.27 (m, 1H), 7.23-7.18 (m, 2H), 7.12-7.05 (m, 3H), 4.99 (dd, J = 9.4, 7.4 Hz, 1H), 3.49 (dd, J = 10.4, 1.5 Hz, 1H),

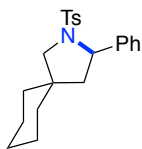
3.34 (d, $J = 10.4$ Hz, 1H), 2.40 (s, 3H), 2.35 (s, 3H), 2.11-2.02 (m, 1H), 1.61 (dd, $J = 12.7, 9.4$ Hz, 1H), 1.06 (s, 3H), 0.80 (s, 3H). ¹³C NMR (75 MHz, CDCl₃): $\delta = 143.1, 141.2, 136.1, 134.2, 130.3, 129.4, 127.5, 126.8, 126.5, 126.3, 61.8, 60.6, 50.0, 38.4, 26.2, 25.9, 21.6, 19.4$.

4,4-Dimethyl-2-(*m*-tolyl)-1-tosylpyrrolidine (17i)



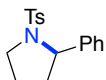
17i was obtained as a white solid (88%) by applying GP2. The NMR data match those reported in literature.⁷⁵ ¹H NMR (400 MHz, CDCl₃): $\delta = 7.54-7.48$ (m, 2H), 7.21-7.18 (m, 2H), 7.14 (t, $J = 7.5$ Hz, 1H), 7.07-7.04 (m, 1H), 7.02-6.96 (m, 2H), 4.69 (dd, $J = 9.5, 7.2$ Hz, 1H), 3.47 (dd, $J = 10.3, 1.5$ Hz, 1H), 3.33 (dd, $J = 10.3, 0.8$ Hz, 1H), 2.39 (s, 3H), 2.26 (d, $J = 0.7$ Hz, 3H), 2.01 (ddd, $J = 12.8, 7.2, 1.5$ Hz, 1H), 1.71 (dd, $J = 12.8, 9.5$ Hz, 1H), 1.06 (s, 3H), 0.79 (s, 3H). ¹³C NMR (100 MHz, CDCl₃): $\delta = 143.0, 142.8, 137.9, 136.3, 129.3, 128.3, 128.0, 127.5, 127.3, 123.9, 63.9, 62.0, 51.7, 38.2, 26.2, 25.8, 21.6, 21.5$.

3-Phenyl-2-tosyl-2-azaspiro[4.5]decane (17j)



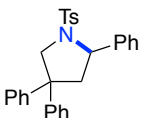
17j was obtained as a white solid (87%) by applying GP2. The NMR data match those reported in literature.⁷² ¹H NMR (300 MHz, CDCl₃): $\delta = 7.59$ (d, $J = 8.2$ Hz, 2H), 7.32-7.21 (m, 7H), 4.63 (dd, $J = 9.4, 7.3$ Hz, 1H), 3.63 (dd, $J = 10.7, 1.4$ Hz, 1H), 3.31 (d, $J = 10.7$ Hz, 1H), 2.42 (s, 3H), 2.12 (ddd, $J = 13.0, 7.2, 1.4$ Hz, 1H), 1.66 (dd, $J = 12.9, 9.4$ Hz, 1H), 1.48-1.24 (m, 8H), 1.06-0.94 (m, 2H). ¹³C NMR (125 MHz, CDCl₃): $\delta = 143.2, 143.1, 135.7, 129.4, 128.4, 127.5, 127.2, 126.5, 63.2, 59.4, 49.7, 42.1, 36.5, 34.0, 26.0, 23.9, 22.9, 21.6$.

2-Phenyl-1-tosylpyrrolidine (17k)



17k was obtained as a white solid (71%) by applying GP2. The NMR data match those reported in literature.⁷² ¹H NMR (300 MHz, CDCl₃): $\delta = 7.68$ (d, $J = 8.3$ Hz, 2H), 7.34-7.20 (m, 7H), 4.80 (dd, $J = 7.8, 3.7$ Hz, 1H), 3.68-3.58 (m, 1H), 3.49-3.38 (m, 1H), 2.43 (s, 3H), 2.07-1.93 (m, 1H), 1.91-1.76 (m, 2H), 1.74-1.59 (m, 1H). ¹³C NMR (75 MHz, CDCl₃): $\delta = 143.4, 143.2, 135.3, 129.7, 128.4, 127.6, 127.1, 126.3, 63.4, 49.5, 35.9, 24.1, 21.6$.

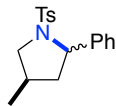
2,4,4-Triphenyl-1-tosylpyrrolidine (17l)



17l was obtained as a white solid (47%) by applying GP2. The NMR data match those reported in literature.⁷² ¹H NMR (500 MHz, CDCl₃): $\delta = 7.35-7.31$ (m, 2H), 7.28-7.22 (m, 6H), 7.20-7.10 (m, 9H), 7.02 (d, $J = 8.0$ Hz, 2H), 4.77 (dd, $J = 10.6, 1.8$ Hz, 1H), 4.69 (dd, $J = 9.9, 6.5$ Hz, 1H), 4.06 (d, $J = 10.6$ Hz, 1H), 3.08 (ddd, $J = 12.9, 6.6, 1.8$ Hz, 1H), 2.66 (dd, $J = 12.9, 9.9$ Hz, 1H), 2.34 (s, 3H). ¹³C NMR (125 MHz, CDCl₃): $\delta = 145.5, 144.3, 142.7, 141.3, 137.1, 129.2, 128.8, 128.7, 128.3, 127.5, 127.4, 127.0, 126.8, 126.8, 126.7, 126.6, 63.3, 59.0, 53.2, 49.2, 21.6$.

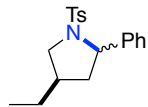
Chapter III. Copper-Catalyzed N-F Bond Activation for Uniform
Intramolecular C-H Amination Yielding Pyrrolidines and Piperidines

4-methyl-2-phenyl-1-tosylpyrrolidine (17m)



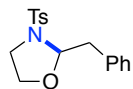
17m was obtained as a colorless oil (84%) in a 1:1 diastereomeric mixture by applying GP2. The NMR data match those reported in literature (trans diastereoisomer described).⁷² ¹H NMR (400 MHz, CDCl₃): δ = 7.62-7.58 (m, 2H), 7.32-7.27 (m, 6H), 7.25-7.19 (m, 1H), 4.64 (dd, J = 9.5, 7.2 Hz, 1H), 3.84 (ddd, J = 11.2, 7.3, 1.4 Hz, 1H), 3.09 (t, J = 10.8 Hz, 1H), 2.43 (s, 3H), 2.40-2.29 (m, 1H), 1.93-1.79 (m, 1H), 1.64-1.40 (m, 1H), 0.95 (d, J = 6.5 Hz, 3H). ¹³C NMR (100 MHz, CDCl₃): δ = 143.4, 143.3, 135.8, 129.6, 128.5, 127.7, 127.2, 126.5, 64.8, 56.8, 45.8, 33.5, 21.7, 16.6.

4-Ethyl-2-phenyl-1-tosylpyrrolidine (17n)



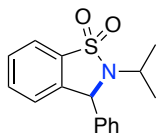
17n was obtained as a colorless oil (77%) in a 1.2:1 diastereomeric mixture by applying GP2. The NMR data match those reported in literature (trans diastereoisomer described).⁷² ¹H NMR (400 MHz, CDCl₃): δ = 7.61-7.57 (m, 2H), 7.31-7.21 (m, 6H), 4.62 (dd, J = 9.5, 7.2 Hz, 1H), 3.87 (ddd, J = 11.1, 7.3, 1.3 Hz, 1H), 3.11 (dd, J = 11.1, 10.4 Hz, 1H), 2.42 (s, 3H), 1.76-1.74 (m, 1H), 1.50-1.42 (m, 1H), 1.38-1.16 (m, 3H), 0.86-0.82 (m, 3H). ¹³C NMR (100 MHz, CDCl₃): δ = 143.5, 143.1, 135.8, 129.6, 128.5, 127.6, 127.2, 126.5, 64.6, 55.3, 43.8, 40.6, 25.5, 21.6, 12.6.

2-Benzyl-3-tosyloxazolidine (17o)



17o was obtained as a white solid (76%) by applying GP2. The NMR data match those reported in literature.²⁰⁷ ¹H NMR (400 MHz, CDCl₃): δ = 7.75-7.71 (m, 2H), 7.34-7.29 (m, 6H), 7.27-7.22 (m, 1H), 5.27 (dd, J = 6.8, 3.0 Hz, 1H), 3.74 (ddd, J = 8.1, 6.3, 4.4 Hz, 1H), 3.41 (ddd, J = 10.7, 6.4, 4.5 Hz, 1H), 3.30-3.22 (m, 1H), 3.21-3.14 (m, 2H), 3.01 (dd, J = 14.0, 6.8 Hz, 1H), 2.43 (s, 3H). ¹³C NMR (125 MHz, CDCl₃): δ = 144.3, 136.2, 134.4, 130.3, 130.1, 128.4, 127.9, 126.9, 91.8, 65.7, 46.9, 42.4, 21.7.

2-isopropyl-3-phenyl-2,3-dihydrobenzo[d]isothiazole 1,1-dioxide (17p)



17p was obtained as a colorless solid (79%) by applying GP2. ¹H NMR (400 MHz, CDCl₃): δ = 7.82-7.78 (m, 1H), 7.49-7.46 (m, 2H), 7.42-7.32 (m, 5H), 7.04-7.01 (m, 1H), 5.55 (s, 1H), 3.94 (hept, J = 6.8 Hz, 1H), 1.47 (d, J = 6.8 Hz, 3H), 1.13 (d, J = 6.7 Hz, 3H). ¹³C NMR (100 MHz, CDCl₃): δ = 139.8, 138.5, 132.9, 129.3, 129.2, 128.9, 127.8, 125.1, 120.9, 62.5, 46.8, 22.0, 20.5. IR ν (cm⁻¹): 2980, 2933, 2876 1661. mp: 131-132 °C. HRMS: Mass calculated for C₁₆H₁₇NNaO₂S: 310.0872, found: 310.0868.

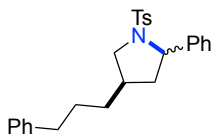
²⁰⁷ L. D. Elliott, J. W. Wrigglesworth, B. Cox, G. C. Lloyd-Jones, K. I. Brooker-Milburn, *Org. Lett.* **2011**, *13*, 728-731.

2-methyl-2-phenyl-1-tosylpyrrolidine (17q)



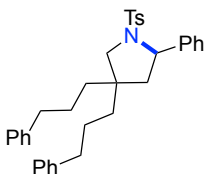
17q was obtained as a colorless oil (78%) by applying GP2. The NMR data match those reported in literature.⁷² ¹H NMR (400 MHz, CDCl₃): δ = 7.61-7.55 (m, 2H), 7.41-7.37 (m, 2H), 7.32-7.27 (m, 2H), 7.25-7.19 (m, 3H), 3.70 (ddd, J = 9.1, 7.1, 5.2 Hz, 1H), 3.55 (dt, J = 9.1, 7.4 Hz, 1H), 2.41 (s, 3H), 2.18-2.09 (m, 1H), 1.98 (ddd, J = 12.3, 8.9, 6.7 Hz, 1H), 1.89 (s, 3H), 1.87-1.79 (m, 2H). ¹³C NMR (100 MHz, CDCl₃): δ = 146.6, 142.7, 138.7, 129.4, 128.2, 127.2, 126.8, 126.0, 70.0, 49.9, 46.0, 26.6, 22.6, 21.6.

2-phenyl-4-(3-phenylpropyl)-1-tosylpyrrolidine (21)



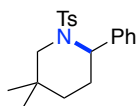
21 was obtained as a colorless oil (61%) in a 1:1 diastereomeric mixture by applying GP2. ¹H NMR (500 MHz, CDCl₃): δ = 7.69-7.65 (m, 2H), 7.62-7.57 (m, 2H), 7.31-7.20 (m, 18H), 7.20-7.14 (m, 2H), 7.12-7.06 (m, 4H), 4.84 (dd, J = 8.5, 2.2 Hz, 1H), 4.62 (dd, J = 9.6, 7.2 Hz, 1H), 3.86 (ddd, J = 11.1, 7.3, 1.3 Hz, 1H), 3.74 (dd, J = 9.4, 7.0 Hz, 1H), 3.10 (t, J = 10.8 Hz, 1H), 2.90 (t, J = 9.4 Hz, 1H), 2.56-2.48 (m, 4H), 2.43 (s, 3H), 2.41 (s, 3H), 2.41-2.35 (m, 1H), 2.27-2.19 (m, 1H), 1.89 (ddd, J=12.3, 6.0, 2.2, 1H), 1.80-1.71 (m, 1H), 1.62-1.43 (m, 7H), 1.37-1.19 (m, 5H). ¹³C NMR (125 MHz, CDCl₃): δ = 143.4, 143.4, 143.3, 143.0, 142.1, 135.7, 135.1, 129.7, 129.6, 128.5, 128.5, 128.5, 128.4, 128.4, 128.4, 127.7, 127.6, 127.3, 127.1, 126.4, 126.2, 126.0, 126.0, 64.5, 63.1, 55.4, 54.5, 44.0, 41.8, 38.8, 36.9, 36.0, 35.9, 32.3, 32.0, 30.0, 30.0, 21.7, 21.7. IR ν (cm⁻¹): 3026, 2923, 2856, 1599. HRMS: Mass calculated for C₂₆H₃₀NO₂S: 420.1992, found: 420.2005.

2-phenyl-4,4-bis(3-phenylpropyl)-1-tosylpyrrolidine (23)



23 was obtained as a colorless oil (44%) by applying GP2. ¹H NMR (500 MHz, CDCl₃): δ = 7.57-7.52 (m, 2H), 7.32-7.20 (m, 12H), 7.20-7.15 (m, 1H), 7.10-7.05 (m, 4H), 4.60 (dd, J = 9.4, 7.3 Hz, 1H), 3.48 (dd, J = 10.7, 1.3 Hz, 1H), 3.28 (d, J = 10.6 Hz, 1H), 2.47 (t, J=7.1, 2H), 2.40 (s, 3H), 2.39-2.26 (m, 2H), 2.07 (dd, J = 13.1, 7.4 Hz, 1H), 1.62 (dd, J = 13.0, 9.5 Hz, 1H), 1.42-1.28 (m, 6H), 1.04-0.98 (m, 2H). ¹³C NMR (125 MHz, CDCl₃): δ = 143.2, 143.1, 142.2, 142.1, 135.8, 129.5, 128.5, 128.5, 128.5, 128.4, 128.4, 127.6, 127.2, 126.5, 126.1, 126.0, 63.4, 59.6, 48.7, 44.3, 36.4, 36.2, 35.9, 33.7, 29.8, 26.7, 25.8, 21.6. IR ν (cm⁻¹): 3026, 2931, 2859, 1600. HRMS: Mass calculated for C₃₅H₄₀NO₂S: 538.2774, found: 538.2791.

5,5-dimethyl-2-phenyl-1-tosylpiperidine (19a)

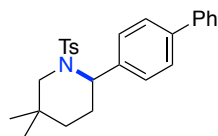


19a was obtained as a white solid (57%) by applying GP2. The NMR data match those reported in literature.⁷⁶ ¹H NMR (400 MHz, CDCl₃): δ = 7.65 (d, J = 8.3 Hz, 2H), 7.25-7.19 (m, 4H), 7.17-7.13 (m, 2H), 5.23 (t, J = 3.9 Hz, 1H), 3.41 (d, J = 13.5 Hz, 1H), 2.86 (d, J = 13.5 Hz, 1H), 2.40 (s, 3H), 2.10 (m, 2H), 1.26-1.21 (m, 2H), 0.80 (s, 3H), 0.79 (s, 3H). ¹³C NMR (125 MHz, CDCl₃): δ =

Chapter III. Copper-Catalyzed N-F Bond Activation for Uniform
Intramolecular C-H Amination Yielding Pyrrolidines and Piperidines

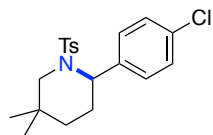
142.9, 139.1, 138.7, 129.5, 128.6, 127.2, 127.1, 126.8, 55.5, 52.7, 32.7, 30.5, 28.8, 25.9, 24.3, 21.6.

2-([1,1'-biphenyl]-4-yl)-5,5-dimethyl-1-tosylpiperidine (19b)



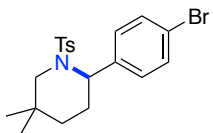
19b was obtained as a white solid (50%) by applying GP2. The NMR data match those reported in literature.⁷⁶ ¹H NMR (400 MHz, CDCl₃): δ = 7.69-7.65 (m, 2H), 7.58-7.54 (m, 2H), 7.49-7.40 (m, 4H), 7.37-7.31 (m, 1H), 7.25-7.20 (m, 4H), 5.31-5.22 (m, 1H), 3.44 (dt, J = 13.5, 1.4 Hz, 1H), 2.91 (d, J = 13.5 Hz, 1H), 2.40 (s, 3H), 2.17-2.07 (m, 2H), 1.36-1.20 (m, 2H), 0.82 (s, 6H). ¹³C NMR (100 MHz, CDCl₃): δ = 142.9, 140.8, 139.7, 138.7, 138.2, 129.6, 128.9, 127.6, 127.4, 127.2, 127.2, 127.1, 55.4, 52.7, 32.7, 30.5, 28.8, 25.9, 24.3, 21.6.

2-(4-chlorophenyl)-5,5-dimethyl-1-tosylpiperidine (19c)



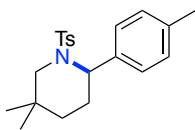
19c was obtained as a colorless oil (42%) by applying GP2. The NMR data match those reported in literature.⁷⁶ ¹H NMR (300 MHz, CDCl₃): δ = 7.65 (d, J = 8.3 Hz, 2H), 7.27-7.17 (m, 4H), 7.09 (dd, J = 8.8, 0.9 Hz, 2H), 5.20-5.14 (m, 1H), 3.39 (d, J = 13.5 Hz, 1H), 2.80 (d, J = 13.5 Hz, 1H), 2.41 (s, 3H), 2.12-2.00 (m, 2H), 1.25-1.14 (m, 2H), 0.79 (s, 3H), 0.77 (s, 3H). ¹³C NMR (75 MHz, CDCl₃): δ = 143.1, 138.5, 137.6, 132.8, 129.6, 128.7, 128.6, 127.1, 55.1, 52.6, 32.6, 30.4, 28.7, 25.8, 24.2, 21.6.

2-(4-bromophenyl)-5,5-dimethyl-1-tosylpiperidine (19d)



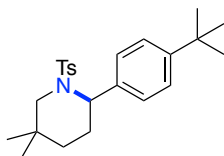
19d was obtained as a white solid (43%) by applying GP2. The NMR data match those reported in literature.⁷⁶ ¹H NMR (400 MHz, CDCl₃): δ = 7.67-7.62 (m, 2H), 7.37-7.34 (m, 1H), 7.25-7.10 (m, 4H), 7.05-7.01 (m, 1H), 5.25-5.11 (m, 1H), 3.44-3.36 (m, 1H), 2.88-2.77 (m, 1H), 2.41-2.39 (m, 3H), 2.15-1.99 (m, 2H), 1.24-1.17 (m, 2H), 0.81-0.75 (m, 6H). ¹³C NMR (100 MHz, CDCl₃): δ = 143.1, 138.5, 138.2, 131.7, 129.6, 129.5, 128.9, 128.6, 127.2, 127.1, 127.1, 120.9, 55.3, 52.7, 32.6, 30.5, 28.7, 25.8, 24.2, 21.6.

5,5-dimethyl-2-(p-tolyl)-1-tosylpiperidine (19e)



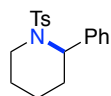
19e was obtained as a white solid (47%) by applying GP2. The NMR data match those reported in literature.⁷⁶ ¹H NMR (400 MHz, CDCl₃): δ = 7.68-7.62 (m, 2H), 7.25-7.19 (m, 2H), 7.07-7.00 (m, 4H), 5.18 (d, J = 3.3 Hz, 1H), 3.39 (dt, J = 13.5, 1.4 Hz, 1H), 2.85 (d, J = 13.4 Hz, 1H), 2.40 (s, 3H), 2.30 (s, 3H), 2.13-2.02 (m, 2H), 1.30-1.21 (m, 2H), 0.80 (s, 3H), 0.79 (s, 3H). ¹³C NMR (100 MHz, CDCl₃): δ = 142.8, 138.8, 136.4, 135.9, 129.5, 129.2, 127.2, 127.0, 55.3, 52.6, 32.7, 30.5, 29.8, 28.7, 25.8, 24.3, 21.6, 21.0.

2-(4-(tert-Butyl)phenyl)-5,5-dimethylpiperidine (19f)



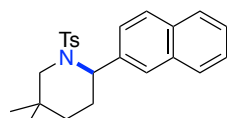
19f was obtained as a colorless oil (64%) by applying GP2. The NMR data match those reported in literature.⁷⁶ ¹H NMR (300 MHz, CDCl₃): δ = 7.61 (d, J = 8.3 Hz, 2H), 7.25-7.16 (m, 4H), 7.09-7.05 (m, 2H), 5.18 (t, J = 3.9 Hz, 1H), 3.46-3.36 (m, 1H), 2.88 (d, J = 13.4 Hz, 1H), 2.39 (s, 3H), 2.11-2.03 (m, 2H), 1.37-1.19 (m, 12H), 0.81 (s, 6H). ¹³C NMR (75 MHz, CDCl₃): δ = 149.6, 142.7, 138.7, 136.0, 129.4, 127.2, 126.8, 125.4, 55.3, 52.7, 34.5, 32.7, 31.5, 30.5, 28.8, 25.9, 24.3, 21.6.

2-phenyl-1-tosylpiperidine (19g)



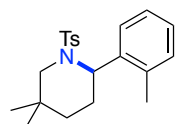
19g was obtained as a white solid (38%) by applying GP2. The NMR data match those reported in literature.⁷⁶ ¹H NMR (400 MHz, CDCl₃): δ = 7.78-7.73 (m, 2H), 7.37-7.27 (m, 7H), 5.27 (d, J = 5.1 Hz, 1H), 3.87-3.80 (m, 1H), 3.07-2.96 (m, 1H), 2.44 (s, 3H), 2.24-2.17 (m, 1H), 1.72-1.58 (m, 1H), 1.50-1.23 (m, 4H). ¹³C NMR (100 MHz, CDCl₃): δ = 143.1, 139.0, 138.9, 129.8, 128.7, 127.2, 127.1, 126.9, 55.4, 42.0, 27.4, 24.4, 21.7, 19.1.

5,5-dimethyl-2-(naphthalen-2-yl)-1-tosylpiperidine (19h)



19h was obtained as a colorless oil (56%) by applying GP2. ¹H NMR (300 MHz, CDCl₃): δ = 7.81-7.76 (m, 1H), 7.73 (d, J = 8.6 Hz, 1H), 7.68 (d, J = 8.3 Hz, 2H), 7.59-7.53 (m, 1H), 7.47-7.41 (m, 2H), 7.38 (s, 1H), 7.30 (dd, J = 8.6, 2.0 Hz, 1H), 7.21-7.17 (m, 2H), 5.41-5.35 (m, 1H), 3.50 (d, J = 13.3 Hz, 1H), 2.95 (d, J = 13.3 Hz, 1H), 2.37 (s, 3H), 2.30-2.14 (m, 2H), 1.32-1.24 (m, 2H), 0.89 (s, 3H), 0.80 (s, 3H). ¹³C NMR (75 MHz, CDCl₃): δ = 143.0, 138.7, 136.3, 133.3, 132.3, 129.6, 128.3, 128.0, 127.5, 127.1, 126.1, 126.1, 125.9, 125.1, 55.7, 52.9, 32.8, 30.5, 28.7, 26.0, 24.3, 21.6. IR ν (cm⁻¹): 2951, 1598. HRMS: Mass calculated for C₂₄H₂₇NNaO₂S: 416.1655, found: 416.1660.

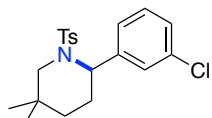
5,5-dimethyl-2-(o-tolyl)-1-tosylpiperidine (19i)



19i was obtained as a white solid (42%) by applying GP2. The NMR data match those reported in literature.⁷⁶ ¹H NMR (500 MHz, CDCl₃): δ = 7.29-7.25 (m, 2H), 7.08-7.05 (m, 1H), 7.04-6.99 (m, 3H), 6.89 (d, J = 7.8 Hz, 1H), 6.78 (td, J = 7.5, 1.6 Hz, 1H), 5.08 (t, J = 5.8 Hz, 1H), 3.37 (dd, J = 12.6, 1.1 Hz, 1H), 3.29 (d, J = 12.6 Hz, 1H), 2.35 (s, 3H), 2.33 (s, 3H), 2.07-1.99 (m, 1H), 1.72-1.65 (m, 1H), 1.43 (ddd, J = 13.8, 10.2, 3.7 Hz, 1H), 1.30-1.25 (m, 1H), 1.04 (s, 3H), 1.03 (s, 3H). ¹³C NMR (125 MHz, CDCl₃): δ = 142.5, 140.1, 137.4, 135.0, 130.8, 129.0, 127.2, 126.9, 126.7, 125.4, 55.2, 54.0, 33.4, 30.7, 27.9, 27.9, 25.8, 21.5, 19.7.

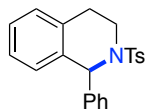
2-(3-chlorophenyl)-5,5-dimethyl-1-tosylpiperidine (19j)

Chapter III. Copper-Catalyzed N-F Bond Activation for Uniform
Intramolecular C-H Amination Yielding Pyrrolidines and Piperidines



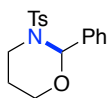
19j was obtained as a colorless oil (29%) by applying GP2. ¹H NMR (400 MHz, CDCl₃): δ = 7.65-7.62 (m, 2H), 7.25-7.22 (m, 2H), 7.17-7.13 (m, 2H), 7.08-7.04 (m, 1H), 6.95-6.92 (m, 1H), 5.17 (t, J = 4.8 Hz, 1H), 3.44 (dt, J = 13.4, 1.3, Hz 1H), 2.81 (d, J = 13.4 Hz, 1H), 2.41 (s, 3H), 2.15-2.04 (m, 2H), 1.26-1.19 (m, 2H), 0.84 (s, 3H), 0.82 (s, 3H). ¹³C NMR (100 MHz, CDCl₃): δ = 143.2, 141.4, 138.5, 134.6, 129.8, 129.7, 127.3, 127.1, 127.0, 125.3, 55.2, 52.8, 32.7, 30.4, 28.7, 26.0, 24.2, 21.6. IR ν (cm⁻¹): 2923, 1596. HRMS: Mass calculated for C₂₀H₂₄ClNNaO₂S: 400.1108, found: 400.1098.

1-Phenyl-2-tosyl-1,2,3,4-tetrahydroisoquinoline (19k)



19k was obtained as a white solid (70%) by applying GP2. The NMR data match those reported in literature.⁷⁶ ¹H NMR (500 MHz, CDCl₃): δ = 7.56-7.53 (m, 2H), 7.28-7.23 (m, 5H), 7.22-7.17 (m, 2H), 7.14-7.11 (m, 2H), 7.09-7.07 (m, 2H), 7.01-6.96 (m, 2H), 6.24 (s, 1H), 3.77 (dddd, J = 14.2, 6.7, 2.8, 1.3 Hz, 1H), 3.32 (ddd, J = 14.1, 11.1, 5.1 Hz, 1H), 2.68 (ddd, J = 17.3, 11.1, 6.5 Hz, 1H), 2.57 (ddd, J = 16.6, 5.1, 2.8 Hz, 1H), 2.32 (s, 3H), 0.90-0.81 (m, 1H). ¹³C NMR (125 MHz, CDCl₃): δ = 143.0, 141.6, 137.7, 134.1, 133.8, 129.3, 128.9, 128.7, 128.4, 128.3, 127.6, 127.1, 127.0, 126.1, 59.2, 39.1, 26.7, 21.4.

2-phenyl-3-tosyl-1,3-oxazinane (19o)



19o was obtained as a white solid (50%) by applying GP2. The NMR data match those reported in literature.⁷² ¹H NMR (500 MHz, CDCl₃): δ = 7.91-7.87 (m, 2H), 7.51-7.48 (m, 2H), 7.44-7.40 (m, 2H), 7.37-7.31 (m, 3H), 6.69 (s, 1H), 3.88-3.79 (m, 1H), 3.77-3.68 (m, 1H), 3.64-3.55 (m, 1H), 3.31 (ddd, J = 14.9, 13.1, 3.3 Hz, 1H), 2.46 (s, 3H), 1.49-1.36 (m, 1H), 1.05-0.99 (m, 1H). ¹³C NMR (125 MHz, CDCl₃): δ = 143.7, 136.2, 129.9, 129.1, 128.4, 127.7, 127.4, 127.2, 83.8, 60.0, 39.9, 23.2, 21.8.

X-Ray Analytical Data for Compound 24

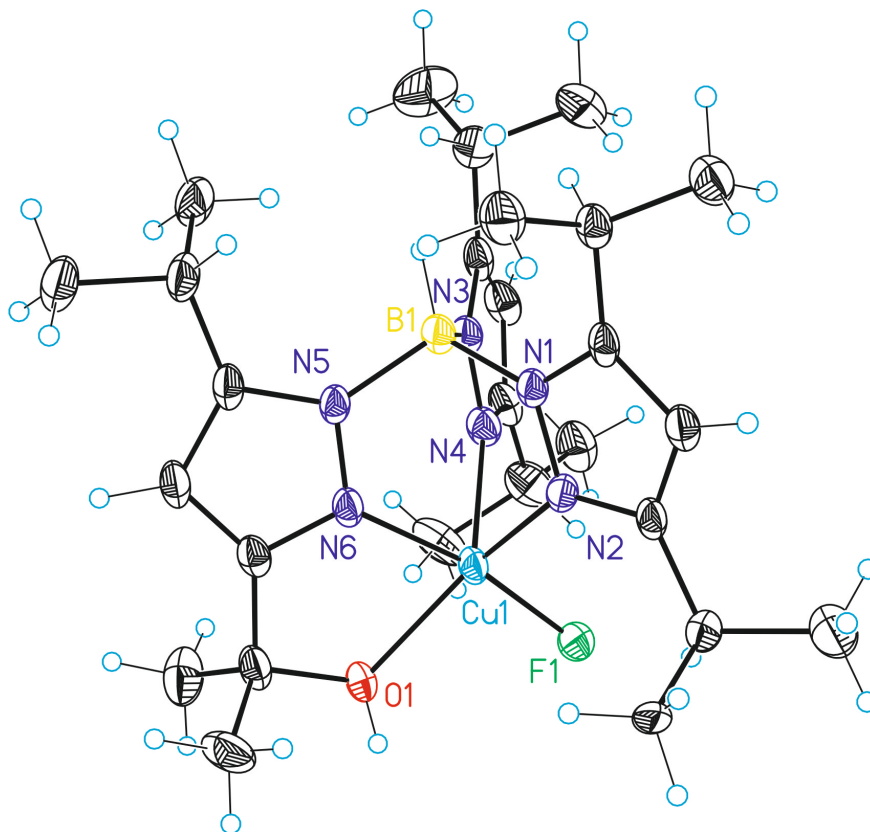


Table S-2. Crystal data and structure refinement for **24**.

Identification code	24	
Empirical formula	C ₃₄ H ₅₄ B Cu F N ₆ O	
Formula weight	656.18	
Temperature	100(2) K	
Wavelength	0.71073 Å	
Crystal system	Monoclinic	
Space group	P2(1)/n	
Unit cell dimensions	a = 11.5174(7)Å	α = 90°.
	b = 13.6246(8)Å	β = 92.828(2)°.

Chapter III. Copper-Catalyzed N-F Bond Activation for Uniform
Intramolecular C-H Amination Yielding Pyrrolidines and Piperidines

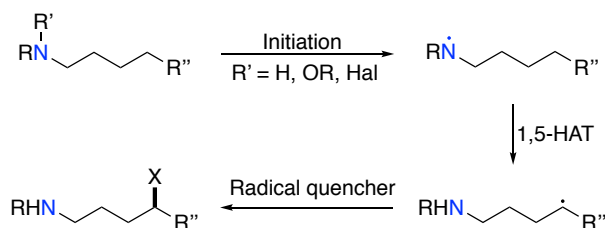
	$c = 22.9510(15)\text{\AA}$	$\gamma = 90^\circ$.
Volume	$3597.1(4)\text{\AA}^3$	
Z	4	
Density (calculated)	1.212 Mg/m^3	
Absorption coefficient	0.646 mm^{-1}	
F(000)	1404	
Crystal size	$0.02 \times 0.02 \times 0.02\text{ mm}^3$	
Theta range for data collection	$1.739\text{ to }27.570^\circ$.	
Index ranges	$-14 \leq h \leq 14, -16 \leq k \leq 17, -29 \leq l \leq 29$	
Reflections collected	34712	
Independent reflections	8292[R(int) = 0.0567]	
Completeness to theta = 27.570°	99.7%	
Absorption correction	Multi-scan	
Max. and min. transmission	0.987 and 0.93	
Refinement method	Full-matrix least-squares on F^2	
Data / restraints / parameters	8292/ 142/ 484	
Goodness-of-fit on F^2	1.030	
Final R indices [$I > 2\sigma(I)$]	$R1 = 0.0497, wR2 = 0.1042$	
R indices (all data)	$R1 = 0.0898, wR2 = 0.1180$	
Largest diff. peak and hole	$0.706\text{ and }-0.394\text{ e.\AA}^{-3}$	

Chapter IV. Iodine Catalysis for C(sp³)-H Fluorination with a Nucleophilic Fluorine Source

Chapter IV. Iodine Catalysis for C(sp³)-H Fluorination
with a Nucleophilic Fluorine Source

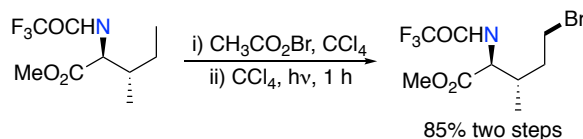
4.1. Introduction: Interrupted Hofmann-Löffler reaction

Through this PhD thesis, it has been highlighted the importance of fluorinated compounds and the relevance for triggering a catalytic *sp*³ C-H fluorination (sections 1.4. and 1.5.). In a formal sense, the methods described in previous sections via the generation of transient nitrogen-centered radicals can be considered as ‘interrupted Hofmann-Löffler’ approaches. Selective functionalization at the δ position then occurs through 1,5-HAT, giving rise to a carbon-centered radical intermediate. In the traditional Hofmann-Löffler reaction, halogenation would take place at this stage to give the corresponding alkyl halide that is intercepted by the pending nitrogen atom in a nucleophilic substitution event. If such intertwined scenario can be prevented, the alkyl halide or the alkyl radical could be employed for further diversification, including C–C or C–heteroatom bond-formations. Such a strategy is particularly attractive, as it represents a useful entry point for aliphatic C–H functionalization at remote sites.²⁰⁸



Scheme 4.1: General working mode for interrupted Hofmann-Löffler protocols.

In 1985, pioneering work of Nikishin demonstrated the potential of amidyl radicals for directed C-H functionalization, resulting in a δ -chlorination protocol employing stoichiometric amounts of CuCl₂ and sodium persulfate.²⁰⁹ Twenty years later, Corey employed this concept for selective bromination of α -aminoacids as a platform for further chemical diversification.²¹⁰ In this case, the activated N-bromoamide compound had to be used as the source of nitrogen radical (Scheme 4.2).



Scheme 4.2: Directed photochemical isoleucine derivative bromination.

Further applications on directed aliphatic C-H halogenation were explored by the synthetic organic community. In 2015 Yu (S.) reported a photochemical chlorination

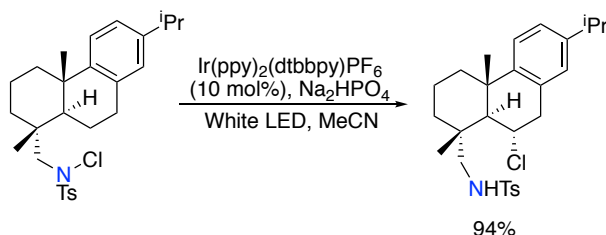
²⁰⁸ G. Kumar, S. Pradhan, I. Chatterjee, *Chem Asian J.* **2020**, *15*, 651-672.

²⁰⁹ G. I. Nikishin, E. I. Troyansky, *Tetrahedron Lett.* **1985**, *26*, 3743-3744.

²¹⁰ B. V. S. Reddy, L. R. Reddy, E. J. Corey, *Org. Lett.* **2006**, *8*, 2819-2821.

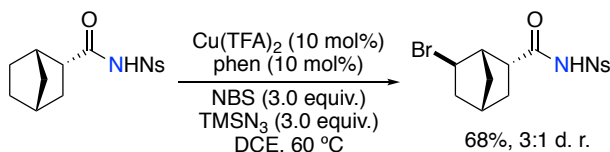
Chapter IV. Iodine Catalysis for C(sp³)-H Fluorination
with a Nucleophilic Fluorine Source

approach employing an iridium-based photoredox catalyst for activation of N-chlorosulfonamides (Scheme 4.3).^{65a}



Scheme 4.3: Iridium catalyzed δ -chlorination conditions for 1,5-chloroamine synthesis.

Among these contributions, Yu (Y.-Q.) reported a related transformation for C-H bromination of amides that did not require the preformation of active N-haloamine species.²¹¹ In this case, mixed BrN_3 species engages in situ N-bromination, which evolves following the Hofmann-Löffler mechanism. The copper catalyst employed for the reaction is involved at the final bromination step of the carbon-centered radical intermediate. With this protocol, the authors could effectively brominate protected amides and terminal amine derivatives as well.



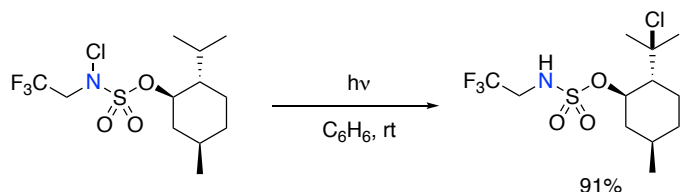
Scheme 4.4: Copper-catalyzed amides C-H bromination protocol.

In 2018, Zare²¹² and Roizen²¹³ reported the use of sulfamate esters as novel directing groups for C-H halogenation. Interestingly, sulfamate esters showed a complete selectivity for 1,6-HAT processes, which is in sharp contrast with what observed before for amidyl radical-based systems. Additionally, these functionalities showed lousy cyclization capacity avoiding the formation of the corresponding Hofmann-Löffler cyclized products. The introduction of such directing group opened new complementary C-H functionalization venues in the context of nitrogen-centered radical chemistry. In the case of Zare, the authors employed a rhodium-based catalytic system with sodium hypochlorite as oxidant to afford bromination at the γ position. On the other hand, Roizen achieved a photochemical transformation from N-chlorosulfamate esters to its corresponding γ -chlorinated products under blue light irradiation (Scheme 4.5).

²¹¹ T. Liu, M. C. Myers, J.-Q. Yu, *Angew. Chem. Int. Ed.* **2017**, *56*, 306-309.

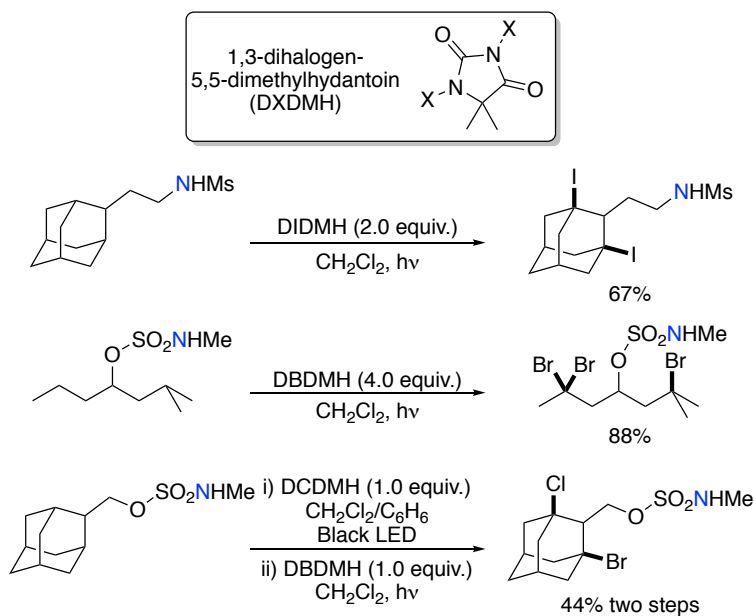
²¹² S. Sathyamoorthi, S. Banerjee, J. Du Bois, N. Z. Burns, R. N. Zare, *Chem. Sci.* **2018**, *9*, 100-104.

²¹³ M. A. Short, J. M. Blackburn, J. L. Roizen, *Angew. Chem. Int. Ed.* **2018**, *57*, 296-299.



Scheme 4.5: Roizen's protocol for photochemical C-H chlorination involving 1,6-HAT.

In 2018, our group also devised a directed aliphatic halogenation methodology at γ and δ positions with different electrophilic halogen sources.²¹⁴ Complementary 1,5- and 1,6-HAT selectivity could be controlled by an appropriate choice of the nitrogen directing group, with dihalogenated hydantoin derivatives as the optimal electrophilic halogen sources. Not only monohalogenation, but polyhalogenation could be effected by using simple sulfonamides as directing groups (Scheme 4.6, top). Even di- and tri-bromination could be achieved in simple linear substrates by employing sulfamate esters (Scheme 4.6, middle). Interestingly, sequential halogenation with different halogen sources could be performed in adamantyl derivatives to achieve mixed halogenated species (Scheme 4.6, bottom).

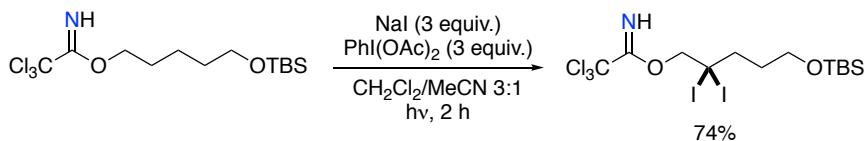


Scheme 4.6: Photochemical polyhalogenation of aliphatic C-H bonds.

²¹⁴ E. D. Castillo, M. D. Martínez, A. E. Bosnidou, T. Duhamel, C. Q. O'Broin, H. Zhang, E. C. Escudero-Adán, M. Martínez-Belmonte, K. Muñiz, *Chem. Eur. J.* **2018**, *24*, 17225-17229.

Chapter IV. Iodine Catalysis for C(sp³)-H Fluorination
with a Nucleophilic Fluorine Source

In 2018, Nagib employed a modification of their imidyl-radical strategy to interrupt the Hofmann-Löffler reaction at the iodination step.²¹⁵ Furthermore, the authors could promote iterative radical processes to formally di-iodinate β -methylene groups through 1,5-HAT from in situ generated imidyl radicals. Additionally, when a NaBr and Bu₄NBr mixture was employed instead of NaI, the corresponding dibrominated products were smoothly obtained.



Scheme 4.7: Nagib's protocol for β -halogenation directed by imidyl radical intermediates.

Within the general area of interrupted Hofmann-Löffler reaction, particularly interesting is the ability of triggering a directed sp^3 C-H fluorination. In this sense, the iron catalytic system reported by Cook for the activation of fluoroamides toward benzylic C-H fluorination¹¹³ and the two approaches from the group of Leonori for aliphatic C-H bond functionalization (which includes C-F bond formation among other C-X bond formations like C-C) are particularly appealing.^{115,116} It is noteworthy that for the latter case the halogen atom for the C-F bond formation arises from an external halogen source which is not involved in the nitrogen functionality, consequently acting as a radical quencher of the key carbon-centered radical intermediate. The same conceptual approach has been employed for triggering C-C²⁰⁸ or C-heteroatom bond-forming reactions, including oxygenation,²¹⁶ azidation,²¹⁷ cyanation,^{116,217b} or carbon-sulfur^{116,217b,218} bond formation.

In all the examples presented so far, the mechanism of the reaction relies on carbon-centered radical trapping strategies for the C-H functionalization event. Thus, only reagents displaying an electrophilic nature such as electrophilic halogen sources could be employed for directed aliphatic functionalization. In 2019, our group reported a Ritter-type amination reaction within the concept of interrupted Hofmann-Löffler reaction that could employ an external nucleophile such as acetonitrile, thus overcoming the limitation to the use of electrophilic radical quenchers.²¹⁹ In this novel approach, iodine catalysis was employed to promote the formation of a key alkyl-iodine(III) intermediate which enabled the nucleophilic displacement with a weak nucleophile such as acetonitrile. Additionally, we introduced sulfamide directing groups

²¹⁵ E. A. Wappes, A. Vanitcha, D. A. Nagib, *Chem. Sci.* **2018**, *9*, 4500-4504.

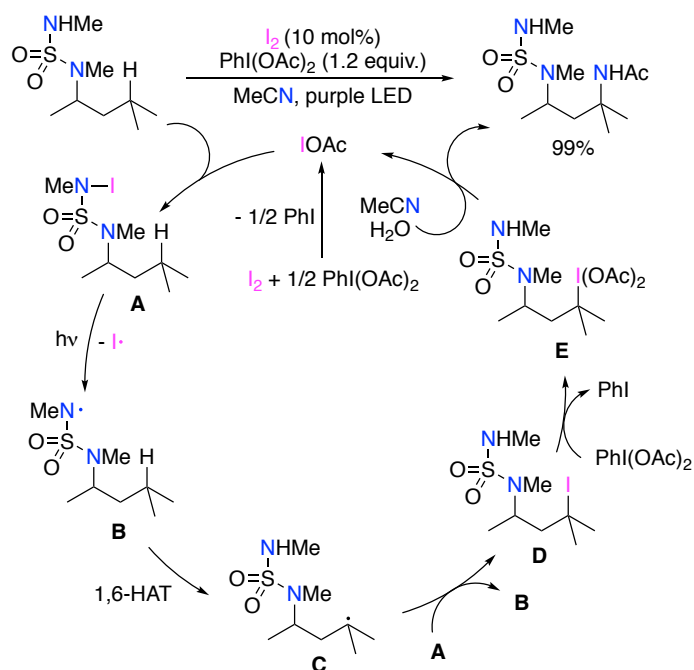
²¹⁶ Y. Tang, Y. Qin, D. Meng, C. Li, J. Wei, M. Yang, *Chem. Sci.* **2018**, *9*, 6374-6378.

²¹⁷ a) X. Bao, Q. Wang, J. Zhu, *Nat. Commun.* **2019**, *10*, 769-776. b) Xia, L. Wang, A. Studer, *Angew. Chem. Int. Ed.* **2018**, *57*, 12940-12944.

²¹⁸ S. K. Ayer, J. L. Roizen, *J. Org. Chem.* **2019**, *84*, 3508-3523.

²¹⁹ T. Duhamel, M. D. Martínez, I. K. Sideri, K. Muñiz, *ACS Catal.* **2019**, *9*, 7741-7745.

as efficient nitrogen-based functionalities for selective 1,6-HAT. Sulfamides showed a kinetically incompetent nucleophilic character that prevented intramolecular C-N bond-forming reaction, thus demonstrating its potential for directed radical-based C-H functionalization.²²⁰ The reaction is believed to be initiated by comproportionation of molecular iodine catalyst with commercial PhI(OAc)₂ oxidant to generate the active electrophilic iodine(I) catalyst (Scheme 4.8). Iodination of the sulfamide starting material followed by homolytic cleavage upon light irradiation affords nitrogen-centered radical **B**. Subsequent selective 1,6-HAT produces carbon-centered radical **C**. At this stage, radical-chain propagation takes place via iodine atom abstraction with **A**, thus generating an alkyl-iodide **D**, an observation corroborated by a quantum yield value of 120. At this stage, a second oxidation of **D** generates a nucleophile alkyl-iodine(III) species **E** that can be intercepted by acetonitrile en route to the targeted *sp*³ C-H amination event.



Scheme 4.8: Iodine-catalyzed Ritter type amination of sulfamides, mechanistic proposal.

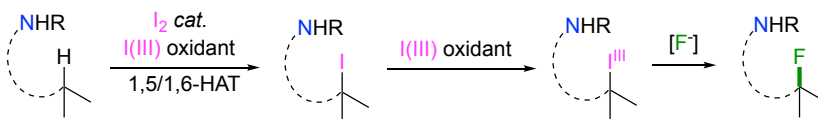
In summary, interrupted Hofmann-Löffler might represent a powerful alternative to enable a direct aliphatic C-H functionalization, including the always elusive *sp*³ C-F bond-formation. At present, however, these reactions are somewhat limited by the electron-rich nature of the in situ generated carbon-centered radical, thus requiring an

²²⁰ The group of Roizen explored sulfamides as radical directing groups for photochemical γ -chlorination: M. A. Short, M. F. Shehata, M. A. Sanders, J. L. Roizen, *Chem. Sci.* **2020**, *11*, 217-223.

Chapter IV. Iodine Catalysis for C(sp³)-H Fluorination
with a Nucleophilic Fluorine Source

electrophilic fluoride source. The use of electrophilic fluorine sources such as NFSI, Selectfluor or NFPY comprises drawbacks like waste generation or toxicity issues, among others, making these sources rather inconvenient for C-F bond-forming reactions. In addition, PET imaging techniques are unlikely to be implemented with these sources due to the difficulty of accessing the corresponding ¹⁸F-sources. Ideally, sp³ C-F bond-forming techniques should be implemented with nucleophilic fluoride sources to meet the above-mentioned challenges. At present, only one system for C(sp³)-H fluorination employing nucleophilic fluoride as fluorine source and involving formation of radical species with manganese-based porphyrin complexes have been reported to date.^{111,112}

Prompted by the knowledge acquired in interrupted Hofmann-Löffler reaction (Scheme 4.8), we envisioned an iodine catalytic system that could generate alkyl iodide(III) supernucleophile species that engages in a nucleophilic displacement with an external fluoride anion, affording a formal directed C(sp³)-H fluorination.



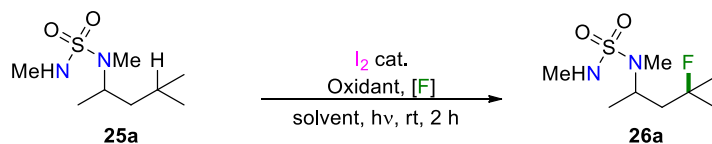
Scheme 4.9: Envisioned concept for metal free directed C(sp³)-H fluorination using nucleophilic fluorine source.

4.2. Results and discussion

We started our optimization studies with sulfamide **25a** possessing a tertiary C-H at the γ position accessible by 1,6-HAT. Sulfamide directing group was chosen because of its position selectivity and observed tendency to avoid cyclization products in similar systems.²¹⁹ Catalytic conditions involving a mixture of 10 mol% of molecular iodine with commercial PhI(OAc)₂ as terminal oxidant together with TBAF as fluorine source in various solvents did not afford any productive fluorination towards product **26a** (Table 4.1, entries 1-3). Other nucleophilic fluorine sources like KHF₂, Bu₄NPh₃SiF₂ or HF solution in pyridine also failed to promote the targeted sp³ fluorination events (entries 4-7). However, the use of Et₃N·3HF in dichloromethane afforded a promising 37% isolated yield of product **26a** after only 2 hours of reaction time (entry 8). Further solvent adjustments increased the yield up to 52% when 1,2-dichloroethane was employed as solvent (entries 9-11). Interestingly, the use of a higher energetic light source such as blue LEDs instead of conventional fluorescent irradiation from the fume hood halogen bulb lights did not lead to an improved yield (entry 12). Actually, formation of various unidentified byproducts were observed in the crude NMR, while much cleaner reaction mixture crudes were obtained employing simple fume hood light. Addition of acid additives like trifluoroacetic acid and acetic acid resulted in degradation of the reaction mixture for the first case whereas increased reaction

performance for the latter (entries 13 and 14). We then studied the nature of the oxidant employed. Strong oxidizing agent $\text{PhI}(\text{O}_2\text{CCF}_3)_2$ lead to complete degradation of the starting material, while hypervalent iodine compound $\text{PhI}(\text{mCBA})_2$ bearing chlorinated benzoate ligands afforded a good 66% yield of **26a** formation (entries 15 and 16). Although a different set of hypervalent iodine(III) oxidants bearing different benzoate ligands were explored, $\text{PhI}(\text{mCBA})_2$ was considered the optimal because of its excellent performance, high stability and low by-product generation (see extended optimization studies -Table 4.2- at the experimental section). Further adjustments on the catalyst loading and oxidant equivalents afforded optimized values of 10 mol% of I_2 and 1.5 equivalents of $\text{PhI}(\text{mCBA})_2$ (entries 17-19). Remarkably, moving back to dichloromethane as solvent from 1,2-dichloethane did not affect the excellent reaction outcome of 88% isolated yield of **26a** (entry 20). Thus, dichloromethane was considered the solvent for the optimized fluorination conditions because of toxicity reasons. Finally, the reaction robustness was corroborated in an experiment performed at 4.9 mmol scale, which afforded an excellent and consistent fluorination of **25a** in 79% isolated yield (entry 21). More importantly, we observed high yields after only 2h reaction time (and even a 50% conversion after 30 min, see entry 22), thus indicating the suitability of this protocol for PET-imaging with nucleophilic ^{18}F sources.

Chapter IV. Iodine Catalysis for C(sp³)-H Fluorination
 with a Nucleophilic Fluorine Source



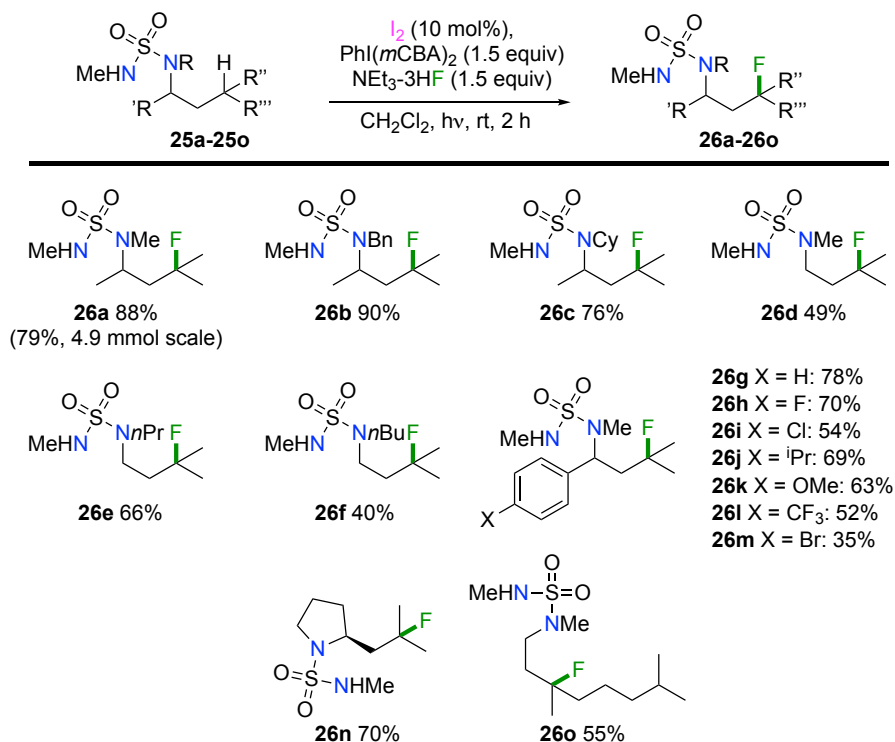
Entry	I_2 mol%	Oxidant (equiv.)	[F] (equiv.)	Solvent	26a yield (%)
1	10	PIDA (1.2)	Bu_4NF (1.5)	CH_2Cl_2	0
2	10	PIDA (1.2)	Bu_4NF (1.5)	CH_3NO_2	0
3	10	PIDA (1.2)	Bu_4NF (1.5)	HFIP	traces
4	10	PIDA (1.2)	KHF_2 (1.5)	CH_2Cl_2	traces
5	10	PIDA (1.2)	$Bu_4NPh_3SiF_2$ (1.5)	$(CH_2Cl)_2$	0
6	10	PIDA (1.2)	$HF.py$ (1.5)	CH_2Cl_2	traces
7	10	PIDA (1.2)	$HF.py$ (1.5)	$CH_2Cl_2/HFIP$	traces
8	10	PIDA (1.2)	$Et_3N.3HF$ (1.5)	CH_2Cl_2	37
9	10	PIDA (1.2)	$Et_3N.3HF$ (1.5)	HFIP	37
10	10	PIDA (1.2)	$Et_3N.3HF$ (1.5)	$CH_2Cl_2/HFIP$	46
11	10	PIDA (1.2)	$Et_3N.3HF$ (1.5)	$(CH_2Cl)_2$	52
12 ^[a]	10	PIDA (1.2)	$Et_3N.3HF$ (1.5)	$(CH_2Cl)_2$	50 ^[b]
13 ^[c]	10	PIDA (1.2)	$Et_3N.3HF$ (1.5)	$(CH_2Cl)_2$	traces
14 ^[d]	10	PIDA (1.2)	$Et_3N.3HF$ (1.5)	$(CH_2Cl)_2$	60 ^[b]
15	10	PIFA (1.2)	$Et_3N.3HF$ (1.5)	$(CH_2Cl)_2$	0
16	10	$PhI(mCBA)_2$ (1.2)	$Et_3N.3HF$ (1.5)	$(CH_2Cl)_2$	66
17	20	$PhI(mCBA)_2$ (1.2)	$Et_3N.3HF$ (1.5)	$(CH_2Cl)_2$	68
18	20	$PhI(mCBA)_2$ (1.5)	$Et_3N.3HF$ (1.5)	$(CH_2Cl)_2$	74
19	10	$PhI(mCBA)_2$ (1.5)	$Et_3N.3HF$ (1.5)	$(CH_2Cl)_2$	88
20	10	$PhI(mCBA)_2$ (1.5)	$Et_3N.3HF$ (1.5)	CH_2Cl_2	88

21 ^[e]	10	PhI(<i>m</i> CBA) ₂ (1.5)	Et ₃ N.3HF (1.5)	CH ₂ Cl ₂	79
22 ^[f]	10	PhI(<i>m</i> CBA) ₂ (1.5)	Et ₃ N.3HF (1.5)	CH ₂ Cl ₂	50 ^[b]

Table 4.1: Optimization studies for aliphatic fluorination. Isolated yields. 0.15 mmol substrate scale. Fluorescent light irradiation. PIDA = (Diacetoxyiodo)benzene. PIFA = [Bis(trifluoroacetoxy)iodo]benzene. [a] Blue LED irradiation. [b] ¹H-NMR conversion. [c] 1 equiv. TFA. [d] 1 equiv. AcOH. [e] 4.9 mmol of substrate. [f] 30 min reaction time.

Once we achieved optimized conditions for directed aliphatic C-H fluorination, we evaluated the scope of the reaction for a series of sulfamide derivatives (Scheme 4.10). Notably, as benzyl or cyclohexyl-containing sulfamides worked equally well, affording the corresponding fluorinated products **26b** and **26c** in excellent yields. Thorpe-Ingold effect was not necessary for the reaction to occur, as showed by the successful fluorination of **26d-26f** bearing no substitution at the carbon backbone. Benzylamide-derived sulfamides **25g-25m** bearing different substitution at the aryl motif could be effectively fluorinated. In this sense, electron-withdrawing and electron-donating groups are perfectly compatible with the reaction conditions. It is worth to particularly highlight substrate **26k** which was obtained in a good 63% isolated yield even displaying a high electron-rich anisole functionality, which usually engages overoxidation problems in similar iodine-catalytic systems. Chiral proline-derived compound **25n** was converted to its fluorinated analogue in a 70% isolated yield. Lastly, compound **25o** offering two different tertiary positions was submitted to reaction conditions. It was observed that only the position accessible through the 1,6-HAT process was fluorinated whereas the distal tertiary C-H bond remained untouched, thus demonstrating that the position selectivity is fully exercised by the sulfamide directing group. In this sense, fluorinated compound **26o** was obtained in 55% isolated yield.

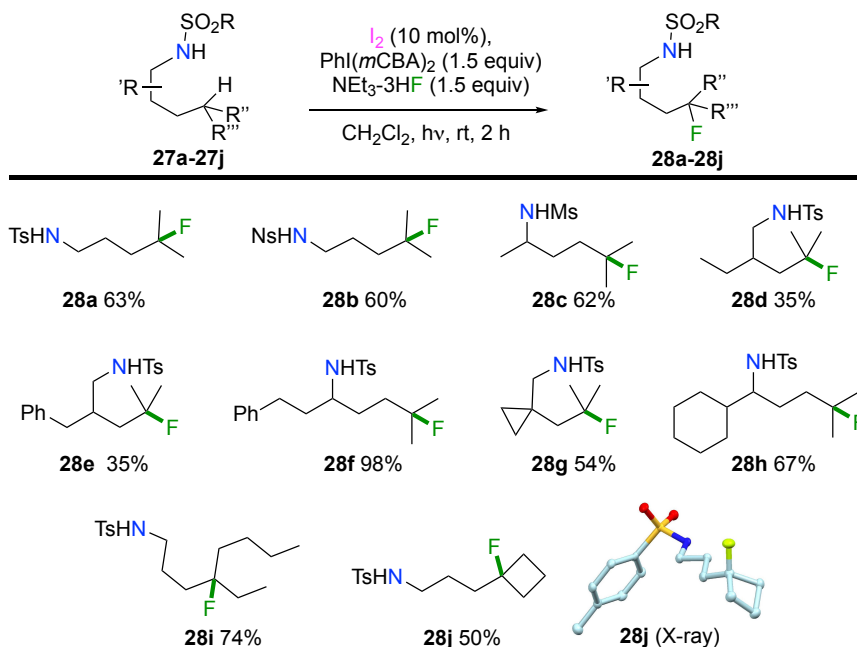
Chapter IV. Iodine Catalysis for C(sp³)-H Fluorination
 with a Nucleophilic Fluorine Source



Scheme 4.10: Sulfamide C(sp³)-H fluorination scope.

Since the general applicability of the reported conditions for preparation of 1,3-aminofluorine scaffolds was demonstrated, we thought about finding alternative radical-based systems that would allow for the access of different aminofluorine substitution patterns. In this sense, our group had experience with sulfonamides as radical directing groups for selective δ -C-H functionalization reactions. However, in our previous experience with sulfonamides in the context of Hofmann-Löffler reaction, these kind of compounds showed a propensity for cyclization reactions. To our delight, when tosylamide **27a** was subjected to reaction conditions for sulfamide fluorination, clean formation of **28a**, which was obtained in a 63% isolated yield, was achieved (Scheme 4.11). The reaction worked with similar performance when other sulfonamide groups like nosylamide or mesylamide were employed (**28b** and **28c**). At the same time, products **28a** and **28b** demonstrated that the reaction does not require Thorpe-Ingold effect to proceed efficiently. Substitution at the alkyl backbone could be equally tolerated as demonstrated by **28d-28f**, even with potentially competing benzylic C-H sites. Compound **28g** bearing cyclopropane substitution at the carbon backbone could be accessed as well and **28h** displaying multiple competing positions at the cyclohexyl moiety posed no problems. Extended aliphatic compound **28i** was obtained in a notable 74% isolated yield. Finally, *ipso*-fluorination at a cyclobutane ring could be performed giving rise to compound **28j**, the structure of which was unambiguously confirmed by

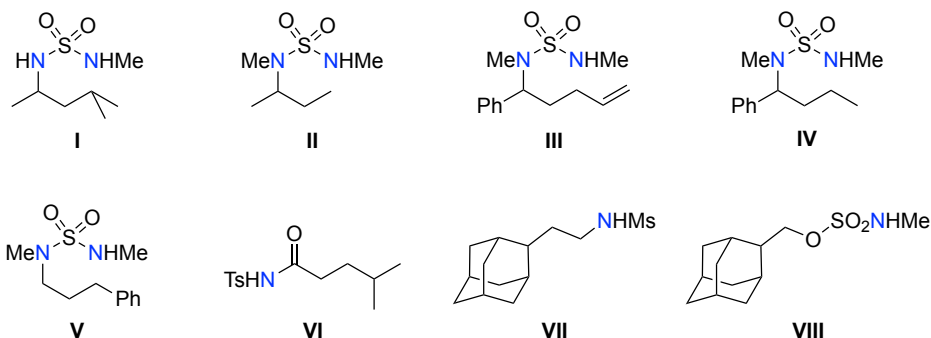
X-ray crystallographic analysis. It is worth noting that, in all of the examples explored, not even traces of the corresponding nitrogen-containing heterocycles arising from Hofmann-Löffler reaction were identified. In addition, a complete regioselectivity was observed at the tertiary C-H bond, probably due to the inherent tendency for triggering 1,5-HAT processes.



Scheme 4.11: Sulfonamide C(sp³)-H fluorination scope.

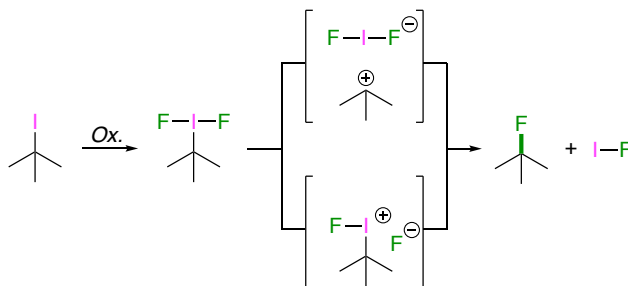
Unfortunately, a number of substrates could not be employed in the targeted *sp*³ fluorination event (Scheme 4.12). In the sulfamide series, substitution at the internal nitrogen was required, as I bearing a free N-H group did not lead to productive fluorination under our optimized conditions. Regarding the regioselectivity, the system is limited to the activation of tertiary C-H sites. Compounds **II** and **III** offering primary an activated allylic position did not provide fluorination. In these cases, recovered starting material and substrate degradation was observed in the crude reaction mixtures. In contrast, compound **IV** bearing an accessible secondary position gave stoichiometric iodination at the mentioned secondary position. In this regard, 20% of iodination product was obtained when using 20% of molecular iodine catalyst among other by-products. This observation is fully consistent with our previously developed work on Ritter-type amination.²¹⁹ Furthermore, secondary benzylic positions such as the one present in sulfamide **V** did not trigger an effective fluorination event. Instead, 20% conversion to the cyclized product together with various byproducts were observed. Unfortunately, other substituted amides such as **VI-VIII** could not be employed as substrates, recovering back the corresponding starting precursor.

Chapter IV. Iodine Catalysis for C(sp³)-H Fluorination
with a Nucleophilic Fluorine Source



Scheme 4.12: Selected non-productive substrates for directed aliphatic C-H fluorination.

Next, we focused our attention on investigating the reaction mechanism. It has been postulated that hypervalent iodine(III) compounds interact with fluoride anions to in situ generate high reactive species such as ArIF₂.²²¹ These species have been studied in great detail and are meant to be key active intermediates involved in fluorination for different catalytic procedures.²²² If these species are generated under our reaction conditions, then the putative alkyl iodide intermediate might be the subject of an oxidation en route to a hypervalent alkyl-iodine(III) containing fluorine species (Scheme 4.13). Such intermediates can evolve via ligand dissociation at iodine or C-I scission, resulting in intermediates that might be prone to C-F bond-forming reaction via nucleophilic displacement.⁷³

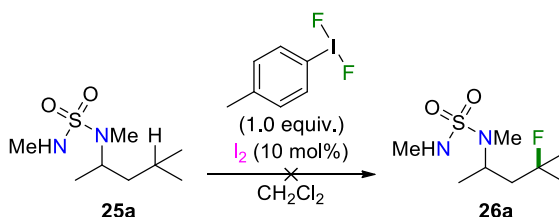


Scheme 4.13: Fluorinated hypervalent alkyl-iodine(III) compounds' evolution to alkyl fluorides.

²²¹ W. Carpenter, *J. Org. Chem.* **1966**, *31*, 2688-2689.

²²² a) X. Huang, W. Liu, J. M. Hooker, J. T. Groves, *Angew. Chem. Int. Ed.* **2015**, *54*, 5241-5245. b) T. J. Nash, G. Pattison, *Eur. J. Org. Chem.* **2015**, 3779-3786. c) I. G. Molnár, R. Gilmour, *J. Am. Chem. Soc.* **2016**, *138*, 5004-5007. d) R. Pluta, P. E. Krach, L. Cavallo, L. Falivene, M. Rueping, *ACS Catal.* **2018**, *8*, 2582-2588. e) M. K. Haj, S. M. Banik, E. N. Jacobsen, *Org. Lett.* **2019**, *21*, 4919-4923.

To explore this possibility, we first synthesized hypervalent iodine(III) compound *p*TollIF₂ following Gilmour's reported procedure.²²³ Subsequently, standard sulfamide substrate **25a** was subjected to fluorination reaction employing molecular iodine in catalytic amounts and stoichiometric amounts of fluorinated hypervalent iodine(III) oxidant in dichloromethane (Scheme 4.14). Interestingly, only unreacted starting material was obtained as the reaction outcome. This observation points toward fluorinated iodine species such as ArIF₂ not being involved in the productive pathway for C-H fluorination. However, one may argue that at conditions depicted in Scheme 4.14, the active catalyst formed would be iodine(I) species such as IF, which could be unproductive for alkyl iodide intermediates formation. In other words, this experiment does not defectively rule out the plausible formation of fluorinated alkyl-iodine(III) species as productive intermediates for C-H fluorination.



Scheme 4.14: Unsuccessful fluorination of **25a** employing *p*TollIF₂.

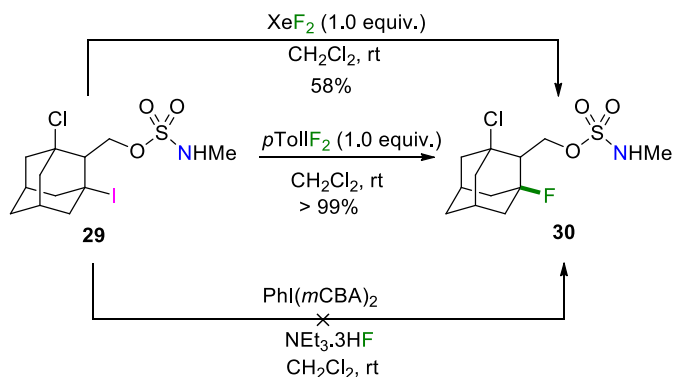
For this reason, reactivity of iodinated adamantane **29** was studied, since such compound could be considered an isolable analogue to the putative alkyl iodide intermediate prior to oxidation. Different reactions were tested to convert **29** in its corresponding oxidized fluorinated alkyl-iodine(III) analogue (Scheme 4.15). Upon reaction with stoichiometric XeF₂, expected fluorinated product **30** was obtained in an isolated 58% yield. Iodinated adamantane compounds are known to be converted to the corresponding adamantane fluorides when treated with fluorine-based oxidants in a fluorodeiodination reaction involving transient formation of fluorinated alkyl-iodine(III) intermediates.^{73, 224} Subsequent reaction with stoichiometric amounts of *p*TollIF₂ resulted in full conversion to fluorinated product **30**, thus demonstrating that an external fluorinated hypervalent iodine(III) oxidant can efficiently promote oxidation of *tert*-alkyl iodide species. In contrast, no product formation was found under our optimized reaction conditions, since unreacted **29** was recovered. From these three experiments we could conclude that the combination of PhI(*m*CBA)₂ and NEt₃·3HF does not generate kinetically competent PhIF₂ species. Consecutively, oxidation to fluorinated alkyl-iodine(III) might not take place in our protocol. In addition, product **30**

²²³ J. C. Sarie, C. Thiehoff, R. J. Mudd, C. G. Daniliuc, G. Kehr, R. Gilmour, *J. Org. Chem.* **2017**, *82*, 11792-11798.

²²⁴ a) S. Rozen, M. Brand, *J. Org. Chem.* **1981**, *46*, 733-736. b) E. W. Della, N. J. Head, *J. Org. Chem.* **1992**, *57*, 2850-2855.

Chapter IV. Iodine Catalysis for C(sp³)-H Fluorination
with a Nucleophilic Fluorine Source

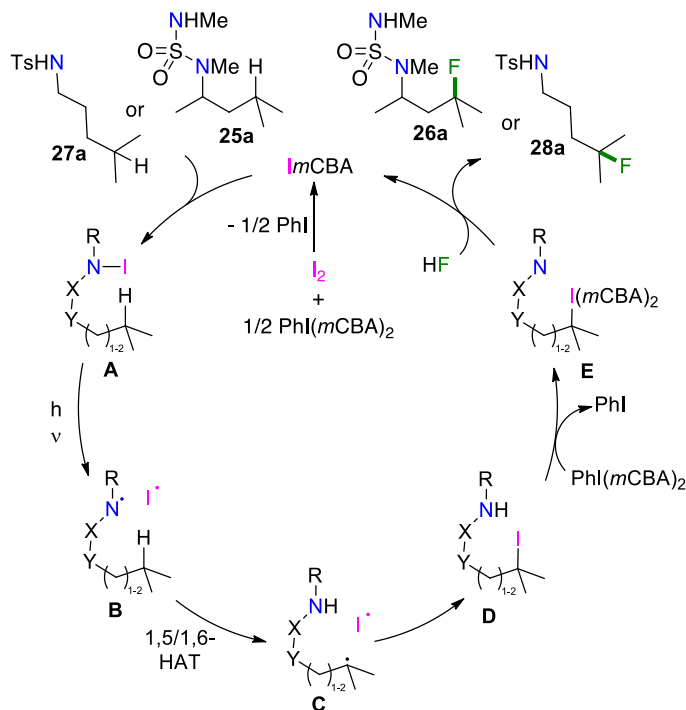
was not formed from **29**, indicating that fluoride introduction takes place in a final nucleophilic substitution event which is impeded by adamantane's rigidity.²²⁵



Scheme 4.15: Control experiments with **29**.

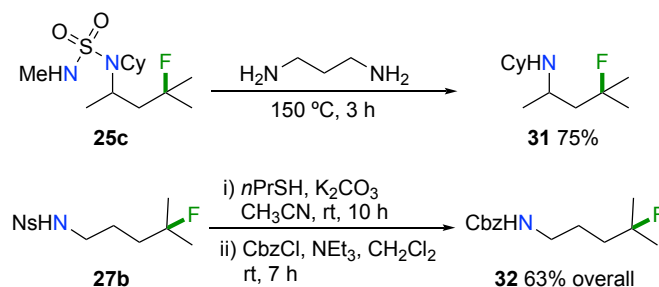
Taking all these observations into consideration, we tentatively propose a mechanistic rationale for our sp^3 C-H fluorination event (Scheme 4.16). The active electrophilic iodine catalyst, *ImCBA*, arises from fast comproportionation of molecular iodine catalyst with hypervalent iodine(III) $\text{PhI}(m\text{CBA})_2$ oxidant. Such iodine(I) compound promotes iodination at the active nitrogen group of the corresponding sulfamide of sulfonamide starting material (exemplified by **25a** and **27a** at Scheme 4.16) to generate N-haloamine species **A**. Homolysis of labile N-I bond accounts from light irradiation, thus generating nitrogen-centered radical **B**. Selective 1,5-HAT and 1,6-HAT for the sulfonamide and sulfamide series respectively affords formation of *tert*-alkyl radical species **C**. Further evolution of carbon-centered radical **C** to alkyl iodide **D** could result from radical recombination or, in an alternative pathway, from iodine abstraction to intermediate **A** to concomitantly deliver **B** in a chain propagation mechanism. To further evaluate the involvement of these two putative pathways, the quantum yield for fluorination of substrate **25a** was measured, obtaining a value of $\Phi = 5$. This result points toward participation of the chain propagation mechanism for generation of **D**. At this stage, oxidation of alkyl iodide **D** by the terminal hypervalent iodine(III) oxidant delivers alkyl-iodine(III) species **E**. Final nucleophilic substitution by the fluoride anion enabled by the presence of the super-nucleophile group delivers smooth formation of fluorinated products such as **26a** and **28a** for the sulfamide and sulfonamide series respectively.

²²⁵ R. A. Rossi, S. M. Palacios, A. N. Santiago, *J. Org. Chem.* **1982**, *47*, 4654-4657.



Scheme 4.16: Mechanistic proposal for iodine-catalyzed directed C(sp³)-H fluorination.

While one might argue that the inclusion of rather sophisticated amine directing groups might constitute a drawback, we found that the deprotection of this motif could easily be accomplished by standard techniques (Scheme 4.17). On one hand, sulfamide deprotection was performed by aminolysis in neat 1,3-aminopropane to afford **31** in 75% isolated yield whereas the nosyl derivative **27b** from the sulfonamide series can be deprotected under standard Fukuyama conditions, resulting in the Cbz-protected derivative **32** after protection of the in situ generated primary amine.



Scheme 4.17: Deprotection toward 1,3- and 1,4-fluoroamine access.

Chapter IV. Iodine Catalysis for C(sp³)-H Fluorination
with a Nucleophilic Fluorine Source

4.3. Conclusions

In summary, we achieved an unprecedented iodine-catalytic system for selective aliphatic C-H fluorination employing simple fluoride as nucleophilic fluorine source. The unique inherent performance of iodine catalysis enables at the same time for the use of such lousy nucleophilic species and for a perfect control of the position selectivity by means of nitrogen-centered radical intermediates. Just by choosing the protecting group nature at the nitrogen moiety, practical fluorination can be performed with complementary selectivity toward preparation of 1,3- and 1,4-fluoroamine compounds within the same experimental conditions. The present work demonstrates the outstanding performance of iodine catalysis for advanced C(sp³)-H functionalization and reveals its potential application for building up molecular complexity. In addition, the use of simple fluoride as fluorine source and the short reaction times suggests potential application for ¹⁸F radiolabeling and late-stage functionalization.

4.4. Experimental section

General Remarks: All solvents and reagents employed were purchased from Aldrich, Acros, TCI and Fluorochem. Column chromatography was performed on silica gel (PanReac AppliChem, Silica Gel 60, 0.063-0.2 mm). NMR spectroscopy was performed on a Bruker Avance 300 MHz, 400 MHz or 500 MHz, respectively. The chemical shifts are given in ppm normalized to the shift of residual chloroform in the deuterated chloroform (δ H = 7.26 ppm and δ C = 77.16 ppm). The multiplicities are stated as follows: s = singlet, bs = broad singlet, d = doublet, t = triplet, q = quartet, m = multiplet. HRMS measurements were performed on a UHPLC-MS-QqTOF (MaXis Impact, Bruker Daltonics) or HPLC-MS-TOF (MicroTOF II, Bruker Daltonics) within the ICIQ service department. IR spectroscopy was performed using a Bruker Alpha instrument in the solid state. Melting points were determined employing a Büchi B-540 instrument. UV-vis spectra were recorded on a Shimadzu UV-2401PC.

General protocol (GP1) for the synthesis of sulfamides: Compounds **25a-25o** were synthesized according to described procedures reported in literature.²¹⁹

General protocol (GP2) for the synthesis of sulfonamides: Compounds **27a-27j** were synthesized according to described procedures reported in literature. For each particular compound, the corresponding nitrile and alkyl bromide were used in the same synthetic sequence.^{72,74,75}

General protocol (GP3) for C-H fluorination: In a flamed-dried Schlenk flask the corresponding sulfamide or sulfonamide (0.15 mmol) was dissolved in 1ml of dry dichloromethane under an argon atmosphere. Subsequently, PhI(mCBA)₂ (0.225 mmol, 1.5 equiv.), NEt₃·3HF (0.225 mmol, 1.5 equiv.) and I₂ (0.015 mmol, 0.1 equiv.) were added to the reaction mixture. The reaction was stirred for 2h under visible light irradiation (fume hood light) and then quenched by addition of saturated aqueous

solution of Na₂S₂O₃ and NaHCO₃. The aqueous phase was extracted twice with dichloromethane and the combined organic fractions were washed with H₂O and brine solution. Subsequently, the organic solvent was evaporated at low pressure. The final fluorinated product was obtained after column chromatography purification on silica gel using *n*-Hex/EtOAc as eluent.

Extended optimization studies:

Entry	I ₂ mol%	Oxidant (equiv.)	[F] (equiv.)	Solvent	26a yield (%)
1	10	PIDA (1.2)	KF, 18-crown-6 (1.5 equiv.)	MeNO ₂	0
2	10	PIDA (1.2)	Et ₃ N.3HF (1.5)	CF ₃ CH ₂ OH	0 ^[a]
3	10	PIDA (1.2)	Et ₃ N.3HF (1.5)	CH ₂ Cl ₂ /HFIP	42
4	10	PIDA (1.2)	Et ₃ N.3HF (0.5)	CH ₂ Cl ₂ /HFIP	39
5	10	PIDA (1.2)	Et ₃ N.3HF (1.5)	HFIP	40 ^[b]
6	20	PIDA (1.5)	Et ₃ N.3HF (1.5)	(CH ₂ Cl) ₂	55
7 ^[c]	20	PIDA (1.5)	Et ₃ N.3HF (1.5)	(CH ₂ Cl) ₂	0
8	20	PhI(<i>m</i> CBA) ₂ (1.5)	Et ₃ N.3HF (1.5)	CH ₂ Cl ₂	71
9	10	PhI(<i>o</i> FBA) ₂ (1.5)	Et ₃ N.3HF (1.5)	(CH ₂ Cl) ₂	73
10	10	PhI(<i>p</i> MeBA) ₂ (1.5)	Et ₃ N.3HF (1.5)	(CH ₂ Cl) ₂	72
11	10	PhI(<i>p</i> BBA) ₂ (1.5)	Et ₃ N.3HF (1.5)	(CH ₂ Cl) ₂	40
12	10	PhI(O ₂ CPh) ₂ (1.5)	Et ₃ N.3HF (1.5)	(CH ₂ Cl) ₂	85
13	10	PhI(<i>m</i> OMeBA) ₂ (1.5)	Et ₃ N.3HF (1.5)	(CH ₂ Cl) ₂	82
14	10	PhI(<i>p</i> OMeBA) ₂ (1.5)	Et ₃ N.3HF (1.5)	(CH ₂ Cl) ₂	58
15	10	PhI(<i>m,m</i> OMeBA) ₂ (1.5)	Et ₃ N.3HF (1.5)	(CH ₂ Cl) ₂	0
16	20	PhI(<i>m</i> OMeBA) ₂ (1.5)	Et ₃ N.3HF (1.5)	CH ₂ Cl ₂	60
17	10	PhI(<i>m</i> OMeBA) ₂ (1.7)	Et ₃ N.3HF (1.5)	CH ₂ Cl ₂	0
18	10	PhI(<i>m</i> OMeBA) ₂ (1.5)	Et ₃ N.3HF (1.5)	CH ₂ Cl ₂	68

Chapter IV. Iodine Catalysis for C(sp³)-H Fluorination
with a Nucleophilic Fluorine Source

19^[d] 10 PhI(mOMeBA)₂ (1.5) Et₃N.3HF (1.5) CH₂Cl₂ 50^[b]

Table 4.2: Optimization studies for aliphatic fluorination. Isolated yields. 0.15 mmol substrate scale. Fluorescent light irradiation. [a] Trifluoroethanol insertion observed. [b] ¹H-NMR conversion. [c] Dilution factor = 4 (4 ml of solvent instead of 1 ml). [d] Blue LED irradiation.

Quantum yield measurements: The procedure for the quantum yield determination was previously described by Melchiorre et al.²²⁶

Preparation of solutions:

A ferrioxalate (Potassium trioxalatoferrate(III) trihydrate) actinometry solution was prepared. Ferrioxalate actinometer solution measures the decomposition of ferric ions to ferrous ions, which are complexed by 1,10-phenanthroline and monitored by UV/Vis absorbance at 510 nm. The moles of iron-phenanthroline complex formed are related to moles of photons absorbed, so this solution is used to calibrate the amount of photons.²²⁷

The solutions were prepared and stored in the dark (red light):

1. Potassium ferrioxalate solution: 294.8 mg of potassium ferrioxalate (commercially available from Alfa Aesar) and 139 μ L of sulfuric acid (96%) were added to a 50 mL volumetric flask, and filled to the mark with water (HPLC grade).
2. Phenanthroline solution: 0.2% by weight of 1,10-phenanthroline in water (100 mg in 50 mL volumetric flask).
3. Buffer solution: to a 50 mL volumetric flask 2.47 g of NaOAc and 0.5 mL of sulfuric acid (96%) were added and filled to the mark with water (HPLC grade).
4. Reaction mixture stock solution 1: 104.16 mg of **25a** was added to a 2.5 mL volumetric flask followed by 386 mg of PhI(mCBA)₂ and 122 μ L of NEt₃.3HF. The mixture was then filled up with HPLC grade dichloromethane.
5. Reaction mixture stock solution 2: 12.7 mg of molecular iodine was added to a 2.5 mL volumetric flask, which was filled up with HPLC grad dichloromethane.

Reaction setup:

- Reaction mixtures: 0.5 mL of the reaction mixture stock 1 solution was added to a 5 mL Schlenk tube (10 cm, 1.2 cm diameter). The Schlenk was placed in front of the xenon lamp at a distance of 10 cm. Then, 0.5 mL of the reaction mixture stock 2 was added. Four different reactions were setup and irradiated for four different times: 30 s, 60 s,

²²⁶ M. Silvi, C. Verrier, Y. P. Rey, L. Buzzetti, P. Melchiorre, *Nat. Chem.* **2017**, *9*, 868-873.

²²⁷ C. G. Hatchard, C. A. Parker, A new sensitive chemical actinometer. II. Potassium ferrioxalate as a standard chemical actinometer, *Proc. R. Soc. Lond. A.* **1956**, *235*, 518-536.

90 s and 120 s. After each reaction was finished, a saturated solution of Na₂CO₃ and Na₂S₂O₃ (1 mL) was added to quench the reaction. A usual work up was done with dichloromethane and an internal standard was added (4,4'-Difluorobenzophenone).

- Actinometer solutions: A Schlenk flask of the same dimensions as used for the reaction mixtures was loaded with 1.0 mL of actinometer solution and placed next to the reaction mixture solution. Four different actinometer solutions were irradiated for 30 s, 60 s, 90 s and 120 s (each irradiation was started at the same time as the reaction mixture irradiations and removed after the times mentioned). After each irradiation the actinometer solutions were carefully transferred into a 10 mL volumetric flask, then 0.5 mL of phenanthroline solution and 2.0 mL of buffer solution were added and the flask was filled up with water. The mixture was kept for at least 1 h in the dark and then analyzed by UV-vis.

Analysis:

- Reaction mixtures: The NMRs of the crude were recorded in order to determine the NMR yield.

- Actinometer solutions: 7 UV-vis spectra were recorded: One each of every irradiated actinometer solution, 1 of a non-irradiated actinometer solution (but complexed with phenanthroline), 1 of a non-irradiated potassium ferrioxalate solution (but not complexed with phenanthroline and non-diluted) and one of the reaction mixture (diluted 1 to 2). The latter three spectra are used to determine the correction factors. From the four irradiated actinometer solutions and the non-irradiated (but complexed) solution, the produced moles of Fe(II) can be determined using the following formula:

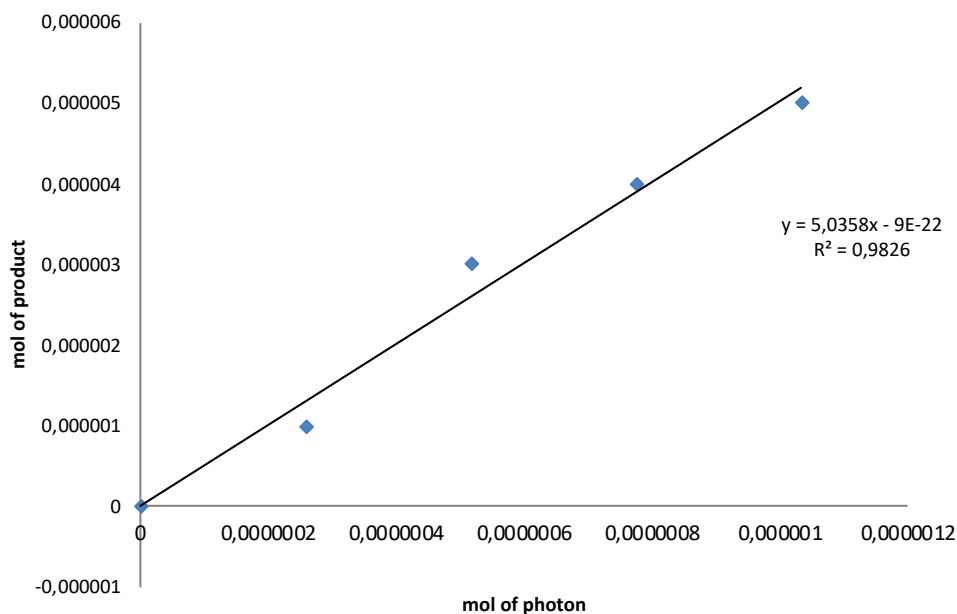
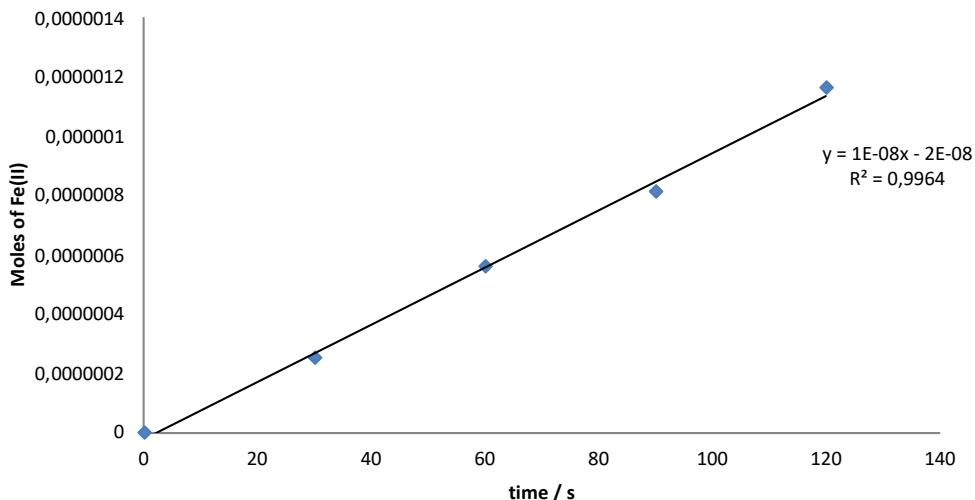
$$\text{Moles of Fe(II)} = \frac{V_1 V_3 \Delta A(510 \text{ nm})}{10^3 V_2 l \epsilon(510 \text{ nm})}$$

Plotting these values vs. the irradiation time of the actinometer solutions, knowing the quantum yield of the actinometer reaction at 400 nm and the correction factor *f* of the noncomplexed, non-irradiated actinometer solution, the photon flux of the lamp at 400 nm and 10 cm of distance through the solution can be determined. The quantum yield of the reaction was then determined by plotting the moles of product formed vs. the moles of photons absorbed, the slope of the linear regression corresponds to the quantum yield.

Chapter IV. Iodine Catalysis for C(sp³)-H Fluorination
 with a Nucleophilic Fluorine Source

Quantum Yield measurements					
time actinometer [sec]					
time [min]	0	0,5	1	1,5	2
time [s]		30	60	90	120
GC Integral P		0,01	0,03	0,04	0,05
GC Integral IS		1	1	1	1
I(P)/I(S)		0,01	0,03	0,04	0,05
corrected n(P)/n(I(S)		0,01	0,03	0,04	0,05
theoretical yield in <i>mmol</i>	0,1				
number of moles of product formed	0	0,000001	0,000003	0,000004	0,000005
Actinometry					
Volume of irradiated solution (V1) [mL]		1			
Volume of aliquot taken from V1 (V2) [mL]		1			
Volume after complexation with Phenanthroline (V3) [mL]		10			
Path length of the cell (l) [cm]		1			
A (510 nm) of reference (complexed solution at t = 0 s)		0,268			
time of actinometer reaction [s]	0	30	60	90	120
A (510 nm) of actinometer solution (complexed sol.; at various t)	0	0,542	0,887	1,168	1,562
ΔA (510 nm)		0,274	0,6190	0,9000	1,2940
ε (510 nm) of Fe(phen) ₂ ⁺ [L/(mol.cm)]		11100			
Moles of Fe ²⁺	0	2,46847E-07	5,57658E-07	8,10811E-07	1,16577E-06
Quantum yield of Fe(II) formation at 400 nm		1,13			
Absorption of actinometer solution (non-complexed) at 400 nm		2,13			
correction factor (f): ratio of absorbed light		0,992586898			
Slope of "Moles Fe(II) vs. Time"		9,65165E-09			
Flux (F) [einstein/s]		8,60507E-09			
Flux (F) * <i>reactiontime</i> [einstein]	0	2,58152E-07	5,16304E-07	7,74457E-07	1,03261E-06
Absorption of reaction mixture at 400 nm		0,576			
Dilution of reaction mixture (1:x); x =		2			
correction factor: ratio of absorbed light for rxn mix (f=1-(10 ^{-A}))		0,929531			
Quantum Yield (φ)		5,42			

Moles Fe(II) vs. time



Conclusion: We obtained a quantum yield of 5.4, which points toward a radical chain mechanism.

2-Methyl-4-(methyl(N-methylsulfamoyl)amino)pentane (25a)



Compound **25a** was synthesized following GP1. Its data matched with those reported in the literature.²¹⁹ ¹H NMR (400 MHz, CDCl₃): $\delta =$

Chapter IV. Iodine Catalysis for C(sp³)-H Fluorination
with a Nucleophilic Fluorine Source

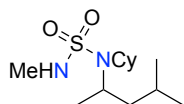
4.07-3.97 (m, 1H), 2.67-2.65 (m, 6H), 1.66-1.55 (m, 1H), 1.46 (ddd, $J = 14.3, 8.9, 5.6$ Hz, 1H), 1.24-1.17 (m, 1H), 1.15 (d, $J = 6.7$ Hz, 3H), 0.94 (d, $J = 6.6$ Hz, 3H), 0.92 (d, $J = 6.7$ Hz, 3H). ¹³C NMR (100 MHz, CDCl₃): $\delta = 51.3, 43.7, 29.4, 27.7, 25.0, 23.0, 22.3, 18.3$.

2-Methyl-4-(benzyl(N-methylsulfamoyl)amino)pentane (25b)



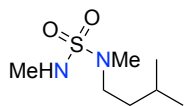
Compound **25b** was synthesized following GP1. Its data matched with those reported in the literature.²¹⁹ ¹H NMR (400 MHz, CDCl₃): $\delta = 7.43-7.38$ (m, 2H), 7.36-7.30 (m, 2H), 7.30-7.25 (m, 1H), 4.33 (d, $J = 15.4$ Hz, 1H), 4.24 (d, $J = 15.4$ Hz, 1H), 3.96 (h, $J = 6.9$ Hz, 1H), 3.67 (bs, 1H), 2.53 (s, 3H), 1.65-1.54 (m, 1H), 1.52-1.44 (m, 1H), 1.29-1.19 (m, 4H), 0.89 (d, $J = 6.5$ Hz, 3H), 0.78 (d, $J = 6.6$ Hz, 3H). ¹³C NMR (100 MHz, CDCl₃): $\delta = 138.5, 128.6, 127.7, 53.3, 47.7, 44.7, 29.4, 25.0, 22.7, 22.4, 19.4$.

2-Methyl-4-(cyclohexyl(N-methylsulfamoyl)amino)pentane (25c)



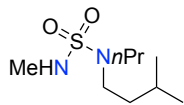
Compound **25c** was synthesized following GP1. Its data matched with those reported in the literature.²¹⁹ ¹H NMR (400 MHz, CDCl₃): $\delta = 3.91$ (bs, 1H), 3.64-3.49 (m, 1H), 3.21-3.07 (m, 1H), 2.67 (s, 3H), 1.88-1.72 (m, 6H), 1.67-1.52 (m, 3H), 1.48-1.38 (m, 1H), 1.5-1.20 (m, 5H), 1.12 (tt, $J = 13.0, 3.2$ Hz, 1H), 0.93 (d, $J = 6.3$ Hz, 3H), 0.90 (d, $J = 6.4$ Hz, 3H). ¹³C NMR (125 MHz, CDCl₃): $\delta = 57.4, 51.7, 45.3, 32.6, 32.4, 29.2, 26.7, 26.7, 25.5, 25.5, 23.6, 22.1, 19.7$.

2-Methyl-4-(methyl(N-methylsulfamoyl)amino)butane (25d)



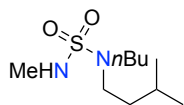
Compound **25d** was synthesized following GP1. Its data matched with those reported in the literature.²¹⁹ ¹H NMR (500 MHz, CDCl₃): $\delta = 3.21-3.14$ (m, 2H), 2.80 (s, 3H), 2.69 (s, 3H), 1.62 (h, $J = 6.7$ Hz, 1H), 1.50-1.43 (m, 2H), 0.92 (d, $J = 6.6$ Hz, 6H). ¹³C NMR (125 MHz, CDCl₃): $\delta = 49.1, 36.7, 34.8, 29.6, 25.8, 22.6$.

2-Methyl-4-(propyl(N-methylsulfamoyl)amino)butane (25e)



Compound **25e** was synthesized following GP1. Its data matched with those reported in the literature.²¹⁹ ¹H NMR (500 MHz, CDCl₃): $\delta = 3.97$ (bs, 1H), 3.23-3.16 (m, 2H), 3.16-3.06 (m, 2H), 2.67 (s, 3H), 1.67-1.53 (m, 3H), 1.53-1.43 (m, 2H), 0.97-0.86 (m, 9H). ¹³C NMR (125 MHz, CDCl₃): $\delta = 49.7, 46.5, 37.3, 29.4, 26.1, 22.6, 21.7, 11.4$.

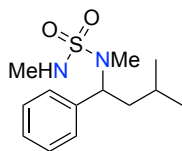
2-Methyl-4-(butyl(N-methylsulfamoyl)amino)butane (25f)



Compound **25f** was synthesized following GP1. Its data matched with those reported in the literature.²¹⁹ ¹H NMR (500 MHz, CDCl₃): $\delta = 3.26-3.14$ (m, 4H), 2.67 (s, 3H), 1.62-1.53 (m, 3H), 1.52-1.45 (m, 2H),

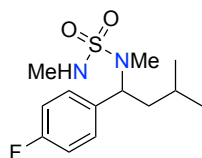
1.37-1.28 (m, 2H), 0.97-0.91 (m, 9H). ¹³C NMR (125 MHz, CDCl₃): δ = 47.7, 46.4, 37.2, 31.1, 30.6, 29.4, 26.1, 22.6, 20.2, 13.9.

2-Methyl-4,4-phenyl-(methyl(N-methylsulfamoyl)amino)butane (25g)



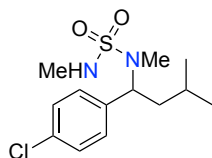
Compound **25g** was synthesized following GP1. Its data matched with those reported in the literature.²¹⁹ ¹H NMR (400 MHz, CDCl₃): δ = 7.41-7.28 (m, 5H), 5.09 (t, *J* = 7.9 Hz, 1H), 3.90 (bs, 1H), 2.64 (s, 3H), 2.54 (s, 3H), 1.92-1.73 (m, 2H), 1.61 (h, *J* = 6.6 Hz, 1H), 0.99 (d, *J* = 6.6 Hz, 3H), 0.96 (d, *J* = 6.6 Hz, 3H). ¹³C NMR (100 MHz, CDCl₃): δ = 139.2, 128.7, 128.3, 128.0, 58.7, 40.1, 29.3, 29.0, 25.0, 22.8, 22.6.

2-Methyl-4,4-p-fluorophenyl-(methyl(N-methylsulfamoyl)amino)butane (25h)



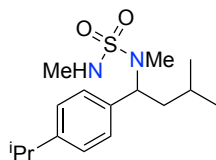
Compound **25h** was synthesized following GP1. Its data matched with those reported in the literature.²¹⁹ ¹H NMR (400 MHz, CDCl₃): δ = 7.40-7.33 (m, 2H), 7.08-7.01 (m, 2H), 5.08 (t, *J* = 7.9 Hz, 1H), 3.92 (bs, 1H), 2.60 (s, 3H), 2.56 (s, 3H), 1.87-1.71 (m, 2H), 1.59 (h, *J* = 6.7 Hz, 1H), 0.99 (d, *J* = 6.6 Hz, 3H), 0.96 (d, *J* = 6.6 Hz, 3H). ¹³C NMR (100 MHz, CDCl₃): δ = 162.4 (d, *J* = 246.6 Hz), 134.9, 129.9 (d, *J* = 8.0 Hz), 115.5 (d, *J* = 21.3 Hz), 57.9, 40.2, 29.3, 28.8, 25.0, 22.8, 22.5. ¹⁹F{¹H} NMR (375 MHz, CDCl₃) δ = -114.42.

2-Methyl-4,4-p-chlorophenyl-(methyl(N-methylsulfamoyl)amino)butane (25i)



Compound **25i** was synthesized following GP1. Its data matched with those reported in the literature.²¹⁹ ¹H NMR (500 MHz, CDCl₃): δ = 7.33 (s, 4H), 5.07 (t, *J* = 8.3 Hz, 1H), 3.93 (bs, 1H), 2.60 (s, 3H), 2.57 (d, *J* = 5.4 Hz, 3H), 1.86-1.71 (m, 2H), 1.64-1.57 (m, 1H), 0.99 (d, *J* = 6.6 Hz, 3H), 0.96 (d, *J* = 6.7 Hz, 3H). ¹³C NMR (125 MHz, CDCl₃): δ = 137.7, 133.9, 129.7, 128.8, 58.0, 40.0, 29.3, 28.9, 25.0, 22.8, 22.4.

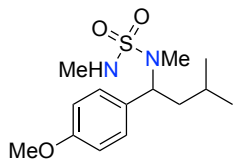
2-Methyl-4,4-(4-isopropylphenyl)-(methyl(N-methylsulfamoyl)amino)butane (25j)



Compound **25j** was synthesized following GP1. Its data matched with those reported in the literature.²¹⁹ ¹H NMR (500 MHz, CDCl₃): δ = 7.32-7.28 (m, 2H), 7.22-7.18 (m, 2H), 5.05 (t, *J* = 7.9 Hz, 1H), 2.89 (p, *J* = 6.9 Hz, 1H), 2.61 (s, 3H), 2.53 (s, 3H), 1.88-1.75 (m, 2H), 1.61 (h, *J* = 6.7 Hz, 1H), 1.24 (d, *J* = 6.9 Hz, 6H), 0.98 (d, *J* = 6.6 Hz, 3H), 0.95 (d, *J* = 6.6 Hz, 3H). ¹³C NMR (125 MHz, CDCl₃): δ = 148.5, 136.4, 128.2, 126.6, 58.4, 40.0, 33.8, 29.2, 28.8, 24.9, 24.0, 24.0, 22.8, 22.5.

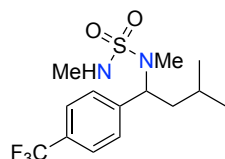
2-Methyl-4,4-p-methoxyphenyl-(methyl(N-methylsulfamoyl)amino)butane (25k)

Chapter IV. Iodine Catalysis for C(sp³)-H Fluorination
with a Nucleophilic Fluorine Source



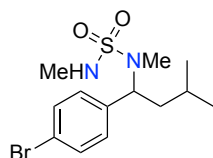
Compound **25k** was synthesized following GP1. Its data matched with those reported in the literature.²¹⁹H NMR (500 MHz, CDCl₃): δ = 7.33-7.29 (m, 2H), 6.90-6.86 (m, 2H), 5.05 (t, J = 7.9 Hz, 1H), 3.81 (s, 3H), 2.61 (s, 3H), 2.55 (d, J = 5.4 Hz, 3H), 1.85-1.72 (m, 2H), 1.63-1.56 (m, 1H), 0.98 (d, J = 6.6 Hz, 3H), 0.95 (d, J = 6.6 Hz, 3H). ¹³C NMR (125 MHz, CDCl₃): δ = 159.3, 131.1, 129.5, 113.9, 58.2, 55.4, 40.2, 29.3, 28.9, 25.0, 22.7, 22.6.

2-Methyl-4,4-(4-trifluoromethylphenyl)-(methyl(N-methylsulfamoyl)amino)butane (25l)



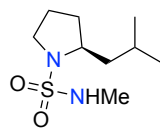
Compound **25l** was synthesized following GP1. Its data matched with those reported in the literature.²¹⁹H NMR (400 MHz, CDCl₃): δ = 7.65-7.59 (m, 2H), 7.53-7.58 (m, 2H), 5.15 (t, J = 7.9 Hz, 1H), 4.01 (bs, 1H), 2.62 (s, 3H), 2.61-2.56 (m, 3H), 1.91-1.74 (m, 2H), 1.64-1.57 (m, 1H), 1.01 (d, J = 6.5 Hz, 3H), 0.97 (d, J = 6.6 Hz, 3H). ¹³C NMR (100 MHz, CDCl₃): δ = 143.3, 130.4, 130.1, 128.6, 125.6 (q, J = 3.8 Hz), 122.8 (q, J = 273.5 Hz), 58.2, 39.9, 29.3, 28.9, 25.0, 22.8, 22.4. ¹⁹F{¹H} NMR (375 MHz, CDCl₃) δ = -62.70.

2-Methyl-4,4-p-bromophenyl-(methyl(N-methylsulfamoyl)amino)butane (25m)



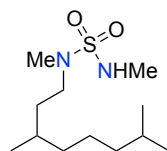
Compound **25m** was synthesized following GP1. Its data matched with those reported in the literature.²¹⁹H NMR (500 MHz, CDCl₃): δ = 7.51-7.45 (m, 2H), 7.29-7.26 (m, 2H), 5.06 (t, J = 7.9 Hz, 1H), 3.92 (bs, 1H), 2.60 (s, 3H), 2.57 (s, 3H), 1.85-1.71 (m, 2H), 1.63-1.56 (m, 1H), 0.99 (d, J = 6.5 Hz, 3H), 0.96 (d, J = 6.7 Hz, 3H). ¹³C NMR (125 MHz, CDCl₃): δ = 138.2, 131.8, 130.0, 122.0, 58.1, 40.0, 29.3, 28.9, 27.1, 25.0, 22.8, 22.5.

(S)-2-Isobutyl-N-methylpyrrolidine-1-sulfonamide (25n)



Compound **25n** was synthesized following GP1. Its data matched with those reported in the literature.²¹⁹H NMR (500 MHz, CDCl₃): δ = 3.99 (bs, 1H), 3.91-3.80 (m, 1H), 3.40 (dt, J = 10.1, 7.3 Hz, 1H), 3.26-3.17 (m, 1H), 2.72 (d, J = 5.3 Hz, 3H), 2.09-1.98 (m, 1H), 1.92-1.86 (m, 2H), 1.71-1.57 (m, 3H), 1.33-1.24 (m, 1H), 0.92 (t, J = 6.4 Hz, 6H). ¹³C NMR (125 MHz, CDCl₃): δ = 59.1, 48.6, 45.2, 31.3, 29.7, 25.7, 24.7, 23.8, 21.8.

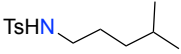
2-Methyl-6-methyl-8-(methyl(N-methylsulfamoyl)amino)octane (25o)



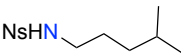
Compound **25o** was synthesized following GP1. Its data matched with those reported in the literature.²¹⁹H NMR (500 MHz, CDCl₃): δ = 3.99 (bs, 1H), 3.24-3.12 (m, 2H), 2.81 (s, 3H), 2.69 (s, 3H), 1.64-1.44 (m, 3H), 1.42-1.35 (m, 1H), 1.34-1.21 (m, 3H), 1.18-1.10 (m, 3H), 0.90 (d, J = 6.6

Hz, 3H), 0.87 (dd, $J = 6.7, 1.0$ Hz, 6H). ¹³C NMR (125 MHz, CDCl₃): $\delta = 48.9, 39.4, 37.3, 34.9, 34.8, 30.6, 29.6, 28.1, 24.8, 22.8, 22.7, 19.6$.

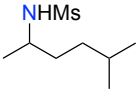
4-methyl-N-(4-methylpentyl)benzenesulfonamide (27a)

 Compound **27a** was synthesized following GP2. Its data matched with those reported in the literature.²¹⁹ ¹H NMR (400 MHz, CDCl₃): $\delta = 7.78-7.72$ (m, 2H), 7.33-7.28 (m, 2H), 4.64 (t, $J = 6.2$ Hz, 1H), 2.90 (q, $J = 7.1$ Hz, 2H), 2.42 (s, 3H), 1.51-1.37 (m, 3H), 1.16-1.07 (m, 2H), 0.83-0.76 (m, 6H). ¹³C NMR (100 MHz, CDCl₃): $\delta = 143.4, 137.2, 129.8, 127.2, 43.6, 35.8, 27.7, 27.6, 22.5, 21.6$.

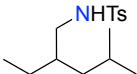
N-(4-methylpentyl)-4-nitrobenzenesulfonamide (27b)

 Compound **27b** was synthesized following GP2, it was obtained as a white solid. ¹H NMR (500 MHz, CDCl₃): $\delta = 8.39-8.34$ (m, 2H), 8.09-8.03 (m, 2H), 4.73 (t, $J = 6.1$ Hz, 1H), 3.00 (td, $J = 7.1, 6.0$ Hz, 2H), 1.53-1.44 (m, 3H), 1.17-1.09 (m, 2H), 0.83-0.81 (m, 6H). ¹³C NMR (125 MHz, CDCl₃): $\delta = 150.2, 146.2, 128.4, 124.5, 43.8, 35.7, 27.7, 27.7, 22.5$. IR ν (cm⁻¹): 3258, 2944, 2873, 1529. HRMS: Mass calculated for C₁₂H₁₈N₂NaO₄S: 309.0879, found: 309.0882. mp: 66 - 67 °C.

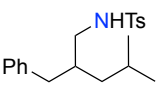
N-(5-methylhexan-2-yl)methanesulfonamide (27c)

 Compound **27c** was synthesized following GP2, it was obtained as a white solid. ¹H NMR (400 MHz, CDCl₃): $\delta = 3.48-3.40$ (m, 1H), 2.96 (s, 3H), 1.59-1.43 (m, 3H), 1.33-1.14 (m, 6H), 0.88 (dd, $J = 6.6, 1.8$ Hz, 6H). ¹³C NMR (100 MHz, CDCl₃): $\delta = 50.8, 42.0, 35.7, 35.0, 28.0, 22.7, 22.6, 22.5$. IR ν (cm⁻¹): 3273, 2954. HRMS: Mass calculated for C₈H₁₉NNaO₂S: 216.1029, found: 216.1026. mp: 38 - 39 °C.

N-(2-ethyl-4-methylpentyl)-4-methylbenzenesulfonamide (27d)

 Compound **27d** was synthesized following GP2, it was obtained as a colorless oil. ¹H NMR (500 MHz, CDCl₃): $\delta = 7.77-7.73$ (m, 2H), 7.33-7.28 (m, 2H), 4.70 (t, $J = 6.3$ Hz, 1H), 2.91-2.75 (m, 2H), 2.42 (s, 3H), 1.50 (p, $J = 6.7$ Hz, 1H), 1.42 (p, $J = 6.3$ Hz, 1H), 1.30-1.22 (m, 2H), 1.03 (t, $J = 7.1$ Hz, 2H), 0.81-0.75 (m, 9H). ¹³C NMR (125 MHz, CDCl₃): $\delta = 143.4, 137.2, 129.8, 127.2, 46.0, 40.8, 36.8, 25.2, 24.2, 22.8, 21.6, 10.6$. IR ν (cm⁻¹): 3283, 2956. HRMS: Mass calculated for C₁₅H₂₅NNaO₂S: 306.1498, found: 306.1504.

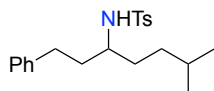
N-(2-benzyl-4-methylpentyl)-4-methylbenzenesulfonamide (27e)

 Compound **27e** was synthesized following GP2, it was obtained as a colorless oil. ¹H NMR (400 MHz, CDCl₃): $\delta = 7.77-7.71$ (m, 2H), 7.32-7.27 (m, 2H), 7.25-7.15 (m, 3H), 7.09-7.02 (m, 2H), 5.14 (t, $J = 6.3$ Hz, 1H), 2.91-2.76 (m, 2H), 2.55 (d, $J = 7.0$ Hz, 2H), 2.42 (s, 3H), 1.91-1.79 (m, 1H), 1.66-1.52 (m, 1H), 1.24-1.04 (m, 2H), 0.80 (dd, $J = 14.8, 6.6$ Hz, 6H). ¹³C NMR (100 MHz, CDCl₃): δ

Chapter IV. Iodine Catalysis for C(sp³)-H Fluorination
with a Nucleophilic Fluorine Source

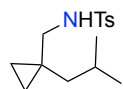
= 143.3, 140.0, 137.0, 129.7, 129.2, 128.3, 127.2, 126.0, 46.0, 40.9, 38.4, 37.6, 25.1, 22.8, 22.5, 21.5. IR ν (cm⁻¹): 3275, 2921. HRMS: Mass calculated for C₂₀H₂₇NNaO₂S: 368.1655, found: 368.1656. mp: 105 - 106 °C.

4-methyl-N-(6-methyl-1-phenylheptan-3-yl)benzenesulfonamide (27f)



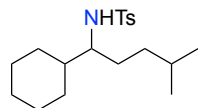
Compound **27f** was synthesized following GP2, it was obtained as a white solid. ¹H NMR (500 MHz, CDCl₃): δ = 7.81-7.77 (m, 2H), 7.31-7.27 (m, 2H), 7.26-7.22 (m, 2H), 7.20-7.15 (m, 1H), 7.07-7.02 (m, 2H), 4.93 (d, *J* = 8.5 Hz, 1H), 3.31-3.20 (m, 1H), 2.66-2.55 (m, 1H), 2.53-2.46 (m, 1H), 2.42 (s, 3H), 1.77-1.68 (m, 1H), 1.67-1.58 (m, 1H), 1.47-1.38 (m, 1H), 1.38-1.27 (m, 2H), 1.10-0.95 (m, 2H), 0.77-0.74 (m, 6H). ¹³C NMR (125 MHz, CDCl₃): δ = 143.2, 141.6, 138.6, 129.7, 128.4, 128.4, 127.2, 125.9, 54.2, 36.8, 34.3, 32.8, 31.8, 27.8, 22.5, 22.4, 21.5. IR ν (cm⁻¹): 3278, 2953, 2867. HRMS: Mass calculated for C₂₁H₂₉NNaO₂S: 382.1811, found: 382.1808. mp: 60 - 61 °C.

N-((1-isobutylcyclopropyl)methyl)-4-methylbenzenesulfonamide (27g)



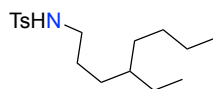
Compound **27g** was synthesized following GP2, it was obtained as a colorless oil. ¹H NMR (500 MHz, CDCl₃): δ = 7.77-7.73 (m, 2H), 7.31-7.27 (m, 2H), 4.92 (t, *J* = 6.0 Hz, 1H), 2.74 (d, *J* = 6.0 Hz, 2H), 2.40 (s, 3H), 1.66-1.55 (m, 1H), 1.12 (d, *J* = 7.4 Hz, 2H), 0.80 (d, *J* = 6.6 Hz, 6H), 0.26-0.23 (m, 4H). ¹³C NMR (125 MHz, CDCl₃): δ = 143.3, 137.0, 129.7, 127.2, 49.2, 43.1, 25.9, 23.0, 21.6, 17.9, 11.0. IR ν (cm⁻¹): 3245, 2951. HRMS: Mass calculated for C₁₅H₂₃NNaO₂S: 304.1342, found: 304.1348. mp: 56 - 57 °C.

N-(1-cyclohexyl-4-methylpentyl)-4-methylbenzenesulfonamide (27h)



Compound **27h** was synthesized following GP2, it was obtained as a colorless oil. ¹H NMR (400 MHz, CDCl₃): δ = 7.76-7.71 (m, 2H), 7.32-7.26 (m, 2H), 4.28 (d, *J* = 9.0 Hz, 1H), 3.09-2.98 (m, 1H), 2.76 (t, *J* = 6.4 Hz, 1H), 2.41 (s, 3H), 1.73-1.57 (m, 6H), 1.40-1.25 (m, 3H), 1.21-1.05 (m, 4H), 0.93-0.82 (m, 2H), 0.71 (dd, *J* = 6.6, 2.7, 6H). ¹³C NMR (100 MHz, CDCl₃): δ = 143.2, 138.8, 129.6, 127.2, 59.3, 41.5, 34.7, 30.7, 29.7, 29.1, 28.4, 27.9, 26.5, 26.4, 25.8, 22.6, 22.4, 21.6. IR ν (cm⁻¹): 3282, 2925, 2853. HRMS: Mass calculated for C₁₉H₃₁NNaO₂S: 360.1968, found: 360.1977.

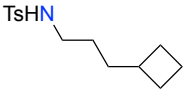
N-(4-ethyloctyl)-4-methylbenzenesulfonamide (27i)



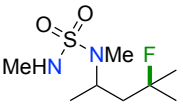
Compound **27i** was synthesized following GP2, it was obtained as a colorless oil. ¹H NMR (500 MHz, CDCl₃): δ = 7.78-7.73 (m, 2H), 7.30-7.26 (m, 2H), 5.03 (bs, 1H), 2.95-2.84 (m, 2H), 2.40 (s, 3H), 1.45-1.34 (m, 2H), 1.26-1.07 (m, 9H), 0.84 (t, *J* = 7.2 Hz, 3H), 0.75 (t, *J* = 7.3 Hz, 3H). ¹³C NMR (125 MHz, CDCl₃): δ = 143.3, 137.2, 129.7, 127.2, 43.8, 38.5, 32.7, 30.1, 28.9, 26.8,

25.7, 23.1, 21.5, 14.2, 10.8. IR ν (cm⁻¹): 3281, 2925, 2858. HRMS: Mass calculated for C₁₇H₂₉NNaO₂S: 334.1811, found: 334.1812.

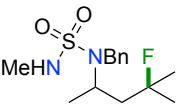
N-(3-cyclobutylpropyl)-4-methylbenzenesulfonamide (27j)

 Compound **27j** was synthesized following GP2, it was obtained as a colorless oil. ¹H NMR (500 MHz, CDCl₃): δ = 7.77-7.72 (m, 2H), 7.31-7.26 (m, 2H), 4.93 (bs, 1H), 2.89-2.83 (m, 2H), 2.40 (s, 3H), 2.17-2.08 (m, 1H), 2.00-1.85 (m, 1H), 1.84-1.66 (m, 2H), 1.56-1.40 (m, 2H), 1.34-1.28 (m, 4H). ¹³C NMR (125 MHz, CDCl₃): δ = 143.3, 137.1, 129.7, 127.2, 43.3, 35.5, 33.8, 28.2, 27.3, 21.6, 18.4. IR ν (cm⁻¹): 3253, 2938. HRMS: Mass calculated for C₁₅H₂₁NNaO₂S: 290.1191, found: 290.1194.

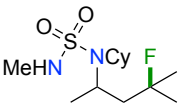
2-Methyl-2-fluoro-4-(methyl(N-methylsulfamoyl)amino)pentane (26a)

 Compound **26a** was synthesized following GP3, it was obtained in 88% yield as a yellow oil. ¹H NMR (400 MHz, CDCl₃): δ = 4.22 (sext, J = 6.7 Hz, 1H), 4.08 (bs, 1H), 2.70 (s, 3H), 2.67 (d, J = 5.4 Hz, 3H), 1.93 (ddd, J = 22.0, 14.7, 6.6 Hz, 1H), 1.70 (ddd, J = 20.0, 14.8, 6.5 Hz, 1H), 1.41 (d, J = 21.5 Hz, 6H), 1.27-1.22 (m, 3H). ¹³C NMR (100 MHz, CDCl₃): δ = 94.9 (d, J = 166.2 Hz), 50.0 (d, J = 2.6 Hz), 45.2 (d, J = 21.8 Hz), 29.4, 28.3, 27.4 (d, J = 24.6 Hz), 26.8 (d, J = 24.8 Hz), 19.5 (d, J = 2.2 Hz). ¹⁹F{¹H} NMR (375 MHz, CDCl₃): δ = -137.23. IR ν (cm⁻¹): 3311, 2975, 2936. HRMS: Mass calculated for C₈H₁₉FN₂NaO₂S: 249.1043, found: 249.1043.

2-Methyl-2-fluoro-4-(benzyl(N-methylsulfamoyl)amino)pentane (26b)

 Compound **26b** was synthesized following GP3, it was obtained in 90% yield as a yellow oil. ¹H NMR (400 MHz, CDCl₃): δ = 7.48-7.27 (m, 5H), 4.31 (s, 2H), 4.11-4.01 (m, 1H), 3.77 (bs, 1H), 2.55 (d, J = 5.4 Hz, 2H), 2.01 (ddd, J = 27.4, 14.7, 3.9 Hz, 1H), 1.80 (ddd, J = 17.6, 14.7, 8.3 Hz, 1H), 1.45-1.18 (m, 9H). ¹³C NMR (100 MHz, CDCl₃): δ = 138.1, 128.8, 128.7, 128.6, 127.9, 127.0, 94.9 (d, J = 166.8 Hz), 52.0, 48.7, 46.8 (d, J = 21.4 Hz), 29.4, 28.1 (d, J = 24.6 Hz), 26.4 (d, J = 24.8 Hz), 20.9 (d, J = 3.1 Hz). ¹⁹F{¹H} NMR (375 MHz, CDCl₃): δ = -138.96. IR ν (cm⁻¹): 3311, 2979, 2936. HRMS: Mass calculated for C₁₄H₂₃FN₂NaO₂S: 325.1356, found: 325.1345.

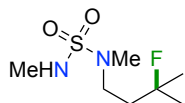
2-Methyl-2-fluoro-4-(cyclohexyl(N-methylsulfamoyl)amino)pentane (26c)

 Compound **26c** was synthesized following GP3, it was obtained in 76% yield as a colorless oil. ¹H NMR (500 MHz, CDCl₃): δ = 4.00 (bs, 1H), 3.77-3.70 (m, 1H), 3.28-3.12 (m, 1H), 2.68-2.66 (m, 3H), 2.20-2.07 (m, 1H), 1.99 (ddd, J = 25.6, 14.7, 2.7 Hz, 1H), 1.89-1.70 (m, 6H), 1.66-1.58 (m, 1H), 1.45-1.35 (m, 9H), 1.34-1.22 (m, 2H), 1.17-1.06 (m, 1H). ¹³C NMR (125 MHz, CDCl₃): δ = 95.0 (d, J = 166.9 Hz), 58.3, 49.6, 48.2 (d, J = 21.7 Hz), 32.2 (d, J = 14.8

Chapter IV. Iodine Catalysis for C(sp³)-H Fluorination
with a Nucleophilic Fluorine Source

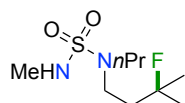
Hz), 29.2, 28.1 (d, *J* = 24.9 Hz), 27.1 (d, *J* = 24.7 Hz), 26.6, 26.6, 25.4, 21.9 (d, *J* = 3.0 Hz). ¹⁹F{¹H} NMR (470 MHz, CDCl₃): δ = -139.48. IR ν (cm⁻¹): 3311, 3303, 2978, 2929, 2855. HRMS: Mass calculated for C₁₃H₂₇FN₂NaO₂S: 317.1669, found: 317.1682.

2-Methyl-2-fluoro-4-(methyl(N-methylsulfamoyl)amino)butane (26d)



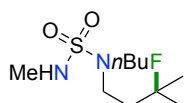
Compound **26d** was synthesized following GP3, it was obtained in 49% yield as a yellow oil. ¹H NMR (400 MHz, CDCl₃): δ = 4.08 (bs, 1H), 3.39-3.23 (m, 2H), 2.83 (s, 3H), 2.70 (d, *J* = 5.3 Hz, 3H), 2.05-1.85 (m, 2H), 1.41 (s, 3H), 1.36 (s, 3H). ¹³C NMR (100 MHz, CDCl₃): δ = 94.5 (d, *J* = 166.1 Hz), 46.3 (d, *J* = 5.8 Hz), 39.0 (d, *J* = 22.5 Hz), 35.1, 29.6, 27.0, 26.8. ¹⁹F{¹H} NMR (375 MHz, CDCl₃): δ = -140.05. IR ν (cm⁻¹): 3311, 2981, 2937. HRMS: Mass calculated for C₇H₁₇FN₂NaO₂S: 235.0887, found: 235.0878.

2-Methyl-2-fluoro-4-(propyl(N-methylsulfamoyl)amino)butane (26e)



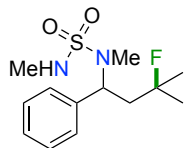
Compound **26e** was synthesized following GP3, it was obtained in 66% yield as a yellow oil. ¹H NMR (400 MHz, CDCl₃): δ = 4.09 (bs, *J* = 5.2 Hz, 1H), 3.40-3.32 (m, 2H), 3.21-3.13 (m, 2H), 2.70 (d, *J* = 5.4 Hz, 3H), 2.03-1.92 (m, 2H), 1.70-1.58 (m, 2H), 1.42 (s, 3H), 1.37 (s, 3H), 0.98-0.91 (t, *J* = 7.4 Hz, 3H). ¹³C NMR (100 MHz, CDCl₃): δ = 94.4 (d, *J* = 165.8 Hz), 49.8, 43.3 (d, *J* = 5.5 Hz), 39.5 (d, *J* = 22.4 Hz), 29.2, 26.9, 26.6, 21.6, 11.2. ¹⁹F{¹H} NMR (375 MHz, CDCl₃): δ = -140.74. IR ν (cm⁻¹): 3307, 2968, 2934, 2876. HRMS: Mass calculated for C₉H₂₁FN₂NaO₂S: 263.1200, found: 263.1201.

2-Methyl-2-fluoro-4-(butyl(N-methylsulfamoyl)amino)butane (26f)



Compound **26f** was synthesized following GP3, it was obtained in 40% yield as a yellowish oil. ¹H NMR (400 MHz, CDCl₃): δ = 4.12 (bs, 1H), 3.37-3.29 (m, 2H), 3.22-3.12 (m, 2H), 2.69-2.65 (m, 3H), 2.02-1.85 (m, 2H), 1.64-1.53 (m, 2H), 1.43-1.22 (m, 6H), 0.98-0.88 (m, 5H). ¹³C NMR (100 MHz, CDCl₃): δ = 94.6 (d, *J* = 165.8 Hz), 48.0, 43.3, 39.6 (d, *J* = 22.3 Hz), 30.6, 29.8, 29.4, 26.9 (d, *J* = 24.6 Hz), 20.1, 13.9. ¹⁹F{¹H} NMR (375 MHz, CDCl₃): δ = -140.72. IR ν (cm⁻¹): 3307, 2959, 5928, 2873. HRMS: Mass calculated for C₁₀H₂₃FN₂NaO₂S: 277.1356, found: 277.1361.

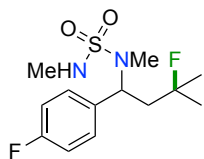
2-Methyl-2-fluoro-4,4-phenyl-(methyl(N-methylsulfamoyl)amino)butane (26g)



Compound **26g** was synthesized following GP3, it was obtained in 78% yield as a yellow oil. ¹H NMR (400 MHz, CDCl₃): δ = 7.46-7.28 (m, 5H), 5.30 (t, *J* = 6.9 Hz, 1H), 3.94 (bs, 1H), 2.67 (s, 3H), 2.57 (d, *J* = 5.4 Hz, 3H), 2.42-2.25 (m, 2H), 1.43 (d, *J* = 2.1 Hz, 3H), 1.38 (d, *J* = 2.1 Hz, 3H). ¹³C NMR (125 MHz, CDCl₃): δ = 139.0, 128.7, 128.3, 128.2, 94.9 (d, *J* = 166.8 Hz), 57.3 (d, *J* = 4.2 Hz), 41.9 (d, *J* = 22.5 Hz), 29.5, 29.3, 27.9 (d, *J* = 24.5 Hz), 26.7 (d, *J* = 24.6 Hz). ¹⁹F{¹H} NMR (470 MHz, CDCl₃): δ = -136.40. IR ν (cm⁻¹): 3312, 2978,

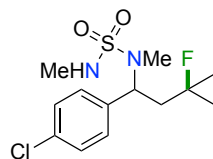
2958, 2918, 2849. HRMS: Mass calculated for C₁₃H₂₁FN₂NaO₂S: 311.1200, found: 311.1200.

2-Methyl-2-fluoro-4,4-p-fluorophenyl-(methyl(N-methylsulfamoyl)amino)butane (26h)



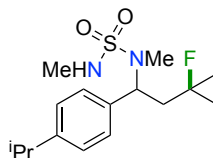
Compound **26h** was synthesized following GP3, it was obtained in 70% yield as a yellow oil. ¹H NMR (400 MHz, CDCl₃): δ = 7.44-7.36 (m, 2H), 7.10-7.00 (m, 2H), 5.30 (t, *J* = 6.9 Hz, 1H), 4.02 (bs, 1H), 2.63 (s, 3H), 2.59 (d, *J* = 5.3 Hz, 3H), 2.41-2.18 (m, 2H), 1.43 (d, *J* = 4.5 Hz, 3H), 1.38 (d, *J* = 4.5 Hz, 3H). ¹³C NMR (125 MHz, CDCl₃): δ = 162.5 (d, *J* = 247.1 Hz), 134.9 (d, *J* = 3.3 Hz), 130.0 (d, *J* = 8.0 Hz), 115.5 (d, *J* = 21.4 Hz), 94.8 (d, *J* = 167.0 Hz), 56.5 (d, *J* = 3.7 Hz), 42.0 (d, *J* = 22.4 Hz), 29.3, 29.3, 27.8 (d, *J* = 24.6 Hz), 26.8 (d, *J* = 24.8 Hz). ¹⁹F{¹H} NMR (470 MHz, CDCl₃): δ = -114.10, -137.01. IR ν (cm⁻¹): 3312, 2980, 2938, 1650, 1510. HRMS: Mass calculated for C₁₃H₂₀F₂N₂NaO₂S: 329.1106, found: 329.1103.

2-Methyl-2-fluoro-4,4-p-chlorophenyl-(methyl(N-methylsulfamoyl)amino)butane (26i)



Compound **26i** was synthesized following GP3, it was obtained in 54% yield as a colorless oil. ¹H NMR (400 MHz, CDCl₃): δ = 7.42-7.29 (m, 4H), 5.29 (t, *J* = 6.9 Hz, 1H), 3.97 (bs, 1H), 2.64-2.58 (m, 6H), 2.39-2.19 (m, 2H), 1.44 (d, *J* = 5.3 Hz, 3H), 1.38 (d, *J* = 5.3 Hz, 3H). ¹³C NMR (125 MHz, CDCl₃): δ = 137.6, 134.1, 129.7, 128.9, 94.7 (d, *J* = 167.4 Hz), 56.5 (d, *J* = 3.6 Hz), 41.8 (d, *J* = 22.3 Hz), 29.8, 29.3, 27.8 (d, *J* = 24.7 Hz), 26.8 (d, *J* = 24.6 Hz). ¹⁹F{¹H} NMR (375 MHz, CDCl₃): δ = -137.21. IR ν (cm⁻¹): 3312, 2976, 2926. HRMS: Mass calculated for C₁₃H₂₀ClFN₂NaO₂S: 345.0810, found: 345.0817.

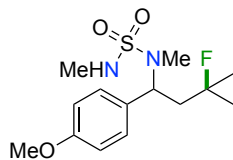
2-Methyl-2-fluoro-4,4-p-isoropopylphenyl-(methyl(N-methylsulfamoyl)amino)butane (26j)



Compound **26j** was synthesized following GP3, it was obtained in 69% yield as a colorless oil. ¹H NMR (400 MHz, CDCl₃): δ = 7.35-7.29 (m, 2H), 7.23-7.18 (m, 2H), 5.27 (t, *J* = 6.9 Hz, 1H), 2.96-2.84 (m, 1H), 2.66 (s, 3H), 2.58 (s, 3H), 2.41-2.18 (m, 2H), 1.43 (s, 3H), 1.38 (s, 3H), 1.26-1.22 (m, 6H). ¹³C NMR (100 MHz, CDCl₃): δ = 148.9, 136.3, 128.2, 126.7, 95.0 (d, *J* = 166.5 Hz), 57.0 (d, *J* = 4.2 Hz), 41.9 (d, *J* = 22.4 Hz), 33.9, 29.8, 29.5, 29.3, 27.9 (d, *J* = 24.5 Hz), 26.6 (d, *J* = 24.6 Hz), 24.1, 24.0. ¹⁹F{¹H} NMR (375 MHz, CDCl₃): δ = -136.27. IR ν (cm⁻¹): 3311, 2959, 2926, 2871. HRMS: Mass calculated for C₁₆H₂₇FN₂NaO₂S: 353.1669, found: 353.1666.

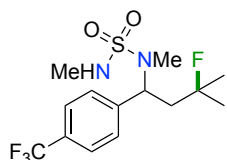
2-Methyl-2-fluoro-4,4-p-methoxyphenyl-(methyl(N-methylsulfamoyl)amino)butane (26k)

Chapter IV. Iodine Catalysis for C(sp³)-H Fluorination
with a Nucleophilic Fluorine Source



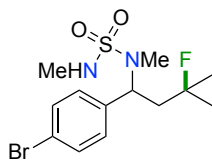
Compound **26k** was synthesized following GP3, it was obtained in 63% yield as a yellow oil. ¹H NMR (500 MHz, CDCl₃): δ = 7.35-7.30 (m, 2H), 6.91-6.86 (m, 2H), 5.24 (t, *J* = 6.9 Hz, 1H), 3.80 (s, 3H), 2.64 (s, 3H), 2.57 (d, *J* = 4.2 Hz, 3H), 2.40-2.21 (m, 2H), 1.42-1.35 (m, 6H). ¹³C NMR (125 MHz, CDCl₃): δ = 159.4, 131.0, 129.5, 114.0, 95.0 (d, *J* = 166.8 Hz), 56.7 (d, *J* = 4.2 Hz), 55.4, 42.1 (d, *J* = 22.6 Hz), 29.8, 29.3, 29.3, 27.8 (d, *J* = 24.5 Hz), 26.7 (d, *J* = 24.5 Hz). ¹⁹F{¹H} NMR (470 MHz, CDCl₃): δ = -136.03. IR ν (cm⁻¹): 3314, 2977, 2935, 1610, 1513. HRMS: Mass calculated for C₁₄H₂₃FN₂NaO₃S: 341.1306, found: 341.1311.

2-Methyl-2-fluoro-4,4-p-trifluoromethylphenyl-(methyl(N-methylsulfamoyl)amino)butane (26l)



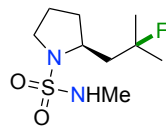
Compound **26l** was synthesized following GP3, it was obtained in 52% yield as a colorless oil. ¹H NMR (400 MHz, CDCl₃): δ = 7.65 (m, *J* = 8.1 Hz, 2H), 7.59-7.53 (m, 2H), 5.41 (t, *J* = 6.9 Hz, 1H), 4.03 (bs, 1H), 2.67 (s, 3H), 2.65 (d, *J* = 4.5 Hz, 3H), 2.45-2.26 (m, 2H), 1.48 (d, *J* = 6.4 Hz, 3H), 1.43 (d, *J* = 6.4 Hz, 3H). ¹³C NMR (125 MHz, CDCl₃): δ = 143.3, 130.7, 128.8, 125.9 (q, *J* = 4.0 Hz), 123.2 (q, *J* = 271.7 Hz), 94.9 (d, *J* = 167.6 Hz), 56.9, 41.8 (d, *J* = 22.2 Hz), 29.6, 29.5, 28.0 (d, *J* = 24.7 Hz), 27.1 (d, *J* = 24.6 Hz). ¹⁹F{¹H} NMR (470 MHz, CDCl₃): δ = -62.72, -137.77. IR ν (cm⁻¹): 3313, 2982, 2939. HRMS: Mass calculated for C₁₄H₂₀F₄N₂NaO₂S: 379.1074, found: 379.1083.

2-Methyl-2-fluoro-4,4-p-bromophenyl-(methyl(N-methylsulfamoyl)amino)butane (26m)



Compound **26m** was synthesized following GP3, it was obtained in 32% yield as a colorless oil. ¹H NMR (500 MHz, CDCl₃): δ = 7.48 (m, 2H), 7.28 (m, 2H), 5.26 (t, *J* = 6.9 Hz, 1H), 3.92 (bs, 1H), 2.61 (s, 3H), 2.59 (s, 3H), 2.36-2.19 (m, 2H), 1.41 (d, *J* = 7.0 Hz, 3H), 1.37 (d, *J* = 7.1 Hz, 3H). ¹³C NMR (100 MHz, CDCl₃): δ = 137.9, 131.7, 129.9, 122.1, 94.6 (d, *J* = 167.6 Hz), 56.4, 41.5 (d, *J* = 22.3 Hz), 29.7, 29.2, 27.7 (d, *J* = 24.7 Hz), 26.6 (d, *J* = 24.7 Hz). ¹⁹F{¹H} NMR (470 MHz, CDCl₃): δ = -137.23. IR ν (cm⁻¹): 3306, 2978, 2924, 2852. HRMS: Mass calculated for C₁₃H₂₀BrFN₂NaO₂S: 389.0305, found: 389.0307.

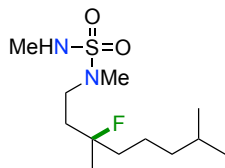
(S)-2-(2-fluoro-2-methylpropyl)-N-methylpyrrolidine-1-sulfonamide (26n)



Compound **26n** was synthesized following GP3, it was obtained in 70% yield as a yellow oil. ¹H NMR (400 MHz, CDCl₃): δ = 4.08 (bs, 1H), 4.02-3.95 (m, 1H), 3.40-3.30 (m, 1H), 3.30-3.19 (m, 1H), 2.73 (d, *J* = 5.4 Hz, 3H), 2.22-2.05 (m, 2H), 1.96-1.75 (m, 4H), 1.45-1.33 (m, 6H). ¹³C NMR (100 MHz, CDCl₃): δ = 95.1 (d, *J* = 165.6 Hz), 57.4, 48.6, 46.8 (d, *J* = 20.5 Hz), 32.7 (d, *J* = 4.1 Hz), 29.7, 29.1 (d, *J* = 24.5 Hz), 25.6 (d, *J* = 24.8 Hz), 24.78. ¹⁹F{¹H} NMR (375 MHz,

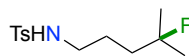
CDCl₃): δ = -138.68. IR ν (cm⁻¹): 3301, 2978, 2958, 2917, 2849. HRMS: Mass calculated for C₉H₁₉FN₂NaO₂S: 261.1043, found: 261.1056.

2-Methyl-6-fluoro-6-methyl-8-(methyl(N-methylsulfamoyl)amino)octane (26o)



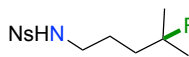
Compound **26o** was synthesized following GP3, it was obtained in 55% yield as a colorless oil. ¹H NMR (500 MHz, CDCl₃): δ = 4.01 (bs, 1H), 3.37-3.22 (m, 2H), 2.82 (s, 3H), 2.69-2.67 (m, 3H), 2.00-1.81 (m, 2H), 1.64-1.50 (m, 3H), 1.40-1.28 (m, 5H), 1.20-1.13 (m, 2H), 0.86 (d, J = 6.6 Hz, 6H). ¹³C NMR (100 MHz, CDCl₃): δ = 96.6 (d, J = 167.7 Hz), 46.4 (d, J = 5.9 Hz), 40.4 (d, J = 22.6 Hz), 39.5, 37.5 (d, J = 22.6 Hz), 35.4, 29.8, 28.2, 24.5 (d, J = 24.9 Hz), 22.9, 22.9, 21.7 (d, J = 6.0 Hz). ¹⁹F{¹H} NMR (470 MHz, CDCl₃): δ = -145.58. IR ν (cm⁻¹): 3308, 2952, 2870. HRMS: Mass calculated for C₁₂H₂₇FN₂NaO₂S: 305.1669, found: 305.1655.

N-(4-fluoro-4-methylpentyl)-4-methylbenzenesulfonamide (28a)



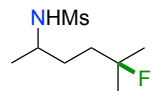
Compound **28a** was synthesized following GP3, it was obtained in 63% yield as a colorless oil. ¹H NMR (500 MHz, CDCl₃): δ = 7.77-7.72 (m, 2H), 7.35-7.27 (m, 2H), 4.38 (t, J = 6.2 Hz, 1H), 3.01-2.93 (m, 2H), 2.43 (s, 3H), 1.63-1.51 (m, 4H), 1.29 (d, J = 21.4 Hz, 6H). ¹³C NMR (125 MHz, CDCl₃): δ = 143.6, 137.2, 129.9, 127.2, 95.4 (d, J = 165.5 Hz), 43.5, 38.2 (d, J = 23.1 Hz), 29.8, 26.7 (d, J = 24.6 Hz), 24.4 (d, J = 4.2 Hz), 21.6. ¹⁹F{¹H} NMR (470 MHz, CDCl₃): δ = -139.04. IR ν (cm⁻¹): 3285, 2977, 2959, 2929, 2871, 1598. HRMS: Mass calculated for C₁₃H₂₀FNNaO₂S: 296.1091, found: 296.1097.

N-(4-fluoro-4-methylpentyl)-4-nitrobenzenesulfonamide (28b)



Compound **28b** was synthesized following GP3, it was obtained in 60% yield as a white solid. ¹H NMR (500 MHz, CDCl₃): δ = 8.39-8.35 (m, 2H), 8.08-8.03 (m, 2H), 4.68 (t, J = 6.2 Hz, 1H), 3.06 (q, J = 6.5 Hz, 2H), 1.69-1.50 (m, 4H), 1.31 (d, J = 21.4 Hz, 6H). ¹³C NMR (125 MHz, CDCl₃): δ = 150.2, 146.2, 128.4, 124.6, 95.4 (d, J = 165.2 Hz), 43.6, 38.0 (d, J = 22.9 Hz), 26.8 (d, J = 24.7 Hz), 24.5 (d, J = 3.8 Hz). ¹⁹F{¹H} NMR (470 MHz, CDCl₃): δ = -139.18. IR ν (cm⁻¹): 3276, 2978, 1529. HRMS: Mass calculated for C₁₂H₁₇FN₂NaO₄S: 327.0785, found: 327.0791. mp: 76 - 77 °C.

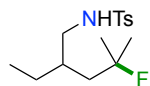
N-(5-fluoro-5-methylhexan-2-yl)methanesulfonamide (28c)



Compound **28c** was synthesized following GP3, it was obtained in 62% yield as a yellow oil. ¹H NMR (400 MHz, CDCl₃): δ = 4.29-4.18 (m, 1H), 3.57-3.41 (m, 1H), 2.97 (s, 3H), 1.82-1.52 (m, 4H), 1.35 (dd, J = 21.4, 2.0 Hz, 5H), 1.26 (d, J = 6.6 Hz, 3H). ¹³C NMR (100 MHz, CDCl₃): δ = 95.3 (d, J = 165.6 Hz), 50.6, 42.0, 37.5 (d, J = 23.0 Hz), 32.0 (d, J = 4.3 Hz), 27.0 (d, J = 18.0 Hz), 26.7 (d, J = 18.0 Hz), 22.6. ¹⁹F{¹H} NMR (375 MHz, CDCl₃): δ = -139.15. IR ν (cm⁻¹): 3282, 2978, 2935, 2873. HRMS: Mass calculated for C₈H₁₈FNNaO₂S: 234.0934, found: 234.0940.

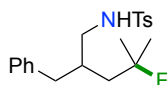
Chapter IV. Iodine Catalysis for C(sp³)-H Fluorination
with a Nucleophilic Fluorine Source

N-(2-ethyl-4-fluoro-4-methylpentyl)-4-methylbenzenesulfonamide (28d)



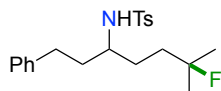
Compound **28d** was synthesized following GP3, it was obtained in 35% yield as a yellow oil. ¹H NMR (500 MHz, CDCl₃): δ = 7.76-7.68 (m, 2H), 7.31-7.28 (m, 2H), 4.58-4.53 (m, 1H), 2.95-2.87 (m, 2H), 2.42 (s, 3H), 1.66-1.60 (m, 1H), 1.61-1.51 (m, 3H), 1.49-1.37 (m, 1H), 1.36-1.24 (m, 6H), 0.84 (t, *J* = 7.4 Hz, 3H). ¹³C NMR (125 MHz, CDCl₃): δ = 143.4, 137.3, 129.8, 127.2, 96.5 (d, *J* = 164.3 Hz), 46.4 (d, *J* = 2.5 Hz), 42.7 (d, *J* = 21.5 Hz), 35.9, 28.4 (d, *J* = 25.1 Hz), 26.1 (d, *J* = 24.7 Hz), 26.0, 21.6, 11.1. ¹⁹F{¹H} NMR (470 MHz, CDCl₃): δ = -137.88. IR ν (cm⁻¹): 2962, 2926, 2874, 2860, 1599. HRMS: Mass calculated for C₁₅H₂₄FNNaO₂S: 324.1409, found: 324.1511.

N-(2-benzyl-4-fluoro-4-methylpentyl)-4-methylbenzenesulfonamide (28e)



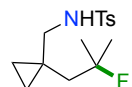
Compound **28e** was synthesized following GP3, it was obtained in 35% yield as a colorless. Colorless oil. 35%. ¹H NMR (400 MHz, CDCl₃): δ = 7.70-7.62 (m, 2H), 7.32-7.23 (m, 5H), 7.14-7.08 (m, 2H), 4.58 (bs, 1H), 2.99-2.86 (m, 2H), 2.69 (dd, *J* = 13.7, 7.3 Hz, 1H), 2.56 (dd, *J* = 13.8, 7.1 Hz, 1H), 2.42 (s, 3H), 2.11-1.98 (m, 1H), 1.71-1.60 (m, 1H), 1.59-1.42 (m, 1H), 1.36-1.17 (m, 6H). ¹³C NMR (125 MHz, CDCl₃): δ = 143.4, 139.8, 137.1, 129.8, 129.4, 128.6, 127.25, 126.4, 96.6 (d, *J* = 164.3 Hz), 46.5 (d, *J* = 2.7 Hz), 42.4 (d, *J* = 21.3 Hz), 39.8, 36.6, 31.6 (d, *J* = 22.3 Hz), 28.5 (d, *J* = 25.0 Hz), 25.9 (d, *J* = 24.6 Hz), 21.6. ¹⁹F{¹H} NMR (375 MHz, CDCl₃): δ = -137.71. IR ν (cm⁻¹): 3284, 3027, 2978, 2927, 2864, 2599. HRMS: Mass calculated for C₂₂H₂₆FNNaO₂S: 386.1560, found: 386.1561.

N-(6-fluoro-6-methyl-1-phenylheptan-3-yl)-4-methylbenzenesulfonamide (28f)



Compound **28f** was synthesized following GP3, it was obtained in 98% yield as a yellow oil. ¹H NMR (400 MHz, CDCl₃): δ = 7.78-7.71 (m, 2H), 7.31-7.27 (m, 2H), 7.25-7.20 (m, 2H), 7.21-7.16 (m, 1H), 7.05-6.98 (m, 2H), 4.41 (d, *J* = 8.7 Hz, 1H), 3.35-3.22 (m, 1H), 2.61-2.45 (m, 2H), 2.42 (s, 3H), 1.76-1.66 (m, 1H), 1.65-1.52 (m, 2H), 1.49-1.36 (m, 2H), 1.32-1.18 (m, 7H). ¹³C NMR (100 MHz, CDCl₃): δ = 143.5, 141.3, 138.4, 129.8, 128.6, 128.4, 127.2, 126.1, 95.2 (d, *J* = 165.6 Hz), 54.1, 37.1, 31.8, 29.3 (d, *J* = 4.4 Hz), 26.8 (d, *J* = 6.2 Hz), 26.6 (d, *J* = 6.3 Hz), 21.6. ¹⁹F{¹H} NMR (375 MHz, CDCl₃): δ = -139.41. IR ν (cm⁻¹): 3276, 3027, 2977, 2925, 1856, 1599. HRMS: Mass calculated for C₂₁H₂₈FNNaO₂S: 400.1717, found: 400.1719.

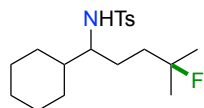
N-((1-(2-fluoro-2-methylpropyl)cyclopropyl)methyl)-4-methylbenzenesulfonamide (28g)



Compound **28g** was synthesized following GP3, it was obtained in 54% yield as a colorless oil. ¹H NMR (500 MHz, CDCl₃): δ = 7.75-7.65 (m, 2H), 7.29-7.26 (m, 2H), 4.87 (bs, 1H), 2.86 (d, *J* = 5.9 Hz, 2H), 2.41 (s, 3H), 1.59 (d, *J* = 26.0 Hz, 2H), 1.36 (d, *J* = 21.8 Hz, 6H), 0.53-0.46 (m, 2H), 0.39-0.30 (m, 2H). ¹³C NMR (125 MHz, CDCl₃): δ = 143.2, 137.8, 129.7, 127.1, 98.1 (d, *J* = 162.0 Hz), 50.4 (d, *J*

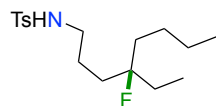
= 3.0 Hz), 45.7 (d, $J = 21.6$ Hz), 31.1, 27.4, 27.2, 21.6, 17.6, 12.2. $^{19}\text{F}\{^1\text{H}\}$ NMR (470 MHz, CDCl_3): $\delta = -136.53$. IR ν (cm^{-1}): 3283, 2980, 2928, 1599. HRMS: Mass calculated for $\text{C}_{15}\text{H}_{22}\text{FNNaO}_2\text{S}$: 322.1247, found: 322.1254.

N-(1-cyclohexyl-4-fluoro-4-methylpentyl)-4-methylbenzenesulfonamide (28h)



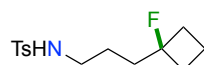
Compound **28h** was synthesized following GP3, it was obtained in 67% yield as a yellow oil. Two full sets of signals were observed due to the presence of two conformers in the cyclohexane moiety. ^1H NMR (400 MHz, CDCl_3): $\delta = 7.78$ -7.69 (m, 4H), 7.32-7.26 (m, 4H), 4.42 (bs, 1H), 4.33 (d, $J = 9.1$ Hz, 1H), 3.10-3.02 (m, 1H), 2.76 (t, $J = 5.8$ Hz, 2H), 2.45-2.38 (m, 6H), 1.75-1.46 (m, 14H), 1.43-1.04 (m, 20H), 1.01-0.78 (m, 6H). ^{13}C NMR (125 MHz, CDCl_3): $\delta = 143.4$, 143.3, 138.8, 137.2, 129.8, 129.7, 127.2, 127.2, 95.3 (d, $J = 165.7$ Hz), 59.2, 49.5, 41.8, 37.9, 37.34 (d, $J = 22.9$ Hz), 30.7, 28.9, 28.6, 26.8, 26.7, 26.6, 26.5, 26.4, 26.4, 26.4, 26.3, 26.1, 26.1, 25.8, 21.6, 21.6. $^{19}\text{F}\{^1\text{H}\}$ NMR (375 MHz, CDCl_3): $\delta = -139.55$. IR ν (cm^{-1}): 3283, 2977, 2923, 2852, 1599. HRMS: Mass calculated for $\text{C}_{19}\text{H}_{30}\text{FNNaO}_2\text{S}$: 378.1873, found: 378.1877.

N-(4-ethyl-4-fluorooctyl)-4-methylbenzenesulfonamide (28i)



Compound **28i** was synthesized following GP3, it was obtained in 74% yield as a dark yellow oil. ^1H NMR (400 MHz, CDCl_3): $\delta = 7.77$ -7.72 (m, 2H), 7.35-7.29 (m, 2H), 3.04-2.91 (m, 2H), 2.43 (s, 3H), 1.63-1.45 (m, 6H), 1.35-1.17 (m, 6H), 0.92-0.87 (t, $J = 7.2$ Hz, 3H), 0.86-0.81 (t, $J = 7.2$ Hz, 3H). ^{13}C NMR (100 MHz, CDCl_3): $\delta = 184.7$, 178.3, 171.0, 168.4, 140.3 (d, $J = 169.7$ Hz), 84.8, 77.2 (d, $J = 22.9$ Hz), 74.8 (d, $J = 23.4$ Hz), 70.6 (d, $J = 23.8$ Hz), 66.7 (d, $J = 6.3$ Hz), 64.9 (d, $J = 4.6$ Hz), 64.3, 62.8, 55.2, 49.0 (d, $J = 7.2$ Hz). $^{19}\text{F}\{^1\text{H}\}$ NMR (375 MHz, CDCl_3): $\delta = -152.13$. IR ν (cm^{-1}): 3283, 2956, 2929, 2871, 1598. HRMS: Mass calculated for $\text{C}_{17}\text{H}_{28}\text{FNNaO}_2\text{S}$: 352.1717, found: 352.1719.

N-(3-(1-fluorocyclobutyl)propyl)-4-methylbenzenesulfonamide (28j)



Compound **28j** was synthesized following GP3, it was obtained in 50% yield as a white solid. ^1H NMR (500 MHz, CDCl_3): $\delta = 7.77$ -7.72 (m, 2H), 7.33-7.29 (m, 2H), 4.50 (bs, 1H), 2.98 (q, $J = 6.6$ Hz, 2H), 2.43 (s, 3H), 2.33-2.18 (m, 2H), 2.05-1.93 (m, 2H), 1.85-1.74 (m, 1H), 1.73-1.63 (m, 2H), 1.62-1.54 (m, 2H), 1.45-1.38 (m, 1H). ^{13}C NMR (125 MHz, CDCl_3): $\delta = 143.6$, 137.2, 129.9, 127.2 (d, $J = 1.7$ Hz), 97.0 (d, $J = 211.3$ Hz), 43.4, 34.1 (d, $J = 23.2$ Hz), 33.5 (d, $J = 21.7$ Hz), 23.7, 23.7, 21.6, 11.7 (d, $J = 13.6$ Hz). $^{19}\text{F}\{^1\text{H}\}$ NMR (470 MHz, CDCl_3): $\delta = -130.79$. IR ν (cm^{-1}): 3243, 2993, 2941, 2868, 1598. HRMS: Mass calculated for $\text{C}_{14}\text{H}_{20}\text{FNNaO}_2\text{S}$: 308.1091, found: 308.1097. mp: 44 - 46 °C.

X-Ray Analytical Data for Compound 28j

Chapter IV. Iodine Catalysis for C(sp³)-H Fluorination
with a Nucleophilic Fluorine Source

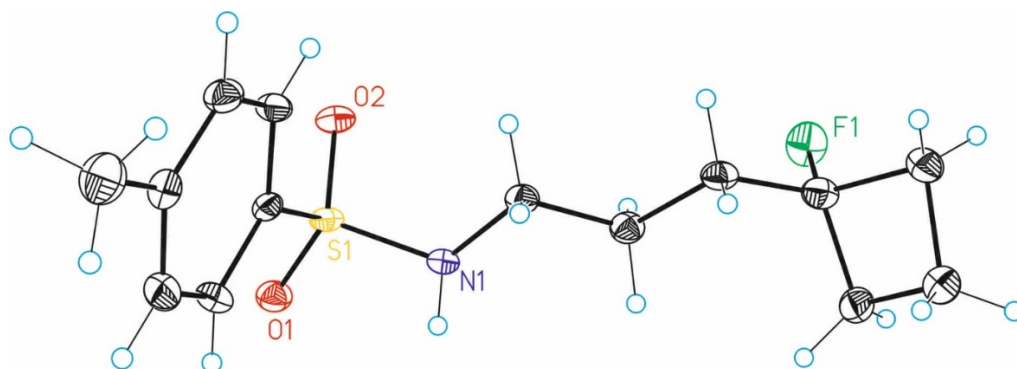
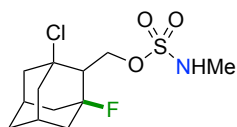


Table S-1. Crystal data and structure refinement for **28j**.

Identification code	28j	
Empirical formula	C ₁₄ H ₂₀ F N O ₂ S	
Formula weight	285.37	
Temperature	100(2)K	
Wavelength	0.71073 Å	
Crystal system	monoclinic	
Space group	C c	
Unit cell dimensions	a = 5.5561(10)Å	α = 90°.
	b = 27.536(5)Å	β = 101.529(5)°.
	c = 9.3762(16)Å	γ = 90°.
Volume	1405.5(4) Å ³	
Z	4	
Density (calculated)	1.349 Mg/m ³	
Absorption coefficient	0.240 mm ⁻¹	
F(000)	608	
Crystal size	0.500 x 0.400 x 0.040 mm ³	
Theta range for data collection	2.665 to 29.249°.	
Index ranges	-6<=h<=7,-37<=k<=36,-12<=l<=11	
Reflections collected	8503	

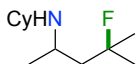
Independent reflections	2749[R(int) = 0.0407]
Completeness to theta =29.249°	95.3%
Absorption correction	Multi-scan
Max. and min. transmission	0.74 and 0.60
Refinement method	Full-matrix least-squares on F ²
Data / restraints / parameters	2749/ 2/ 177
Goodness-of-fit on F ²	1.002
Final R indices [I>2sigma(I)]	R1 = 0.0363, wR2 = 0.0778
R indices (all data)	R1 = 0.0523, wR2 = 0.0862
Largest diff. peak and hole	0.267 and -0.475 e.Å ⁻³

1-chloro-3-fluoroadamantan-2-yl)methyl methylsulfamate (30)



In a flamed-dried Schlenk flask the corresponding iodinated adamantane **30** (0.20 mmol)²¹⁴ was dissolved in 1ml of dry dichloromethane under an argon atmosphere. Subsequently, XeF₂ (0.20 mmol, 1.0 equiv.) was added to the reaction mixture, which was stirred at room temperature overnight. Saturated aqueous solution of Na₂S₂O₃ was added, the aqueous phase was extracted twice with dichloromethane and the combined organic fractions were washed with H₂O and brine solution. The final fluorinated product was obtained in 58% yield as a colorless oil after column chromatography purification on silica gel using *n*-Hex/EtOAc 90:10 as eluent. ¹H NMR (400 MHz, CDCl₃): δ = 4.50 (d, *J* = 3.6 Hz, 2H), 4.41 (bs, 1H), 2.83 (d, *J* = 4.8 Hz, 3H), 2.50-2.46 (m, 1H), 2.40-2.31 (m, 2H), 2.16-2.13 (m, 2H), 2.10-2.03 (m, 1H), 1.99-1.91 (m, 3H), 1.79-1.71 (m, 1H), 1.66-1.56 (m, 3H). ¹³C NMR (100 MHz, CDCl₃): δ = 93.4 (d, *J* = 193.7 Hz), 69.0 (d, *J* = 7.7 Hz), 67.1 (d, *J* = 3.3 Hz), 56.2 (d, *J* = 17.5 Hz), 48.4 (d, *J* = 1.8 Hz), 43.1 (d, *J* = 18.0 Hz), 42.0, 37.0 (d, *J* = 18.2 Hz), 34.1 (d, *J* = 2.0 Hz), 32.2 (d, *J* = 9.9 Hz), 31.6 (d, *J* = 9.8 Hz), 30.0. ¹⁹F{¹H} NMR (375 MHz, CDCl₃): δ = -139.76. IR ν (cm⁻¹): 3320, 2937, 2868. HRMS: Mass calculated for C₁₂H₁₉ClFNNaO₃S: 334.0650, found: 334.0647.

N-(4-fluoro-4-methylpentan-2-yl)cyclohexanamine (31)

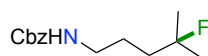


Compound **31** (0.30 mmol) was dissolved in 1mL of 1,3-diaminopropane and the reaction mixture was stirred at 150 °C for 3 hours. The reaction was cooled down to room temperature, diluted with water and extracted with ethyl acetate. After evaporation of the organic fraction, the pure product was obtained as a yellow oil in 75% yield after column chromatography purification on silica gel using *n*-Hex/EtOAc/NEt₃ 90:9:1 as eluent. ¹H NMR (500 MHz, CDCl₃): δ = 3.07 (td, *J* = 6.4, 5.1 Hz, 1H), 2.50-2.43 (m, 1H), 1.99-1.90 (m, 1H), 1.87-1.66 (m, 4H), 1.63-1.47 (m, 2H), 1.37 (dd,

Chapter IV. Iodine Catalysis for C(sp³)-H Fluorination
with a Nucleophilic Fluorine Source

$J = 21.5, 6.1$ Hz, 6H), 1.31-1.10 (m, 3H), 1.09-0.96 (m, 5H). ¹³C NMR (125 MHz, CDCl₃): $\delta = 96.1$ (d, $J = 164.2$ Hz), 53.5, 48.8 (d, $J = 20.7$ Hz), 46.1 (d, $J = 1.6$ Hz), 35.0, 33.6, 27.9 (d, $J = 24.7$ Hz), 27.1 (d, $J = 25.1$ Hz), 26.3, 25.4 (d, $J = 22.9$ Hz), 22.6 (d, $J = 1.9$ Hz). ¹⁹F{¹H} NMR (470 MHz, CDCl₃): $\delta = -136.59$. IR ν (cm⁻¹): 2925, 2853. HRMS: Mass calculated for C₁₂H₂₅FN: 202.1966, found: 202.1964.

Benzyl (4-fluoro-4-methylpentyl)carbamate (32)



Step 1: Fluorinated compound **32** (0.27 mmol) was dissolved in 1 mL of HPLC-grade acetonitrile together with K₂CO₃ (1.36 mmol, 5.0 equiv.) and 1-propanethiol (1.36 mmol, 5.0 equiv.). The reaction mixture was stirred at room temperature until TLC showed total consumption of the starting material (10-12 hours). The reaction was diluted with dichloromethane and extracted with HCl 1M. The aqueous phase was then basified to pH 14 with NaOH and subsequently extracted with dichloromethane. Due to volatility issues, the combined organic phase was acidified with HCl in dioxane prior to evaporation. After solvent removal, the resulted residue was submitted to the following step without any further purification. Step 2: In a flamed-dried Schlenk flask the residue from step 1 was dissolved in dry dichloromethane under an argon atmosphere. NEt₃ (0.67 mmol, 2.5 equiv.) and CbzCl (0.32 mmol, 1.2 equiv.) were added and the reaction was stirred for 6 hours at room temperature. The reaction was quenched with saturated aqueous NH₄Cl solution and subsequently extracted with dichloromethane. The combined organic fractions were washed with H₂O and brine solution and resulting crude was purified by column chromatography on silica gel using *n*-Hex/EtOAc 95:5 as eluent. The pure product **8b** was obtained as a colorless oil in 63% combined yield over two steps. ¹H NMR (500 MHz, CDCl₃): $\delta = 7.39$ -7.29 (m, 5H), 5.10 (s, 2H), 4.78 (bs, 1H), 3.26-3.20 (m, 2H), 1.77-1.70 (m, 2H), 1.64-1.59 (m, 2H), 1.59 (s, 3H), 1.34 (d, $J = 21.4$ Hz, 3H). ¹³C NMR (125 MHz, CDCl₃): $\delta = 156.6, 136.8, 136.7, 128.7, 128.3, 95.4$ (d, $J = 165.3$ Hz), 66.8, 43.1, 41.2 (d, $J = 20.2$ Hz), 38.4 (d, $J = 23.2$ Hz), 32.6, 26.8 (d, $J = 24.7$ Hz). ¹⁹F{¹H} NMR (470 MHz, CDCl₃): $\delta = -138.52$. IR ν (cm⁻¹): 3333, 2933, 1696, 1523. HRMS: Mass calculated for C₁₄H₂₀FNNaO₂: 276.1370, found: 276.1367.

Overall conclusions

This Doctoral Thesis aimed at designing novel protocols for *sp*³ C-N and *sp*³ C-F bond formation in the context of aliphatic C-H functionalization. The most significant conclusions of this scientific journey are summarized below:

- i) We have developed an unprecedented electrochemical C(sp³)-H intramolecular amination method. The reaction proceeds under mild conditions and in an atom-economical fashion, since molecular hydrogen is the sole by-product generated. Not only pyrrolidine, but a wide variety of piperidines could be prepared by employing this methodology. In addition, the reaction could be extended to oxygen-containing heterocycles when employing aliphatic alcohols and carboxylic acids as precursors. Mechanistic investigations were performed in order to understand the reaction mechanism.
- ii) We have accomplished the development of a new Cu-catalytic system for the activation of N-F bonds as a new vehicle for triggering an intramolecular aliphatic C-H amination. By using this protocol, fluorinated sulfonamides could be employed as transferable aminating agents for the synthesis of pyrrolidines and piperidines. Importantly, 6-membered rings can be obtained, thus overriding the natural proclivity for 1,5-HAT processes while expanding the application profile of Hofmann-Löffler reactions. Extensive mechanistic investigations including stoichiometric experiments and theoretical calculations were performed in order to elucidate the reaction mechanism.
- iii) We have developed a new photocatalytic protocol for aliphatic *sp*³ C-H fluorination employing nucleophilic fluorine as fluorine source. This technique makes use of hypervalent alkyl-iodine(III) intermediates generated in situ, allowing to access different fluoroamine products via site-selective 1,5- or 1,6-HAT by a judicious choice of the amine-directing group utilized. Taking into consideration the short reaction times required for effecting the targeted transformation, we anticipate that this technique might be used for incorporating ¹⁸F-isotopes, thus holding promise for PET-imaging techniques.

UNIVERSITAT ROVIRA I VIRGLI
NEW STRATEGIES FOR C(SP³)-H FUNCTIONALIZATION
Daniel Bafaluy Español

UNIVERSITAT ROVIRA I VIRGLI
NEW STRATEGIES FOR C(SP³)-H FUNCTIONALIZATION
Daniel Bafaluy Español

UNIVERSITAT ROVIRA I VIRGLI
NEW STRATEGIES FOR C(SP³)-H FUNCTIONALIZATION
Daniel Bafaluy Español

